Hydrogen Peroxide as an Oxidiser for Medium-Lift Launch Vehicles

A Performance and Integration Analysis

Michaël Staelens
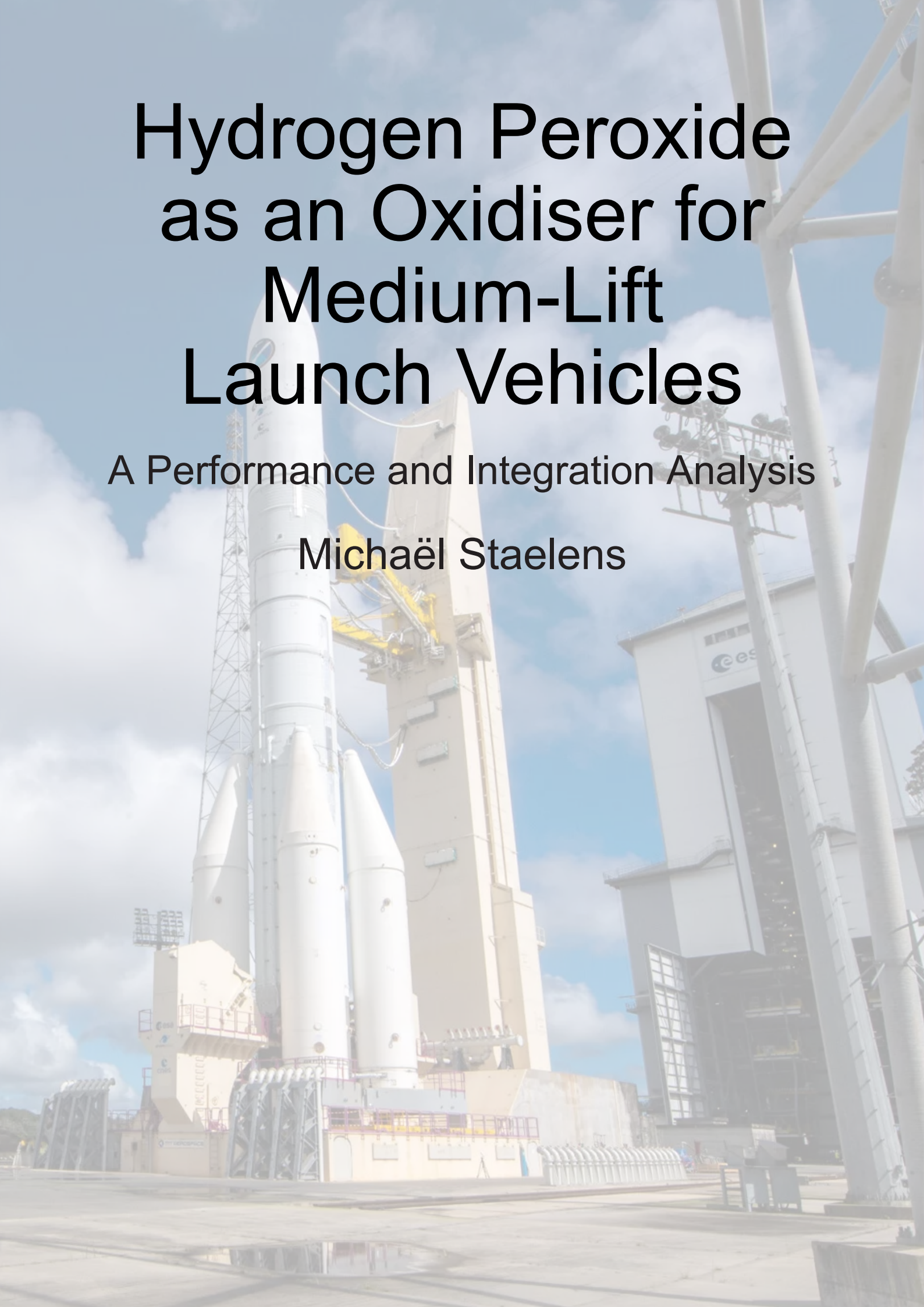
Hydrogen Peroxide as an Oxidiser for Medium-Lift Launch Vehicles

A Performance and Integration Analysis

by

Michaël Staelens

to obtain the degree of Master of Science
at the Delft University of Technology,
to be defended publicly on **Thursday January 25, 2024 at 14:00**

*TU*Delft

Acknowledgements

Abstract

Cryogenic and semi-cryogenic propellants are the most commonly used liquid propellants for applications in medium-lift launch vehicles. Despite their high performance, the storage requirements for these propellants often lead to complex, heavy, and voluminous structures. The only storable propellant used in medium-lift launch vehicles, UDMH/NTO, comes with its own problems of high toxicity and reduced performance. A promising alternative to this could be storable fuels with highly concentrated hydrogen peroxide (HTP) as an oxidiser. Despite a shorter history of dedicated development, HTP has proved itself an effective oxidiser for in-space applications and small-lift launch vehicles. Therefore, the question could be raised towards the potential of this oxidiser for applications in medium-lift launch vehicles. In this study, the application potential of an HTP-based storable bi-propellant for medium-lift expendable launch vehicles was investigated. To this extent, a large selection of green storable fuels was considered to find the most suitable propellant for this application.

Both the integration and compatibility potential of the propellants and the propulsive and mass performance potential were investigated. The integration and compatibility potential were evaluated through a qualitative assessment based on non-performance-related propellant characteristics. Furthermore, eight fuels were subjected to a more detailed assessment covering the criteria of handling toxicity, environmental toxicity, material compatibility, handling and storage, development level, and coolant qualities. RP-1 was found to be the most suitable fuel with respect to the specific criteria, while ethanol, methanol, isooctane, and isopropanol were also found to be promising alternatives. A launch vehicle model was created to evaluate the propulsive and mass potential of twelve fuels proposed based on earlier findings. This model included a propulsion model, a mass and sizing model, and an aerodynamics and trajectory model, which were all connected through a global optimisation model. In terms of propulsive potential, the cryogenic propellant hydrolox was predicted to have a 25% higher vacuum specific impulse than the best-performing HTP-based propellant DMAZ/HTP. In terms of the specific impulse density, kerosene-derivative fuels in combination with HTP were predicted to have a better performance than hydrolox and than that other conventional storable propellant UDMH/NTO. The optimised gross lift-off mass for the launch vehicle concepts employing HTP was found to be 42-61% higher than the gross lift-off mass of Ariane 6 predicted through the model. Separately, the payload capability of the HTP-based launch vehicle concepts was predicted to be at least 38% lower. In both cases, RP-1/HTP was reported to be the HTP-based propellant with the best performance, while DMAZ, isooctane, and isopropanol could be regarded as suitable alternatives. All of these propellants also outperformed UDMH/NTO. Through a sensitivity analysis, it was discovered that up to $270kg$ additional payload could be taken to GTO upon considering elevated chamber pressures in the HTP-based engine design. In the end, the high potential and promise of HTP were confirmed as it was concluded that increased development efforts towards HTP-based storable bi-propellant rocket engines could not only lead to a promising alternative to cryogenic propellants but could also allow for the complete replacement of toxic hydrazine-derivative fuels.

Contents

Abbreviations

Abbreviation	Definition
A62	Ariane 6 *(2 boosters configuration)*
A64	Ariane 6 *(4 boosters configuration)*
ADN	Ammonium Dinatramide
AHP	Analytical Hierarchy Process
AQAO	Anthraquinone Auto-Oxidation
CEA	Chemical Equilibrium Analysis
CH_4	Liquid Methane
CI	Consistency Index
CNES	Centre National d'Etudes Spatiales *(French)*
CR	Consistency Ratio
DETA	Diethylenetriamine
DLR	Deutsches Zentrum für Luft- und Raumfahrt *(German)*
DMAZ	2-dimethylaminoethylazide
ECHA	European Chemicals Agency
FRT	First Stage Recovery Tool
GA	Genetic Algorithm
GG	Gas Generator Cycle
GHS	Global Harmonised System of Classification and Labelling of Chemicals
GLOM	Gross Lift-off Mass
GRASP	GReen Advanced Space Propulsion
GTO	Geostationary Transfer Orbit
HTP	High Test Peroxide
HTP	Highly Concentrated Hydrogen Peroxide
IDT	Ignition Delay Time
IL	Ionic liquid
IRT	Ideal Rocket Theory
LEO	Low Earth Orbit
LH	Liquid Hydrogen
LLPM	Lower-stage Liquid Propellant Module
LOX	Liquid Oxygen
MDF	Multi-Discipline Feasible Method
MDO	Multidisciplinary Design Optimisation
MER	Mass Estimation Relation
MMH	Monomethyl Hydrazine
NASA	National Aeronautics and Space Administration
NFPA	US National Fire Protection Association
NTO	Dinitrogen Tetroxide
O/F	Oxidiser-to-Fuel Ratio
OMS	Orbital Manoeuvring System
PICE	Propellant Integration and Compatibility Evaluation
POST	Program to Optimise Simulated Trajectories
RCS	Reaction Control System

Abbreviation	Definition
REACH	Registration, Evaluation, Authorisation and Restriction of Chemicals
RI	Random Index Value
RP-1	Rocket Propellant 1
RPA	Rocket Propulsion Analysis
RSE	Residual Standard Error
SC	Spacecraft
SRB	Solid rocket booster
SVHC	Substances of Very High Concern for Authorization
SVP	Saturated Vapour Pressure
THF	Tetrahydrofuran
Threshold Limit Value	TLV
TMPDA	N,N,N',N'–tetramethylpropane–1,3-diamine
TRL	Technology Readiness Level
Tudat	TU Delft Astrodynamics Toolbox
UDMH	Unsymmetrical Dimethylhydrazine
ULPM	Upper-stage Liquid Propellant Module
US76	US 1976 Standard Atmosphere Model
VHI	Vapour Hazard Index
WEL	Workplace Exposure Limit

List of Symbols

Latin Symbols

Symbol	Definition	Units
A_e	Nozzle Exit Area	$[m^2]$
A_t	Nozzle Throat Area	$[m^2]$
a	Aerodynamic acceleration	$\left[\frac{m}{s^2}\right]$
C_D	Drag Coefficient	$[-]$
C_F	Thrust coefficient	$[-]$
C_L	Lift Coefficient	$[-]$
C_S	Side Force Coefficient	$[-]$
c^*	Characteristic Velocity	$\left[\frac{m}{s}\right]$
c_p	Specific Heat Capacity	$\left[\frac{J}{kg \cdot K}\right]$
D	Diameter	$[m]$
D	Drag Force	$[N]$
D_f	Fuel Tank Diameter	$[m]$
D_{ox}	Oxidiser Tank Diameter	$[m]$
D_s	Stage Diameter	$[m]$
F	Thrust Force	$[N]$
F_{core}	Core Stage Thrust Force	$[N]$
F_G	Gravitational Force	$[N]$
F_{SL}	Sea Level Thrust	$[N]$
F_{SRB}	Booster Stage Thrust Force	$[N]$
F_u	Ullage Factor	$[-]$
F_{vac}	Vacuum Thrust	$[N]$
$f_{mutation}$	Mutation Factor	$[-]$
G	Universal Gravitational Constant	$\left[\frac{N \cdot m2}{kg^2}\right]$
g_0	Earth Gravitational Constant	$\left[\frac{m}{s^2}\right]$
H	Altitude	$[m]$
h	Heat Transfer Coefficient	$\left[\frac{W}{m^2 \cdot K}\right]$
I_{sp}	Specific Impulse	$[s]$
$I_{sp,SL}$	Sea Level Specific Impulse	$[s]$
$I_{sp,SRB}$	Booster Specific Impulse	$[s]$
$I_{sp,vac}$	Vacuum Specific Impulse	$[s]$
k	Thermal conductivity	$\left[\frac{W}{m \cdot K}\right]$
L	Lift Force	$[N]$
L_0	Core Stage Length Constant	$[m]$
L_f	Fuel Tank Length	$[m]$
L_{ox}	Oxidiser Tank Length	$[m]$
L_{S1}	Core Stage Length	$[m]$
L_{S2}	Upper Stage Length	$[m]$
L_{tot}	Total Launch Vehicle Length	$[m]$
M	Mach Number	$[-]$
M_{const}	Construction Mass	$[kg]$
M_{dry}	Dry Mass	$[kg]$

Symbol	Definition	Units
M_E	Earth Mass	kg
M_{eng}	Engine Mass	$[kg]$
M_{LV}	Launch Vehicle Mass	$[kg]$
M_p	Propellant Mass	$[kg]$
M_{pay}	Payload Mass	$[kg]$
M_{S2}	Upper Stage Mass	$[kg]$
M_w	Molecular Weight	$\left[\frac{kg}{kmol}\right]$
M_{wet}	Wet Mass	$[kg]$
$\dot{m}$	Mass Flow	$[kg/s]$
N_{eng}	Number of Engines	$[-]$
O	Trajectory Objective Function	$[-]$
P_r	Prandtl Number	$[-]$
p	Roll Rate	$[\frac{rad}{s}]$
p_a	Ambient Pressure	$[Pa]$
p_c	Chamber Pressure	$[Pa]$
p_e	Nozzle Exit Pressure	$[Pa]$
q	Dynamic Pressure	$[Pa]$
q	Pitch Rate	$[\frac{rad}{s}]$
R	Distance to Center	$[m]$
R	Specific gas constant	$\left[\frac{N \cdot m}{kg \cdot K}\right]$
R^2	Coefficient of Determination	$[-]$
R_a	Universal Gas Constant	$\left[\frac{N \cdot m}{mol \cdot K}\right]$
R_E	Earth Radius	$[m]$
R_e	Reynolds Number	$[-]$
r	Yaw Rate	$[\frac{rad}{s}]$
S	Side Force	$[N]$
S_{core}	Core Stage Surface Area	$[s]$
S_{ref}	Reference Area	$[m^2]$
S_{SRB}	Booster Surface Area	$[s]$
S_{upper}	Upper Stage Surface Area	$[s]$
T	Temperature	$[K]$
T_B	Coolant Bulk Temperature	$[K]$
T_c	Chamber temperature	$[K]$
T_W	Coolant Wall Temperature	$[K]$
t_b	Burn Time	$[s]$
t_{core}	Core Stage Burn Time	$[s]$
t_{SRB}	Booster Stage Burn Time	$[s]$
V	Velocity	$[\frac{m}{s}]$
V	Volume	$[m^3]$
V_e	Exhaust velocity	$[\frac{m}{s}]$
$V_e q$	Equivalent Exhaust velocity	$[\frac{m}{s}]$
V_f	Fuel Volume	$[m^3]$
V_G	Relative Ground velocity	$[\frac{m}{s}]$
V_{ox}	Oxidiser Volume	$[m^3]$
V_{s2}	Upper Stage Volume	$[m^3]$

Greek Symbols

Symbol	Definition	Units
α	Angle of Attack	[°]
β	Sideslip Angle	[°]
$\beta_{S,c}$	Stage-Specific Fineness Ratio Constraint	[−]
β_{S1}	Core Stage Fineness Ratio	[−]
β_{S2}	Upper Stage Fineness Ratio	[−]
β_{tot}	Total Launch Vehicle Fineness Ratio	[−]
χ	Heading Angle	[°]
$\Delta\gamma_e$	Flight Path End State Difference	[°]
ΔH_e	Altitude End State Difference	[m]
ΔH_{max}	Altitude Max State Difference	[m]
ΔV_e	Velocity End State Difference	$\left[\frac{m}{s}\right]$
δ	Latitude	[°]
ϵ	Nozzle Area Ratio	[−]
Γ	Vandenkerckhove Number	[−]
γ	Flight Path Angle	[°]
γ	Specific Heat Ratio	[−]
λ	Longitude	[°]
λ_{max}	Maximum Eigenvalue	[−]
μ	Dynamic Viscosity	[$Pa \cdot s$]
μ	Bank Angle	[°]
μ_E	Earth Gravitational Parameter	$\left[\frac{m^3}{s^2}\right]$
ω	Earth Rotational Rate	$\left[\frac{rad}{s}\right]$
ρ	Density	$\left[\frac{kg}{m^3}\right]$
ρ_f	Fuel Density	$\left[\frac{kg}{m^3}\right]$
ρ_{ox}	Oxidiser Density	$\left[\frac{kg}{m^3}\right]$
ρ_{S2}	Upper Stage Density	$\left[\frac{kg}{m^3}\right]$
θ	Pitch Angle	[°]
ζ_F	Thrust Correction Factor	[−]
ζ_{isp}	Specific Impulse Correction Factor	[−]
ζ_m	Mass Flow Correction Factor	[−]

List of Figures

List of Tables

1.Introduction

A remarkable characteristic of the space industry is the continuous strive to improve existing technology and to develop new innovative systems. This effort has made space more accessible and more attractive for further research initiatives, which have pushed the industry into a cycle of constant innovation and improvement. Studying ongoing trends and exploring the potential of new innovative systems is an essential factor in sustaining this cycle. As can be deduced from Figure 1.1, the annual number of objects to be launched into space, which includes all objects launched into Earth orbit and beyond, has increased tenfold compared to a decade ago. A major reason for this significant development in recent years has been the increase in accessibility to space due to the influx of new providers, both through increased commercial activity and through the interest and resources from national agencies that were not considered to be traditional spacefaring nations a decade ago.
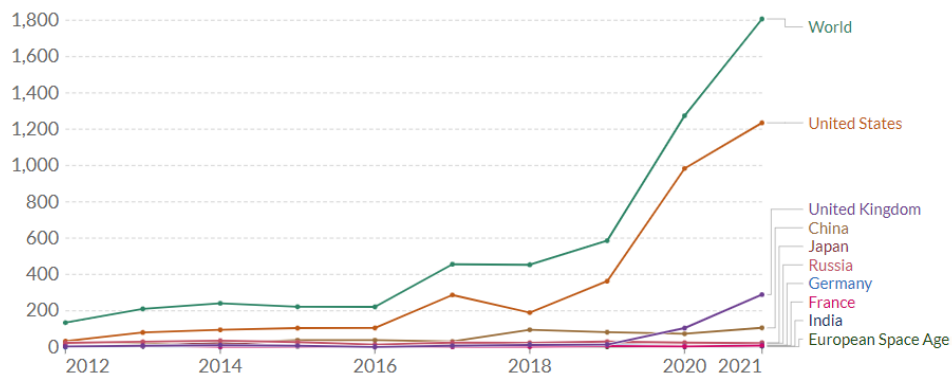
Figure 1.1: Annual number of objects launched into space since 2012[2]

As interest in space grows, so does the need to improve existing solutions and push the boundaries of what is possible. This also applies to the systems that bring humanity to space; Launch vehicles. One design choice that significantly influences the performance of launch vehicles and could thus allow for noticeable improvement is the choice of propellant. Cryogenic and semi-cryogenic bi-propellants are currently the most commonly used liquid propellants for medium-lift launch vehicles. Despite their high performance, the storage requirements for these propellants often lead to complex, heavy, and voluminous structures. The only storable liquid propellant currently used in medium-lift launch vehicles, hydrazine combined with nitrogen tetroxide, comes with its own problems of reduced performance and high toxicity. The latter is a major drawback, as the space industry has been in search of green alternatives to replace toxic propellants following similar developments in the aviation industry. This is motivated by proposals to ban hydrazine.[3][4]

A relatively non-toxic and promising green propellant and oxidizer that has been reintroduced onto the scene is hydrogen peroxide. Despite a shorter history of dedicated development, hight test peroxide or highly concentrated hydrogen peroxide (HTP) has been proven an effective oxidiser for in-space applications and small-lift launch vehicles. A recent study by Elferink[5] treated the design optimisation for an upper stage of an expendable launch vehicle design using green storable propellants. In his work, he proved the value and the potential of HTP as an oxidiser for bi-propellants in propulsive applications for launch vehicles.[5] From a literature review prior to this study, it became evident that while the use of HTP-based propellants for in-space applications and small-lift has been investigated, their full potential remains unexplored. Therefore, the next step is to raise the question towards the potential of this oxidiser for applications in medium-lift launch vehicles.

Main research objective: Perform a performance and integration potential analysis for the use of a hydrogen peroxide based bi-propellant into the core stage of a medium-lift expendable launch vehicle to further map the potential of hydrogen peroxide for space applications.

Main research question: What are the integration and performance potential of a green hydrogen peroxide-based bi-propellant in the core stage of a medium-weight expendable launch vehicle?

To effectively treat the topics brought forward in the main research objective and question set for this research, a set of subquestions could be defined. These show the intent to investigate different aspects of the launch vehicle design, as both the integration and compatibility potential, as well as the performance potential of the propellants, are subject to evaluation.

- RQ-CI-01: Which non-performance-related design drivers allow for candidate fuels to be assessed based on their compatibility and integration potential with hydrogen peroxide for launch vehicle applications?
- RQ-CI-02: Which storable fuel shows the most compatibility and integration potential in combination with highly concentrated hydrogen peroxide with respect to a set of specific non-performance-related design drivers for launch vehicle applications?
- RQ-PERF-01: What is the propulsion performance potential of storable non-toxic fuels combined with hydrogen peroxide?
- RQ-PERF-02: How does the integration of selected green bi-propellants in the core stage of a medium-lift expendable launch vehicle affect the payload capability of the vehicle?

To accommodate the answering of these questions, two main research segments are set up. The first research segment, referred to as the *Baseline fuel assessment*, is aimed at narrowing down the initially large selection of proposed fuels and at evaluating the integration and compatibility potential of the remaining fuels. For this purpose, a surface-level assessment and a more detailed assessment are consecutively performed, thereby relying on non-performance related criteria. For the second, a model is created, referred to as the *vehicle performance model*. This should enable the prediction of the performance of the launch vehicle concepts employing the proposed HTP-based propellants in a relevant setting. Ultimately, a global optimisation model is created to optimise for the gross lift-off mass and the payload capability of the launch vehicle concepts based on the Ariane 6 reference case.

To support the claims made in this introduction and to provide a theoretical framework to further define this research, a literature study will be performed and presented in Chapter 2. This will then allow for a research goal and, subsequently, a set of research objectives and research questions for this study to be formulated in Chapter 3. Then, the methodology for this study will be outlined in Chapter 4, where a brief definition and orientation will be provided for the two main research segments that were considered in this study. The setup and methods behind the first research segment will be introduced in Chapter 5, after which the results and findings will be presented in Chapter 6. Next, the setup and methods behind the second research segment will be introduced in Chapter 7, after which the results and findings will be presented in Chapter 8. This will then allow for a series of conclusions to be drawn and subsequently for recommendations for further study to be given in Chapter 9 and 10, respectively.

2.Literature review

Before introducing the research goal and questions for this study, it is important to provide a foundation for setting up this research definition. As such, the chapter will serve to place this study within a relevant theoretical framework. To this extent, the current state of relevant technologies and the need for further research will be investigated. As per the core of this study, the main topics that will be reviewed in this chapter are ongoing launch vehicle trends and the characteristics and applicability of hydrogen peroxide for this purpose.

2.1. Launch vehicle development trends

Less than a century ago, institutional causes were at the basis of high launch costs, as commercialisation of the launch vehicle industry was limited and national agencies were mostly interested in reliability and performance over other design drivers such as cost and environmental concerns. Today, significant trends can be identified in the development of new launch vehicles, as these other design drivers have gained ever more importance.[6] As the space industry and the political scene behind it evolve, so do the launch vehicle development needs and strategies. As such, it is important to identify the market needs and orientation when considering launch vehicle design. Knowledge of launch vehicle development trends and design drivers is thus a crucial factor in setting up launch vehicle design studies.

2.1.1. Areas of development

An important evolution in terms of launch vehicle development and design trends are the areas of the design which are prioritised and from which major design drivers are derived. Whereas reliability and performance were in the past the most important drivers for designs such as that of the Space Shuttle, other areas of development have gained prominence in recent years.[6] Prime examples are considerations of cost, complexity, environmental consequences, and adjustment to payload scaling.[7][8] Important factors in this evolution are an increase in commercialisation and competitiveness within the industry, a shift in priorities and regulations on the political scene, and developments in other areas of the space industry such as the growing trend of scaling down spacecraft (SC).[6][8][9]

Miniaturisation of spacecraft

The launch vehicle industry was founded on the effort to provide the service of bringing payload to space. In developing new generations of launch vehicles, it is thus evident that the launch vehicle designs and capabilities need to be scaled with the market needs and trends. A major trend in recent years has been the miniaturisation of spacecraft and their components, as can be deduced from Figure 2.1.[8][10] As such, the payload mass to orbit needs have been significantly reduced. Another major trend made possible by miniaturisation is the deployment of constellations, resulting in a rising need for multi-object launches. Here, the launch vehicle industry has shown to be reactive, as illustrated by the development efforts made by major global launch providers. The rideshare services offered by SpaceX[11] and the multi-launch service that is developed for the upcoming Ariane 6 launch vehicle by ArianeGroup[12] are prime examples. The commercialisation and miniaturisation of the space industry have not only increased the supply and demand for launch services but have also sparked the need for cost-effective launch solutions. Thus, several new launch vehicles focused on the small-lift launch market share are currently in development to further answer this need and to offer an alternative to rideshare on medium-lift launch vehicles.[8]
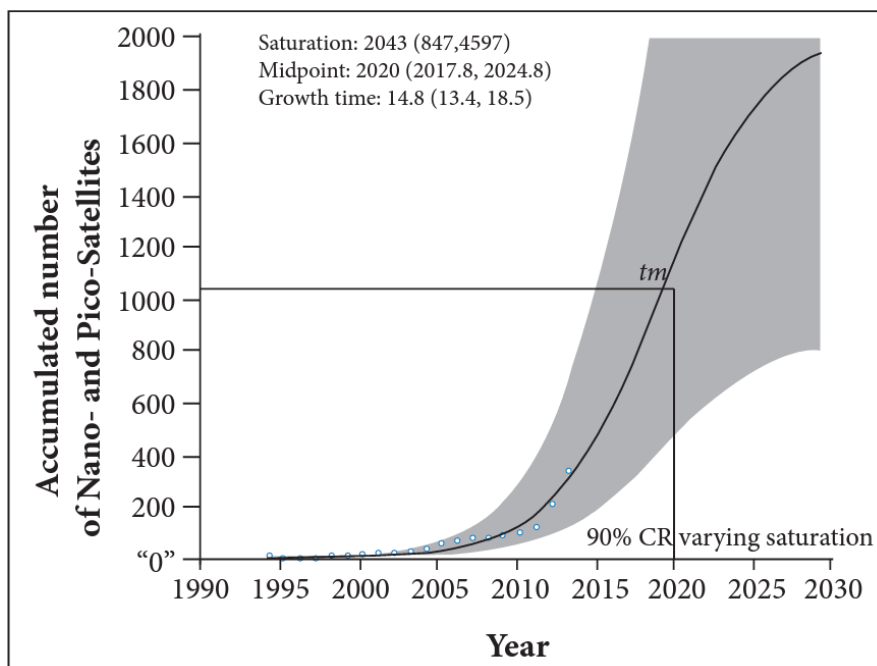
Figure 2.1: History and forecast of the number of accumulated nano- and pico-satellites (< 10 kg of wet mass) using a logistic growth model. The black line is the model output, the white dots represent the input data (period between 1995 and 2014) and the gray region shows the range of curve with saturation values within 90% of confi dence interval. The midpoint of the growth process is given by "tm" [8]

Cost and complexity

Wertz and Larson described high launch costs as "the greatest limiting factor to expanded space exploitation and exploration".[13] Indeed, the costs of launch vehicles have become a significant driver in recent design and development efforts.[6][7][8] As such, several cost reduction strategies have been proposed. Unsurprisingly, several of these propositions address the complexity of launch vehicle design as a result of the identified relation between system complexity and the cost of the system's development and production. Here, simplified vehicle configurations, increased simplicity and design margins, and reduced complexity of structurally demanding components are prominent cost reduction strategies.[6][13]

Environmental considerations

In recent years, the space industry has been in search of green alternatives to replace toxic propellants following similar developments in the aviation industry. This motivation can be illustrated by European proposals to ban hydrazine, a conventional but toxic propellant.[14] As such, environmental considerations have become important drivers in the design and development of new launch vehicles. Especially for new systems, research and green initiatives have become crucial as to ensure long-term competitiveness. Therefore, environmental considerations are not only a result of market adaption, but also of anticipation and proactive measures for future competitiveness.[7][9] It is also worth noting the effects of propellant selection on other design drivers, as the complexity and structural build of primarily propulsion systems is directly related to propellant properties. Next to that, availability concerns, volatility, and ease of handling are all factors that directly relate the choice of propellant to systems costs.[9][15] Following these realisations, it can be concluded that propellants would form an interesting basis for further research on the topic of launch vehicle design and development.

2.1.2. Launch vehicle propellants

In the space industry, various classes and subclasses of propellants are employed in several different applications. As each propellant combination carries a specific set of characteristics, it is crucial to have a base understanding of these characteristics concerning the design purpose and to have knowledge of their common applications. The two classes of propellants that are deemed most relevant and developed for launch vehicle applications are those of solid propellants and liquid propellants.[16]

Solid propellants

Following the idea that the fundamental difference between the different types of chemical propellants is the state of matter of the fuel/oxidiser combinations, a definition for solid propellants can be deduced.[17] Solid propellants are chemical propellants in which both the fuel and the oxidiser are characteristically stored in a condensed, solid state of matter.[18] Within the class of solid propellants, further classification efforts can be made. The two major types of solid propellants to be differentiated are homogeneous and heterogeneous propellant grains. In the case of the former, fuel and oxidiser are combined in the same module, while the latter, which are also referred to as composite solid propellants, are composed of separate fuel and oxidiser modules blended together in a binder material.[16]

Solid propellant systems are generally recognised for their simple designs, high reliability, and low-cost characteristics.[16][17] This is reflected by the small number of essential components incorporated in these rocket designs. As a result, common applications for solid rocket propellant engines are launch vehicle boosters and stages for which little to no autonomous flexibility and constant burn are required. Advantages and disadvantages of solid rocket propellants are given in Table 2.1.

Table 2.1: Advantages and drawbacks of solid propellants[16]

Advantages	Drawbacks
· Simple design	· High explosion/fire potential
· Easy to operate	· Risk of performance reduction in case of grain cracks
· Little preflight checks needed	· Motor reqork required before reuse
· Will not leak, spill or slosh	· Ignition system required
· Throttle/restart can be preprogrammed	· Only preprogrammed throttleability/restart
· Long storage capabilities	· Limited restart capabilities
· More compact due to higher density	· Limited fire duration
· Some potential for reuse	· Hot fire testing not possible prior to use
· Several flight-proven (Technology Readiness Level (TRL) 9) systems	· Once ignited, thrust and duration are set (no option to control or adapt to changes in the environment during flight)
	· Sensitive to rough handling and transport
	· Self-ignition precautions are needed

Liquid propellants

In classifying chemical propellants based on the state of matter of the fuel and oxidiser that make up the propellant, a class of liquid propellants could be identified in which both the fuel and the oxidiser are characteristically stored in a liquid state. Similar to the class of solid propellants, a first subdivision can be made in the class of liquid propellants, thereby differentiating between two main types labelled as monopropellants and bi-propellants, respectively. Whereas in the case of monopropellants the oxidiser and the fuel are essentially combined into one molecule or as a mixture, fuel and oxidiser are kept separated for bi-propellant combinations. As a direct result, monopropellant systems are less complex and require only one propellant tank and feed system compared to the two tanks and feed systems required for bi-propellant systems. Yet, due to a

distinct difference in performance and storability, both liquid propellant types are used in different applications. Hereby, bi-propellants are mostly used for launch vehicle applications in booster stages, core stages, and upper stages. Monopropellants are often preferred for in-space propulsion or attitude control applications.[16][19] As was the case for solid rocket propellants, Sutton[16] has composed a list concerning common advantages related to liquid rocket propellant systems. This can be found inTable 2.2 and includes only general advantages and drawbacks that are relevant for most systems of this type.

Table 2.2: Advantages and drawbacks of liquid propellants[16]

Advantages	Drawbacks
· Possibility of random restart and throttling	· Relatively complex design
· Several flight-proven (TRL 9) systems	· Risk of spilling, leaking, sloshing
· Higher relative performance (specific impulse, thrust) capabilities	· Non-hypergolic propellants require an ignition system
· Possibility of thrust termination and control	· Tank pressurisation needed
· Possibility of hot fire tests before flight	· Combustion instabilities are harder to control
· Cooling by on-board propellant possible	· More volume needed for storage
· Can withstand many ambient temperature cycles without deterioration	· Need special design provisions for restart in zero gravity (not relevant for launch vehicles)
· Low inert propulsion system mass	
· Possibility of component redundancy for increased reliability	

Given their relevance and great variety in terms of launch vehicle applications, it is worth further exploring some of the subclasses of liquid propellants. Propellant components that are in a gaseous state at ambient temperatures and are liquified at extremely cold temperatures are labelled cryogenic propellants. In order to store these propellants in their liquid state, additional storage tank elements are needed to allow for venting, cooling and insulation. This leads to an effective increase in structural mass for cryogenic propellant storage. Despite this mass surplus, cryogenic propellants are often considered due to their excellent specific impulse and overall favourable performance properties. Liquid oxygen (LOX) is the most used cryogenic oxidizer, while liquid hydrogen (LH) and liquid methane are commonly used cryogenic fuels. Liquid oxygen is, however, also often combined with hydrocarbon fuels, such as kerosene, which are stored in a liquid state at ambient conditions and are thus not cryogenic fuels. Such a propellant combination, where either the oxidiser or the fuel is a cryogenic propellant and the other propellant component is not, is referred to as a semi-cryogenic propellant. Common propellant components for cryogenic propellants are LOX as an oxidiser, and LH or liquid methane (CH_4) as fuels.[16][20]

As opposed to cryogenic propellants, storable propellants are propellants that are storable in their liquid state at ambient conditions, indicating room temperature and modest pressure. A differentiation can be made between Earth-storable propellants, such as hydrogen peroxide and kerosene, which are storable in their liquid state at Earth ambient conditions, and space-storable propellants, such as ammonia, which are storable in their liquid state at Space ambient conditions. When considering launch vehicle applications, Earth storable propellants are typically those that are referred to as storable propellants. These storable propellants can lead to weight savings in launch vehicle structures as opposed to cryogenic propellants, at the cost of a performance reduction. Examples of storable propellants are nitrogen tetroxide (NTO), unsymmetrical dimethyl hydrazine (UDMH), monomethyl hydrazine (MMH), and highly concentrated hydrogen peroxide or high test peroxide (HTP).[16][20] An important characteristic that is inherent to some common storable propellant combinations such as MMH/NTO is hypergolicity. Hypergolic propellants, as opposed to propellants that require external stimuli for ignition to occur, are propellants that ignite spontaneously when mixed. Hypergolic systems are most desirable for in-space applications such as satellite reac-

tion control systems (RCS) or orbit manoeuvring systems (OMS) to allow for an overall less complex system at the cost of a performance reduction.[20] For most hypergolic propellants, it holds that the properties that make them hypergolic also make them extremely toxic, thus placing additional strain on the environment and increasing the cost needed for handling and processing the propellant.[16]

Comparison of propellant classes
Despite the fact that the aforementioned propellant classes are grouped under the term liquid propellants, there is a large variety of applications and characteristics to be related to each of these types of liquid propellants. An overview can be found in Table 2.3. Note that this is a general overview, including only a selected range of characteristics and applications. It can be deduced that cryogenic and semi-cryogenic bi-propellants are the most commonly selected types of liquid propellants for use in medium-lift and heavy-lift launch vehicles. That indicated that the excellent performance characteristics displayed by these types of liquid propellants are dominant in the decision for integration over less favourable characteristics such as higher density and additional storage and cooling concerns. It can also be concluded that the combination of LOX and CH_4, also referred to as methalox, is considered in several more recent launch vehicle concepts and also in future concepts that are currently still in development. Another interesting observation is the less featured use of bi-propellant combinations based on highly concentrated hydrogen peroxide. Given the high density, low cost, non-toxic nature and ease of storage related to this chemical, it would be interesting to further study the capabilities of this propellant in launch vehicle propulsive applications.

Another way of classifying propellants is by distinguishing between green and non-green or toxic propellants. The term "green propellants" refers to a elatively novel classification and does, as a result, not have one agreed-upon description. These propellants are commonly referred to as propellants that are less damaging to the environment. This includes characteristics such as lower toxicity levels, corrosiveness or hypergolic reaction. A more extreme description involves propellants that are completely harmless to humans and the environment. Examples of propellants often classified as green are ammonium dinatramide propellants (ADN) and hydrogen peroxide.[16] Note that common propellant components such as LOX and LH are also accepted by the Registration, Evaluation, Authorisation and Restriction of Chemicals (REACH) agreement and could be classified as green propellants.[1] Hydrazine is the most common example of a liquid rocket propellant that is not green. It is dangerous to both humans, making it difficult and costly to handle and process this propellant, and the environment. This take was invigorated by the fact that the propellant was added to the list of substances of very high concern for authorization (SVHC) by REACH legislation of the European Chemicals Agency (ECHA).[4][21]

The term green propellants does not imply that this class of propellants are entirely clean alternatives that do not result in any negative impacts on the environment. Rather, these propellants tend to be generally safer to handle than conventional propellants, resulting in reduced costs associated with propellant storage, transport, and operations.[22] Indeed, green propellants offer additional benefits past adherence to governmental regulations. As these are generally more easy to handle and safer to use, costs associated with handling, storage, and transportation are often reduced.[15] Additionally, due to their less volatile nature, reduced operations costs and quicker turnaround times are also benefits connected with the use of green propellants.[9] Currently, only a small selection of highly developed green propellant systems exist, most of which are cryogenic or semi-cryogenic solutions e.g., hydrolox and methalox. It would, therefore, be interesting to widen this range to allow for more optimal selection for specific applications. One example here, it the need for more complex and structurally heavy systems when using cryogenic propellants.[19] As complexity has become an important design driver in launch vehicle development efforts, it would be interesting to further develop green storable propellant solutions as to provide high-performance green alternatives for such applications. One such alternative would be hydrogen peroxide, which

---

[1]https://www.space-propulsion.com/new-technologies/alternative-propellants.html

given its heritage and relative stage of development and research efforts, could be an interesting propellant component to be considered in the near future.

Table 2.3: Characteristics, classifications and general applications for commonly used liquid propellants[20] (S0 = booster stage ; S1 = core stage ; S2 = upper stage

Combinations	Classification	Common applications	Specific applications	Characteristics
LOX/LH	Cryogenic	S0/1/2	Saturn V (S2/3) Delta IV (S1/2) Ariane 5/6 (S1/2) Vulcan Centaur (S2)	· Highest I_{sp} · High thrust · Non-toxic · Low density · Difficult storage · Long development history
LOX/CH_4	Cryogenic	S0/1	New Glenn (S1) Vulcan Centaur (S1) Starship (S1/2)	· High I_{sp} · High thrust · Non-toxic · Lower density · Difficult storage · High development interest
LOX /hydrocarbon	Semi-cryogenic	S0/1	Saturn V (S1) Falcon Heavy (S0/1/2) Electron (S1/2)	· High I_{sp} · High thrust · Non-toxic · Higher density · Easier storage
NTO/UDMH or NTO/MMH	Storable Hypergolic	S1/2 Satellites RCS OMS	Titan II GLV (S1/S2) Space shuttle (OMS/RCS) LM-3 (S2)	· Instant restart · High development level · Long term storage · Easy storage conditions · Lower I_{sp} and thrust levels · Toxic
MMH or UDMH	Storable Monopropellant	Satellites RCS	Satellites	· Instant restart · High development level · Long term storage · Easy storage conditions · Low I_{sp} and thrust levels · Toxic
HTP	Storable Monopropellant	Satellites RCS	Satellites Centaur (RCS)	· Non-toxic · Low I_{sp} and thrust levels · Easy storage conditions · Lower development level
HTP /hydrocarbon	Storable	S1/2 OMS RCS	Black knight (S1) Black arrow (S1/S2)	· Non-toxic · Promising I_{sp} and thrust levels · Easy storage conditions · Lower development level · High density

2.2. Hydrogen peroxide

In the discussion of green propellants, hydrogen peroxide is often proposed as a prominent replacement for toxic propellants such as hydrazine. Hydrogen peroxide could find application both as a monopropellant and as an oxidiser for bi-propellant based propulsion systems. Due to its moderate characteristics, it could also be worth exploring this oxidiser for application in launch vehicle propellants. Therefore, this section is meant to provide an overview of hydrogen peroxide, including its most important characteristics, its advantages and its drawbacks.

2.2.1. A brief history of hydrogen peroxide

Despite the sudden rise of interest over the last decade, hydrogen peroxide has been around since the nineteenth century, when it was first discovered as a result of a reaction between barium peroxide and nitric acid.[23] In the years leading up to World War II, the concentration of hydrogen peroxide solutions had been increased to a level that saw it fit for introduction in propellant applications. The height of the use of concentrated hydrogen peroxide as a propellant came when the United Kingdom started developing it as a powerful oxidiser in combination with kerosene. This led to the production of various systems, such as the Gamma 201/301 and the Spectre engines.[24] In the period of the 1970s and the 1980s, not coincidentally in the same time frame as the termination of the active UK space program, the usage of hydrogen peroxide in propellant applications was drastically reduced in favour of hydrazine, LOX, and NTO based propellant combinations.[25]

Given the choice of alternative propellants, which have now become conventional, over hydrogen peroxide based combinations, it would be natural to question its value. Yet, it is important to frame this transition in the context of its time period. In the past, little hypergolic combinations were known for hydrogen peroxide and its performance was deemed inferior to the potential displayed by novel propellants such as hydrazine. As performance was valued over other characteristics such as operations costs, environmental issues, and toxicity, other propellants were favoured for further development.[25] This is, to some extent, in contrast with modern-day rocket propellant development philosophies, as concerns regarding the cost of rocket programs and their effects on the environment are ever-growing.

2.2.2. Strengths and weaknesses

As was mentioned, a major reason for phasing out hydrogen peroxide in propellant applications was its, at the time, relatively weak performance with respect to alternative propellants. Another important factor was the criticism offered by prominent scientists such as Clark[26], who favoured the novel propellant hydrazine. His criticism was founded on some of the supposed weaknesses of hydrogen peroxide, such as its detonation risk, stability and storability issues, lack of hypergolic reaction with fuels and its relatively high freezing/melting point. In recent years, many of these criticisms have been reassessed as to give way for the reevaluation and subsequent reintroduction of HTP in propellant applications.

Material compatibility and volatility

An important drawback of hydrogen peroxide as a propellant in space applications is its incompatibility with several relevant aerospace materials. From the material compatibility chart provided in Appendix A, it can be deduced that hydrogen peroxide, especially at the high concentrations in which it is used for space applications, should not come in contact with several common materials e.g., stainless steel, copper, acetal, and carbon steel.[27] This introduces constraints on the design of propulsion systems for hydrogen peroxide, which could prove disadvantageous with respect to important design drivers such as cost and weight. Indeed, early incidents have been reported, supporting the claim of HTP being a dangerous and unstable propellant when in contact with incompatible materials.[28] Here, especially organic dirt and flammable materials have proven to be catalysts for dangerous HTP reactions. Important to note is that the experiments performed by Clark were to some extent incomplete in that the volatile and dangerous nature of the substance hydrazine was insufficiently recognised.[29] This is validated by the information on substance hazards provided on the database from the ECHA[30]. It should be recognised that the processing and handling of chemicals is often not without danger. Safety protocol and regulations related to HTP

will therefore be treated in this section.

Stability
The stability of HTP in both vented and sealed environments is a topic that often has it disregarded for use in-space applications. Due to its supposed fast decomposition rate, it is expected to not meet the storability requirements set for most space missions. Cases have been reported in the 1960s when HTP was used on space missions for periods between three and five years. As some missions, however, require propellant storage in sealed environments for periods exceeding 15 years, this thus renders the performance characteristics regarding the use of HTP in such environments inadequate and in need of further development. It has been proven, however, that the substance can be stored for longer time periods in vented containers, corresponding to the environment of launch vehicles in the months leading up to the launch.[31] Other research reported a drop of less than 0.4% in concentration per year for high concentrations of HTP in such environments for a period upwards of 15 years.[32] This thus shows the promise for the integration of this substance in these types of applications, as well as the need for further studies to replicate and verify these results.

Performance
The main reason for phasing out hydrogen peroxide in the past century was its relatively lower performance with respect to NTO/MMH and LOX, as well as its general lack of hypergolic reactions with high-energy fuels. Recent works, however, have claimed that HTP is amongst the highest-performing propellant components, second only to LOX, which has its own limitations.[25][33] Similarly, recent research and developments have shown not only the existence of viable hypergolic reactions of HTP with a number of fuels, but also that catalysing agents can be added to indirectly provide these reactions or to provide quasi-hypergolic reactions.[29] These will be discussed later on in this section.

Strengths
Apart from its performance benefits and benign environmental nature, especially with respect to NTO/MMH, there are also some other benefits in using HTP which have magnified the current interest in its development over most other green propellants. One such benefit is its high relative density and in addition to this the high oxidiser-to-fuel (O/F) ratio in most HTP-based propellant combinations. This thus allows for weight and cost reduction in its support structures. On top of that, HTP is characterised by its low vapor pressure, high specific heat and its non-reactive nature with the atmosphere. Finally, it is also important to note that HTP is generally more cost-effective than conventional propellants, both in terms of its base cost, as well as its storage and handling costs and the costs related to its support structures.[25][33]

2.2.3. Notable characteristics
Properties related to the chemical nature of quasi-pure hydrogen peroxide (i.e., hydrogen peroxide with a near 100% concentration) were tabulated in Table 2.4. Note that the melting point (or freezing point) of hydrogen peroxide is close to the freezing point of water and, therefore, set at a relatively high temperature. A factor to consider here is that of the super-cooling ability due to the absence of foreign nucleates in highly concentrated hydrogen peroxide solutions, which essentially allows for the freezing process of the liquid to be slowed down when brought below its freezing point.[23][34]

Table 2.4: Chemical characteristics for quasi-pure hydrogen peroxide[33][35]

Characteristic	Value	Unit
Density (@273.15K)	1470	kg/m^3
Density (@293.15K)	1450	kg/m^3
Melting point	272.72	K
Boiling point	423.35	K
Viscosity (@273.15K)	1.819	$mPa.s$
Viscosity (@293.15K)	1.249	$mPa.s$
Autoignition temperature	395.15	K
Flashpoint	348.15	K
Critical temperature	730.15	K

Next to the chemical characteristics related to quasi-pure HTP, several other notable characteristics related to HTP can be found in Table 2.5.

Table 2.5: Other characteristics for 95%+ hydrogen peroxide

Characteristic	Value	Unit
Toxicity hazard codes	H271, H302, H332, H314 [30]	/
Cost estimate	4.14 [36]	$\$/L$
Shelf life (sealed, in space)	>3 [32]	$Years$
Shelf life (vented containers)	>15 [32]	$Years$

2.2.4. Reaction process and production

In order to assess the use and the reaction state of hydrogen peroxide, it is important to have a deeper understanding of its common reaction processes. These are mostly observed in its production and in specific applications.

Hydrogen peroxide reaction processes

Hydrogen peroxide contains a peroxide bond. This single oxygen-oxygen bond is intrinsically weak and unstable. As a result, hydrogen peroxide can easily be decomposed. It is also known to decompose over time into water and oxygen, thereby releasing free radicals[37]:

$$H_2O_2(l)(98\%+) \rightarrow H_2O + \frac{1}{2}O_2 - 98.1kJ/mol \tag{2.1}$$
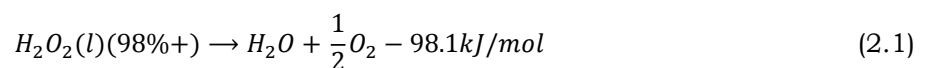
It is important to realise that this decomposition process is directly affected by several environmental factors. Most notable are the size of the initial hydrogen peroxide concentration, the presence of reactive metal ions such as copper, the ambient temperature and the pH value. These relationships are presented in Figure 2.2a-2.3b, respectively.[38]

A fuel that has for a long time been known to be hypergolic with hydrogen peroxide is hydrazine (and its derivatives). It has been found that a reaction between hydrazine and hydrogen peroxide can readily occur through the presence of a small amount of metal ions:[39]

$$2H_2O_2 + N_2H_4 \xrightarrow{metalion} N_2 + 4H_2O \tag{2.2}$$
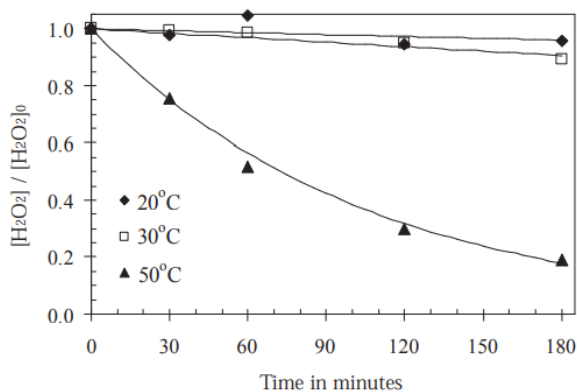
(a) The effects of ambient temperature on the decomposition process of hydrogen peroxide
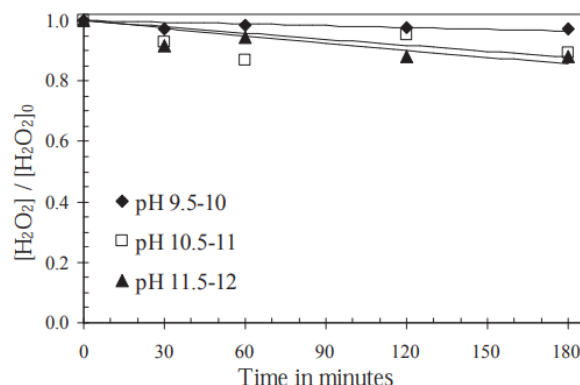
(b) The effects of pH values on the decomposition process of hydrogen peroxide.

Figure 2.3: The effects of ambient temperature and pH values on the decomposition process of hydrogen peroxide [38]
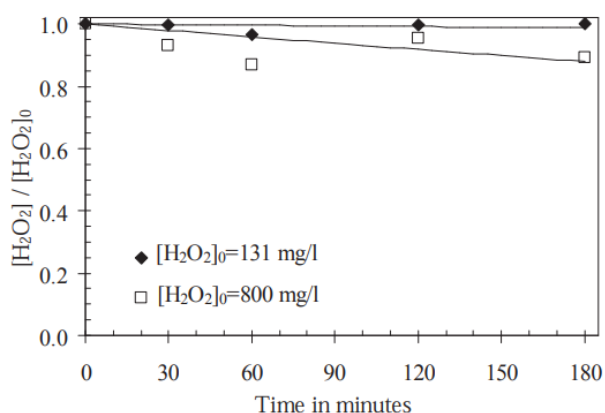
(a) The effects of initial concentration on the decomposition process of hydrogen peroxide
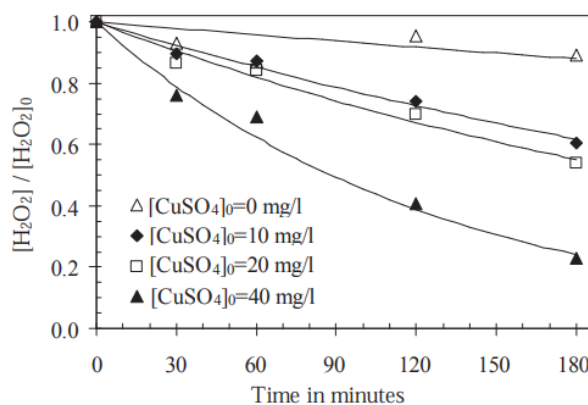
(b) The effects of metal ions such as copper on the decomposition process of hydrogen peroxide.

Figure 2.2: The effects of initial concentration and metal ions on the decomposition process of hydrogen peroxide [38]

Production of hydrogen peroxide

The most commonly used industrial processes with respect to producing hydrogen peroxide are electrochemical cathode reduction of oxygen, electrolysis and a process known as anthraquinone auto-oxidation (AQAO). Among these, AQAO is the method most considered for industrial applications, which makes up 95-99% of global hydrogen peroxide production. This method is based on a cyclic process, visualised in Figure 2.4, in which anthraquinone is put through subsequent stages of hydrogenation, oxidation, hydrogen peroxide extraction, and working solution purification. In the first phase of the process, the polycyclic aromatic hydrocarbon anthraquinone is converted into tetrahydroalkyl-anthrahydroquinone through hydrogenation. In order to promote this process, the solid anthraquinone powder is dissolved in a working fluid together with a catalytic additive, often palladium. Next, traces of catalyst and undissolved anthraquinone are filtered out, after which hydrogen peroxide is formed in an organic state from the tetrahydroalkyl-anthrahydroquinone through a process of auto-oxidation. Using demineralised water, this hydrogen peroxide is extracted, after which the working fluid is treated to recover anthraquinone products for future processes. Note that the recovered products are degraded throughout the process and are thus post-treated before reuse. Also, note that the crude hydrogen peroxide product extracted through the process needs to be further purified to realise mass concentration specific to the intended applications. Common purification methods include repeated sequences of vacuum suction and distillation.[40]
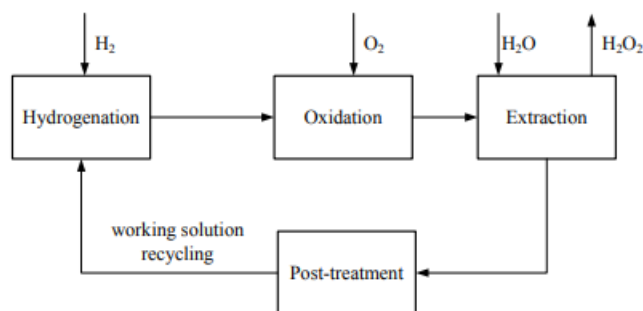
Figure 2.4: Fundamental concept of an AQAO process[40]

Hydrogen peroxide is often considered for green rocket propellant applications due to its relatively non-toxic nature and good propulsive performance characteristics. A consideration to be made, however, is that the matured process of AQAO, which is used at an industrial scale, leads to the production of a significant amount of waste, both through the regeneration process of the working fluid and through the wastewater resulting from the oxidation process.[41] Recent studies and research have been put towards making these processes more environmentally friendly through more controlled input of resources. Alternatively, more efficient and environmentally friendly processes, such as the direct synthesis of hydrogen peroxide from molecular hydrogen and oxygen are being proposed and refined to phase out more wasteful processes such as AQAO.[40][42]

Currently, common purification methods to attain highly concentrated solutions of hydrogen peroxide include repeated sequences of vacuum suction and distillation. These methods are, however, costly and have a limited reach. For specific applications, such as the use of hydrogen peroxide for rocket propellants, high concentrations of hydrogen peroxide of 95+% are needed. New purification processes, such as the technology in development by SolvGe, have the potential to drastically reduce the cost of production while also reducing the complexity of the process and eliminating the need for risk-inducing factors such as transportation. The patented technology introduced by SolvGe in 2021 is, in essence, a hydrogen peroxide printer that allows for the conversion of low concentrations of hydrogen peroxide to highly concentrated hydrogen peroxide solutions up to 99%. This conversion is performed in an inert environment through a simple, passive, gas-based process. SolvGe aims to reduce the cost of hydrogen peroxide and make it more accessible throughout Europe for a variety of applications through this scalable, portable and safe-to-operate system. Following the current progress made by the company, the production price of hydrogen peroxide is expected to evolve to around 0.80$ per kg in the near future. The concentration process proposed by SolvGe would require an approximate energy consumption of $16.74 MJ/kg$, making it far more efficient than AQAO processes.[5]

2.2.5. Safety and handling

Hydrogen peroxide is generally considered to be non-toxic and relatively easy to handle. This is what makes it very appealing for propulsive applications purposes in the space industry as compared to more toxic and dangerous chemicals such as hydrazine. It is, however, imperative to be aware of the specific characteristics of hydrogen peroxide such that it can be approached and handled with the right care.

The Global Harmonised System of Classification and Labelling of Chemicals (GHS) includes nine main classes that are concerned with different kinds of toxicity and hazards applying to chemical compounds.[43] The hazard codes relevant to hydrogen peroxide are listed below. The level of severity to which these codes apply is dependent on the concentration of the hydrogen peroxide in the working solutions. For applications in the space industry, this is generally high. The relevance of these codes with respect to the handling process of hydrogen peroxide should be a first indication in hazard assessments.

- H271: Oxidising liquids - Hazard category 1 (GHS Class 2: Flammables)

- H302: Acute toxicity (oral) - Hazard category 4 (GHS Class 7: Irritants)
- H314: Skin corrosion - Hazard category 1B (GHS Class 5: Corrosives)
- H332: Acute toxicity (inhalation) - Hazard category 4 (GHS Class 7: Irritants)

From the GHS labels applicable to hydrogen peroxide, it can be deduced that despite rather mild features with respect to overall toxicity, it should still be approached with care. It is imperative that a hazard assessment is performed to select suitable protective equipment before working with hydrogen peroxide. Among the most present safety hazards for highly concentrated solutions of hydrogen peroxide is skin contact with microscopic droplets, which could lead to benign but painful spots. As such, it is important to limit the amount of exposed skin. Another important consideration to be made is the reaction of hydrogen peroxide with flammable materials or organic dirt. Wearing leather items or similar fabrics should thus be avoided when handling hydrogen peroxide, even in small concentrations.[37] Finally, it was mentioned that some chemical mixtures promote the decomposition of hydrogen peroxide. These catalytic additives are crucial to effective propellant solutions based on hydrogen peroxide. It is important to keep these chemical compounds away from hydrogen peroxide solutions so as not to prematurely trigger decomposition reactions.[37][40]

Given that is crucial to prevent the decomposition of hydrogen peroxide before use, it is generally recommended to store the chemical solution in a sealed-off and dark environment. This is especially important for high concentrations of hydrogen peroxide. Next to that, the presence of traces of catalysts that could trigger hydrogen peroxide decomposition reactions should be verified and limited. Multiple studies regarding the effects of environmental factors on hydrogen peroxide have been conducted. Figure 2.2a-2.3b give a good overview of these effects and taking into account these findings is important to allow for effective storage of hydrogen peroxide.[40] Finally, it is important to consider the compatibility of hydrogen peroxide with the materials used in the storage tanks. This is a crucial consideration not only for temporary storage facilities but also for the design of the storage tanks in hydrogen peroxide-based propellant applications.

2.2.6. The potential of hydrogen peroxide in launch vehicle applications

When trying to assess the potential of an existing propellant solution for a specific application, it is evident that the historic use of the propellant in similar relevant applications should be considered. In the case of hydrogen peroxide, a prime example are the Gamma 301 and the Spectre engines.[24] These were employed on the first stage of the Black Knight launch vehicle and on the Blue Steel ballistic missile, respectively, both of which were developed and used in the 1960s by the government of the United Kingdom (UK). Of the Black Knight launch vehicle, which is considered a small-lift launch vehicle, 22 effective launches were performed, all of which were deemed a success.[44] In pursuit of similar success, a UK-base company has recently started developing Skyrora XL, a derivative launch vehicle based on Black Knight.[45]

A recent study by Elferink[5] treated the design optimisation for an upper stage of an expendable launch vehicle design using a hydrogen peroxide-based green storable propellant. He considered the integration of green storable non-toxic bi-propellant combinations based on hydrogen peroxide in upper-stage modules for expendable launch vehicles for the purpose of decreasing weight and complexity and increasing the cost and reliability of the design. It was chosen to assess the potential of this technology, referred to as prototype X, from the perspective of cost-benefit, payload performance and technical feasibility. Initial results showed potential dry mass reductions of over 20% and cost-per-flight reduction of up to 8.9% compared to hydrolox-based upper stages. The Ariane 6 launch vehicle was chosen to be the main reference vehicle. It was, however, found that the reduced performance of storable green propellants could implicate a reduced payload performance of over 300%. Therefore, further analysis was performed to prove that propellant optimisation and structural modifications to the upper stage design could potentially lead to an overall payload performance increase to rival hydrolox-based solutions. Due to this conclusion, it was recommended by the author to expand the study towards reusable launch vehicles, hybrid propellant solutions and the main stage modules for expendable launch vehicles.[5]

3. Research definition

The theoretical framework provided in Chapter 2 was set up with the intention of providing more context to the topics investigated in this study. Its contents can be combined into a research definition. In this chapter, the research goal and subsequent research questions and objectives set for this study will be outlined. In doing so, a distinction will be made between the two main research segments which were considered for this study.

3.1. Research goal

Based on the findings from the literature study and conclusions drawn regarding the need for further study and the framework needed to support this, a more definitive research goal could be formulated. This allowed for a more narrow and clear research field and acted as a driving factor in this study. It was defined as:

> *To further map the potential of hydrogen peroxide in space applications by assessing the performance and integration potential of a low-toxicity storable bi-propellant employing highly concentrated hydrogen peroxide as an oxidiser in the core stage of an expendable medium-lift launch vehicle.*

Several elements were included in this research goal statement in order to provide effective boundaries to the scope of the study. The objective of selecting storable fuels with low toxicity levels to be employed in combination with hydrogen peroxide was stated. Next, the field of relevant applications to which the propellants in this study were to be tailored was narrowed down to the core stage of expendable medium-lift launch vehicles.

3.2. Research objectives and questions

The aim of the literature review in Chapter 2 was to build a foundation for further research on the subject of the applicability of hydrogen peroxide in space and launch vehicle applications. This would give an opportunity to expand on the study performed by Elferink[5] concerning the applicability of hydrogen peroxide in launch vehicle upper stages. The insights gained from the literature review have allowed for two main topics to be identified for this study: integration and compatibility potential and performance potential. The former refers to the study of fuel candidates in combination with hydrogen peroxide to assess their potential and suitability with respect to earlier stated objectives of storability and toxicity, as well as several other design drivers that are not directly related to vehicle performance. This would thus allow for an effective evaluation of the compatibility of different fuel candidates with hydrogen peroxide and their more general potential to be integrated into launch vehicle systems. The topic of performance potential covers the propulsive and mass performance of launch vehicle designs employing the proposed green hydrogen peroxide-based bi-propellants. With these topics in mind, a main research objective and main research question could be defined for this study:

> *Main research objective: Perform a performance and integration potential analysis for the use of a hydrogen peroxide based bi-propellant into the core stage of a medium-lift expendable launch vehicle to further map the potential of hydrogen peroxide for space applications.*

> *Main research question: What are the integration and performance potential of a green hydrogen peroxide-based bi-propellant in the core stage of a medium-weight expendable launch vehicle?*

For the above-stated research objective and research question, a set of sub-questions and sub-objectives could be derived. These were defined with respect to the topics of integration potential and performance potential. Studying these subdivisions will allow for the general research question to be answered and thus for the general research objective to be satisfied.

3.2.1. Compatibility and integration potential research definition

In Chapter 1, it was indicated that this study could be classified as a launch vehicle design and optimisation study. To allow for an effective design, several different design drivers could be considered, not all of which are directly related to the performance of the launch vehicle in which the propellant is to be employed. Several drivers and criteria cover the viability and suitability of fuels and are thus good indicators for the compatibility and integration potential of the propellant within the propulsion system outside of factors related to the performance of the vehicle. As such, a separate assessment of different fuel candidates with respect to these criteria could provide for a more complete and valuable analysis if properly investigated. A first sub-objective statement and a set of sub-questions could thus be defined with respect to the topic of fuel integration potential.

Compatibility and integration potential research objective

> To investigate the compatibility and integration potential of various fuel candidates in combination with highly concentrated hydrogen peroxide with respect to design drivers that are not directly related to launch vehicle propulsion and mass performance.

Compatibility and integration potential research questions

- RQ-CI-01: Which non-performance-related design drivers allow for candidate fuels to be assessed based on their compatibility and integration potential with hydrogen peroxide for launch vehicle applications?
- RQ-CI-02: Which storable fuel shows the most compatibility and integration potential in combination with highly concentrated hydrogen peroxide with respect to a set of specific non-performance-related design drivers for launch vehicle applications?

3.2.2. Performance potential research definition

Next to investigating the compatibility and integration potential of several candidate fuels, the second research subject outlined in the research goal statement is that of performance potential. In this part of the study, the emphasis will be on assessing the capabilities of proposed launch vehicle designs from a perspective of propulsion and mass performance. As such, a research objective and a set of research questions could be formulated to set up this study.

Performance potential research objective

> To investigate the performance potential of employing storable propellants based on hydrogen peroxide as an oxidiser on the core stage of a medium-weight launch vehicle with respect to overall launch vehicle propulsion and mass performance definitions.

Performance potential research questions

- RQ-PERF-01: What is the propulsion performance potential of storable non-toxic fuels combined with hydrogen peroxide?
- RQ-PERF-01-A: Which storable non-toxic fuels combined with hydrogen peroxide show the closest specific impulse performance with respect to the reference conventional propellant hydrolox?
- RQ-PERF-01-B: How close can hydrogen peroxide based bi-propellants come to conventional reference propellants in terms of impulse performance?

- RQ-PERF-02: How does the integration of selected green bi-propellants in the core stage of a medium-lift expendable launch vehicle affect the payload capability of the vehicle?
- RQ-PERF-02-A: Which weight and sizing benefits can be achieved by the integration of selected green bi-propellants in a medium-lift expendable reference launch vehicle?
- RQ-PERF-02-B: What is the difference in mass that can be brought into orbit after integration of selected green bi-propellants in a medium-lift expendable reference launch vehicle?

4.Methodology

To support the objectives stated in Chapter 3 and to subsequently find an answer to the research questions that are central to this study, a general structure for the proposed research methodology will be outlined here. Based on the research goal, several similar and relevant studies will first be examined, after which the chosen methodology and setup for this research will be introduced. Next, a series of hypotheses for this study will be formulated based on literature, to provide a means for comparison of results later on. To allow for a more defined and unambiguous research framework, a reference launch vehicle and any other relevant reference data will also be introduced here.

4.1. Design and optimisation studies in literature

In Chapter 3, a research goal and subsequent research objectives were defined following a need for further study identified as a result of the literature study presented in Chapter 2. Following this more detailed research definition, an extended literature study was needed to provide a reliable and complete framework for the research to be conducted. As such, the methods employed in similar studies will be explored in this section.

4.1.1. Fuel selection

An important factor in the overall performance and the general design of a launch vehicle is the choice of propellant. In Chapter 2, it was found that the most commonly used type of propellants for launch vehicle applications are bi-propellants. Even when a bi-propellant system is selected, however, many different subdivisions of propellant still remain, and a selection process specific to the design objectives for the launch vehicle is desirable.

The work by Guerrieri et al.[46] is a study that focused on a propellant selection for two micro-resistojet concepts: the vaporizing liquid micro-resistojet and the low-pressure micro-resistojet. In this work, a methodology was proposed that is composed of four sequential stages with the goal of selecting the propellant most suitable to the proposed application. As a first step, a data collection effort was performed, in which data relevant for the next stages of the selection process were collected for a wide range of candidate propellants. Next, a preliminary feasibility assessment was made based on a small set of essential criteria directly derived from requirements, such as the state of matter of the candidate propellants under the expected storage conditions. This allowed for propellants that were in direct opposition to the system requirements to be discarded early on in the selection process. The main stage of the selection process designed to assess the suitability of the candidate propellants with respect to the proposed application was the Analytical Hierarchy Process (AHP) and Pugh matrix assessment. An AHP tool was used to determine relative weights for a set of criteria derived from design objectives and requirements. This essentially required a number of experts to make a pairwise comparison for the criteria, after which the relative weights, as well as a standard deviation to these weights, could be determined. These weights were then used as input for the Pugh matrix, in which the propellants were scored with respect to the proposed criteria. Following this scoring process, a small group of the most promising propellants was selected for further consideration in the final stage. This final stage covered a detailed analysis which allowed for the performance and the applicability of the propellants to be estimated more accurately in the specific setting of the proposed system.[46] It could be argued that the reviewed methodology is a five-stage process rather than a set of only four sequential stages. The requirements generation was not stated as an official stage in the selection process but can be deemed crucial and influential with respect to the other stages of the process and the eventual selection results. Overall, the methodology applied to this study could allow for an effective and specific base for a theoretical propellant selection to be performed.

The Green Advanced Space Propulsion (GRASP) project was an effort funded by the European Commission with the goal of investigating green propulsion and the possibility of replacing toxic

conventional propellants such as hydrazine in future settings. A very wide range of propellants, including monopropellants and bi-propellants, was considered, and an extensive methodology was proposed to aid the selection process. It is worth noting that the overall selection requirements and criteria were less specific than for other fuel selection efforts, such as the study by Guerrieri et al.[46], due to the wider and less specific scope of the project. Four main stages were identified for the assessment process. Making use of available literature, as well as analytical and numerical modelling efforts, a theoretical assessment of the potential of the propellants with respect to prespecified objectives was first performed. Here, crucial elements were data collection and a top-level trade-off based on the criteria of toxicity, performance, storability, and technology readiness level. Given this method allowed for a large number of candidate propellants to be assessed in an efficient manner, a similar approach could be considered to answer the research questions with respect to the topic of compatibility and integration potential (RQ-CI-01 and RQ-CI-02). After this theoretical assessment, the properties of a proposed selection of propellants were further investigated by means of an experimental evaluation, including considerations such as the ignition properties and the decomposition properties. Laboratory-type propulsion systems were then tested to provide further theoretical and experimental information on the applicability, performance and integration potential of the propellant candidates. Finally, a small selection of propellants was subjected to a final experimental assessment through more advanced systems, referred to as elegant bread board models. Overall, six propellants were considered in this final phase, and the large-scale selection process allowed for further research and derivative propellant selection efforts to be conducted.[47][48][49][50]

4.1.2. Numerical models
In literature, several studies and research works can be found that have focused on the design and optimisation of launch vehicles. Often, these studies make use of numerical models to provide a quantitative basis for their design efforts and their design conclusions. From the research questions stated in Section 3.2.1, it could be deduced that following a similar approach could prove beneficial for this thesis study. As such, propulsion-centered models and mass-centered models could provide a basis for answering the research questions related to the topics of propulsion and mass performance (RQ-PERF-01 and RQ-PERF-02), respectively. Reviewing the methods and models used in launch vehicle design and optimisation studies could give more insight into which models could prove relevant for this thesis study.

In the work of Balesdent[51] and various similar works, four top-level models were used. These models, referred to as modules making up the general model, were an aerodynamics model, a propulsion model, a weight and sizing model, and a trajectory model. In the aerodynamics model, observed Mach numbers were interpolated to obtain drag coefficient results to be inputted in the trajectory model, which allowed for a relative state definition and determination throughout the vehicle trajectory. Overall geometry and mass budgets were set up in the weight and sizing module, making use of the PERSEUS model developed by Centre National d'Etudes Spatiales (CNES)[52] and estimation relationships introduced by Humble et al.[53] and by Sutton and Biblarz[16]. Finally, The propulsion model allowed for propulsive performance and thermodynamic properties to be determined and to be transferred to other modules.[51]

Propulsion models
Throughout several launch vehicle design and optimisation studies, a combination of models is used similar to the work of Balesdent. Overall, the disciplines of propulsion, aerodynamics, trajectory analysis, cost, and weight and sizing are addressed to some extent in these studies. Bayley[54] and Braun et al.[55] both set up a case-specific model for the propulsion module based on adaptations from literature and fundamental propulsion theory. Other studies, such as the works by Dresia et al.[56], van Kesteren[57], van Beers[58], Ernst[59], Iyer[60], Vandamme[61], Elferink[5], and Wiegand et al.[62] have made use of existing specialised software for combustion modelling. The former six opted for the Chemical Equilibrium with Applications (CEA) tool[63] by the National Aeronautics and Space Administration (NASA), while the latter two chose the Rocket Propulsion Analysis (RPA) tool[64], which is effectively verified and validated with CEA. In most of these stud-

ies, ideal rocket theory (IRT) or similar propulsion theories were used to augment or verify the results extracted from these software tools. CEA and RPA Lite are design analysis tools that can model equilibrium conditions and combustion performances, which makes them highly relevant in providing the means to answer RQ-PERF-01.

Aerodynamics and trajectory models
For trajectory analysis, Braun et al.[55] suggested the use of the Program to Optimise Simulated Trajectories (POST) software by NASA[65], which allows for the trajectory to effectively be modelled using numerical integration techniques and a set of final state conditions.[66] Bayley[54] documented the use of a six-degrees-of-freedom flight dynamics simulator, developed to be case-specific, and the AeroDesign software to set up his trajectory and aerodynamics models, respectively, for his launch vehicle design efforts. Several recent studies at Delft University of Technology, including the works by van Kesteren[57], van Beers[58], Dijkstra Hoefsloot[67], and Vandamme[61] have opted to make use of Tudat[68], a software platform originating from the Astrodynamics and Space Missions department at TU Delft that allows for computational support tasks in Python and C++ related to astrodynamics and space research. In addition to this, an older version of the Missile Datcom software[69] was used to add aerodynamic properties to the model. Finally, studies by Iyer[60], Rozemeijer[70], and Contant[71] made use of the first stage recovery tool (FRT), which was originally developed by Rozemeijer. This was combined with RasAero II[72] to add aerodynamic properties to the model.

Weights and sizing models
A module that is commonly used in studies regarding launch vehicle design and optimisation is the mass and sizing model. Dresia et al.[56] and Elferink[5] made use of mass fraction theory. Relations described by Zandbergen[73] and by Barrere et al.[74] allow for fundamental mass fractions to be expressed in terms of other launch vehicle characteristics such as the specific impulse of the different rocket stages. This gives an opportunity to find an effective expression for the payload performance of the launch vehicle. The studies performed by Bayley[54] and Wiegand et al.[62] made use of historical data and available literature to set up regression analyses in determining stage and component weights. The former also followed a bottom-up approach starting from a subsystem level and verifying overall system stability by means of inertia studies. Finally, Braun et al.[55] opted for the use of the CONSIZ software by NASA[75], which requires only limited inputs. The software is, however, outdated and should thus be combined with adequate verification tools.

4.1.3. Optimisation methods
It was identified earlier that optimisation of the design is crucial for the analysis of the influence of new modifications on aspects of launch vehicle performance. From Balesdent[51], it was deduced that effective optimisation involves a multidisciplinary assessment process, meaning that a balance should be found between different elements of the design. Multidisciplinary design optimisation (MDO) is an engineering concept developed to simplify the solving of complex multidisciplinary design problems. MDO methods can be applied to allow for global multidisciplinary optimisation efforts in which either one or multiple optimisers are employed to find global optima based on user-defined objectives.[51] Effective optimisation methods will allow for the research questions stated with respect to vehicle performance potential (RQ-PERF-01 and RQ-PERF-02) to be approached more efficiently as it will allow for a more elaborate, optimised, and effective analysis and assessment of the influence of new modifications on vehicle performance.

An MDO used by Duranté et al.[76] and several other launch vehicle design optimisation efforts is the MultiDiscipline Feasible (MDF) method, which makes use of a single global optimiser to handle all of the identified design variables across the coupled disciplines. This method has been found to be most relevant to small design problems and is reported to be very resource-expensive to use.[51][76] Some MDO methods such as the bi-level integrated systems synthesis method applied by Sobieszczanski-Sobieski et al.[77] are set up to consider multiple discipline-specific optimisers at

the subsystem level in combination with a global optimiser at the system level. This allows for more targeted and design-specific optimisation at the cost of added complexity. This method requires more knowledge of the subsystem level and should thus be applied for detailed design efforts, but could potentially be simplified for use in this study.[77] In a recent performance analysis and design study, Wiegand et al.[62] made use of the optimal control software CAMTOS to aid in optimisation efforts.[78] This software uses the European Space Agency's (ESA) non-linear programming solver WORHP[79] and a single-component decomposition approach to allow for effective integration of design constraints. It is mostly used for conceptual and preliminary design, and it is considered a relevant tool for validation activities.[62]

Gradient-based optimisation methods are generally simple optimisation algorithms in which optima are found using an iterative process based on the gradient of the objective function. Examples of these are the Newtonian method and the steepest descent method. A noteworthy characteristic of most gradient-based optimisation methods is that it could lead to finding local optima, even where global optima are preferred. Therefore, an accurate initial solution estimate is often required. In the work "Gradient Based Optimization Methods", other important problems and advantages related to gradient-based optimisation are described and modifications and quasi-alternative methods to allow for more effective optimisation efforts are suggested.[80]

Genetic algorithms (GA) are numerical optimisation algorithms inspired by genetics and natural selection. Bayley[54] differentiates it from other MDO methods in that it is built to facilitate the improvement of an initial population of solutions to a design problem rather than pure optimisation. An initial population of guesses of the solution is first randomly generated, after which the quality and level of desirability of the solutions with respect to the objective are assessed, referred to by Coley[81] as determining the fitness of the solution. The best of these solutions are then selected from the population to find solutions that can more closely approach the objective. Finally, an operator is applied to provide mutation to the solution selection process to avoid a loss in diversity in the population of solutions. The main advantages of GA are the simplicity of the method and the fact that no exact initial solutions or gradient information are required, while extensive solution areas are explored to come to accurate solutions to the objective problem. Disadvantages are the reduced certainty with respect to whether the final solution is a global optimum and the lack of robustness of the method. This thus implies the need for additional verification efforts.[54][56][81] An efficient implementation for genetic algorithms exists in the programming language Python through the use of e.g., the DEAP package or the *scipy.optimize.differential_evolution* package.[82]

4.2. General setup

Following a review of the various methods found in literature concerning launch vehicle design and optimisation efforts, the methodology chosen for this study will be outlined in this section. The framework of this study and its main constituents will thus be introduced here. Important considerations in this setup are the research objective, the extent of the available resources, and the scope of the research.

4.2.1. Proposed methodology overview

Prior to proposing a methodology, it is important to first present the different considerations and specifics that apply to this study. It was found that due to the time-dependent nature of the study and a lack of experience, a theoretical assessment should be preferred over an experimental setup or a combination of a theoretical and an experimental setup. Next to that, the research goal stated a specific need for low-toxicity, storable bi-propellants employing hydrogen peroxide as an oxidiser. This implies that a fuel selection process would be needed to find a suitable fuel in accordance with the research objectives defined in Chapter 3. Another important consideration is the availability of software for modelling purposes. Here, only publicly available or free software was considered. This includes software for which licenses were provided by TU Delft.

Following the methodologies used in similar works, as presented in Section 4.1, as well as the aforementioned considerations, a general methodology scheme could be proposed for this study. Central to this scheme are two main research segments: a baseline fuel assessment and a vehicle performance model. The former module is a top-level assessment of fuel characteristics as derived from literature and support sources, while the latter is a more in-depth numerical assessment for which existing software and coding tools are employed. Note that these segments were set up to correspond to the two main research topics introduced in Chapter 3 as to allow for the research questions to be optimally addressed. As the first segment is a top-level assessment of important fuel characteristics, it could be used as an effective tool to eliminate unsuitable fuels, as per the criteria derived from the research objective, in the early stage of the study. As a result, by performing the research segments consecutively, a smaller number of fuels need to be considered for the more resource-intensive vehicle performance model. Prior to the setup of these segments, a set of requirements will be formulated to ensure compliance of these modules with respect to the research goal, the research questions, and the research questions introduced in Chapter 3. This can be considered the third research segment. The fuel selection and launch vehicle design process will consist of a series of consecutive steps, which will be designed in a manner that allows for iterative design techniques to be applied. A visualisation of the proposed methodology can be found in Figure 4.1.

In this methodology chart, the different research segments are visualised together with the modules they are comprised of. The *general launch vehicle definition*, which will be treated in this chapter, is mainly a preparatory research segment. This can be deduced from the activities making up this segment, as they are mainly aimed at providing a solid basis and constraints to the study. Next to that, the requirements set up and the data gathered in this segment also allowed for verification and validation activities in a later stage of the study. The next research segment to be considered is the *baseline fuel assessment*, which is closely linked with the research topic regarding the integration and compatibility potential of different candidate fuels in combination with HTP. As mentioned earlier, this segment was a means of eliminating unsuitable fuels from the study with the goal of making a selection of the most promising fuels to be considered in the vehicle performance assessment. As such, a set of requirements and assumptions will first be set up, which will allow for the definition of relevant criteria for the fuels to be evaluated. Next, a top-level preliminary feasibility assessment will allow for a first selection to be made and for a better picture to be formed regarding the expected potential of the selected candidate fuels. An *availability assessment* will then follow to both make an estimate of the availability of the ground resources for each of the fuels and to determine the availability of fuel data for further assessment. Finally, the remaining fuels will be subjected to a more detailed evaluation, referred to as the *propellant integration and compatibility evaluation or PICE*. Here, an AHP tool will be employed to make a more detailed assessment of the fuel characteristics that are not directly related to performance. The final research segment will be based on a numerical model similar to those introduced in Section 4.1. Again, a set of requirements and assumptions will first be set up to provide a structured base for this numerical model. Finally, the *vehicle performance models* will be connected together to allow for multidisciplinary optimisation to be performed.
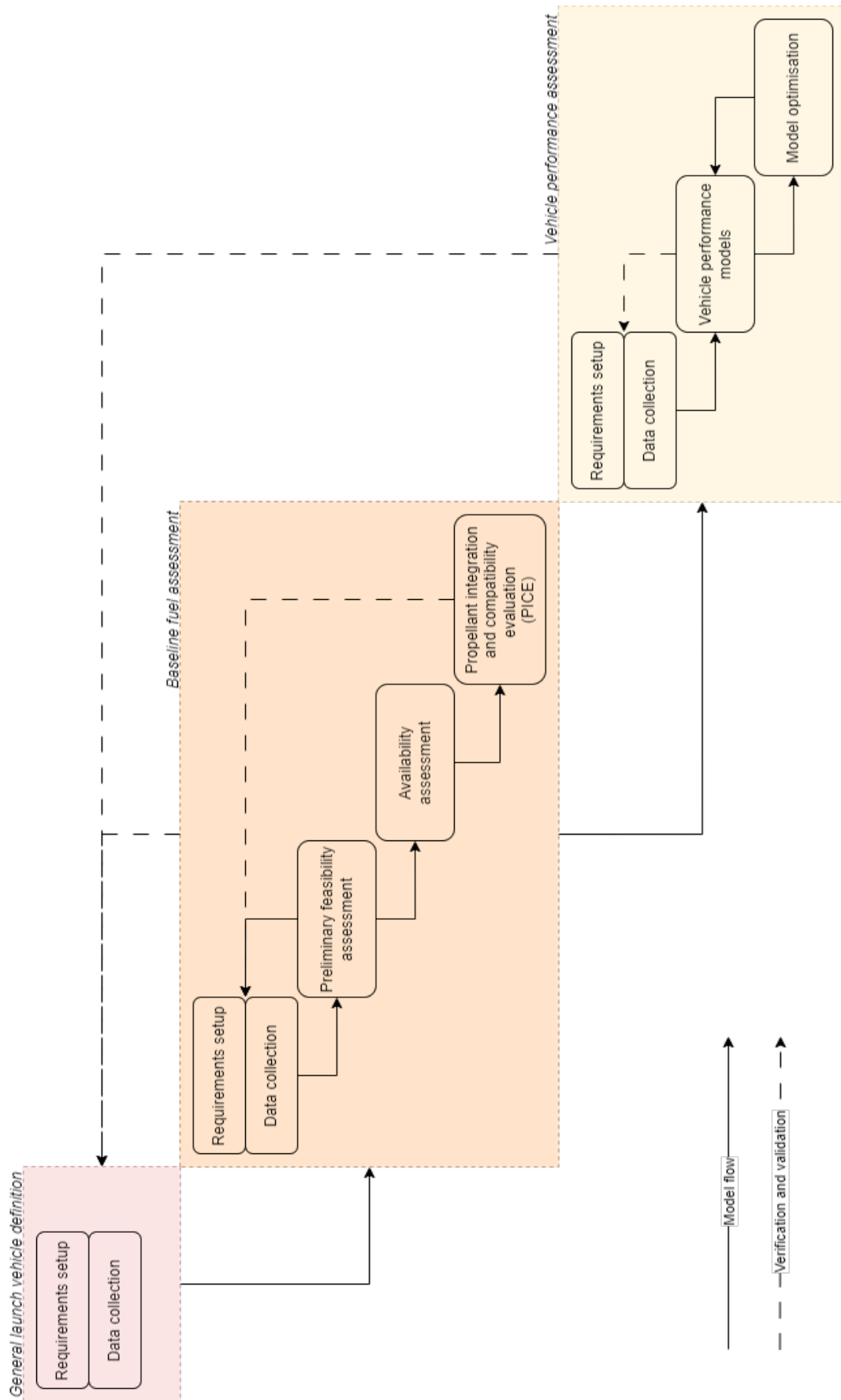
Figure 4.1: N2 chart of the proposed methodology for this study

Requirements setup

From the research questions and objectives stated in Chapter 3, it can be deduced that the extent of the research conducted in this study is limited by specific boundaries. Translating the research definition into requirements will allow for an efficient design process in accordance with these imposed boundaries. In several of the works introduced in Section 4.1, including the studies by Elferink[5] and Bayley[54], a set of requirements were formulated as to provide a foundation and constraints with respect to the design efforts. Next to that, a reference launch vehicle was selected for most of these launch vehicle design and optimisation studies to narrow the scope of the research and the design and to allow for effective validation efforts to be performed. Subsequently, a reference launch vehicle will also be selected for this study based on several factors, including the availability of information and relevance with respect to the stated research goal and reference studies. This reference launch vehicle, described in Section 4.4, will also allow for a set of general design requirements to be set up in a more defined manner.

Data collection

It was mentioned that an integral part of this study will be the model validation efforts for which a reference launch vehicle will be used. It is thus imperative that the necessary data is gathered to provide the means to perform this validation effort. Therefore, the data collection step is considered of high importance to the overall design process. It is worth noting that throughout each of the research segments, several data collection activities will be performed. This includes collecting data regarding the non-performance-related characteristics of the proposed fuels for the preliminary feasibility assessment and the PICE module. Next to that, other data will be needed to set up numerical models depending on relations derived from historical data. Finally, data will need to be collected for the reference propellants to which the proposed propellant combinations will be compared. As with the requirements setup, the data collection step can be considered to be subject to iteration. As the relevant design modules are developed, the available data sets will need to be reevaluated and augmented with additional data to increase the overall effectiveness of the design modules.

Design tools

Throughout this study, the main programming environment that will be employed for setting up and connecting analytical and quantitative models will be Python[83]. The reasons for this are familiarity with the programming as well as the wide area of applications it offers with respect to academic design and optimisation efforts via scientific and numerical methods. The open-source functionality has allowed for the overall functionality and range of applications to be rapidly expanded. A prime example of this is the package developed for the implementation of genetic algorithms in problem-solving.

Due to the multi-disciplinary nature of the considered design problem, MDO methods would be most suited for optimisation efforts. An optimiser method that is considered for use is the GA method, due to the implementation of this method in similar studies regarding conceptual launch vehicle design, as well as the ease of use of this method and its applicability to Python through the *scipy.optimize.differential_evolution* package. This method is often considered for launch vehicle design efforts because it does not require the input of an initial solution. This comes at the cost of more expensive computation efforts and reduced accuracy. A reference launch vehicle will be used, which would imply the possibility of defining an initial solution. It is, however, hard to predict whether to what extent the proposed propellant combinations integrated in the reference launch vehicle will approach this solution. In fact, based on the study by Elferink[5], considerable deviations from this initial solution could be expected. Therefore, GA optimisation methods could be considered relevant for this study.

4.2.2. Baseline fuel assessment

The baseline assessment could be considered critical to making an initial selection of fuels to be evaluated in the more resource-intensive vehicle performance assessment. Due to the wide range of potential fuels, a combination of the methods employed in the GRASP project[47][50][49] and the methods described by Guerrieri et al.[46] will be adapted and modified for this study.

Preliminary feasibility assessment

A preliminary feasibility assessment will be performed, in which all propellants will be subjected to a surface-level assessment regarding the minimum requirements for certain propellant characteristics. These are related to combustion stability with HTP, state at expected storage conditions, overall (maximum) toxicity levels, and minimum performance levels. These criteria were selected due to their suitability for surface-level assessment and their relevance with respect to this trade-off study. Based on this assessment, a first selection of promising fuels will be made, and unsuitable fuel candidates will be discarded. Furthermore, it will also give an initial idea of the greater potential and range of the considered fuels.

Availability assessment

Following the outcome of the preliminary feasibility assessment, the remaining fuels will be subjected to another "elimination" assessment before being considered for the more detailed PICE module. In this availability assessment, the availability of all remaining fuels and their ground resources will be checked, as this is considered to be a killer criterion due to its implications with respect to cost and transportation needs. It is also important to determine that the selected fuels are not at risk of becoming scarce in the future so as to not waste resources on research and development efforts for a fuel that is only interesting for short-term use. Furthermore, the existence and development stage of production techniques and facilities are directly related to the overall fuel cost. This criterion is investigated separately from the preliminary feasibility assessment due to the time-consuming nature of the availability assessment, which thus makes it more efficient to consider only a small selection of fuels. Another aspect to be considered in the availability assessment is that of data availability. As the PICE module will require a larger amount of verified data to allow for a reliable and conclusive result to be obtained, it is crucial to assess the availability of data for each of the selected fuels prior to committing resources to further study. As such, this aspect will also be considered as part of the availability assessment.

PICE

The fuels selected following the preliminary feasibility assessment and the availability assessment will be subjected to a trade-off, for which an AHP tool will be employed. This will allow for a more narrow selection of promising fuels to be made for the research intent. The goal of this trade-off is to further explore the potential of the fuels with respect to integration in the launch vehicle propulsion system regarding characteristics other than pure performance. Next to that, compatibility with hydrogen peroxide and relevant propulsion system components will be assessed. More specific criteria were defined with respect to the baseline fuel assessment, after which experts in this field were contacted to provide relative weightings to these criteria. The criteria considered were safety and toxicity, ease of use, development level, and coolant qualities. Although some of these criteria are similar to those considered for the preliminary feasibility assessment, a more detailed assessment and a deeper take on the relevant fuel characteristics were considered as part of PICE. Overall, this trade-off should allow for an effective and quantifiable comparison to be made between the proposed fuels with respect to characteristics, other than performance properties, that are deemed most relevant for launch vehicle propellants.

4.2.3. Vehicle performance assessment

It is expected that only a small selection of fuels will result from the baseline fuel assessment. These fuels will be subjected to a final assessment, in which numerical models will be employed to estimate the effects of propellant choice on the propulsive and mass performance potential of a reference launch vehicle. Here, two main study cases were formulated. For the first case, the gross lift-off mass (GLOM) will be assessed by estimating the payload-carrying capacity of launch vehicle designs for a fixed payload mass and a set of trajectory objectives based on the final core stage separation velocity, altitude, and flight path angle. In a second case, the expected payload capability will be estimated for a fixed gross lift-off mass and a similar set of trajectory objectives. For each of these cases, an optimised result will be targeted using a multi-disciplinary approach. Both cases will not only give an insight into the performance potential of different fuel/HTP combinations, but they will also allow for future studies to estimate the relative cost potential of these combinations as these are, to a large extent, related to absolute and relative mass fractions. The most promising

fuels will then be selected for further review. In order to accurately assess the performance of these propellant combinations, an important factor in the selection of fitting models will be the level of verification and accuracy of the models based on previous studies. Next to this, continuous verification and validation activities will be performed to ensure a low level of errors and good knowledge of the overall accuracy level of the models.

From the extended literature presented in Section 4.1, a common sequence of models for launch vehicle design and optimisation studies could be identified. Therefore, a similar approach will be followed here. A general overview of the connection between these modules and their relevance has been given in Figure 4.2. The modules described here are a propulsion model (which is essential to answer RQ-PERF-01), a mass and sizing model, and an aerodynamics and trajectory model. A short summary of the methods selected for each of these models will be presented below. Note that the global optimisation model, which has not been included in Figure 4.2, adds additional connections between the models and affects the relative importance of the inputs identified for the vehicle performance models.

Propulsion model
For the propulsion model, the CEA tool by NASA will be used. It should be noted that access needs to be requested for this. It was found, based on literature and comparable design efforts, that both CEA and RPA Lite, which was also considered, provide sufficient accuracy and combustion modelling information to be applied to conceptual launch vehicle design and for RQ-PERF-01 to be answered. The choice was made to select CEA as a basis for the propulsion model primarily because of the wide use and heritage in other studies such as the works by Dresia et al.[56], van Kesteren[57], van Beers[58], Ernst[59], Iyer[60], and Vandamme[61]. Next to that, use could be made of RocketCEA, a Python extension derived from the original CEA tool, which allowed for a database to be easily set up. The outputs generated through RocketCEA were combined with ideal rocket theory and correction factors derived from historical data to assemble the propulsion module.

Mass and sizing model
For mass and sizing, an approach will be considered that is centred around historical data, mass fractions and established mass models, similar to the model suggested by Dresia et al.[56]. This approach is expected to have limited accuracy but can be deemed sufficient for conceptual design efforts and provides a good baseline while being less computationally expensive. The models constructed by Akin[84] and Zandbergen[85] will both be considered. As to provide higher accuracy for this approach, additional verification and validation activities will be performed to verify the relevance of the used data sets and to validate the results by means of comparison with outcomes using reference cases. The mass and sizing model will allow for a relative payload mass fraction to be derived and, thus, for the effects of the propellant modifications on the payload mass to be assessed. This will thus allow for an answer to RQ-PERF-02 to be provided.

Aerodynamics and trajectory model
For the trajectory model, the Tudat[68] software Python extension will be used. The advantage of using this package as a basis is the fact that fundamental verification activities have already been performed and that several previous studies have already proven its effectiveness and accuracy for launch vehicle trajectory applications. This thus allows for more time to be invested in more detailed verification and validation activities as well as model modifications. In addition to this, RASAero II[86] was used to add aerodynamic properties to the model.
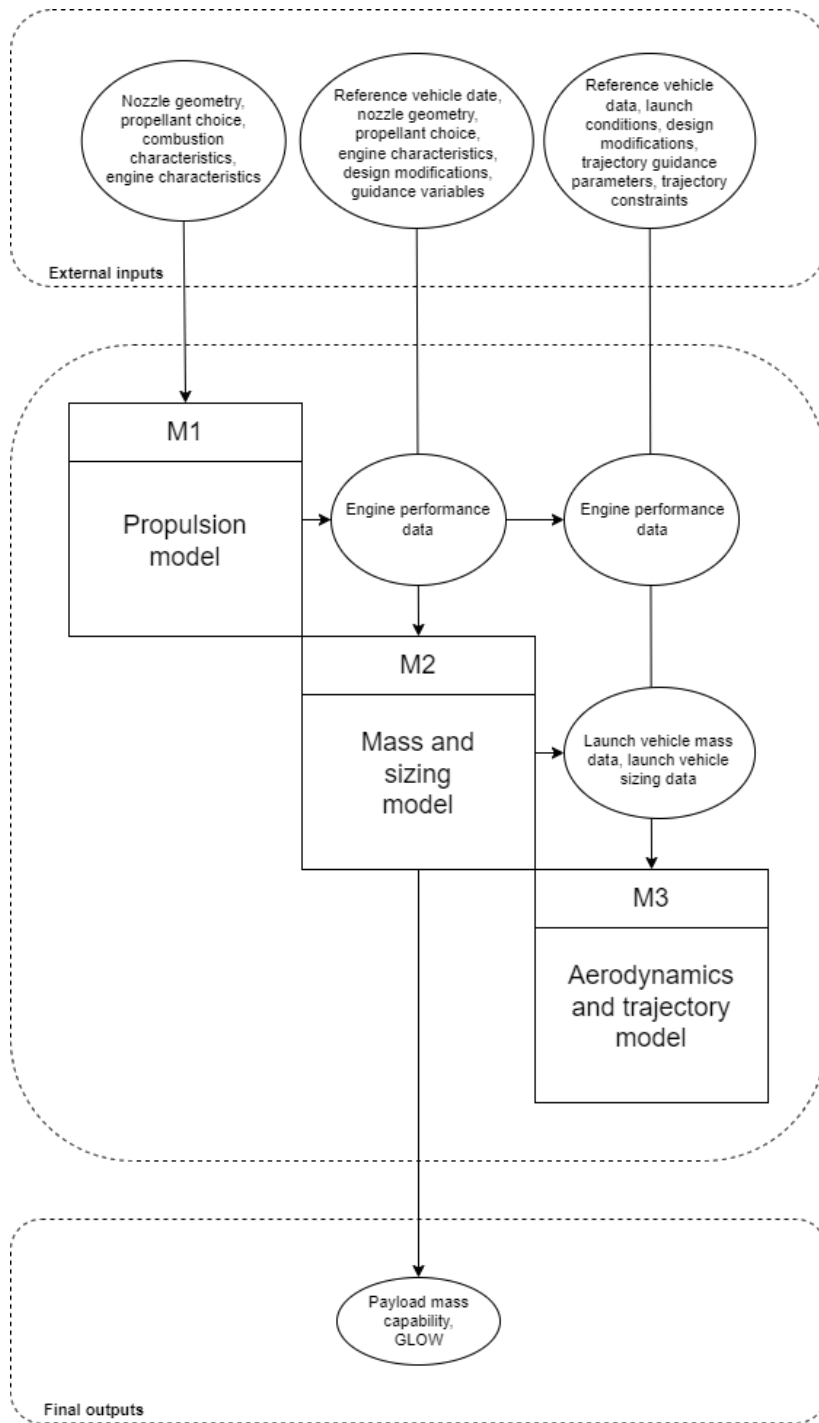
Figure 4.2: N2 chart representing the structure for the vehicle performance models

4.3. Hypotheses

A set of hypotheses with respect to the expected research results and answers to the research questions, formulated in Section 3.2, will be presented here. Similar design efforts available in literature will be used as a foundation to ensure that these predictions are logical and anchored. This will allow for an effective comparison at the end of this study and will thus allow for the results obtained from this study, as well as the expected results deduced from available literature, to be critically assessed for validity and relevance in the framework of this research topic.

RQ-PERF-01

From literature, an estimate can be made of the performance, in terms of vacuum specific impulse, of various non-toxic storable fuels in combination with HTP as an oxidiser. This will allow for an answer to be predicted to RQ-PERF-01. In research conducted by Okninski et al.[87], it is concluded that the specific impulse performance of hydrocarbon fuels, such as methane, isooctane and Jet-A, in combination with HTP is in the range of $310s$ to $320s$ for an optimum oxidiser-to-fuel ratio. A similar performance is described by Florczuk et al.[88], where the performances of various HTP-based propellant combinations are mapped and it is concluded that the highest attainable specific impulses for these combinations range from $315s$ to $335s$. It was also remarked that the best-performing fuel was DMAZ. This same finding was stated by Elferink[5], who estimated the vacuum specific impulse of the DMAZ-HTP propellant combination at $341s$. In similar sources, the performance discussion is often concluded by denoting the relatively high specific impulse density of HTP-based propellant combinations as compared to conventional propellants such as hydrolox. Similar observations are expected to be made in this study. The performance of conventional cryogenic propellants can best be derived from existing applications. ArianeGroup reports a specific impulse of $432s$ for its Vulcain 2.1 engine, which is driven by the cryogenic hydrolox propellant.[89] Aerojet Rocketdyne reports a similar specific impulse performance of $410s$ for its RS-68 rocket engine, which used the same propellant.[90] Based on these observations, it could be predicted that the performance in terms of specific impulse of the storable non-toxic fuels in combination with HTP will be significantly less compared to conventional cryogenic propellants such as hydrolox, in the order of 25-30%. Next to this, it could be derived from literature that the measured specific impulse performances of these proposed combinations will be found to be in a close range for the highest performing combinations.

RQ-PERF-02

From launch vehicle design and optimisation studies by Bayley[54] and Dresia et al.[56], intuitive predictions with respect to the effects of the specific impulse of propellants on the optimised launch vehicle masses can be confirmed. As supported by ideal rocket theory, the specific impulse is an influential factor to the gross lift-off mass of the vehicle as it symbolises the effectiveness of the propellant mass use. From launch vehicle design and optimisation studies by Bayley[54] and Dresia et al.[56], relevant conclusions can be derived from the final launch vehicle design comparison tables with respect to the importance of the specific impulse characteristic. It was found that the integration of propellants displaying a lower specific impulse as compared to conventional cryogenic propellants, would lead to a significant increase in the overall GLOM of the vehicle. It should, however, be noted that when considering ascent trajectories through an atmosphere, aerodynamics and drag considerations are also very influential to the overall vehicle mass. As such, Elferink[5] argued the specific impulse density to be a more relevant performance indicator, as it combines both the specific impulse of propellant and its density, and thereby thus the effective propellant and vehicle volume.

Elferink[5] followed a different approach to scale the effectiveness of the proposed upper-stage propellant alterations. For a fixed total upper stage mass, it was shown that a propellant with a reduced specific impulse performance would result in a decrease of the available payload mass of approximately 70% and, thus, a reduction of the overall payload performance of the launch vehicle. Here, it was argued that intensive development efforts specific to the proposed propellant could reduce this number to a more favourable result. Next to that, due to the addition of atmospheric

and, thus, drag considerations for the design of lower stages of a launch vehicle, the density of the proposed propellants would also become a more influential factor next to the specific impulse. This is illustrated by calculations made by Elferink, which estimate a vehicle size reduction of up to 33%. As such, a better payload performance is expected for high-density storable propellants if compared to a conventional propellant such as hydrolox, which has a rather low density.[5]

Following the conclusions drawn from these launch vehicle design and optimisation efforts, a similar prediction can be made with respect to the optimised gross lift-off mass and payload capability for the design case proposed in this study to formulate a prediction for RQ-PERF-02. It is expected that the integration of a storable non-toxic propellant employing HTP as an oxidiser will lead to an increase of the GLOM of the launch vehicle, or otherwise a decrease of its payload-carrying capabilities for a design case in which the GLOM is kept constant, given that no major structural modifications are proposed other than those that are directly derived from a transition from cryogenic propellants to storable propellants. Due to the higher density of hydrogen peroxide based bi-propellants as compared to hydrolox, however, the size of the launch vehicle is expected to be reduced to an extent that the drag gains might allow for a payload capability more similar i.e., within 50%, to that of launch vehicles employing cryogenic propellants.

4.4. Reference launch vehicle: Ariane 6

A constant in the launch vehicle design and optimisation studies described in Section 4.1 is the use of a reference launch vehicle with the intent of setting up a frame of reference for the study and providing an effective means of comparison for the final optimisation results. Here, the selection of specific reference vehicles is mostly a result of relevant parameters, including the status of the vehicle with respect to the current market, the relevance of the vehicle with respect to the research goal, the origin country of the vehicle and that of the institution to which the study is linked, and the availability of information on the vehicle. Bayley[54], for example, selected Titan II SLV due to the reliability and extent of the available information. Dresia[56] opted for Falcon 9 due to the relevance of this vehicle in the current market. Finally, Dijkstra Hoefsloot[67] selected Electron due to the relevance of this vehicle to his feasibility study on the recovery of small-lift launch vehicles.

A primary motivation for this study was to expand on the work performed by Elferink[5], thereby making use of the foundation that he built with respect to analysing the potential of hydrogen peroxide in launch vehicle applications. In his work, Ariane 6 was selected as a reference launch vehicle to provide an effective comparison with an upper-stage design based on hydrogen peroxide. It would thus be evident to opt for the same reference vehicle as a basis for this study. Furthermore, Ariane 6 is also highly relevant as it was designed to replace Ariane 5 as the main European launch vehicle for medium to heavy-weight payload missions. In relation to this, it is worth noting that Delft University, the institution to which this study is linked, is based in Europe. Finally, the information available on Ariane 6 is more extensive compared to other relevant launch vehicles, including Falcon 9, Angara, and the Long March series.

4.4.1. General Ariane 6 description

Ariane 6 is the newest launch vehicle in a series of launch vehicles by the French company ArianeGroup. By decision of ESA, the Ariane 6 development programme was initiated in 2014 to safeguard European independence and competitiveness with respect to space launching capabilities in a growing industry. This was required due to the influx of new spacefaring nations, such as China and India, and private ventures into the industry, which has led to a worldwide trend of decreasing launch costs. To allow Europe to keep up with this trend, the main goal set for the Ariane 6 programme was thus to develop a launch vehicle that could bring payload into orbit at half the cost per kilogram as compared to the Ariane 5 launch vehicle. Here, the use of tried and tested technologies, in combination with new innovative technologies, lower production costs, and a bigger role for the industry, have been considered key elements towards achieving this goal. Ariane 6 is expected to have its maiden flight in 2024.[91]

The design of Ariane 6 features a multitude of elements and characteristics from its predecessor Ariane 5 to decrease overall development costs and guarantee a high level of reliability for the new launch vehicle. Similar to Ariane 5, the Ariane 6 launch vehicle will consist of two stages[1], for which both the upper stage and the lower stage are characterised by liquid cryogenic propellant modules. To provide additional thrust at lift-off, it will be equipped with either two or four P120C solid rocket boosters (SRB). Two different versions of the launch vehicle thus exist, referred to as A62 (equipped with 2 SRB) and A64 (equipped with 4 SRB), to facilitate a larger variety of payloads and missions. These configurations are depicted in Figure 4.3.[12][92] As a result of this flexibility in the design and in accordance with the central design ideology for the new launch vehicle, it will be possible to employ Ariane 6 for a wide range of applications. This includes single payload launch, dual payload launch, multi-payload launch, constellations and low earth orbit (LEO) microsat constellation missions for A62, and additionally, the launch of large scientific spacecraft and heavier payloads with A64 to virtually any type of orbit that is currently in demand. For A62, a payload capability of up to $10.3 metric\ tons$ was stated to LEO, and a payload capability of up to 4.5-5$metric\ tons$ to geostationary transfer orbit (GTO), effectively making this configuration a medium-weight launch vehicle by NASA classification. For A64, a payload capability of up to $21.6 metric\ tons$ was stated to LEO, and a payload capability of up to $11.5 metric\ tons$ to GTO, effectively making this configuration a heavy-weight launch vehicle by NASA classification.[92][93]
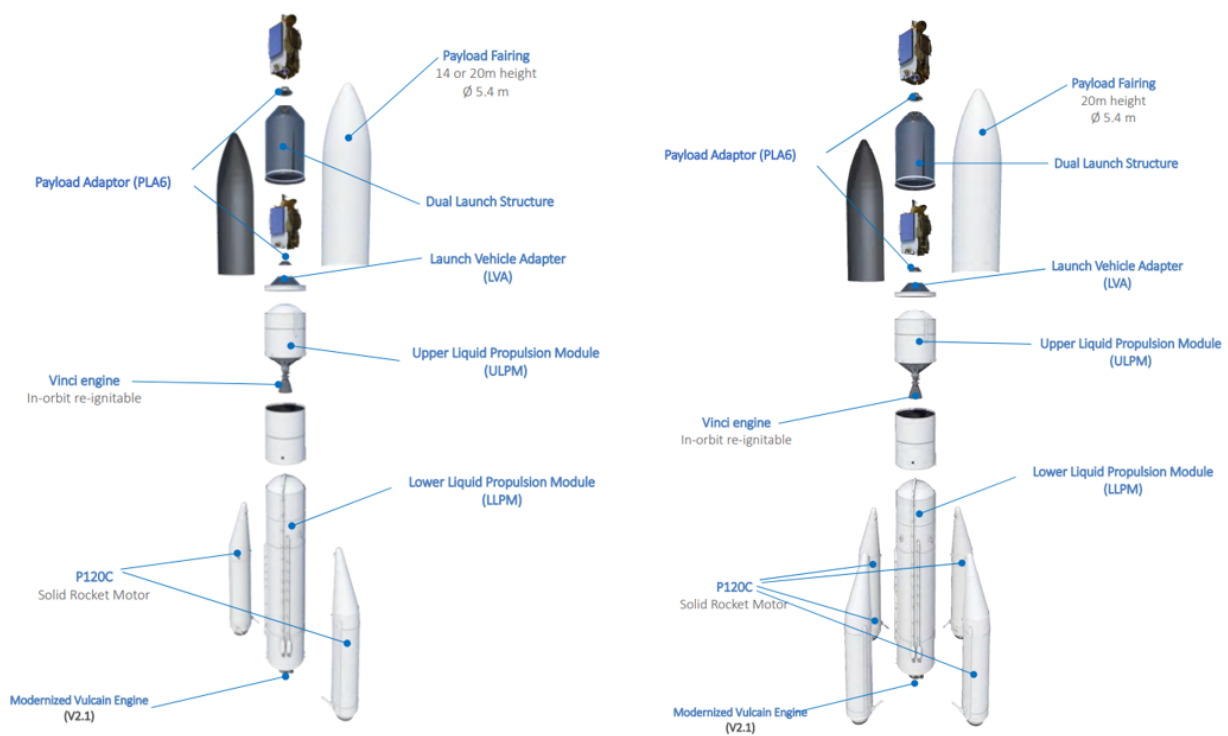
Figure 4.3: The Ariane 6 can be launched with two configuration: A62 (left) and A64 (right)

The Ariane 6 launch vehicle will have an estimated height of 57 to $63m$, depending on the fairing selection. The A62 configuration will be characterised by a maximum gross mass at lift-off of $530 metric\ tons$, while the A64 configuration will be characterised by a maximum gross mass at lift-off of $860 metric\ tons$. It was estimated that an overall thrust force of $8MN$ (A62) or $15MN$ (A64) would be needed in order for the necessary accelerations to be provided for the vehicles in their loaded state for maximum payload conditions.[91] Due to the aforementioned reasons of heritage and standardisation, overall development costs for the combined Ariane 6 and Vega C programmes were limited to an estimated $3.8 Beuros$.[94] It is worth noting that ArianeGroup seems to have succeeded in its efforts to reduce launch cost for the new launch vehicles to half of the cost-per-launch

---

[1]Three stages if the booster stage is considered a separate stage.

for the Ariane 5, which were estimated to be in the range of 175$Meuros$. The expected launch costs for the new Ariane 6 launch vehicle are expected to be in the range of 75$Meuros$ and 115$Meuros$ for the A62 configuration and the A64 configuration, respectively.[95][96]

4.4.2. Ariane 6 core stage

A standard GTO mission profile for Ariane 6 in A62 configuration is provided on the website of supplier ArianeGroup. At lift-off, it sees both of the solid rocket boosters (SRB) ignited together with the core stage engine. After approximately 130-135s of burn time, the solid rocket boosters jettisoned at which point they will have contributed to the vehicle reaching a height of close to 59km and a speed of 1.5km/s. After this point, the vehicle will be propelled solely by the lower-stage liquid propellant module (LLPM) under the impulse of the core stage engine, a Vulcain 2.1 engine. This should result in further acceleration of the vehicle to over 4.6km/s, after which the Vulcain 2.1 engine shutdown occurs, and the LLPM is separated from the vehicle at an altitude of 210km. Thereafter, the upper-stage Liquid propulsion module (ULPM) is used to conduct mission-specific manoeuvres and deliver the payload to its final orbit. For the A64, a similar standard mission profile is presented, albeit with different velocity and height values for crucial mission stages. The boosters are jettisoned after a height of approximately 72km is reached, a point at which the launch vehicle should have been accelerated to a velocity of 2.4km/s. The LLPM is later separated at a height of 209km and a velocity of 5.6km/s.[97]

Table 4.1: Vulcain 2.1 engine by ArianeGroup characteristics[89] (*Estimated values from other sources than manufacturer[98], NF = Not Found)

Characteristic	Value	Unit
Engine name	Vulcain 2.1	/
Manufacturer	ArianeGroup	/
Fuel/Oxidiser	LH/LOX	/
Classification	Cryogenic	/
Vehicle(s)	Ariane 6	/
Status	Tested	/
Overall mixture ratio	6.03	/
Thrust (vacuum)	1371	kN
Thrust (sea level)	960*	kN
Specific impulse (vacuum)	432	s
Specific impulse (sea level)	318*	s
Area ratio	61.5*	/
Nozzle exit diameter	2.1	m
Length	3.6	m
Engine cycle	GG	/
Single burn life	480-650*	s
Throttleability	NF	%
Mass	1650	kg
Chamber pressure	11.9	Mpa

©ArianeGroup Holding
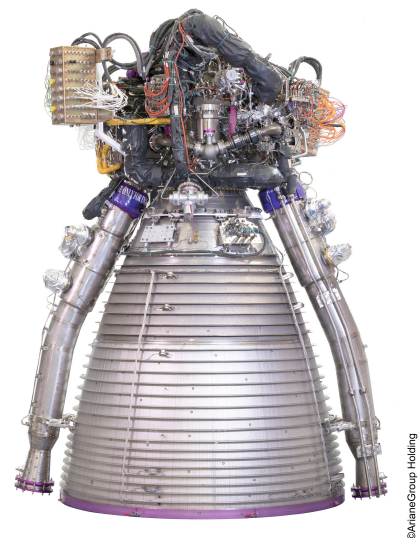
Figure 4.4: Vulcain 2.1 engine by ArianeGroup[89]

The main elements which the LLPM is comprised of are the liquid propellant tanks, the Vulcain 2.1 engine, and the parts providing structural and functional support to those systems. As with the Ariane 5 LLPM, cryogenic propellants were opted for in the design of the Ariane 6 LLPM. As liquid oxygen and liquid hydrogen need to be kept in very cold conditions, -182°C and –253°C respectively, the storage tanks were designed with additional reinforcements and thermal insulation materials. For nominal missions, an estimated 150$metric\ tons$ of liquid propellant will be stored in the LLPM.[91] The Vulcain engine series are rocket engines developed by Ariane Group specifically to be flown on the core stage of Ariane 5 and future Ariane adaptations such as Ariane 6. Vulcain 2.1 is an iteration of a previous engine in the series, Vulcain 2, with the aim of increased reliability and efficiency, and reduced costs. Already tested, this engine, depicted in Table 4.4, will first be flown on the Ariane 6 launch vehicle.[89][98] Featuring a simple gas generator (GG) combustion cycle and the LH/LOX cryogenic propellant combination, the Vulcain 2.1 displays an estimated nominal vacuum thrust of 1371kN in combination with a vacuum specific impulse of 432s. An interesting feature is the addition of 3D-printed components to the new Vulcain 2.1 design.[89] Characteristics specific to the Vulcain 2.1 engine are listed in Table 4.1. Note that not all data listed here was derived directly from the manufacturer and that all data should be approached with some sense of doubt.

While the maiden flight for the Ariane 6 launch vehicle is only planned for late 2024[99], the P120C solid rocket boosters installed to provide the necessary thrust to allow for lift-off have already been flight-tested in a mission scenario. These boosters were directly derived from the boosters used on the first stage of the smaller Vega-C launch vehicle, which was first launched in 2022.[100] P120C SRB are each filled with 142$metric\ tons$ of solid propellant to provide an estimated average thrust of 4.5MN each for the first 130-135s of flight. An important design change with respect to the boosters used on the Ariane 5 launch vehicle is the use of composite casings to achieve further weight and cost reduction for the overall vehicle.[91][101]

Table 4.2: P120C solid rocket booster characteristics[101]

Characteristic	Value	Unit
Average thrust	4.5	MN
Burn time	132.8	s
Propellant mass	143.6	tons
Dry mass	11	tons
Specific impulse	278.5	s
Diameter	3.4	m
Height	11.7	m

4.4.3. Reference configuration selection

In selecting the Ariane 6 launch vehicle, two different launch vehicle configurations were suggested for consideration. Although both A62 and A64 are effectively variations of the same launch vehicle, there are some key differences to be recognised between the two configurations with the amount of solid rocket boosters being mounted onto the vehicle being the most defining of these differences. As the core stage and the upper stage of the launch vehicle remain virtually unchanged, the Ariane 6 can relatively easily be modified into different configurations. As a result of the thrust increment provided by the additional boosters, a difference in mission capabilities and mission profiles can be observed between the two configurations. These key distinctions were tabulated in Table 4.3. An evident benefit of this dual configuration design is thus the wide range of missions which can be supported with this vehicle. Given that this flexibility of launch configurations is a crucial part of the Ariane 6 design, it would be evident to consider both of these configurations as reference cases for this design and optimisation study. This would, however, make the study more computationally demanding while also making it less focused, as the optimisation objectives would need to be set up as a consensus between the two configurations to ensure a uniform design for the core stage, as is the case for Ariane 6. Finally, it is also worth noting the difference in the area of application between

the two configurations. Whereas the A64 configuration is by definition a heavy-lift launch vehicle, the A62 configuration is a medium-lift launch vehicle, which is more in line with the research goal that was presented for this study. In the study by Elferink[5], it was found that the lower specific impulse performance of HTP configuration was more impactful for the lighter A62 launch vehicle configuration. Furthermore, it was found that the effect of structural weight changes was also more noticeable in the A62 configuration. This trend will thus be transferred into this study. The main focus will be on the A62 reference case, while the application of the design solution in the A64 configuration will be briefly touched upon in the concluding remarks.

Table 4.3: Ariane 6 characteristics for the A62 configuration and the A64 configuration[12][102]

Characteristic	A62 value	A64 value	Unit
Modes	Single launch	Dual launch	/
	Dual launch	Multi-launch	/
	Multi-launch	Large scientific SC	/
	Constellation	Heavy mission	/
	LEO microsat constellation	Constellation	/
		LEO microsat constellation	/
Max LEO performance	10.3	21.6	tons
Max GTO performance	4.5-5	11.5	tons
Number of SRB	2	4	/
Lift-off thrust	8	15	MN
Launch cost	75	115	M euros
Max gross lift-off mass	530	860	tons
P120c separation altitude	58754.4	71563.3	m
P120c separation speed	1515.1	2392.8	m/s
LLPM separation altitude	209869	209245.6	m
LLPM separation speed	4625.5	5588.5	m/s

4.4.4. General design requirements

To allow for the design activities performed in this study to culminate in a launch vehicle design that aligns with the intended specifics deduced from the research objectives, it was crucial to derive a set of requirements. These requirements were mostly guiding the setup of the vehicle performance model and the optimisation objective functions, thereby introducing the necessary constraints. Therefore, the main matter of importance in setting up these requirements was to make them relevant to the research and the research goal such that effective verification of the requirements at the end of the design stage could lead to an unambiguous conclusion concerning the relevance of the launch vehicle design with respect to the predetermined research objectives and research questions.

The resulting requirements can be found in Table 4.4. Next to the research goal and the research objectives, the reference vehicle introduced in Section 4.4 was also used as a main source for setting up these requirements. Most of the requirements were thus derived from more general specifications with respect to the design and the intended mission characteristics of the launch vehicle and do not need further discussion. To determine the upper stage separation altitude and velocity accuracy, specified in REQ-VEH-06 and REQ-VEH-07, two sources were taken into account. The $1.3km$ accuracy is based on the typical standard deviation on the perigee altitude for standard GTO mission as specified in the Ariane 6 user manual.[12] For the velocity accuracy, the flight data of two Ariane 5 missions, VA226 and VA229, was compared and a margin was applied to get a rough idea of a typical accuracy at this stage of the trajectory. REQ-VEH-11 to REQ-VEH-13 were based on the reference vehicle design and were included for simplicity and to include some

base constraints into the vehicle sizing model.

Table 4.4: Guiding requirements for the new *HTP Launch Vehicle*

Identifier	Requirement	Derived from
REQ-VEH-01	The *HTP Launch Vehicle* shall consist of two stages and a booster stage.	Reference vehicle
REQ-VEH-02	The *HTP Launch Vehicle* shall be an expendable launch vehicle.	Research goal
REQ-VEH-03	The propellant used on the core stage of the *HTP Launch Vehicle* shall be storable.	Research goal
REQ-VEH-04	The propellant used on the core stage of the *HTP Launch Vehicle* shall be of low toxicity.	Research goal
REQ-VEH-05	The propellant used on the core stage of the *HTP Launch Vehicle* shall employ hydrogen peroxide as an oxidiser.	Research goal
REQ-VEH-06	The *HTP Launch Vehicle* shall be able to deliver the upper stage to an altitude of 209.9±1.3km.	Reference vehicle
REQ-VEH-07	The *HTP Launch Vehicle* shall be able to deliver the upper stage to the intended altitude with a relative velocity of 4.625±0.3km/s.	Reference vehicle
REQ-VEH-08	The *HTP Launch Vehicle* shall be launched from Kourou	Reference vehicle
REQ-VEH-09	The initial flight phase shall be powered by a core stage of the *HTP Launch Vehicle* consisting of a liquid bi-propellant propulsion system supported by a booster stage consisting of either two P120C solid rocket boosters.	Reference vehicle, research goal
REQ-VEH-10	The upper stage of the *HTP Launch Vehicle* shall be the same as the upper stage employed by the Ariane 6 launch vehicle.	Design study choice
REQ-VEH-11	The *HTP Launch Vehicle* main stage shall have separate oxidiser and fuel tanks.	Reference vehicle, safety concerns
REQ-VEH-12	The *HTP Launch Vehicle* main stage shall have single oxidiser and fuel tanks.	Reliability, reference vehicle
REQ-VEH-13	The propellant tanks employed in the *HTP Launch Vehicle* main stage shall be of a cylindrical design with elliptical caps.	Reference vehicle, [103]

5.Baseline fuel assessment setup

In Chapter 4, two main research segments were introduced, the first of which was referred to as the baseline fuel assessment. The idea behind this research segment was twofold: to narrow down the large selection of fuels before running the computationally intensive and time-demanding vehicle performance assessment and to assess the fuels on relevant characteristics not directly related to performance. The latter would not only allow for a more complete mapping of the fuel options, but it would also eliminate the bias towards strictly high-performance fuels that would be introduced in any one assessment including performance-related characteristics. This research segment was also set up as a basis for answering RQ-CI-01 and RQ-CI-02.

In this chapter, the structure of this research segment will first be outlined, after which the framework of respective modules will be explored in more depth. The results of this setup will be reported in Chapter 6

5.1. Baseline fuel assessment structure

An N2 chart depicting the flow for the proposed methodology for this study was provided in Figure 4.1. From this, the four consecutive phases making up the *baseline fuel assessment* research segment can be derived. These phases were mostly based on the fuel selection methods employed by Guerrieri et al.[46] and by the GRASP[47][48] project. The following phases make up the baseline fuel assessment research segment:

1. Requirements setup and data collection
2. Preliminary feasibility assessment
3. Availability assessment
4. Propellant integration and compatibility evaluation (PICE)

The first phase of the baseline fuel assessment could be considered a preparatory phase, as a more precise and constrained definition of the assessment was provided. Next to this, a large database of candidate fuels was assembled based on literature and some of the key requirements introduced for the assessment. It is worth noting that the requirements setup and data collection processes were revisited several times throughout this research segment to allow for a dynamic assessment with continuous verification efforts and, if needed, reiterations. As the pool of potential candidate fuels was expected to be rather large, there was a need for a top-level assessment of some key fuel characteristics to narrow down the selection significantly without the need for extensive study or data review. As such, a preliminary feasibility assessment was set up where the candidate fuels were assessed based on four key factors derived from the requirements setup and similar studies on the topic of propellant selection. A rather important factor that is often considered in the selection of propellants for launch vehicle propulsion is the availability of its constituents, as is illustrated by Briggs et al.[9]. The availability of fuels is directly related to the overall fuel cost but also to the long-term potential of the fuels and, therefore, the program as a whole. The availability assessment was considered a separate phase of this research segment as availability data collection is too time-consuming to apply on the initial selection of fuel candidates on one hand, and because of the need for the second component of the availability assessment for the setup of the PICE assessment on the other hand. This second component was focused on the availability of data needed for further assessment for the reason of eliminating fuel candidates for which an insufficient amount of data was available. Two goals were identified for the baseline fuel assessment: narrowing down the selection of candidate fuels and providing a more complete and comparative mapping of the fuel candidates. While the former was largely achieved with the preliminary feasibility assessment and the availability assessment, the latter was introduced in the final phase of this research segment. In this phase, the PICE assessment and the AHP tool were used to provide a more detailed quantitative comparison of the fuel candidates with respect to several non-performance related characteristics.

As per the introduction of this section, an important activity in this research segment was the setup of relevant requirements to guide and constrain the baseline fuel assessment. The results of this requirements setup were tabulated in Table 5.1. A few key requirements (REQ-BFA-01 and REQ-BFA-02) were derived directly from the research goal. Others were added based on similar studies from literature to add additional value to the assessment results and to add additional constraining factors to the preliminary feasibility assessment. The stability requirement (REQ-BFA-04) was proposed by Guerrieri at al.[46] to introduce safety considerations into the fuel assessment. In the GRASP project, one of the main factors of the preliminary propellant selection process was a performance assessment through the characteristics of specific impulse and specific impulse density. This was done to ensure a minimum level of performance amongst the selected propellant candidates. A similar performance-based requirement (REQ-BFA-03) was introduced here to ensure a minimum performance level justified by the performance potential research objective.

Table 5.1: Requirements for the *baseline fuel assessment* research segment

ID	Statement	Derived from
REQ-BFA-01	The selected fuel shall be liquid in a temperature range of 0 to 40 degrees Celcius.	RQ-VEH-02 (and research goal)
REQ-BFA-02	The selected fuel shall be characterised in literature by a negligible to low toxicity level.	RQ-VEH-02 (and research goal)
REQ-BFA-03	The selected fuel shall have a reported specific impulse performance with HTP of at least 300 [s].	Performance objective considerations
REQ-BFA-04	The selected fuel shall not be characterised by low combustion stability (in combination with HTP).	Safety and reliability considerations

Throughout this research segment, several data collection efforts were made. First, an initial selection of potential fuels was performed based on information found in literature. Important sources here were studies of green propellants and subsequent applications, existing HTP-based propulsion applications, and similar design and optimisation studies for which HTP was considered. HTP-based experimental research papers, which mostly investigated performance, stability, and reactivity, were also considered. These same sources were also used for data needed for the preliminary feasibility assessment, as the criteria for this assessment were mostly covered there as well. Further data collection was performed to obtain more detailed data for the availability assessment and the PICE assessment. The aforementioned sources were mostly complemented with data published by fuel component manufacturers and chemical agencies. The data sources were mostly limited to established institutions to ensure a certain level of validity and reliability within the datasets used for the different assessments. Next to that, data verification was introduced by collecting data values from different sources to find the final data values through weighted averaging methods such as the three-point estimate.

5.2. Preliminary feasibility assessment setup

The preliminary feasibility assessment was introduced as an essential part of the baseline fuel assessment research segment. Guerrieri et al.[46] employed a similar assessment in a study on the *"Selection and characterisation of green propellants for micro-resistojets"* to select those fluids that were deemed feasible to work on for the proposed application. In this study, a similar objective was posed for this assessment as it was used to reduce the number of potential fuel candidates by selecting those deemed most feasible and interesting for further study concerning the stated research goal and intended application. For this purpose, four elimination criteria were chosen based on the key requirements presented in Table 5.1 to allow for a surface-level assessment of all considered fuel candidates within the initial selection pool. The following criteria were chosen:

- Combustion stability (with HTP)
- Storage state
- Overall toxicity threshold

- Minimum performance

Fuels that did not display the required characteristics for these four criteria were subsequently not considered for the ensuing phases of the study. As to ensure a decisive yet time-efficient assessment process, the fuel candidates were scored for the elimination criteria on a surface level, meaning that mostly qualitative or easily defined quantitative evaluations were used. The definition of the four elimination criteria and the preferred assessment method will be briefly discussed.

Combustion stability

The first criterion to be considered is the stability criterion. Two primary definitions could be given to stability when considering it for the selection of rocket fuel. Chemical stability covers the stability of the composition of fuels, in which stable fuels are characterised by a low decomposition rate. This is especially relevant for applications where long storage life or reactive storage environments are prime considerations.[16][104] For launch vehicle applications, a more relevant stability definition is that of combustion stability, which is related to the ability of an engine to sustain a steady and controlled propellant burn. Here, the level of reactivity of the constituents is an important factor, and the use of compatible propellant components is an important consideration.[105]

Combustion stability is one of the aspects of safety that is considered in the aforementioned study by Guerrieri et al. He argues that it is an influential factor in the overall reliability of the system and the risk posed to the transported payload.[46] As such, it was deemed evident to require a minimum level of combustion stability for the system. Hence, REQ-BFA-04 was added to the list of requirements for this research segment. From the formulation of this requirement, it can be deduced that it is rather difficult to provide a useful quantifiable assessment score to each of the fuel candidates on the basis of combustion stability with HTP. As such, qualitative scoring was preferred, in which fuels that were in literature, i.e., studies on propellant characteristics and experimental research, characterised by low stability, were marked as such and were thus removed from the pool of fuel candidates.

Storage state

In the context of this study, the storage state of a propellant component is defined as the state of the substance in storage at the expected storage conditions. One of the advantages of opting for hydrogen peroxide as an oxidiser for launch vehicle propulsion is that it is a storable propellant, meaning that it is in a liquid state at ambient conditions i.e., at sea-level pressure and temperature. This generally allows for less complex and less structurally heavy systems as compared to cryogenic oxidisers such as liquid oxygen.[106] To optimally benefit from this advantage, the aim for this study was constrained to the use of storable bi-propellants, meaning that the selected fuel should also be liquid at ambient conditions. This constraint is reflected in the research goal statement.

To ensure an efficient storage process, some margin was added to the centre point of $293.15K$ (20°C). Here, the transition points of hydrogen peroxide were used as a reference. As the freezing point of hydrogen peroxide is $272.72K$, see Table 2.4, it was decided to add a margin of $20K$ to the centre point. This margin should also compensate for a shift in the fuel freezing and boiling points due to the pressure in the fuel tanks. The relevant temperature range is reflected in the formulation of REQ-BFA-01, from which this criterion was effectively derived. As a result, fuel candidates that are not in a liquid state between $273.15K$ and $313.15K$ (0°C and 40°C) at atmospheric pressure conditions were disregarded for further study.

Overall toxicity threshold

In the context of rocket propellants, toxicity refers to the harmful effects that a substance could have on the environment and human health. Here, both the effects of exposure and waste during the handling and processing of the propellants could be considered, as well as the effects of the combustion products after the burning of the propellants. Next to its favourable storage stage, hydrogen peroxide is also considered a good advantageous choice for a propellant oxidiser in terms of toxicity. This is especially important given the recent industry trends towards green propellants characterised by a low toxicity level and the (impending) bans on highly toxic substances issued by

governmental bodies.[3][4] Following a similar reasoning as for the storable nature of HTP, the aim of this study introduced a constraint regarding the use of only low-toxicity bi-propellants. This is reflected in the research goal statement and subsequently in REQ-PFA-02.

It is possible to quantify the toxicity of a substance through several ways e.g., LD_{50} values. It is, however, a time-demanding process to work out an effective and complete toxicity evaluation method and to gather the necessary data on a large selection of fuels. As such, it was opted to limit the toxicity evaluations for the preliminary feasibility assessment to be strictly qualitative. As such, evaluations found in literature, i.e., studies on green propellant characteristics and experimental research, were used as a basis to assess the pool of fuel candidates and eliminate fuels characterised by a high level of toxicity. To compensate for this rather inaccurate method of assessment, fuels characterised by a medium toxicity level were not rejected, as opposed to the low toxicity level stated in requirement REQ-PFA-02.

Minimum performance

An important measure in assessing the performance of a rocket propellant, and by extent the engine in which it is employed, is its specific impulse (I_{sp}). This essentially describes the efficiency of the propellant as it relates to the thrust force produced per unit of mass flow. A propellant with a high specific impulse would thus display a high level of thrust relative to the propellant mass needed to generate this thrust.[16]

In the introduction to this research segment, it was indicated that the focus would be on the assessment of the fuel candidates concerning characteristics that are not directly related to performance. Yet, the main goal of the preliminary feasibility assessment was to allow for the initial selection of fuel candidates to be narrowed down in an efficient manner so as to exclude unsuitable fuels from subsequent assessments that are deemed more time-demanding or computationally expensive. As performance will be a major factor in the *vehicle performance assessment* research segment, it was decided to include a minimum performance criterion as part of the preliminary feasibility assessment to eliminate fuels that are known to display insufficient performance in combination with hydrogen peroxide. To this extent, REQ-PFA-03 was added to Table 5.1, specifying a lower limit for the expected specific impulse performance. To determine this lower limit, the study by Scharlemann[50], covering some preliminary results of the GRASP project, was used as a reference. He considered the specific impulse performance of NTO/MMH (sea-level I_{sp} of 323s) to be a valid limit given that this is currently the most used storable bi-propellant in propulsion applications. From the study by Elferink[5], another reference value could be derived, as all of the fuels he considered for his study displayed a vacuum specific impulse with HTP of at least 326s. Given that this concerns vacuum specific impulse, it is a much lower boundary value than the one proposed by Scharlemann. In fact, it could be argued that most of the fuels considered by Elferink would not be suitable according to those standards. The reason for this could partially be a matter of the data and the engine settings used for estimating the performances of the bi-propellant combinations. Furthermore, the nature of the data, either derived theoretically or experimentally, could also have a significant effect on the performance values, as Scharlemann himself indicated. Another reason for the observed performance difference is that while NTO/MMH displays a rather high specific impulse performance, its density is often lower than that of HTP-based propellants, which thus implies the need for more heavy voluminous structures and, as a result, increased vehicle weight and drag. Similar to the other criteria considered for the preliminary feasibility assessment, data obtained from literature was used to assess the fuel candidates' specific impulse performance. As such, the assumed deviations due to using different datasets were considered when defining a boundary value for REQ-PFA-03.

Development status

In performing the preliminary feasibility assessment, an unofficial fifth criterion was taken into account with the development status. The development status of a rocket propellant refers to the level to which it has been investigated and optimised for integration in rocket engines or other intended applications. A high development level indicates a lot of advancements and research into a propellant and therefore could indicate improved performance and reliability in subsequent applications.[107] Selecting fuel candidates that are characterised by a high development level would be

favourable as it would reduce the need for further development and would ensure the level of certainty with which the performance and related characteristics of the propellant can be stated. Fuels characterised by a low development level are the opposite in that more resources will be needed to research, develop, and advance the required technology. Next to that, a low development level poses a risk in that it could imply currently unidentified drawbacks of the propellant that could lead to problems in later stages of the design.[50][107] The development status was marked as an unofficial criterion because of the lack of consistent evaluation over the initial pool of fuel candidates. Instead, the development status was taken into account when explicit mention was made of it, as was the case for the propellants considered in the study by Scharlemann[50]. Insufficient data or literature was available for some fuels to allow for a surface-level assessment. In these cases, it was also assumed that the development level of these fuels, generally or in combination with HTP, was simply too low to allow for further assessment.

5.3. PICE criteria selection

Whereas the main objective of the *preliminary feasibility assessment* and the *availability assessment* was to narrow down the selection of candidate fuels based on surface-level assessment methods, the *propellant integration and compatibility evaluation* was created to add more value to the *baseline fuel assessment* research segment by providing a means of comparison for the most promising fuels. This was done by providing a more detailed assessment of the non-performance-related characteristics of the leftover fuels. In setting up the structure for this evaluation, an extended literature study was first performed to select a set of relevant and informative criteria based on similar studies. A more in-depth assessment method was then worked out for each of these criteria to provide quantitative scoring for each of the fuels. Finally, the criteria were weighted using an AHP process.

The choice of assessment criteria was an essential factor to provide an effective basis of comparison for the non-performance-related characteristics of the proposed fuel candidates. Here, it was deemed that a small number of diverse criteria would allow for the most informative and conclusive comparison. To this purpose, a small literature study was performed in which the assessment criteria proposed through similar studies were investigated and subsequently evaluated with respect to their suitability for this study. For this brief literature review, the studies by Bombelli et al.[108], Carlotti and Maggi[109], Elferink[5], Guerrieri et al.[46], Kurilov et al.[110], and Scharlemann[50] were considered as these studies focused on the assessment of green propellants for rocket propulsion purposes. Furthermore, the works by Briggs and Milthorpe[9] and McClendon et al.[111] were included due to their focus on propellant selection for launch vehicle applications. An overview of the assessment criteria found in the aforementioned studies is given in Table 5.2, including the final decision with respect to the selection of the criteria for the PICE assessment. Below, each of the criteria will briefly be discussed, and a reasoning for the criteria selection will be provided.

Availability

Both Elferink and Briggs and Milthorpe suggest availability as a criterion for launch vehicle propellant selection. Hereby, both studies indicate the relation between availability and cost. Furthermore, Briggs and Milthorpe argue the importance of this criterion with respect to transport and storage needs. In this study, the availability of the proposed fuel candidates was considered in an availability assessment before the PICE assessment. Due to this reason, and because important factors such as transport and storage are considered through other criteria, it was deemed unnecessary to include the availability criterion in the PICE assessment.

Cost

Cost is a major design driver for space applications. As such, it was put forward as an important criterion in the propellant selection process in several studies. Briggs and Milthorpe argue that the total propellant cost is not only made up of the onboard propellant cost but also the propellant consumed during testing. Despite stressing the importance of cost as a criterion, it could be deduced from Elferink that the board propellant cost makes up only a small fraction, less than 1%, of the total operations cost of a launch vehicle stage. Additionally, it is worth pointing out that the

total life cycle cost of a propellant is, to an extent, also related to the ease of handling, storage, toxicity, and material compatibility of the propellant, as stated by Carlotti and Maggi. As such, the cost criterion is indirectly assessed through several other criteria considered in PICE. Finally, assessing the full effects of the propellant choice on the overall launch vehicle cost would require a more in-depth analysis, including complex optimisation models to account for the full effects of the propellant choice on structure and development costs. This was deemed outside of the scope of this study. It was also illustrated by Drenthe[112] that most launch vehicle costs can be expressed as a function of the component mass. The mass performance optimisation performed in the second research segment of this study should thus also be a good indication of the overall launch vehicle costs. Therefore, it was decided not to include cost as a criterion in the PICE assessment.

Development
In giving an overview of the GRASP project, Scharlemann mentions the assessment of proposed propellants for the development status criterion. Here, it is discussed that for propellants for which a higher level of development exists, the opportunity for short-term applicability in relevant applications exists. Furthermore, a high development status implies less need for cost-intensive development efforts and a better knowledge of the drawbacks of the propellants. Because of this, and because a high development level would be highly favourable for the application in this study, it was decided to include the development level as a criterion for the PICE assessment.

Toxicity
Due to the relevance of the subject to the proposed applications, several of the aforementioned studies propose either environmental toxicity or toxicity related to human health and safety (or both) as an essential assessment criterion. Scharlemann mentions the multi-faceted nature of a thorough toxicity assessment, and this is echoed through the other studies as the toxicity criterion is approached from different angles. Yet, generally, it is argued that toxicity is important to mitigate systems risks, decrease costs, and ensure the long-term viability of future designs. As such, both main classifications of toxicity were included in this study.

Handling and safety, storage, and material compatibility
The criteria of handling and safety, material compatibility, and storage come back in most of the studies considered in this literature review. Here, the importance of these criteria is stressed with respect to the implications on ease of handling and integration into launch vehicle systems. Both Elferink and Carlotti and Maggi include several subcriteria under the umbrella of handling and storage, hereby mostly considering the relevance of this criterion to physical hazards and to operations risks. Similarly, material compatibility was considered an essential criterion as this both concerns the applicability of propellants in existing systems and the ease with which the propellants can be handled and stored. It could thus be concluded that these criteria relate to propellant integration and compatibility potential, which were both indicated to be major components of this study. As such, these criteria were all included in the PICE assessment under ease of use.

Ignition properties
Good ignition properties, and in particular hypergolicity, are important characteristics for bi-propellants. The hypergolicity of a bi-propellant relates to the potential of a propellant to spontaneously combust upon mixing without the need for heavy and complex ignition systems or performance-reducing additives. Thus, Kurilov et al. mention the importance of hypergolicity to allow for simple and quick engine start-up, thereby avoiding the accumulation of highly energetic chemicals in the combustion chamber and the subsequent increased risk of engine destruction or cut-off. Bombelli adds to this the need for rapid thrust built-up and easy reignition to ensure high operational reliability and increased efficiency. Due to the relative novelty of HTP-based high-performance storable bi-propellants, little experimental data exists on the hypergolicity potential of the proposed fuel candidates in combination with HTP. As such, it could not be considered as a criterion for the PICE assessment. Therefore, it was recommended in Chapter 10 to conduct additional experimental research regarding the hypergolicity potential of the proposed bi-propellant combinations.

Performance
A criterion that can not be ignored in the selection of propellant for launch vehicle applications, and by extension most space applications, is performance. Here, the pure propulsive potential of the propellants, either expressed through the specific impulse or the specific impulse density, or the mass performance potential, which is essentially obtained by optimising the vehicle for a specific mass objective, could be considered. Indeed, both of these performance potential evaluations were also indicated to be the main objectives of this study. As per the methodology proposed in Chapter 4, however, this will be considered in the second research segment, while the first research segment is centered around characteristics that are not directly related to performance. As such, performance was not included as an assessment criterion in the PICE assessment.

Political concerns
Briggs and Milthrope argue the importance of political considerations in selecting a launch vehicle propellant. Here, it is important to note that their study is specifically built around the case of an Australian launch vehicle. In this study, the selected reference case is of European origin, and the availability assessment was also conducted from this perspective. However, this is a large institution to consider for assessing political considerations. To keep the scope of this study as wide and diverse as possible and to reduce the complexity of this research segment, it was decided not to include political concerns in the PICE assessment.

Coolant qualities
The coolant qualities of the fuel candidates were considered as a criterion in the PICE assessment, even though it was not proposed as a criterion in similar studies on propellant selection. It was argued that this criterion was particularly relevant for this study as a result of the objectives indicated in the research goal, which implied the use of hydrogen peroxide and the integration of the propellants in high-thrust applications. A more detailed reasoning for including this criterion will be given at a later point in this section as the assessment methods for the criterion are discussed.

Table 5.2: Potential assessment criteria considered for the PICE assessment based on similar studies

Criterion	Reference studies	PICE?
Availability	[5][9]	No
Coolant qualities	/	Coolant qualities
Cost	[5][9][108][109][110][111]	No
Development	[50]	Yes, Development level
Environmental toxicity	[9][109]	Yes, Toxicity
Handling and safety	[5][9][46][108][109]	Yes, Ease of Use
Ignition properties	[108][110][111]	No
Material compatibility	[5][108][109]	Yes, Ease of Use
Performance (mass)	[5][108][109]	No
Performance (propulsive)	[5][9][46][50][109][110]	No
Political concerns	[9]	No
Storage	[5][50][108][109][110]	Yes, Ease of Use
Temperature sensitivity	[110][111]	Yes, Ease of Use & Coolant qualities
Toxicity and safety	[9][46][50][108][109][110]	Yes, Toxicity

An overview of the criteria and subcriteria included in the PICE assessment was visualised in Figure 5.1. An additional level of subcriteria could be added based on the assessment methods that will be introduced in Section 5.4, but this was left out to ensure a clear overview.
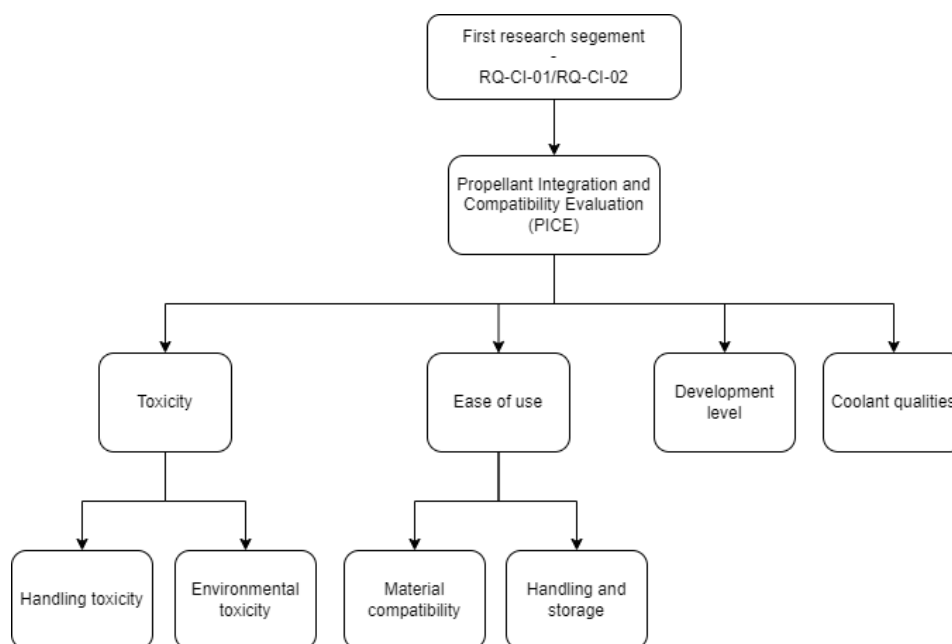
Figure 5.1: Criteria and subcriteria considered for the PICE assessment

5.4. PICE criteria assessment methods

A quantitative assessment method was worked out for each of the proposed criteria to provide an effective and well-founded comparative basis for the PICE assessment. The reasoning and setup of these assessment methods will discussed in this subsection, and component weights will be provided where needed.

5.4.1. Safety and toxicity

Earlier, toxicity was defined as concerning the harmful effects that a substance could have on the environment and human health. From this definition, two main areas of influence could thus be identified: environmental impact and human health. As such, it was considered important to study both of these areas separately to provide a more complete assessment of the extent of the toxicity of each fuel considered for the PICE assessment.

In setting up an effective assessment method for the toxicity of chemical substances, the work by Carlotti and Maggi[109] was used as a main reference. Here, a combined scoring through several health and toxicity classifications was proposed.

As a prelude to this detailed assessment method, the REACH Regulation (EC N. 1907/2006) was taken into consideration. Through REACH, several regulations have been introduced to effectively monitor the processing and use of chemicals amongst European manufacturers and importers. An important document included in REACH Annex XIV is the list of Substances of Very High Concern (SVHC). The highly toxic chemicals on this list have been restricted from use after a given date, with the exception of cases granted special authority for specific use. For this study, all fuels were cross-referenced with the SVHC list to filter out any banned chemicals before considering them for more detailed assessment efforts.[3][14]

An important classification to be considered was the Globally Harmonized System (GHS) of classification and labelling of hazardous chemicals, which was created by the United Nations (UN) after the 1992 Rio Earth summit in an attempt to install a more globally recognisable and simple toxicity classification system. The system is made up of three major hazard groups: Physical hazards, health hazards, and environmental hazards. These groups were further subdivided into classes concerned with different kinds of toxicity and hazards related to the overarching groups. These were tabulated in Table 5.3.[43] The GHS classification was integrated into the PICE assessment by considering both the physical hazard group and the health hazard group for the handling toxicity

criterion, while the environmental hazard group was used to assess fuels with respect to the environmental toxicity criterion. In the latter, a differentiation was made between acute and chronic toxicity effects to provide further insight into the effective toxicity of each of the fuel candidates.

Table 5.3: GHS major hazard groups and subclasses[113]

Environmental hazards
Hazardous to the aquatic environment (acute and chronic)
Hazardous to the ozone layer

Health hazards
Acute toxicity
Skin corrosion/irritation
Serious eye damage/eye irritation
Respiratory or skin sensitisation
Germ cell mutagenicity
Carcinogenicity
Reproductive toxicity
Specific target organ toxicity - single exposure
Specific target organ toxicity - repeated exposure
Aspiration hazard

Physical hazards
Explosives
Flammable gases
Aerosols
Oxidising gases
Gases under pressure
Flammable liquids
Flammable solids
Self-reactive substances and mixtures
Pyrophoric liquids
Pyrophoric solids
Self-heating substances and mixtures
Substances and mixtures which, in contact with water, emit flammable gases
Oxidising liquids
Oxidising solids
Organic peroxides
Corrosive to metals

Based on GHS, chemicals were assigned relevant hazard codes reflecting both the applicable hazards and the extent of the hazard through the category under which the hazard statement is classified. Here, chemicals with category 1 statements are considered highly toxic or dangerous concerning the relevant hazard class, while low toxicity levels characterise chemicals with category 4 statements. Based on this defined range, a scoring system was set up for the fuels based on their H-statements found in the ECHA database. This scoring system is represented in Table 5.4. It was deemed that following the reasoning in other GHS classification and toxicity studies, such as the study by Carlotti and Maggi[109], a chemical with a category 1 evaluation should be deemed far more toxic than a chemical with a category 2 evaluation. This was assumed because the range of category 1 evaluations goes from the highest toxicity limits for category 2 evaluations to an undefined/unconstraint toxicity level. A similar idea was followed in determining the scoring of

category 3/4 evaluations. Due to insufficient expert knowledge, all subclasses within the physical and health hazard groups were given equal weight.

The NFPA 704 rating, referred to as the "Standard System for the Identification of the Hazards of Materials for Emergency Response", was first proposed in 1954 by the Committee on Fire Hazards of Materials and has since been revised on multiple occasions. With this classification, the US National Fire Protection Association (NFPA) aimed to bring more uniformity to the hazard classification system and to allow for quick assessment of potential dangers that specific chemicals may pose. In the present day, NFPA rating labels are often found on the labels of boxes holding industrial materials or chemicals.[114][115] A symbol that is characteristic of the NFPA 704 hazard identification is the hazard diamond, shown in Figure 5.2. Here, the degree of danger of a substance is indicated with respect to the categories of health hazards (blue), flammability hazards (red), and instability hazards (yellow). Additionally, special hazards e.g., "oxidiser", are indicated in the withe segment if applicable. The degree of danger is quantified by a number from 0 (indicating a minimal hazard) to four (indicating a severe hazard).[115]
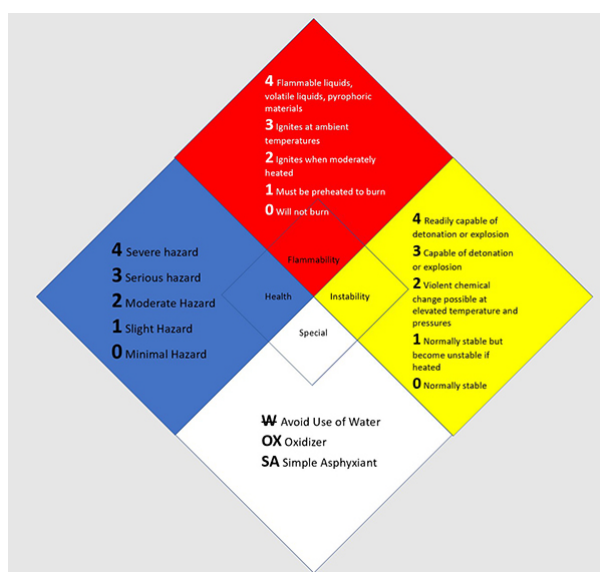
Figure 5.2: NFPA rating diamond[115]

While the NFPA rating covers topics similar to the GHS classification, it was chosen to incorporate both to allow for the identification of inconsistencies between the two systems and to provide a more complete mapping of the candidate fuels in this study in accordance with several major global hazard classification systems. As a result, the scoring system used for the NFPA ratings, which can be found in Table 5.4, was similar to that of the GHS classification, albeit inversed given the inverse relation between both classification systems. Note that only the NFPA health rating was taken into account for the handling toxicity assessment, as the flammability and instability classes were deemed more relevant for the storage and handling assessment.

A final indicator for the hazards and toxicity levels of chemicals that was included in the handling toxicity assessment is the Vapour Hazard Index (VHI). William Popendorf, who introduced this metric in 1984, describes the use of VHI as a method "to predict the relative hazards of vapour concentrations of proposed substitute solvents".[116] It is effectively a representative quantification of the danger of exposure to the headspace of a formerly enclosed substance, comparable to the danger of exposure to a substance in a closed container when taking off the lid. This is because VHI is essentially the logarithmic representation of the ratio of two important measures for indicating the toxicity or dangerous nature of a chemical, these being the Saturated Vapour Pressure (SVP) and the Workplace Exposure Limit (WEL). The former is an indicator of the volatility of a substance as it is a measure of the tendency of a liquid to transition to the vapour phase in a specific environment, while the latter is essentially a toxicity index as it represents the threshold dose or concentration that a

person can be exposed to within a specific timeframe (8 hours in a definition by Pitt[117]) without experiencing adverse effects. The VHI is thus obtained through the following relation:[117][116]

$$VHI = log\left(\frac{SVP}{WEL}\right) \tag{5.1}$$

where both SVP and WEL are expressed in ppm, and VHI is effectively unitless.

One of the reasons for considering toxicity as a criterion was the (European) ban issued for very toxic chemicals such as hydrazine as a result of their inclusion on the list of SVHC.[3][14] Therefore, it was chosen to use hydrazine, which is considered a conventional propellant in space applications, as a reference. A similar approach was taken by Carlotti et al.[109], where it was also proposed to use the VHI value for hydrazine ($VPI(MMH) = 3.7$) as a reference value for a medium toxicity evaluation, with any chemicals characterised by a higher VHI value being classified as highly toxic. As it was decided that this led to a little conclusive result, an additional border value was implemented, this being an order of magnitude lower than the VHI value of hydrazine. The resulting scoring system can be found in Table 5.4. The same scoring values were assumed as for the NFPA and GHS scoring systems.

Table 5.4: Scoring system for the components of the safety and toxicity criterion

	Very toxic ->Non-toxic			
Scores	15	5	1	0
GHS	Cat.1	Cat.2	Cat.3,4	NA / 0 score
NFPA	Cat.4	Cat.3	Cat.2	Cat.1
VPI	VPI >VPI(MMH)	VPI(MMH) >VPI >3.7	3.7 >VPI >2.7	2.7 >VPI

A final task that was imperative in setting up the handling toxicity assessment was determining a relative weighting for each component making up the handling toxicity criterion. First, a comparison was made between the GHS and NFPA classifications concerning relevance to this study. It was argued that GHS is a globally accepted classification with harmonised (i.e., consistent) input from a wide range of entities and companies, while NFPA is a national US-based system that is bound by a systematic assessment procedure and specific regulations. As a result, there are quite a few discrepancies in the evaluation of health hazards for chemicals by different companies. Therefore, the NFPA rating was used as a validation factor, meaning that it was mostly used to check for discrepancies or major differences with the GHS-based assessment, in which case the values found for both classifications were verified again. Next to that, the NFPA rating was still given a small weight to provide balance in case of persisting discrepancies. Finally, both Poppendorf[116] and Carlotti et al.[109] stressed the importance of VHI for toxicity assessments. However, it was argued that both components making up the VHI value of a chemical, SVP and WEL, are incorporated in the hazard statements assigned by the GHS classification. As such, VHI was given a relative weight equal to half of the combined weights of the two GHS-based components i.e., the physical hazard group and the health hazard group. The relative weightings for the handling toxicity criterion can be found tabulated in Table 5.5.

For the environmental toxicity assessment, only influences on the aquatic environment were considered, as no hazard statements were found relating the candidate fuels to harmful effects on the ozone layer. A simple 50/50 weighting was argued for the two components, acute aquatic toxicity and chronic aquatic toxicity, making up the criterion. The relative weightings for the environmental toxicity criterion can be found tabulated in Table 5.6.

Table 5.5: Relative weighting for the components of the handling toxicity criterion

	GHS physical hazards	**GHS health hazards**	**NFPA**	**VPI**
Component weights	0.3	0.3	0.15	0.25

Table 5.6: Relative weighting for the components of the environmental toxicity criterion

	GHS acute aquatic toxicity	GHS chronic aquatic toxicity
Component weights	0.5	0.5

5.4.2. Ease of use

Another assessment criterion introduced by several of the aforementioned studies was that of "handling and storage". Here, several subcriteria were considered to assess propellants based on their physical and chemical properties with respect to flammability, compatibility, stability, and storage requirements.[109] In this study, a similar approach was adopted, although the collection of subcriteria was here referred to as *ease of use* as this was deemed a more comprehensive term to describe the combined meaning of both material compatibility considerations and handling and storage considerations. Elferink[5] also considered both material compatibility and handling and storage in his propellant selection assessment, albeit as separate criteria. It should be noted that his approach placed any toxicity considerations within the criterion of handling and storage. For this study, it was deemed that there was too much difference in the meaning and implications of a toxicity assessment, as introduced earlier in this section, and an assessment focused on other aspects of handling and storage, such as flammability and instability of the propellants. Therefore, it was opted for these criteria to be split here rather than to follow an approach similar to Elferink. Based on this introduction of similar works, the criterion of *ease of use* in this study could be defined as the evaluation of all aspects of the candidate fuels, except for toxicity characteristics, that relate to their suitability for seamless handling and integration into the overall propulsion system design.

Ease of use - Material compatibility

Most rocket propellants are known to be very reactive, which is a reason for their effectiveness but also brings with it other problems. In a study on accidents related to the accident spilling of hyperbolic propellants, Nufer[118] illustrated the fiery or explosive potential of such reactive propellants upon coming in contact with materials they are not compatible with. Other, less violent chemical reactions due to a lack of compatibility with container materials could also introduce impurities in the propellant or could result in corrosion and degradation of the container material, with the result of reduced performance in both cases.[109] Therefore, the need was identified to assess the compatibility of the candidate fuels with commonly used aerospace materials in essential components of the propulsion system with which the fuels are expected to come into contact.

In his study, Elferink[5] provided a qualitative assessment for the materials compatibility of the considered fuels on the basis of general compatibility with major material groups used in aerospace applications, these being metals, elastomers, and plastics. This method was not refined enough for this study as it does not differentiate between the relative importance of these material classes with respect to relevant applications. It also does not take into consideration the difference in compatibility with materials belonging to the same class e.g., aluminium and steel. Carlotti and Maggi[109] took a similar approach by performing a qualitative assessment of the materials compatibility of considered propellants over a range of materials commonly used in space applications. Propellants were subsequently labelled as compatible with "a limited set of standard materials", "a substantial set of standard materials", or "more than 90% of considered standard materials".

For this study, the evaluations in previous works were considered valuable but also too limited. Therefore, a method was developed to quantify the material compatibility criterion based on several factors of importance:

- A list was created of the most important components of the propulsion system with which the fuel was expected to come into contact. Based works in literature[16][19][106][119][120], these components were given a weighting based on the extent of the contact of the fuel with this component before and during operations.
- A list of relevant, commonly used space materials was composed, after which each material was given an importance weight based on which of the aforementioned components the materials are commonly used for.

- A qualitative assessment was made for the compatibility of the fuels with the selected aerospace materials, similar to Carlotti and Maggi. Information provided by suppliers and manufacturers such as Graco Inc.[121] was used to make these assessments. It should be noted that a material score could not be found for all variations of common aerospace materials. Most of the main material groups were, however, included.

By combining these three important factors discussed above, a quantitative evaluation could be made for the material compatibility of the fuels with respect to relevant components and materials in propulsion systems. The advantage of the assessment method proposed in this study for the materials compatibility criterion as compared to the other studies presented earlier in this section is the level of informativeness and the inclusion of a bias towards more important materials. As such, fuels that display good compatibility with materials covering all main components were, by default, scored better. Note that it was also considered to include cost and material density considerations in the assignment of relative material importance weights. It was, however, decided that this would add too much complexity to the assessment method and that leaving it out would allow for more freedom in future designs employing this assessment method.

Ease of use - Storage and handling
The second subcriterion that was considered in defining ease of use was the *handling and storage* subcriterion. It was set up to evaluate all practical aspects, with the exception of toxicity considerations, related to the safe handling and easy storage of the candidate fuels. This included considerations of flammability, stability, vapour pressure, and transition temperatures. In assessing the handling and storage of fuels, Elferink[5] opted to give a qualitative scoring for handling characteristics ranging from dangerous to safe, and to provide information on the shelf life and common storage methods of the fuels. Carlotti and Maggi[109] chose to set up a more quantitative assessment by considering the liquid range of the propellant and the reactivity of the propellant to account for storage characteristics and by considering the vapour pressure and the flammability of the propellant in representing the ease and safety of handling. As indicated before, the focus of PICE is on providing a more complete and informative mapping and ranking of the candidate fuels through quantitative assessment methods. As such, the assessment methods proposed by Carlotti and Maggi[109] were adopted and altered to fit this study. It was also argued that while the shelf life of a propellant gives an important quantified basis for comparison relevant to space applications, it is not as relevant for the proposed reference case of this study as the storage time of propellants for launch vehicle core stage engines was expected to be well under 24 months, which is the shortest shelf life reported by Elferink[5].

A characteristic that is commonly investigated in propellant selection studies to assess the storability of considered propellants for liquid propulsion systems is the liquid range of the propellants. This means that the freezing point and the boiling point of the propellants are considered with respect to prespecified reference points chosen based on the intended application.[49][110] These reference transition temperatures were the main consideration in setting up this part of the handling and storage assessment. In military applications, these requirements are generally rather strict, often requiring the propellants to be at least liquid in a range of -60 to 60°C.[122] Kurilov et al.[110] suggested a similar reference value for the minimum boiling temperature, but with a softer requirement on the freezing temperature of -20°C in their study on green hyperbolic bi-propellants for common space applications. Both Scharlemann[50] and Carlotti and Maggi[109] considered reference values for the freezing temperature close to that of hydrazine, with values of 0°C and 2°C respectively. The former then considered a boiling temperature of 70°C based on Kurilov et al.[110], while the latter considered a reference boiling temperature of 115°C in correspondence with the boiling temperature of hydrazine. For the application of launch vehicle core stage engines, it was argued that the temperature variations in the temperature tanks could be kept within the margins proposed by Carlotti and Maggi[109]. As such, it was decided to evaluate the candidate fuels on their transition temperatures compared to a reference liquid range of 0 to 70°C.

Two major elements in assessing the ease of handling of a propellant are its flammability and its reactivity levels. Flammability refers to the ease with which chemicals ignite and produce vapours.

Although highly flammable fuels are often excellent candidates for high-performance applications and allow for more simplicity in the ignition system, they are also more susceptible to spontaneous ignition under deviating environments, thus leading to increased handling and storage risks. The instability of a rocket propellant refers to its characteristic susceptibility to readily react violently in reaction to small external triggers. Like flammability, highly unstable fuels thus pose major handling and storage risks and are relevant factors concerning the overall reliability of the system. The health hazard NFPA rating classifications were employed to support the toxicity assessment criterion. Two other hazard groups defined by the NFPA rating system are the flammability and instability hazards, respectively, as indicated in Figure 5.2. As such, the assessment method proposed for the NFPA health hazard group was adopted here for the handling and storage criterion to provide further insight into the flammability and stability of the candidate fuels.

Another subcriterion that was proposed by Carlotti and Maggi[109] was the vapour pressure. For vapour pressure, it was first decided to set a similar value of 1 bar as a threshold value for a positive rating of fuels. Upon inspection, however, it was found that all fuels considered in this trade-off had a characteristic vapour pressure well below this threshold value. Therefore, the vapour pressure criterion was ultimately excluded from the handling and storage assessment. It is worth noting that the vapour pressure is still included in the trade-off through the toxicity criterion. The vapour hazard index was used to assess the danger and toxicity of the respective fuels by considering both the saturated vapour pressure and a threshold limit value (TLV), in this case the workplace exposure limit.

In determining relative weights of importance for the components of the handling and storage criterion, equal importance was given to the liquid range transition temperatures and to the NFPA hazard groups. Furthermore, it was found that the instability, although a relevant point of assessment, was not a very decisive factor given the generally high stability of the candidate fuels. As such, it was given a lower relative weight than the flammability hazard rating. An overview of the relative weights assigned to the components of the handling and storage criterion can be found in Table 5.7.

Table 5.7: Relative weighting for the components of the handling and storage criterion

	NFPA flammability hazards	**NFPA instability hazards**	**Freezing temperature**	**Boiling temperature**
Component weights	0.4	0.1	0.25	0.25

Development level

As outlined in Section 5.3, the development level of propellants is an assessment criterion that is considered less often in propellant selection studies. The reason for this is that it is a criterion that is not directly related to any chemical or physical characteristics of the considered propellants, but rather a result of historical factors such as political concerns, availability of the propellant and advancements of technology at the time of previous development efforts, and the novelty of the considered propellants. This makes it a less evident choice of criterion for studies purely focused on assessing the general suitability of propellants for aerospace applications. Studies such as the GRASP project[47][50], however, do show an interest in the heritage and level of maturity of the systems developed for considered propellants due to external reasons such as cost and the need for quick replacements for banned substances such as hydrazine.[4] Indeed, for this study, it was identified that there are some compelling reasons for considering development level as a criterion for the fuel assessment process. It was considered that selecting fuels that are characterised by a high level of development (in combination with HTP) could lead to major savings both in terms of development cost and development time. Another argument for the selection of developed fuels was not only the availability of information on the characteristics of these fuels, but also the level of certainty associated with this information. As such, this would reduce the risk of finding bad or even unacceptable characteristics after investing considerable resources in future development

efforts.

The key metric employed in assessing the development level of the candidate fuels was the Technology Readiness Scale (TRL). This scale, visualised in Figure 5.3, is often used in the space industry to indicate the maturity of a system with respect to qualification for use in space applications. It is worth noting that different institutions employ varying definitions of this scale. Yet, the core principles are generally the same, as TRL 1 relates to a system at the start of research with nothing but basic principles observed, while a TRL of 9 indicates a system that is fully proven in the operation environment.[123] For this study, it was chosen to use the ESA scale due to its relevance with respect to the reference launch vehicle.
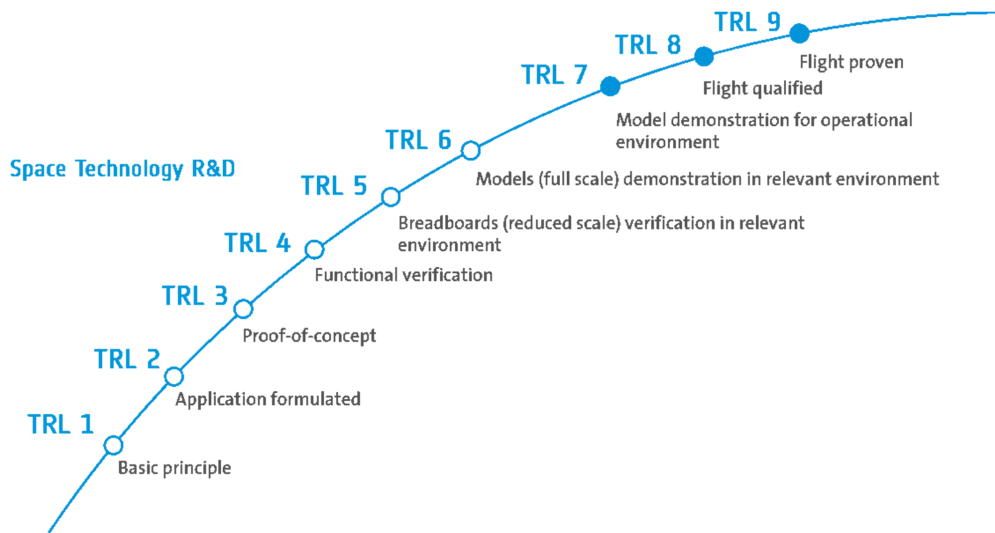
Figure 5.3: Technology Readiness Levels (TRL) scale in accordance with ESA standards[123]

In assessing the candidate fuels with respect to the development level criterion, both development efforts with HTP and without HTP were considered, although the emphasis was on the latter. Next to that, the relevance of the developed applications was also considered. In determining the scoring for each TRL level, an exponential factor was applied to identify the leaps in technological advancement between TRL 3 and TRL 4 and later between TRL 6 and TRL 7. As such, Equation 5.2 was used to score the different TRL levels, where X refers to the respective TRL level and a is the factor applied to account for leaps in technological developments between subsequent triplets of TRL levels. Here, a equals 1 for TRL 1 to TRL 3, 2 for TRL 4 to TRL 6, and 3 for TRL 7 to TRL 9.

$$Score = \frac{TRLX}{9}2^a \tag{5.2}$$

Coolant qualities

Hydrogen peroxide has been proven to be a decent coolant in applications considering regenerative cooling in HTP-based bi-propellant engines.[124] In Section 2.2.2, an important drawback of the use of HTP in space applications was addressed with its incompatibility with several commonly used aerospace materials. It was argued that this poses a problem not only in current development efforts, as the valve materials need to be carefully selected, and the selection of materials that can be considered is limited, which could thus make this a leading factor over other important design drivers such as mass and cost. Furthermore, this limited materials compatibility could put a constraining factor on future development efforts, such as the transition to lightweight additively manufactured structures e.g., Inconel alloy 718 based structures.[125] Next to that, HTP is known to quickly decompose at high temperatures, thereby releasing highly reactive decomposition products.[126] This, in turn, also increases the risk of the system when using hydrogen peroxide for coolant applications. As such, it was deemed that mapping the potential of the candidate fuels

with respect to their coolant qualities would provide a crucial foundation to lead future development efforts in investigating alternatives to the use of HTP for cooling purposes in regenerative bi-propellant engines if problems were to arise.

The convective heat transfer coefficient is a measure of the effectiveness of a cooling layer or a series of cooling layers. It encompasses geometric factors, characteristics of the coolant, and the state of the coolant environment. The convective heat transfer coefficient, which is mostly obtained experimentally, is often expressed through either the Stanton or the Nusselt number. Equation 5.3 is a derivative of the Sieder-Tate equation, where the Nusselt number has been converted to the heat transfer coefficient. The Sieder-Tate equation was originally proposed as a modification of the Dittus-Boelter equation and is generally valid for turbulent flows with an increased Reynolds number.[18][127][128]

$$h = 0.025 \frac{k \cdot Re^{0.8} \cdot Pr^{0.4} \cdot T_b^{0.55}}{D \cdot T_w^{0.55}} \tag{5.3}$$

where h is the heat transfer coefficient, k is the thermal conductivity of the coolant, R_e is the Reynolds number, P_r is the Prandtl number, T_b and T_w are the temperatures of the bulk of the coolant and the coolant at the combustion chamber wall, respectively. In this relation, both T_b and T_w are variables that are not depending on the choice of coolant. The Reynolds number can be expressed as a function of μ, the dynamic viscosity of the coolant, while the Prandtl number can be expressed as a function of μ, k, and c_p. Here, c_p is the specific heat capacity of the coolant. Based on this dissection of the Sieder-Tate equation, the heat transfer coefficient can thus be expressed as a function of three characteristics of the selected coolant, as shown in Equation 5.4.[128]

$$h = f(k^{0.6}, \mu^{0.4}, c_p^{0.4}) \tag{5.4}$$

where:

- μ : Dynamic viscosity [$Pa \cdot s$]
- c_p : Specific heat capacity [$\frac{J}{kg \cdot K}$]
- k : Thermal conductivity [$\frac{W}{m \cdot K}$]

From the heat transfer equations presented above, it follows that the heat transfer coefficient can effectively be related to the thermal conductivity, the specific heat capacity, and the dynamic viscosity of the coolant. Here, it was found that the relation between the heat transfer coefficient and these independent variables is not linear but rather that it depends on a set of exponential factors. These respective factors were used for assigning relative weights to the components. An overview of the relative weights assigned to the components of the coolant qualities criterion can be found in Table 5.8.

Table 5.8: Relative weighting for the components of the coolant qualities criterion

	Thermal conductivity	Specific heat capacity	Dynamic viscosity
Component weights	0.43	0.29	0.29

5.5. PICE criteria weighting

To perform the PICE assessment, use was made of an Analytical Hierarchy Process (AHP). This method was developed by Thomas Saaty to provide a structured approach to analysing and solving complex decision-making problems. As the name suggests, the problem is shaped into a hierarchy structure including a goal, criteria and subcriteria, and options considered for trade-off. At the basis of the mathematical model behind AHP methods are a series of pairwise comparison matrices. Here, elements of the same levels of the hierarchy structure are compared to each other regarding the objectives set by their overcoupling element one level above. This pairwise comparison is made

by specifying the importance of one element to the other with respect to the overcoupling element in accordance with the scoring definitions stated in Table 5.9.[129][130]

Table 5.9: Definition and explanation of the scores applied in pairwise comparison for AHP[131]

Intensity	Definition	Explanation
1	Equal	Two items contribute equally to the objective.
3	Moderate	Experience and judgment slightly favor one item over another.
5	Strong	Experience and judgment strongly favor one item over another.
7	Very strong	An item is strongly favored and its dominance demonstrated in practice.
9	Extreme	The evidence favoring one activity over another is of the highest possible order of affirmation
2,4,6,8	Intermediate values	When compromise is needed.

Once the pairwise comparison matrices are constructed and normalised, the relative worth of each option and the consistency of the assessment are then found by solving for the eigenvector and the maximum eigenvalue of the matrix, respectively. Consistency refers to the extent to which the solution is exempt from random judgment. It is expressed through the Consistency Index (CI) and the Consistency Ratio (CR), which are found through Equation 5.5 and 5.6, respectively. Here, λ_{max} represents the maximum eigenvalue, n represents the number of elements making up the comparison, and RI is a random index determined from the average of a large number of matrices with random judgement. Generally, CR values below 0.1 indicate a high level of consistency in the pairwise comparison matrix.

$$CI = \frac{\lambda_{max} - n}{n - 1} \tag{5.5}$$

$$CR = \frac{CI}{RI} \tag{5.6}$$

In this study, the AHP tool of Dutch Space B.V. by Thijs Methot was used.[131] This choice was made due to the fact that this tool was already validated, relatively user-friendly, and because it was used in a similar study by Elferink[5]. Next to that, the tool allowed for modifications to be made to the base code and for multiple expert weightings to be considered in its setup. As such, the input of 12 people with relevance to the topic of this study, referred to as experts, was used to decide on relative importance weights to the criteria and subcriteria introduced in Section 5.4. The background of the experts included three engineers from ESA, four propulsion and systems engineers active in the industry, three professors from the space flight department at Delft University of Technology, and three master students preparing a master's thesis on similar topics. All experts were sent a preliminary version of the document provided in Appendix B, which provided a short and objective overview of this study and of the (sub)criteria considered in this assessment.

With such a high number of experts providing input on the weighing of the criteria, it could be expected that there would be a level of variation in the resulting weights. In Figure 5.4, the initial distribution of weights given by the experts to each of the criteria can be observed. It followed that for some criteria e.g., coolant qualities, the relative weights assigned by the experts were relatively similar except for some outliers, resulting in a compressed box plot. For other criteria, however, the distribution of weights was much larger, resulting in elongated box plots. It could also be observed that half of the experts had a level of inconsistency in their pairwise comparison matrices exceeding the aforementioned limit of 0.1
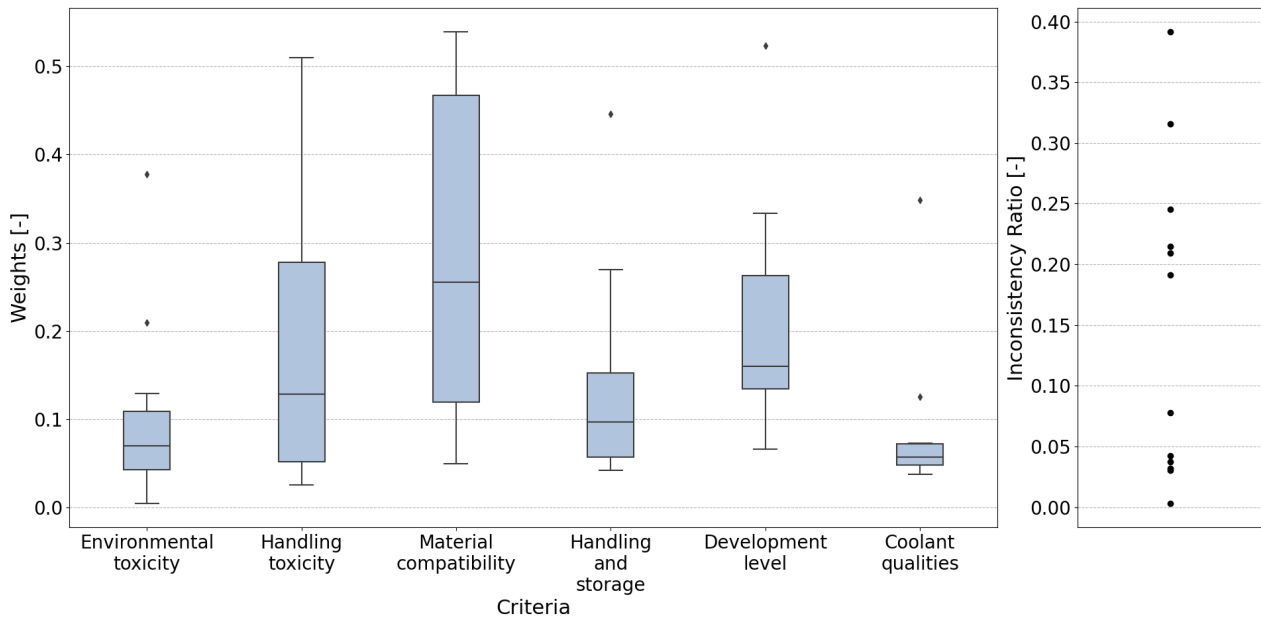
Figure 5.4: A boxplot detailing the distribution of criteria weights provided by experts (left) and a spread of the inconsistency ratios observed in the pairwise comparison matrices provided by the experts (right)

The AHP tool used in this study included some metrics to identify and remove outliers in the assessment. Informativeness is a variable representing the extent to which the evaluation applied to a series of elements on a level of the hierarchy is definitive based on the deviation of different scoring outputs from the mean. It is a function of the number of experts, as the maximum level of informativeness is equal to the number of expert inputs considered for the evaluation and the level of similarity of the provided input.[131] To increase the informativeness of an evaluation, the tool allowed for specific experts to be excluded from this evaluation. Due to the disconnection of this exclusion between different evaluations, the informativeness of each evaluation could be adjusted separately while maintaining a sufficiently high number of inputs. Ultimately, three or four expert inputs were excluded from each evaluation to arrive at a minimum informativeness level of over 50% for each evaluation, as shown in Table 5.10.

Table 5.10: Level of informativeness of the three (sub)criteria evaluations before and after excluding outliers. The maximum level of informativeness is equal to the number of expert inputs considered, with the maximum level of informativeness for each evaluation being equal to 12 before excluding any outliers.

Evaluation	Informativeness before	Informativeness after	Number of experts excluded	Number of experts left
Main criteria	-3.7	5.33	3	9
Toxicity subcriteria	2.61	7.27	4	8
Ease of use subcriteria	2.36	7.2	3	9

In Figure 5.5, the relative weights assigned to the criteria, before and after excluding outliers, were visualised. Here, the *toxicity* and *ease of use* criteria were represented by their respective subcriteria. The final weights were also tabulated in Table 5.11. The highest relative weight was assigned to the material compatibility criterion, at almost four times the weight of the lowest-weighted criterion, environmental toxicity. It is interesting to remark on the noticeable shift in relative weights for most of the criteria after removing outliers using the AHP tool functionalities. For handling toxicity and coolant qualities, this shift was rather small, indicating a high level of agreement amongst the experts regarding the relative importance of these criteria.
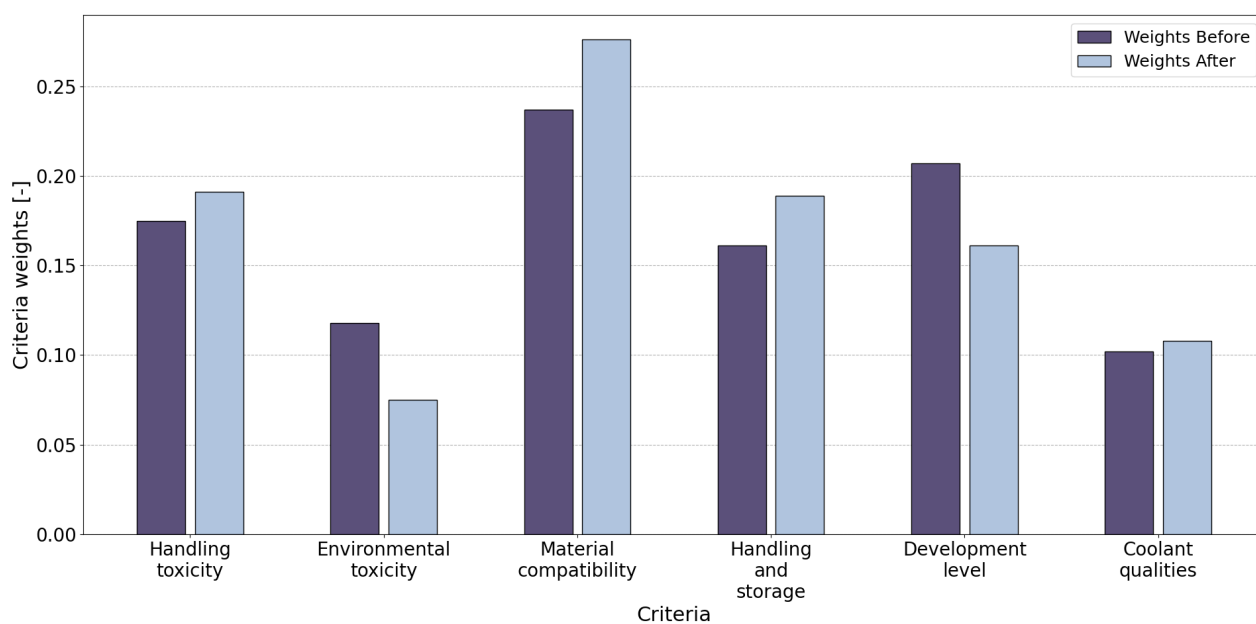
Figure 5.5: Relative weights assigned to the (sub)criteria, before and after removing outliers, as a result of pairwise comparisons by experts

Table 5.11: Relative weights assigned to the (sub)criteria, after removing outliers, as a result of pairwise comparisons by experts

Main criterion	Sub criterion	Weight
Toxicity		0.293
	Handling toxicity	0.191
	Environmental toxicity	0.075
Ease of use		0.398
	Material compatibility	0.276
	Handling and storage	0.189
Development level		0.161
Coolant qualities		0.108

5.6. Chapter summary

In this chapter, the setup of the *baseline fuel assessment* was described, which is the first of 2 research segments central to this study. The objectives of this first research segment are to narrow down the large selection of potential fuels in anticipation of the second research segment, and to assess the remaining fuels based on a series of non-performance related characteristics. To this extent, the baseline fuel assessment was divided into four phases. After a brief *requirements setup and data collection* phase, four key criteria were selected to be considered in the *preliminary feasibility assessment*: combustion stability, storage stage, toxicity threshold, and minimum performance. These criteria were set up to allow for unsuitable fuels to be eliminated from further assessment, mostly through evaluations based on literature and without detailed and time-consuming assessment methods. The setup of an *availability assessment* was described, where the availability of fuel sources and the availability of data for a more detailed assessment were identified to be the most suitable assessment criteria.

For the final phase, referred to as the *propellant integration and compatibility evaluation* or PICE,

a more quantitative approach was described as a scoring system was developed for a total of six (sub)criteria. Through an extended literature review, the following criteria were found to be most relevant and applicable to this assessment: handling toxicity, environmental toxicity, material compatibility, handling and storage, development level, and coolant qualities. To provide relative weighting to the criteria, an AHP tool was used through which the inputs of twelve experts were considered. An informativeness factor was used to filter outliers from these inputs to reach a high level of consistency in the amongst the expert scoring. This resulted in the relative weights presented in Table 5.11. Most notably, the highest weight was given to the material compatibility criterion, while the lowest criterion was found for the environmental toxicity criterion. Furthermore, it was found that for the handling toxicity and the coolant qualities criteria, only a small shift in relative weights was observed after removing outliers. This indicates a high level of agreement amongst experts regarding the importance of these criteria.

6. Baseline fuel assessment results

As per the setup of this study presented in Chapter 4, two main research segments were identified. The first of these research segments, which was referred to as the *baseline fuel assessment*, was aimed *investigating the compatibility and integration potential of various fuel candidates in combination with highly concentrated hydrogen peroxide with respect to design drivers that are not directly related to launch vehicle propulsion and mass performance*, in accordance with the compatibility and integration potential research objective defined in Chapter 3. As such, the two main research questions for the second research segment were defined as:

- RQ-CI-01: Which non-performance-related design drivers allow for candidate fuels to be assessed based on their compatibility and integration potential with hydrogen peroxide for launch vehicle applications?
- RQ-CI-02: Which storable fuel shows the most compatibility and integration potential in combination with highly concentrated hydrogen peroxide with respect to a set of specific non-performance-related design drivers for launch vehicle applications?

The setup of the baseline fuel assessment was discussed in Chapter 5. A combination of qualitative surface-level assessments, followed by a more detailed quantitative assessment, allowed for an answer to be provided to the above-stated research questions. Through a preliminary fuel selection, including a preliminary feasibility assessment and an availability assessment, the initial selection of fuels proposed for this study could be narrowed down. This allowed for a more detailed assessment to be performed on the remaining fuels, and thus for a well-founded and conclusive answer to be found to *RQ-CI-02*. This detailed assessment, referred to as PICE, also allowed for the value of several assessment criteria to be evaluated with respect to the specifications of the propellant selection performed in this study, thereby providing an answer to *RQ-CI-01*. The results of the preliminary fuel selection will be discussed in Section 6.1, after which the results of the PICE assessment will be presented and analysed in Section 6.2.

6.1. Preliminary fuel selection

At the basis of the baseline fuel assessment introduced in Chapter 5 was an initial selection of candidate fuels that were thought to have potential for combination with HTP in launch vehicle applications. A major driver in selecting these initial fuels were the objectives of low toxicity and storability, as per the research goal specified in Chapter 3. Following these objectives, a total of 86 fuels were selected based on various sources in literature. Here, proven effectiveness with hydrogen peroxide and hypergolicity were considered desirable, but not required.

The *preliminary feasibility assessment* was constructed to be a mostly qualitative surface-level assessment of some key fuel characteristics to significantly narrow down the selection of fuels without the need for extensive study or data review. As such, the initial selection of candidate fuels was subjected to this assessment concerning the criteria of combustion stability, required storage state, overall toxicity threshold, and minimum performance levels. On this basis, 58 fuels were rejected and thus excluded from further analysis. Subsequent to this first assessment, an *availability assessment* was performed on the remaining fuels to assess the availability of resources needed to synthesise the fuels and the availability of information to perform the more detailed *PICE* assessment. Seven more fuels were excluded from further analysis on this basis. As such, 21 fuels were originally considered for the PICE assessment. Ultimately, only eight fuels were effectively compared with the AHP tool. Therefore, it is important to discuss a number of fuels that were ultimately not considered for the PICE assessment and to give some more context to the considerations that led to this selection.

- **Block 0**: This fuel was first introduced following studies by the US Navy in the 1990s. It is a combination of methanol and manganese acetate tetrahydrate. As the latter is an effective

catalyst in reactions with hydrogen peroxide, ensuring short ignition delay times (IDT), it was considered highly relevant for this study. Block 0 was, however, reported to have a lack of stability on storage and found to have a lower specific impulse density with HTP than the conventional MMH/NTO combination.[104][132] Methanol was considered in the *PICE* assessment as a replacement for Block 0 due to its generally good properties.

- **BMIM SCN/EMIM SCN**: Ionic Liquids (ILs) are salts liquid at room temperature that can contain specific cations or anions which could influence their physical properties and potentially make them good fuels hyperbolic with hydrogen peroxide. Recently, a study was performed by the German Aerospace Center (DLR) on the hypergolicity and the performance of two ILs, these being BMIM SCN and EMIM SCN, thereby reporting low IDT and high specific impulse density.[133] Although they were deemed highly relevant and interesting for this study, not enough data could be found on these ILs to perform a detailed assessment and effectively compare them with other candidate fuels.

- **DETA**: Diethylenetriamine or DETA is a storable substance from the amino group and was identified as a potential fuel in several studies due to the high reactivity and performance displayed in combination with hydrogen peroxide. Additionally, it mixes well with catalysts such as sodium borohydride ($NaBH_4$), thus further improving the IDT potential.[50][88][104][134] Although initially considered for the *PICE* assessment, it was quickly found that DETA displays a high level of toxicity, at which point is was excluded from further evaluation in favour of more suitable fuels.

- **DMAZ**: 2-Dimethylaminoethylazide or DMAZ was considered as it was mentioned to be a high-performance, low-toxicity fuel in several studies. In the study by Elferink[5], it was subsequently selected as the most suitable fuel for further development in HTP-based launch vehicle applications. As it was first created and developed by the US Army and later NASA, the availability of DMAZ is limited for use, and the stocks are expected to be low. Additionally, information on DMAZ was found to be limited to a selected few sources, with most available information originating from a preliminary review study by Mellor[135]. Here, it was found that the information available was insufficient to perform a detailed assessment as per the assessment methods presented in Section 5.4. Instead, it was included as a reference fuel in the vehicle performance model constructed in the second research segment.

- **JP-series fuels**: These hydrocarbon fuels were first introduced by the US government and are mostly used for military applications. As such, most of these fuels are not available in Europe. Jet-A and RP-1 are other hydrocarbon fuels similar to the JP-series fuels. The former, which is reported to be quite similar to JP-8, is a common fuel within the aviation industry and is more widely available, while the latter, which is essentially highly refined kerosene, is used in several launch vehicle applications such as the Falcon 9 core stage engines. Amongst the JP-series fuels, JP-10 is reported to have the highest performance, and JP-4, JP-5, JP-8, and JP-10 have all been tested with HTP and several catalysts. Despite the lack of availability in Europe, it was decided to include RP-1 in the *PICE* assessment due to its relevance and its similarity with the hydrocarbon fuels used on some European launch vehicles. Furthermore, it was also decided to include Jet-A fuel and JP-10 in the *vehicle performance model*, while the other JP-series fuels were left out due to their inferior performance compared to JP-10. Jet-A fuel was also reported to be inferior to JP-10, but it was included regardless due to it being more widely available.[50][88][104]

- **TMEDA**: TEMED or TMEDA is a chemical compound that was considered for further study in the GRASP project. The use of this chemical was not found in any other sources investigated during the literature phase of this study. Since its characteristics were reported to be favourable in the GRASP project, it was at first considered to include TMEDA in the *PICE* assessment. Yet, after having performed the first part of this assessment concerning the toxicity criterion, it was found that the toxicity of this chemical is comparable to that of DETA. It was thus decided to exclude TMEDA from further assessment.

- **Stock-3**: Due to their historical use as a solvent and overall attractive properties, glymes were considered and used in several fuel mixtures. Among these mixtures were the Stock series fuels, developed by Kang et al.[136]. The original fuel in this series, known as Stock-0, was developed by Mahakali et al.[137] and served as a reference fuel for developing the next two

iterations: Stock-1 and Stock-2. It was, however, observed that both Stock-1 and Stock-2 became unstable quickly in storage conditions.[104][136] A new iteration was thus created with Stock-3, comprising mainly DETA and tetrahydrofuran (THF). This fuel showed promise in terms of performance, hypergolicity with HTP, and storability. A 500 N scale non-toxic hypergolic bi-propellant thruster ground model was equipped with a combination of HTP and Stock-3, which exceeded the performance of the previous iteration that was equipped with Stock-2 fuel. It should, however, be noted that DETA is considered a hazard class 3 chemical, which thus precludes the use of Stock-3 in green propellant applications.[138]

A complete overview of the preliminary fuel selection process can be found in Appendix C. Here, the evaluations for the different criteria considered in the *preliminary feasibility assessment* were provided. Next to that, the final assessment in which each fuel was considered was stated, together with a reason for exclusion if applicable. Ultimately, eight fuels were considered for the complete *PICE* assessment, with a further four fuels added for optimisation through the *vehicle performance model*. An overview of the fuels considered for these elements can be found in Table 6.1. In Appendix D, relevant physical and chemical characteristics were tabulated for each of the fuels that were still considered for the PICE assessment.

Table 6.1: Fuels considered for the PICE assessment and additional fuels considered for the vehicle performance model

PICE assessment	Vehicle performance model
Ethanol	DMAZ
Isooctane	Jet-A
Isopropanol	JP-10
Methanol	Methane
RP-1/Kerosene	
TMPDA	
Toluene	
Turpentine	

While the preliminary feasibility assessment proved to be a decisive factor in this study, the reliability and effectiveness of this part of the baseline fuel assessment are worth discussing. As was repeatedly mentioned in Chapter 5, where the setup of this assessment was discussed, the preliminary fuel assessment was based on qualitative surface-level evaluations, relying on information found in literature. As such, it is worth noting that relevant information and data found here were, at times, contradicting. In making evaluations, specific definitions used by different authors had to be brought together into decisive and consistent evaluations. Whereas the aim was to verify data by consulting multiple sources for each evaluation, it was often found that a lack of sources prevented effective data verification or an evaluation from being made at all. Indeed, from the overview of evaluations provided in Appendix C, it can be observed that a lack of sources was one of the most common reasons for excluding fuels from further study. Although this could imply rejecting some fuels with a high potential for the intended application, it was also an indication of low development of the specific fuel, which could indicate a lack of potential or poor characteristics. Furthermore, this lack of sources would have proven to be an obstacle in subsequent assessment of these fuels through the PICE assessment or the vehicle performance model.

While the availability, or the lack thereof, of data and information for the preliminary feasibility assessment is a key discussion point, it should be stated that this obstacle was not as relevant for all of the assessment criteria. Based on the reported evaluations, it could be concluded that *toxicity* was an effective and conclusive criterion, for which a good amount of consistent data could be found in literature. As such, it ensured that highly toxic fuels were excluded from the study, which was important as per the research goal. Not only toxicity but also the state of the fuel at the expected *storage conditions* was an important factor put forward through the research goal. Similarly, this

criterion and the way in which it was evaluated proved to be very decisive and effective for the preliminary feasibility assessment. Additionally, fuels for which poor storage characteristics were explicitly mentioned in literature could be excluded through this criterion. The assessment criterion for which the least amount of data was available is the *combustion stability* criterion. Although this criterion is very valuable in identifying fuels that would be unsuitable for the intended application, it is rarely touched upon in literature, especially when considering fuels for which fewer experiments or research has been performed. Although the combustion stability criterion allowed for a few unstable fuels to be identified, it would be more suitable in a more detailed and experimental study. While evaluating the fuels with respect to the *performance* criterion, it was found that a lot of variation exists amongst the definitions for performance used by different authors. The parameter used for comparing performance and the different engine settings led to a high variation in the reported performance data. As such, minimum performance was treated as a light and non-decisive criterion. It is, however, a highly relevant criterion and eliminating low-performance fuels without needing a detailed and dedicated assessment or model would be desirable. Therefore, it is recommended that a dedicated study is performed to assess a high number of HTP-based bi-propellant fuels with respect to one specific performance definition and for a single set of engine input settings. This could prove valuable in future development efforts focused on HTP as it would allow for quick and consistent performance evaluations.

6.2. PICE results

Based on the assessment structure outlined in Chapter 5, the AHP tool was used to compare the fuels presented in Table 6.1 with respect to the non-performance-related characteristics considered in the *PICE* assessment. The results plotted in Figure 6.1 (left) show the relative score of the fuels with respect to the respective criteria as well as an overview of the contribution of these criteria to the variation in the total fuel scores. Note that due to the nature of AHP trade-offs, the sum of the final scores of all fuels equals 1. The scores are thus mostly relevant within the frame of reference of this study for mutual comparison between the proposed fuels. It could be observed that *RP-1* is the fuel that displayed the best overall performance with respect to the considered criteria, while *methanol*, *ethanol*, *isooctane*, and *isopropanol* could all be considered acceptable alternatives with similar performance. The biggest factors in the high score found for RP-1 were the contribution from the development level and the material compatibility criteria. The former was mostly the result of the advanced level of development of RP-1 and RP-1 derivatives (with HTP) as compared to the other fuels considered, while the latter could be attributed to the high relative weight assigned to the material compatibility criterion.

As to investigate the impact of specific criteria on the AHP results, the standard deviation for each criterion was also plotted in Figure 6.1 (right). In the context of this assessment, the standard deviation is a measure of the spread in scores observed for the specific criteria. It shows that the highest deviations could be observed for the development level criterion and the material compatibility criterion, while the lowest deviations were found for the handling toxicity criterion and the handling and storage criterion. The effectiveness of the *preliminary feasibility assessment* was arguably an important factor in these results, as the surface-level toxicity assessment and combustion stability assessment allowed for the most toxic and unstable fuels to be excluded from the study at an early stage. Including more toxic fuels such as DETA could have led to a higher level of deviation observed for these respective criteria.

It could be argued that one of the weaknesses of an AHP trade-off is the increased level of subjectivity in the weighing of the criteria. This was mitigated by considering a larger number of experts from different fields and by excluding outliers to obtain a higher level of informativeness for evaluating the criteria, as per the discussion in Section 5.5. To illustrate the robustness of the final results of the AHP assessment, a sensitivity analysis was performed to mark the effect of the relative criteria weights on the final results. To do this, a total of 500 simulations were performed in which the weights of the individual criteria were given a random incremental increase or decrease between 0% and 30%. Three times the standard deviation from these results was used as an error margin on each final fuel score to account for 99.7% of the score variations. It can be observed in Figure 6.2

that RP-1 remained the most suitable fuel with respect to the considered criteria. Another notable result was the relatively low margin of uncertainty in some of the fuel scores, as was the case for ethanol. Upon further inspection of the results, it was found that this could be explained by the consistent score of ethanol for all of the criteria as opposed to other fuels, such as methanol, for which some criteria were scored considerably higher than others. Overall, it seems that the final results could be considered relatively robust and that few inaccuracies were introduced by the choice of AHP as a trade-off tool for this assessment.
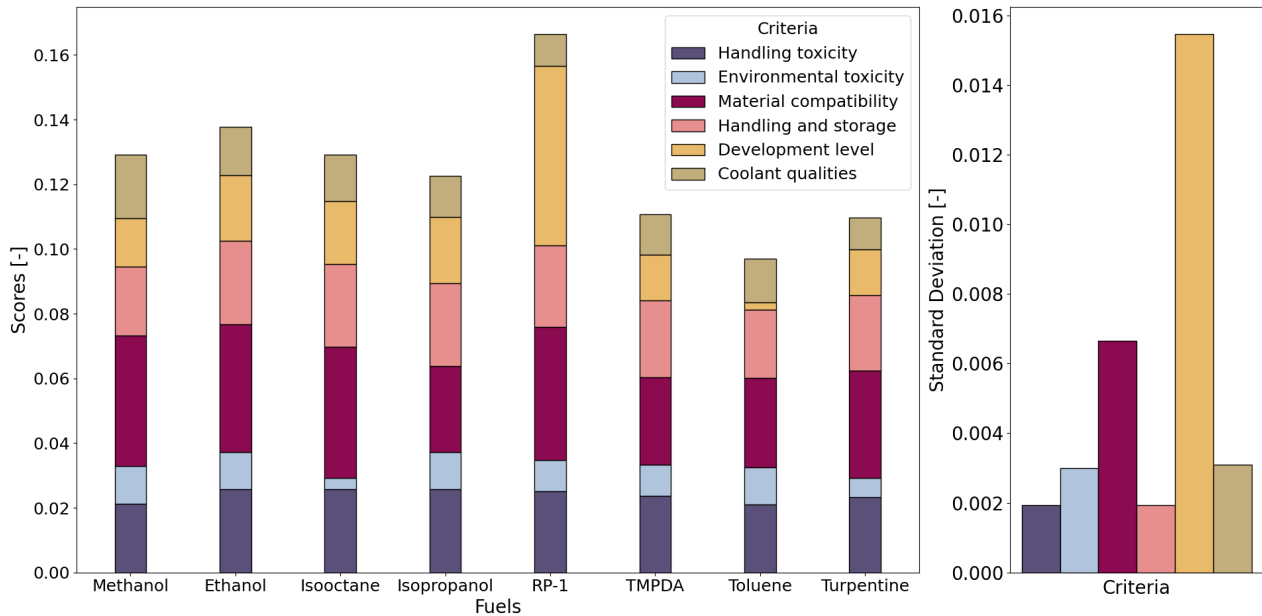
Figure 6.1: Final results of the AHP trade-off including an overview of the contribution of the different criteria to the overall fuels scores (left) and the standard deviation observed in the scores of the fuels for each of the criteria (right)
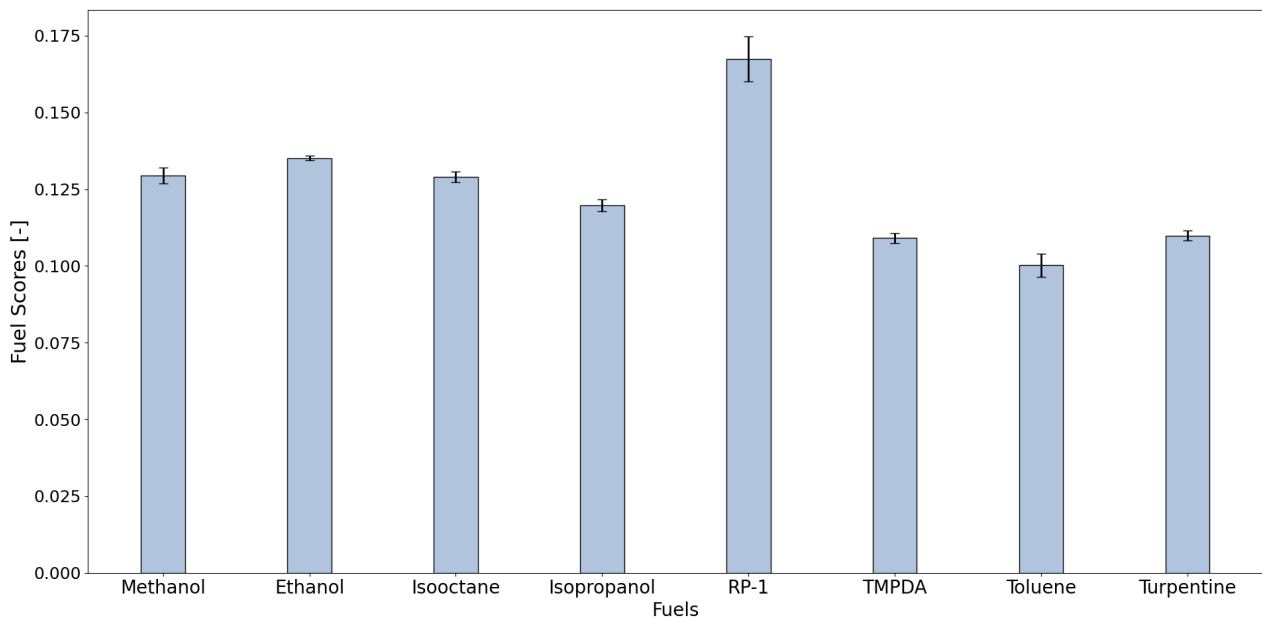
Figure 6.2: The final fuel scores taken from the average of 500 simulations as a result of unique combinations of the criteria weights by applying an incremental increase or decrease between 0% and 30% to the standard weights. The error bars (3σ) show the level of variations observed in the final results.

The conclusion of this research segment allowed for an answer to be formulated to the two research questions related to the compatibility and integration potential of the proposed green propellant fuels in launch vehicle applications. As an answer to **RQ-CI-01**, it was first argued in Section 5.3 that based on similar studies and the specifications of the system considered for this study, toxicity, handling and safety, material compatibility, development level, and coolant qualities are the most relevant non-performance related design drivers for candidate fuels to be assessed based on their compatibility and integration potential with hydrogen peroxide for launch vehicle applications. Thereafter, it was found that based on the inputs from various experts with respect to the topics of systems engineering and propulsion engineering, materials compatibility, handling toxicity, and handling and storage could be deemed the most important of the aforementioned design drivers. Combustion stability and (propulsive) performance proved to be less ideal criteria for surface-level fuel assessments due to a lack of data and consistent criteria definitions in literature. To allow for more conclusive and reliable fuel selections in future studies, it was recommended that dedicated studies and experiments be performed into the performance, combustion stability, and ignition delay times of a large selection of HTP-based bi-propellant combinations.

In attempting to provide an answer to **RQ-CI-02**, a large selection of candidate fuels was initially considered. After a preliminary fuel selection process and a more detailed assessment, it was found that RP-1 (and, by extension, other kerosene derivatives) could be considered the most suitable fuel for combination with highly concentrated hydrogen peroxide in launch vehicle propulsion applications on the basis of the non-performance-related design drivers considered in this study. Methanol, ethanol, isooctane, and isopropanol also showed to be promising alternatives. Furthermore, the robustness of this conclusion was proven through a sensitivity analysis.

6.3. Chapter summary

In this chapter, the results of the first research segment were presented and discussed, the setup of which was described in Chapter 5. Through the preliminary feasibility assessment, 58 fuels were excluded from further analysis. Another seven fuels were rejected following the availability assessment. Overall, it was found that a lack of sources was one of the most common reasons for excluding fuels from further study. Furthermore, both the toxicity criterion and the storage state criterion were found to be very suitable and decisive for surface-level assessments. For the combustion stability and the minimum performance criterion, a lack of sources and variety in the collected data were reported to be the primary reasons for these criteria being less decisive for the preliminary fuel selection.

Following a brief discussion of a selection of the remaining fuels, eight fuels were ultimately considered for the PICE assessment: ethanol, isooctane, isopropanol, methanol, RP-1/kerosene, TMPDA, toluene, and turpentine. It was found that RP-1 is the most suitable fuel with respect to the integration and compatibility criteria considered in the PICE assessment. Ethanol, methanol, isooctane, and isopropanol could all be considered promising alternatives. It could be observed that material compatibility and development level were the two most decisive criteria in the PICE assessment. This indicates the value of these criteria for these types of detailed fuel assessments. It also shows the effectiveness of the toxicity criterion in the preliminary feasibility assessment, as little more distinction could be made in the more detailed PICE assessment. Overall, both RQ-CI-01 and RQ-CI-02 were answered in this chapter, and RP-1 and other kerosene derivatives were concluded to be the most promising fuels for future use with HTP in light of the considered criteria.

7. Vehicle performance model setup

In Chapter 5, the setup and reasoning behind the assessment structure for the first research segment was discussed. As that segment was concerned with the non-performance-related characteristics of the proposed fuels, the corresponding assessment structure was rather qualitative in nature. In the second research segment, an answer was sought to *RQ-PERF-01* and *RQ-PERF-02*, relating to the performance potential of the HTP-based propellant combinations selected in the first research segment. Here, an analytical modelling approach was preferred to allow for the results to be quantified and put through a comparative analysis. In this chapter, the setup and reasoning behind the so-called *vehicle performance model* will be outlined. This will cover the various submodels that were created to support this, including a global optimisation model.

7.1. Vehicle performance model overview

As mentioned, the second research segment was set up to provide an answer to research questions *RQ-PERF-01* and *RQ-PERF-02* through an analytical and numerical model. Both research questions are related to the performance of the proposed HTP-based propellants, with *RQ-PERF-01* specifically covering the propulsion potential of the propellants and *RQ-PERF-02* covering the mass performance of the corresponding launch vehicle concepts. The model created to answer these questions is referred to as the *vehicle performance model*. An overview of the vehicle performance model, its submodels, and its main outputs can be found in Figure 7.1. In this section, each of these models will be discussed briefly as to provide an overview of the elements discussed in this chapter.

Three main models make up the vehicle performance model: the *propulsion model*, the *mass and sizing model*, and the *aerodynamics and trajectory model*. The first of these models, the propulsion model, was set up to answer *RQ-PERF-01* and to provide performance characteristics of the engine concepts as inputs to the other models. This model was created using CEA, for the purpose of modelling the combustion process, and ideal rocket theory. More details and the setup of this model will be discussed in Section 7.2. The mass and sizing model was created to provide scaling of these respective parameters to the proposed launch vehicle concepts corresponding to the choice of propellant for the core stage. Further subdivision was made between the mass and sizing submodels within this model. The former was set up using existing mass estimation relations and inputs from the propulsion model and the guidance model, while the latter was based on scaling and sizing ratios derived from the reference launch vehicle Ariane 6(2). The aerodynamics and trajectory model was created to allow for the states of the proposed launch vehicle concepts to be propagated to the objective states over a realistic trajectory. The trajectory model was based on modules from Tudat, a software platform originating from the Astrodynamics and Space Missions department at TU Delft that allows for computational support tasks in Python and C++ related to astrodynamics and space research. This was supplemented with an aerodynamics model based on inputs from RASAero II, which allowed for the drag coefficient to be defined as a function of the vehicle geometry, velocity state, and angle of attack state at each step during the trajectory. To enable the feasibility of proposed launch vehicle concepts to be assessed, a trajectory optimisation model was created. Here, a set of guidance inputs was optimised through a genetic algorithm for specific trajectory objective states derived from the trajectory of the reference launch vehicle.

To allow for *RQ-PERF-02* to be answered, a global optimisation model was created through which the proposed launch vehicle concepts were optimised for their mass performance. Rather than limit this mass optimisation study to the payload capability of the launch vehicles, another case was added as a means of verification and to allow for a more complete comparison to be made. As such, the two optimisation cases considered in this study were:

- **Case I (GLOM):** For a fixed payload, upper stage, and boosters mass, what minimum gross-lift-off-weight is needed for the conceptual launch vehicles to reach the required end state

conditions?
- **Case II (Payload capability):** For a fixed gross-lift-off mass and boosters mass, what is the maximum payload (upper stage + useful payload) that can be brought on the conceptual launch vehicles while reaching the required end state conditions?

It is important to note that the payload capability referred to in the second optimisation case is the payload capability of the booster stage and the core stage rather than that of the complete launch vehicle. This means that the payload mass considered here is the sum of the upper stage mass and the useful payload mass, where the latter refers to the mass of the payload put in orbit after burnout and separation of the upper stage. The reason for using this definition of payload in this study was to simplify the vehicle performance model as the proposed HTP-based propellants and the subsequent design modifications are integrated into the core stage of the launch vehicle, while the upper stage is left virtually unchanged.
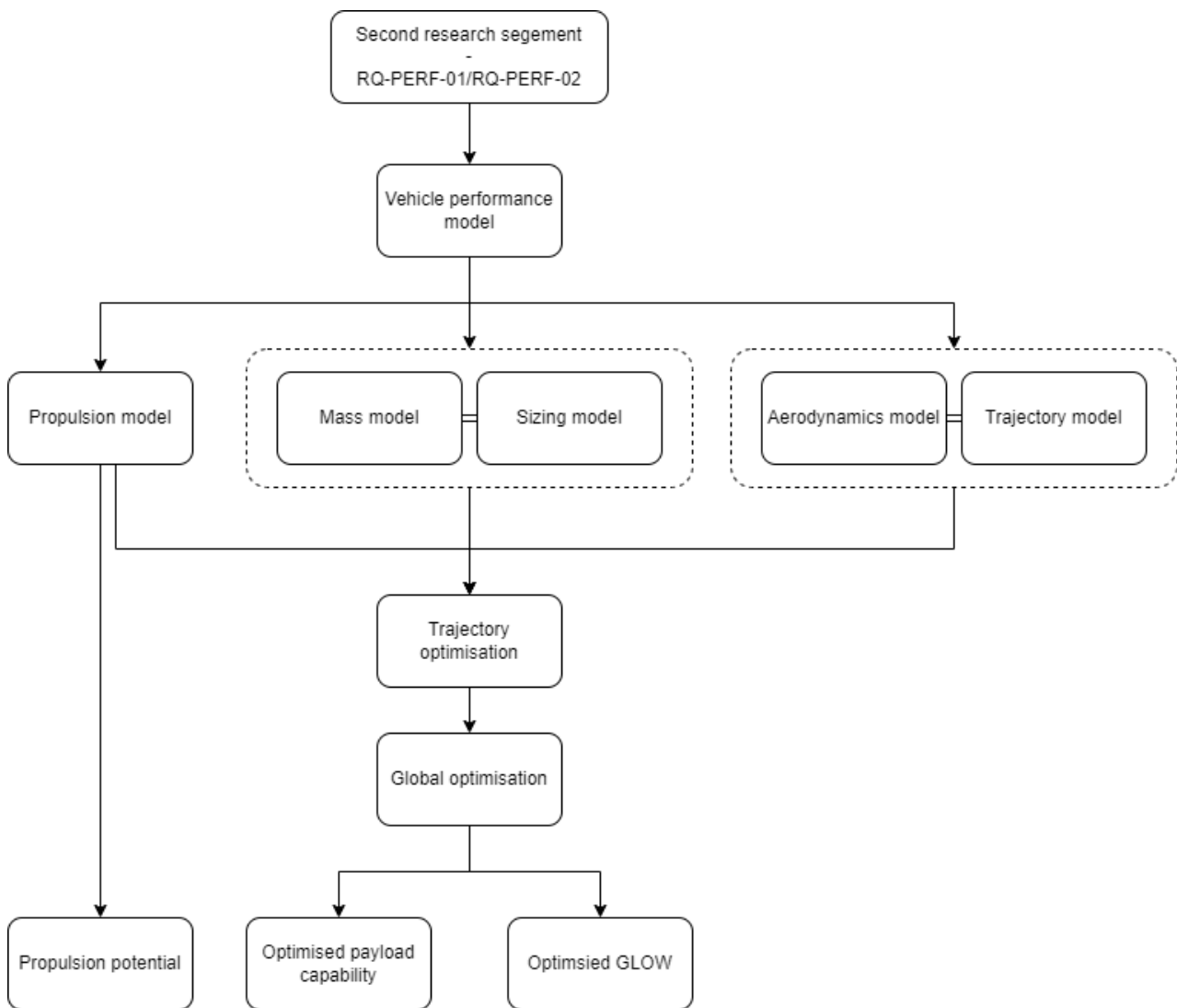
Figure 7.1: Overview of the setup of the vehicle performance model, relevant submodels, and main outputs for the second research segment

7.2. Propulsion model

As per Figure 4.2, the propulsion model was the first model necessary to create the vehicle performance model. This model allowed for several essential engine performance parameters to be modelled and, therefore, for a fundamental and reliable framework to be provided for the trajectory

model. Next to that, this model was needed to estimate the propulsive performance potential of the considered bi-propellant combinations and was thus a key element in answering *RQ-PERF-01*.

7.2.1. Ideal rocket theory

Before going into the structure of the model, it is worth discussing its underlying theory and main outputs and their relevance to the system. As mass is expelled through the nozzle of the rocket engine, a force is generated that provides propulsion to the system. This thrust force is characteristic of the selected engine that drives the rocket to overcome gravitational forces and obtain the acceleration needed to reach the intended orbit. Considering the effects of pressure forces on the effective engine performance, the thrust can be approximated by Equation 7.1. Here, p_e is the pressure observed at the nozzle exit, p_a is the ambient air pressure, and A_e is the area of the nozzle exhaust exit. Note that rocket thrust is expected to be variable during flight, as the ambient air pressure decreases with increasing altitude. If a state were to be assumed where the exit pressure is equal to the ambient pressure throughout the whole trajectory, which can only be approximated by an adaptable nozzle, these terms can be neglected. In this case, a simpler expression based on exhaust momentum flux is left, where $\dot{m}$ is the mass flow at the engine exit and V_e is the exhaust velocity. The mass flow is another important output of the propulsion model, as it describes the amount of propellant that is expelled by the engine each second at a point during flight.[16][139]

$$F = \dot{m}V_e + (p_e - p_a)A_e = \dot{m}U_{eq} \tag{7.1}$$

The specific impulse is a performance parameter that is specific mostly to the selected propellant. It is, in essence, a measure of the efficiency with which the available propellant mass is used to provide a velocity increment to the system, i.e., a measure of how efficiently the propellant is converted to workable impulse. An expression for the specific impulse is given in Equation 7.2, where V_eq is the equivalent exhaust velocity, which is a substitute for the exhaust velocity that also includes pressure losses, as indicated in Equation 7.1. Here, g_0 is the gravitational mass constant at sea level, which represents the acceleration due to gravity at sea level. The thrust and the mass flow are then connected to the specific impulse through Equation 7.3.[16][19]

$$I_{sp} = \frac{U_{eq}}{g_0} \tag{7.2}$$

$$F = I_{sp}g_0\dot{m} \tag{7.3}$$

Generally, launch vehicles are characterised by their high total impulse, which essentially indicates a high total energy exchange during launch sequences. This can also be deducted from the components that make up the total impulse, as shown in Equation 7.4. Here, F is the thrust over time, M_p is the total propellant mass, V_e is the exhaust velocity, and t_b is the total burn time. This last term can be found using Equation 7.5. Note that the total impulse is thus dependent on the amount of propellant mass brought on board. Although it still gives an indication of the overall vehicle performance and the required component type, the total impulse is not as reliable in indicating the potential of propellants and engines as the specific impulse.[16][18]

$$I_{tot} = \int_0^{t_b} F dt = F t_b = M_p V_e \tag{7.4}$$

$$t_b = M_p/\dot{m} \tag{7.5}$$

As outlined in Section 4.2.1, the theory central to the propulsion model is Ideal Rocket Theory (IRT), which allows for rocket propulsion variables to be related through simplified, but reasonably accurate, expressions. Primary assumptions include[16]:

- The working fluid and exhaust gases are homogeneous and of constant composition.
- Exhaust gases obey the ideal gas law.

- In the nozzle, a one-dimensional, steady and isentropic flow is observed.
- The flow is adiabatic.
- Boundary layer and wall friction effects may be neglected.
- The propellant flow rate is constant.
- No discontinuities or shock waves are observed in the nozzle flow.
- A chemical equilibrium exists in the combustion chamber.
- Non-cryogenic propellants are stored at ambient temperature.
- The thrust vector is parallel with the nozzle outlet.

Similar to the specific impulse, the characteristic velocity, c^*, is a metric for the potential of propellants in terms of energy levels for propulsion purposes. As can be derived from Equation 7.6, the characteristic velocity is a function of several factors that are directly related to the combustion of the selected bi-propellants. Here, R_a is the universal gas constant, T is the combustion chamber temperature, and M_w is the molecular weight of the propellant. Γ is the propellant-specific Vandenkerckhove number, which is a function of the specific heat ratio, as can be observed in Equation 7.7.[16][19]

$$c^\star = \frac{\sqrt{R_A T_c / M_w}}{\Gamma} \tag{7.6}$$

$$\Gamma = \sqrt{\gamma}\left(\frac{2}{\gamma+1}\right)^{\frac{\gamma+1}{2(\gamma-1)}} \tag{7.7}$$

The characteristic velocity could be used to formulate a relation to find the first important output from the propulsion model, this being the critical mass flow of the engine. Furthermore, it can be observed from Equation 7.8 that the mass flow also depends on two other variables that are defined the engine design, these being the nozzle throat area, A_t, and the chamber pressure, P_c.[16][18]

$$\dot{m} = P_c A_t / c^\star \tag{7.8}$$

The thrust coefficient is a dimensionless parameter that is useful to better express the performance of engines and propellant combinations as it shows to which degree the thrust is amplified by the nozzle, thus quantifying the effectiveness of the nozzle geometry. As can be deducted from Equation 7.9, the thrust coefficient is directly related to both the thermodynamic properties of the gas in the combustion chamber and the engine nozzle geometry. Similar to the rocket thrust, the ambient pressure is used to calculate the thrust coefficient, thus making this a parameter that is variable during flight as the launch vehicle gains altitude.[140][19]

$$C_F = \frac{F}{p_c A_t} = \Gamma \sqrt{\frac{2\gamma}{\gamma-1}\left(1-\left(\frac{p_e}{p_c}\right)^{\left(\frac{\gamma-1}{\gamma}\right)}\right)} + \left(\frac{p_e}{p_c} - \frac{p_a}{p_c}\right)\frac{A_e}{A_t} \tag{7.9}$$

An important term in Equation 7.9 is the pressure ratio, which relates the pressure at the nozzle exit to the chamber pressure. The pressure ratio was found using an iterative process to solve Equation 7.10, a relation only valid for compressible flow.

$$\frac{A_e}{A_t} = \frac{\Gamma}{\sqrt{\frac{2\gamma}{\gamma-1}\cdot\left(\frac{p_e}{p_c}\right)^{\left(\frac{2}{\gamma}\right)}\left(1-\left(\frac{p_e}{p_c}\right)^{\left(\frac{\gamma-1}{\gamma}\right)}\right)}} \tag{7.10}$$

From Equation 7.2, it could be observed that the second major output variable of the propulsion model, the specific impulse, depends directly on the equivalent exhaust velocity, which is found as the product of the characteristic velocity and the thrust coefficient, as per Equation 7.11. Finally,

with both the mass flow and the equivalent exhaust velocity defined, the thrust of the engine could also be calculated using Equation 7.1

$$U_{\mathrm{eq}} = c^\star C_F \tag{7.11}$$

7.2.2. Propulsion model variables

From the aforementioned relations on ideal rocket theory, it follows that several input variables were needed to find the required performance characteristics of the engine model. Whereas some of these input variables, mostly those related to the engine design and the nozzle geometry, can readily be specified, others, such as the chamber temperature and the combustion gas characteristics, would require further combustion modelling and analysis. For this purpose, it was decided to make use of the CEA tool by NASA[63], which was available on request through the NASA website. This validated and specialised software allowed the equilibrium conditions and combustion processes of rocket engines to be modelled based on a small number of simple inputs concerning the selected engine design settings and propellants.
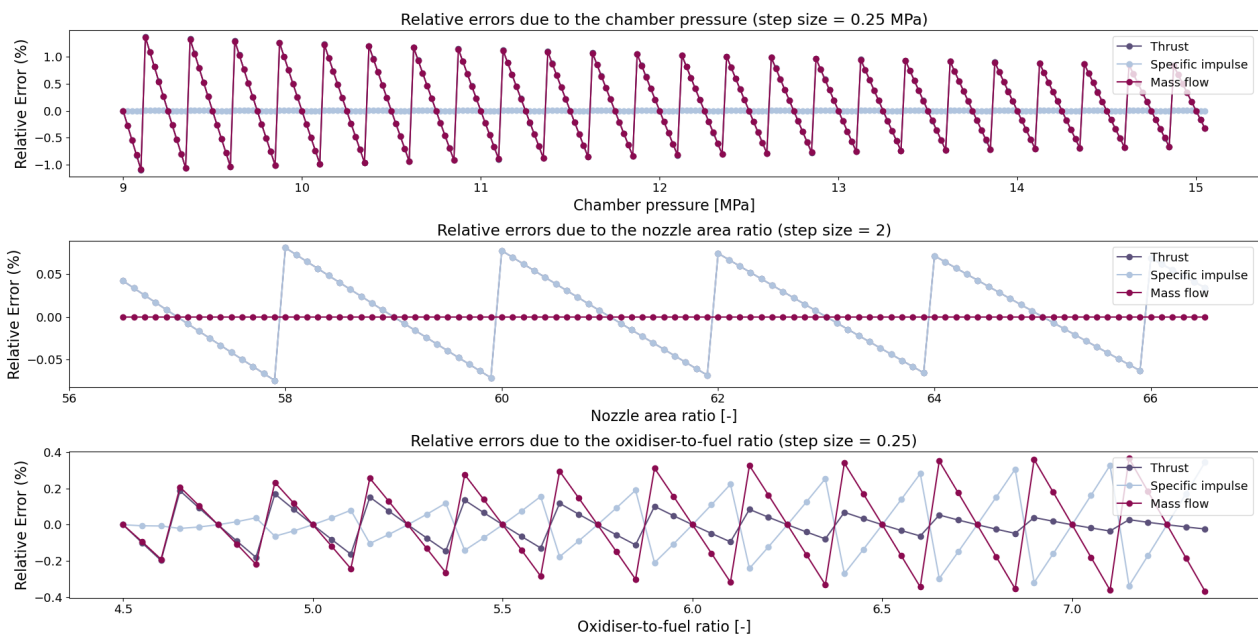
Figure 7.2: The errors introduced in the thrust, specific impulse, and mass flow outputs as a result of the step sizes introduced in the combustion tables for the chamber pressure (top), nozzle area ratio (middle), and propellant oxidiser-to-fuel ratio (bottom), respectively. Note that in the top and middle graphs, the thrust errors coincide with the specific impulse errors due to the nature of the IRT relations. The Vulcain 2 engine and propellant (LH2/LOX) were used as a reference to create these plots.

Rather than integrate the CEA software directly into the propulsion model, it was chosen to tabulate relevant data for all of the considered propellant combinations. Although this significantly decreased the complexity of the model, it also introduced some inaccuracies in the results as the number of data points for each propellant table was limited by the stepsize introduced in the input variables upon creating these combustion tables. This meant that in the propulsion model, the input variables were rounded to the nearest value based on the combustion tables obtained from CEA. Therefore, this effort was a trade-off between computation speed and accuracy. The errors introduced into the model through the stepsize in the combustion tables were visualised in Figure 7.2, where the effect of the stepsize (here for a cryogenic hydrolox engine) is clearly visible in the shape of the graphs. As the input value increases, it is initially rounded down to the closest match in the combustion tables, leading to an underestimation. Once the input value increases further, it is rounded up to the next closest match in the combustion tables, leading to an overestimation and the "jumps", which can be observed in the error graphs. From Figure 7.2, it can furthermore be observed that the maximum error was found to be below 1.5% and that the most

influential input variable was, in fact, the chamber pressure, as could be expected based on the relations introduced through ideal rocket theory.

An overview of the main model input and outputs could be compiled from the CEA tool used to set up the combustion tables and the IRT relations used to calculate the desired model outputs. This overview can be found in Table 7.1.

Table 7.1: Propulsion model variables

Variable	Symbol	Units	Type
Chamber pressure	P_c	Pa	Input
Nozzle area ratio	ϵ	-	Input
Nozzle throat area	A_t	m^2	Input
Oxidiser-to-fuel ratio	O/F	-	Input
Mass flow	$\dot{m}$	kg/s	Output
Specific impulse	I_{sp}	s	Output
Thrust	F	N	Output

7.2.3. Propulsion model validation and correction factors

The use of ideal rocket theory to estimate the performance of the rocket engines leaned on several assumptions that allowed for the model to be constructed using simple relations, thereby eliminating the need for complex and computationally demanding modelling efforts. These assumptions and simplifications did, however, also introduce inaccuracies in the model, as the obtained results were those of an ideal rocket engine. In reality, incomplete combustion, non-ideal gas behaviour, flow separation, and other non-ideal factors are bound to reduce the overall effectiveness and performance of the rocket engine and had to be somehow accounted for to allow for the propulsion model to provide accurate predictions of the engine performance outputs. In literature, this problem is generally solved by introducing so-called quality factors or correction factors into theoretical models, which describe the ratio of real imperfect performance elements to ideal performance elements. Although correction factors can be applied to several different parameters, it was decided to limit the number of correction factors in this study to two, applied to the specific impulse and the mass flow, respectively. This also directly imposed a correction factor on the thrust, as it is related to the ideal specific impulse and the ideal mass flow through:[16][18]

$$F_{real} = \zeta_m \dot{m}_{id} \zeta_{isp} I_{sp,id} \tag{7.12}$$

where ζ_m is the mass flow correction factor, also known as the discharge correction factor, and ζ_{isp} is the specific impulse correction factor. The subscripts *real* and *id* refer to the real and ideal values for the performance elements, respectively.

Historical engine data was used to obtain relevant data for the correction factors. A detailed overview of the characteristics of the engines considered for this analysis can be found in Appendix E. In Table 7.3, the errors observed by estimating the values of thrust, specific impulse, and mass flow with the propulsion model without any correction factors were tabulated for a total of thirteen engines considered in this study. This comparison was made for performance at vacuum conditions to allow for the effects and any inaccuracies introduced by the atmosphere to be neglected. Based on this data, the correction factors needed to minimise the observed errors were derived to be $\zeta_m = 1.01$ and $\zeta_{isp} = 0.93$, respectively. The errors observed by comparing the engine data through the modified propulsion model, including correction factors, were tabulated in Table 7.4. It should be noted that an attempt was made to derive correction factors based on only the most entries, these being cryogenic, core stage engines. However, no notable differences were found.

To obtain more reliable and relevant results for the correction factors with respect to this study, a second set of correction factors was derived based on a selection of engines excluding notable outliers. The exclusion of the RS-68A, RS-25, and J-2 engines led to the new correction factors to

be $\zeta_m = 1.07$ and $\zeta_{isp} = 0.93$, respectively. An overview of the mean error and the error standard deviation in the engine data can be found in Table 7.2 for the three cases considered in this analysis (no correction factors, correction factors with outliers, and correction factors without outliers). It was concluded that excluding outliers from the analysis only led to marginally better results for the thrust estimations while inducing less accurate estimates for the mass flow and the specific impulse. Therefore, it was decided to employ the initial set of correction factors in the propulsion model for the remainder of this study. Furthermore, the correction factors were found to be agreeable with typical ranges for these factors described in literature. In particular, the comparison was made with Rozemeijer[70], who achieved a similar level of performance estimation accuracy in his study, albeit with a remarkably low value for the mass flow correction factor.

Table 7.2: Mean errors and standard deviation of the errors observed amongst engines based on specific sets of correction factors and a comparison of these correction factors to values found in literature.

	No correction factors	Outliers included	Outliers excluded	Humble et al. [106]	Sutton [16]	Rozemeijer [70]
ζ_m	1	1.01	1.07	0.98-1.15	>1	0.95
ζ_{isp}	1	0.93	0.93	0.85-1.03	>0.85	0.98
ζ_f	1	0.94	1	0.92-1	>0.85	0.93
Mass flow mean error [%]	0.1	0.7	3.8	-	-	2.7
Mass flow standard deviation [%]	11.1	11.3	12.4	-	-	13.8
Isp mean error [%]	7.3	0.0	-0.4	-	-	0.3
Isp standard deviation [%]	1.4	1.3	1.5	-	-	3.0
Thrust mean error [%]	7.9	1.7	0.0	-	-	2.2
Thrust standard deviation [%]	10.4	9.8	7.1	-	-	11.6

It is worth noting that while initially attempted, it was not pursued to derive a set of correction factors specifically for storable engines. The reason for this was the lack of reliable and relevant data available to employ for this analysis. Data on current HTP-based launch systems, such as those developed by the British company Skyrora, is very limited, while retired models, such as the Gamma 301 engine used on the Black Knight launch vehicles, were not included due to the complexity of the multi-chamber design. Finally, it was found that the reported performance of the storable engines included in the analysis showed to be sufficiently agreeable with what was predicted through the propulsion model after applying the same set of correction factors that will be used to predict the performance of the cryogenic engines. As such, no further adjustments were made to the correction factors regarding compatibility with storable engines.

Table 7.3: Real thrust, specific impulse, and mass flow of launch vehicle engines at vacuum conditions compared to model predictions before applying correction factors

Engine specifications		Thrust			Specific impulse			Mass flow		
Name	Type	Real [kN]	Model [kN]	Error [%]	Real [kN]	Model [kN]	Error [%]	Real [kN]	Model [kN]	Error [%]
RS-68A	Cryogenic	3558	4461	25.4	411	444	8.0	883	1023	15.9
RS-25	Cryogenic	2278	2695	18.3	452	471	4.2	514	582	13.2
HM7B	Cryogenic	65	68	4.6	446	482	8.1	15	14	-6.7
J-2	Cryogenic	1033	1260	22.0	421	454	7.8	250	283	13.2
RL10B-2	Cryogenic	110	126	14.5	466	494	6.0	24	26	8.3
Vinci	Cryogenic	180	193	7.2	467	495	6.0	39	39	0.6
Vulcain 2.1	Cryogenic	1371	1323	-3.5	432	469	8.6	326	287	-12.0
Vulcain 2	Cryogenic	1140	1051	-7.8	431	467	8.4	258	229	-11.2
LE-5B	Cryogenic	137	151	10.2	449	487	8.5	33	31	-6.8
LE-7A	Cryogenic	1098	1213	10.5	438	466	6.4	262	265	1.1
Viking 5C	Storable	758	731	-3.6	278	302	8.6	278	246	-11.5
Vikas 4B	Storable	804.5	788	-2.1	302	325	7.6	285	246	-13.8
RD-275M	Storable	1832	1968	7.4	316	335	6.1	539	597	10.7

Table 7.4: Real thrust, specific impulse, and mass flow of launch vehicle engines at vacuum conditions compared to model predictions after applying correction factors

Engine specifications		Thrust			Specific impulse			Mass flow		
Name	Type	Real [kN]	Model [kN]	Error [%]	Real [kN]	Model [kN]	Error [%]	Real [kN]	Model [kN]	Error [%]
RS-68A	Cryogenic	3558	4203	18.1	411	414	0.7	883	1034	17.1
RS-25	Cryogenic	2278	2539	11.5	452	439	-2.8	514	588	14.4
HM7B	Cryogenic	65	64	-1.4	446	449	0.8	15	14	-5.7
J-2	Cryogenic	1033	1187	14.9	421	423	0.6	250	286	14.4
RL10B-2	Cryogenic	110	119	7.9	466	461	-1.1	24	26	9.5
Vinci	Cryogenic	180	182	1.0	467	462	-1.2	39	39	1.7
Vulcain 2.1	Cryogenic	1371	1247	-9.1	432	437	1.2	326	290	-11.0
Vulcain 2	Cryogenic	1140	990	-13.1	431	435	1.0	258	231	-10.3
LE-5B	Cryogenic	137	142	3.9	449	454	1.1	33	31	-5.8
LE-7A	Cryogenic	1098	1143	4.1	438	435	-0.8	262	265	2.1
Viking 5C	Storable	758	689	-9.1	278	282	1.3	278	246	-10.6
Vikas 4B	Storable	804.5	742	-7.7	302	303	0.4	285	246	-12.9
RD-275M	Storable	1832	1854	1.2	316	312	-1.1	539	597	11.9

Table 7.5: Real thrust, specific impulse, and mass flow of launch vehicle engines at vacuum conditions compared to model predictions after applying correction factors and excluding outliers

Engine specifications		Thrust			Specific impulse			Mass flow		
Name	Type	Real [kN]	Model [kN]	Error [%]	Real [kN]	Model [kN]	Error [%]	Real [kN]	Model [kN]	Error [%]
HM7B	Cryogenic	65	68	4.4	446	482	0.4	15	14	0.2
RL10B-2	Cryogenic	110	126	14.3	466	494	-1.5	24	26	16.4
Vinci	Cryogenic	180	193	7.0	467	495	-1.5	39	39	8.1
Vulcain 2.1	Cryogenic	1371	1323	-3.7	432	469	0.9	326	287	-5.4
Vulcain 2	Cryogenic	1140	1051	-8.0	431	467	0.7	258	229	-4.7
LE-5B	Cryogenic	137	151	10.0	449	487	0.8	33	31	0.1
LE-7A	Cryogenic	1098	1213	10.3	438	466	-1.1	262	265	8.6
Viking 5C	Storable	758	731	-3.7	278	302	1.0	278	246	-5.0
Vikas 4B	Storable	804.5	788	-2.2	302	325	0.0	285	246	-7.4
RD-275M	Storable	1832	1968	7.2	316	335	-1.4	539	597	14.7

7.2.4. Propulsion model constraints
In setting up the propulsion model, several constraints and assumptions were taken into account. The most important of these are discussed here.

Number of thrust chambers
Next to the regular single-chamber engines considered for the validation of the propulsion model, engines exist that are designed with multiple thrust chambers. An example of such an engine is the Gamma 301 rocket engine, which was designed with four thrust chambers operating on a kerosene/HTP propellant.[44] The intuitive advantages of these multi-chamber designs are higher fault tolerance, a more varied throttle range, increased thrust, and a more compact design. Upon validating the model, significant errors were observed when trying to predict the performance of engines with a multi-chamber design. Thus, It was assumed that the dynamics and processes in these engines are too complex to be modelled with IRT. A constraint was placed on the model, limiting the performance prediction range to engines with only one thrust chamber.

Input boundaries
As per Table 7.1, the propulsion model allows for four input variables to be defined. It was decided to impose boundaries on these input variables to ensure a high level of validity and a minimum level of error within the model predictions. These boundary values were derived from the minimum and maximum engine design parameters observed amongst the reference engine listed in Table E.1. Here, it could be observed that for the reference engines operating at these boundary values, the error of the model was already somewhat significant. This is illustrated by the RS-68A, for which the maximum throat area and exit diameter were reported amongst the reference engines and for which the highest errors were observed in the validation process, as can be seen in Table 7.3. Additionally, the propulsion model was not tested for engines outside of these boundaries, meaning that no information is available on the accuracy of the model outside of the imposed boundary ranges. Therefore, it was deemed a conservative choice to impose these constraints.

7.3. Mass and sizing model
The second main model to be set up in creating a numerical framework for the vehicle performance model was the mass and sizing model. This model was essential in providing a quantitative basis for comparing the payload capabilities of the proposed launch vehicle concepts and in setting up relevant mass and size inputs for the aerodynamics and trajectory model. As such, it was crucial for answering RQ-PERF-02.

7.3.1. Mass model selection and validation
As this study focused on the integration of new HTP-based bi-propellant combinations into the core stage of an existing reference launch vehicle, this being Ariane 6, it was necessary to estimate the effects of these propellant choices on the mass of the core stage. This was important as it implied a shift in the mass distribution of the launch vehicle concepts over their different stages, which in turn affected the trajectory and the payload capabilities of the launch vehicle concepts. As explained in Section 4.2.1, the mass model was created using existing mass estimation relations (MER) based on historical data. For this purpose, two different sets of MERs were considered, these being the relations by Akin[84] and those by Zandbergen[73]. Akin follows a bottom-up approach in which the masses of several relevant launch vehicle components are estimated and later summed together to come to a final estimate for the launch vehicle (stage) mass. Although this method provides a more detailed and complete overview of the mass distribution of the launch vehicle, it was also found to require more inputs and more complex modelling. Zandbergen requires fewer inputs but was found to be less informative, and the accuracy of this approach for this study has to be investigated due to the wide validity range of the MERs.

In order to make a well-founded choice on which relations to integrate into the mass estimation model, a comparative analysis was performed in which simplified models based on Akin and Zandbergen were used to estimate the dry mass of the liquid-propellant based core stages of five medium-lift launch vehicles. Here, both Ariane 5 and Ariane 6 were considered due to the relevance of these vehicles to the study. Furthermore, with H-IIB, Ariane 6, and GSLV Mk.III, three more recent

launch vehicle models were considered. Therefore, including these launch vehicles in the analysis allowed for the transferability of the MERs and their ability to accurately predict the masses of modern launch vehicles to be tested. It should be noted that while this approach proved valuable for the analysis, the information found on these three launch vehicles was deemed less reliable and was thus treated more critically. Finally, both GSLV Mk.III and Atlas V 401 were selected to evaluate the effectiveness of the proposed MERs for launch vehicle stages employing engines working with (partially) storable propellants. Detailed results of the errors observed in launch vehicle stage mass predictions using Akin and Zandbergen were tabulated in Table 7.7. Next to the dry stage mass of the selected launch vehicle stages, the propellant and residual mass of the stages and the gross lift-off mass (GLOM) of the launch vehicles were estimated to provide a more complete overview of the accuracy of the MERs.

Upon inspecting the errors in Table 7.7, several important observations could be made. It was clear that with both sets of MERs, the dry stage masses were underestimated in most cases. These underestimation errors were most significant for the model constructed with Akin. Another interesting observation was that Zandbergen proved to be more accurate for older launch vehicle models. This is sensible as these vehicles were most likely part of the data sets used to create Zandbergen's MERs. Yet, as a result of technological advancements and the use of more lightweight materials, it was expected that the masses of more recent launch vehicles would be overestimated. The error observed in the predicted gross lift-off mass was generally rather low, where especially for the reference vehicle, Ariane 6, both the models based on Akin and Zandbergen resulted in very agreeable estimates. The GLOM error was found to be larger for the Atlas V 401 case, where the error was mostly the result of a significant overestimation of the stage propellant mass. Here, it was argued that the multi-chamber configuration of the RD-180 engine could have been an influential factor in this large error, as it was thought to require more advanced modelling for accurate predictions of the mass flow and other characteristics.

Table 7.6: Mean errors observed in launch vehicle stage mass predictions by Zandbergen (Z) and by Akin (A) with respect to the real (R) component masses.

	GLOM		Stage dry mass	
	Mean error [%]	Standard deviation [%]	Mean error [%]	Standard deviation [%]
Akin	0.71	4.16	-82.84	34.44
Akin + residual	0.71	4.16	-32.21	24.43
Zandbergen	1.79	4.84	-15.60	18.85
Zandbergen + residual	1.79	4.84	6.41	17.04

One reason for the continuous underestimation of the stage dry masses with the MERs by Zandbergen and Akin was thought to be the exclusion of the residual propellant mass in the dry mass budgets upon setting up the MERs. This residual mass refers to the additional propellant mass that is either left in the propellant tank or that is left in the propellant tanks at the point of stage separation. A factor of 1.02, or 2%, was used to account for this factor.[106] While this is propellant mass, it is not used during flight and thus carried on the launch vehicle up to the point of stage separation. Given the close approximation of the propellant mass over the five cases and the more significant errors observed in the dry mass estimations, it was believed that the residual mass was considered part of the dry mass budgets for most values found in literature, while it was not considered in the MERs created by Zandbergen and Akin Adding these residual mass terms to the mass model predictions let to overall more agreeable estimates.

In Table 7.6, the mean and standard deviation of the observed errors across all five cases for both mass estimation models can be found. From this, the conclusions drawn from Table 7.7 were confirmed as the model based on Akin led to larger errors and less accuracy than the model based on Zandbergen. Due to the magnitude of the observed errors, it was also deemed that Akin could not be used to predict system masses for this study accurately. As the magnitude of the mean error

and standard deviations for the model based on Zandbergen were 15.60% and 18.5%, respectively, it was thought that this model was sufficiently accurate for use in this study. Furthermore, when considering the residual volume as part of the dry mass budget, the accuracy of the model was improved even further, with a magnitude of the mean error and standard deviations of 6.41% and 17.04%, respectively. This factor was found to be especially effective for the more recent launch vehicles. As such, the modelling approach of using MERs by Zandbergen with an additional input of the residual propellant mass was selected for this study.

Table 7.7: Comparison of errors observed in launch vehicle stage mass predictions by Zandbergen (Z) and by Akin (A) with respect to the real (R) component masses.

	LLPM (Ariane 6)		H173 (Ariane 5)		CCB (Atlas V 401)		First stage (H-IIB)		L110 (GSLV Mk.III)	
Oxidiser	LOX		LOX		LOX		LOX		NTO	
Fuel	LH2		LH2		RP-1		LH2		UDMH	
Stage burn time [s]	429		540		253		352		203	
Stage # engines	1		1		1		2		2	
Nozzle area ratio [-]	61.5		45		36.9		52		13.9	
O/F [-]	6.03		5.3		2.72		5.9		1.7	
Vaccuum thrust [kN]	1371		1340		4152		1078		766	
Mass flow [kg/s]	326		316		1250		246		275	
	Mass [kg]	Model error [%]	Mass [kg]	Model error [%]	Mass [kg]	Model error [%]	Mass [kg]	Model error [%]	Mass [kg]	Model error [%]
GLOM (R)	530000	0.00	777000	0.00	334500	0.00	531000	0.00	630600	0.00
GLOM (Z)	530359	0.07	781623	0.59	372988	10.32	522819	-1.56	627625	-0.47
GLOM (A)	526326	-0.70	777453	0.06	363292	7.93	517216	-2.66	623836	-1.08
Stage dry mass (R)	15637	0.00	14700	0.00	21054	0.00	24200	0.00	10600	0.00
Stage dry mass (Z)	13345	-17.18	15270	3.74	21056	0.01	16884	-43.33	8742	-21.26
Stage dry mass (A)	9312	-67.93	11100	-32.43	11360	-85.34	11281	-114.51	4953	-114.00
Stage propellant mass (R)	140000	0.00	170000	0.00	284089	0.00	177800	0.00	115000	0.00
Stage propellant mass (Z/A)	139854	-0.10	170640	0.38	316250	10.17	173466	-2.50	111650	-3.00
Stage residual mass (Z/A)	2797	-	3413	-	6325	-	3469	-	2233	-

7.3.2. Mass model setup and variables

As per the research goal of this study and the research questions related to vehicle performance, in particular RQ-PERF-02, the most essential outputs of the mass estimation model were identified to be the gross lift-off mass and the payload capability of the proposed launch vehicle concepts. As argued earlier in this section, the proposed integration of new HTP-based bi-propellant combinations was targeted at the core stage. Therefore, the masses of the main components of the core stage were labelled as output variables for the model, while the other stages of the launch vehicle were considered constants based on the Ariane 6 reference vehicle.

A top-level distinction to be made in terms of the main mass components of the core stage was between the wet mass and the dry mass of the core stage. The former is found by adding the latter to the core stage propellant mass, as per Equation 7.13, where M_{wet} is the wet mass, M_{dry} is the dry mass, and M_p is the propellant mass of the stage.

$$M_{wet} = M_{dry} + M_p \tag{7.13}$$

The MERs by Zandbergen effectively allowed for the dry mass of the core stage to be calculated. Here, Equation 7.14 was presented as the central equation, where M_{const} is the construction mass, N_{eng} is the number of engines, and M_{eng} is the mass per engine.[73]

$$M_{dry} = M_{const} + N_{eng}M_{eng} \tag{7.14}$$

The construction mass or mass of construction is a term referring to the collection of all components making up the dry mass of a stage, except for the engines. The main contributions to this construction mass come from the mass of the propellant tanks, avionics, wiring, skin (if applicable), and insulation. Zandbergen makes an important distinction as Equation 7.15 expresses the construction mass in function of the propellant mass for cryogenic stages, while a separate relation, Equation 7.16, was created for semi-cryogenic and storable stages. Note that both the input and the outputs are measured in metric tons.[73]

$$M_{const} = 0.0641M_p + 2.083 \tag{7.15}$$

$$M_{const} = 0.0461M_p + 1.876 \tag{7.16}$$

Zandbergen created a separate set of MERs for the purpose of accurately estimating engine masses since these make up a large part of the total dry mass of launch vehicle stages and since further distinction needed to be made between pump-fed systems and pressure-fed systems. Equation 7.17 shows the engine mass in function of the vacuum thrust of the engine for cryogenic engines, while Equation 7.18 covers engines using semi-cryogenic and storable bi-propellants. Here, the engine mass is expressed in kilograms, while the vacuum thrust is expressed in Newtons.[85]

$$M_{eng} = 0.00514F_{vac}^{0.92068} \tag{7.17}$$

$$M_{eng} = 0.0011F_{vac} + 27.702 \tag{7.18}$$

When using existing MERs, it is important to state a measure of the validity range and accuracy to justify the applicability of these relations to the study and to identify relevant constraints with respect to the implementation of these relations in models. Therefore, the validity range, number of data points, residual standard error (RSE) and R^2 value for each of the MERs created by Zandbergen were tabulated in Table 7.8.

Table 7.8: validity range, number of data points, residual standard error (RSE) and R^2 for the MER created by Zandbergen[73][85]

Equation	Validity range	# Data points	RSE [%]	R^2
7.15	8.5-427 [t] (Propellant mass)	26	36.3	0.941
7.16	0.5-2037.5 [t] (Propellant mass)	34	40.1	0.9845
7.17	50-3500 [kN] (Vaccuum thrust)	22	13.1	0.991
7.18	50-3500 [kN] (Vaccuum thrust)	25	25.8	0.987

Most of the total wet mass of the core stage is made up of its propellant mass. As such, it was deemed crucial to define a relation such that this output variable could be calculated in a consistent and uncomplex manner. Therefore, the propellant mass was defined as the multiplication product of the total mass flow in the core stage propulsion system and the engine burn time through Equation 7.19. Here, N_{eng} is the number of engines, $\dot{m}_{eng}$ is the mass flow per engine, and t_b is the burn time of the stage i.e., the time between engine ignition and engine shutdown.

$$M_p = N_{eng} \dot{m}_{eng} t_b \qquad (7.19)$$

As per the overview of the vehicle performance model in Section 7.1, two main cases were defined for the launch vehicle optimisation effort, these being the optimisation of the gross lift-off mass and the payload capability, respectively. As such, the GLOM and the payload mass were considered the main output variables for the mass model. Although these output variables are inherently different, the mass estimation and sizing of the core stage remained the same for both cases. The only difference lies in the approach to the problem. For the cases of GLOM and payload capability, the following approaches were adopted:

- **Case I (GLOM):** In the case where the GLOM was set to be the main output for the mass estimation model, the payload mass was constrained to be a constant in accordance with the payload for the reference case i.e., Ariane 6(2) to a geostationary transfer orbit and the specific separation altitude/velocity given by the mission profile. Subsequently, the masses of the different stages were then summed to obtain the GLOM. From Table 4.3, the constant value for the payload mass can be found to be 4.5t.

- **Case II (Payload capability):** In the case where the payload capability was set to be the main output for the mass estimation model, the GLOM was constrained to be a constant in accordance with the GLOM for the reference case i.e., Ariane 6(2) to a geostationary transfer orbit and the specific separation altitude/velocity given by the mission profile. Subsequently, the payload mass was found to be the difference between the GLOM and the summed masses of the core stage and the boosters, respectively. From Table 4.3, the constant value for the GLOM can be found to be 530t.

It is worth repeating the definition of payload capability within this study, as stated in Section 7.1. Rather than referring to the useful mass that is brought into its required orbit by the launch vehicle systems, the payload in this study is a term used to refer to the collection of systems left after the separation of the core stage. It thus encompasses both the useful launch vehicle payload and the complete second stage. In this regard, the payload capability is referred to as the payload capability of the boosters and the core stage rather than that of the entire launch vehicle. Based on the mass budget presented in Table 7.9, this "core stage payload mass" would be 52t rather than the 4.5t that is the useful payload mass. The useful payload of the launch vehicle was estimated from this by multiplying the obtained payload capability of the core stage, which is effectively the summed mass of the second stage and the useful payload of the launch vehicle, with a factor representing

the payload ratio for the second stage.

An important set of constants in the mass estimation model, regardless of the selected case, were the masses of the non-variable stages of the reference launch vehicle. Therefore, it was important to have a clear and well-defined mass budget for the Ariane 6 in its 2-booster configuration. This mass budget, including the mass values for the main launch vehicle stage components, can be found in Table 7.9. In the original mass budget, $19t$ was unaccounted for as compared to the reference GLOM found in literature. It was argued that this mass deficit could come from systems such as the interstages, unburned solid propellant, the payload adapter, the vehicle equipment bay, and other support systems. Therefore, this unaccounted mass was evenly distributed over the three main stages, leading to the adjusted mass budget in Table 7.9.

Table 7.9: Original and adjusted mass budgets for the Ariane 6 reference vehicle with a 2-booster configuration

Stage	Stage component masses	Original mass budget	Adjusted mass budget
Booster stage	Boosters dry mass	22	22
	Boosters propellant mass	288	288
	Booster stage other	0	6
Core stage	Core stage dry mass	16	16
	Core stage propellant mass	140	140
	Core stage other	0	6
Upper stage	Upper stage dry mass	7	7
	Upper stage propellant mass	31	31
	Fairing	2.5	2.5
	Upper stage other	0	7
General	Payload mass	4.5	4.5
	GLOM	511	530
	Unaccounted mass	19	0

From the MERs and the general setup introduced in this section, a list of the main input and output variables for the mass estimation model could be compiled. This overview can be found in Table 7.10.

Table 7.10: Mass model variables

Variable	Symbol	Units	Type
Core stage burn time	t_b	s	Input
Engine mass flow	$\dot{m}_{eng}$	kg/s	Input
Engine vacuum thrust	F_{vac}	N	Input
Number of engines	N_{eng}	-	Input
Gross lift-off mass	$GLOM$	kg	Input/Output
Payload mass	M_{pay}	kg	Input/Output
Core stage dry mass	M_{dry}	kg	Output
Core stage propellant mass	M_p	kg	Output
Core stage wet mass	M_{wet}	kg	Output

7.3.3. Sizing model setup and variables

While characterised by a lower performance as compared to hydrolox systems, a major advantage of HTP-based bi-propellants is their high density. This advantage is reflected to some extent in the mass, but also more significantly in the size of the systems employing HTP-based bi-propellants. Smaller launch vehicle designs, in turn, lead to significant gains in terms of aerodynamic efficiency. As such, including a sizing tool in this study was deemed highly important.

For this study, the main purpose of the sizing model was to obtain an estimate of the main outer dimensions of the proposed launch vehicle concepts. As such, a set of simple relations was created to estimate the lengths and diameters of the main stages and, with that, the overall vehicle length. Due to the nature of this study, the most variable components within the sizing model were found to be the core stage propellant tanks. Based on the propellant mass estimated through the mass model, the fuel tank and the oxidiser tank volumes for the core stage were found using Equation 7.20 and 7.21, respectively. Here, M_p is the total propellant mass, O/F is the oxidiser-to-fuel ratio of the propellant, ρ_f is the density of the fuel, ρ_{ox} is the density of the oxidiser, and F_u is the ullage factor. The latter is a factor introduced to estimate the unfilled volume in propellant tanks needed to account for the thermal expansion of the propellant. It was set at 1.02 based on Humble et al.[106].

$$V_f = \frac{M_p}{(1 + O/F)\rho_f}F_u \tag{7.20}$$

$$V_{ox} = \frac{M_p \cdot O/F}{(1 + O/F)\rho_{ox}}F_u \tag{7.21}$$

As will be discussed in Section 7.5.1, the stage diameter was an essential input in determining the aerodynamic coefficients of the launch vehicle concepts through the aerodynamics model. Therefore, the stage diameter was arguably the most important output variable of the sizing model. Several factors were considered to determine the stage diameter for launch vehicle concepts, thereby striking a balance between aerodynamic efficiency, structural integrity, and payload needs. It is important to remark that it was assumed that the launch vehicle concepts are not tapered, meaning that the diameter could be considered constant over the full length and both the core stage and the upper stage of the vehicles. As such, a dynamic model had to be created, for which constraints of both the upper stage and lower stage of the launch vehicle concepts are considered to find an optimum stage diameter. This was deemed to be especially relevant for Case II of this study regarding the optimisation of the payload capability, as this required a high number of variations in the masses of the upper stage and the payload to be considered. To allow for maximum aerodynamic efficiency while ensuring structural integrity, the maximum fineness ratio constraint was introduced, as will be explained in Section 7.3.5. The fineness ratio is a measure of the slenderness of a launch vehicle as it relates the total length of a launch vehicle to its diameter. Based on maximum fineness ratio constraints derived from literature and volume estimates, an initial minimum diameter could be derived for both stages as per Equation 7.22. Here, $\beta_{s,c}$ refers to the stage-specific fineness ratio constraint, and V_s refers to the stage volume estimates.

$$D = \left(\frac{4V_s}{\pi\beta_{s,c}}\right)^3 \tag{7.22}$$

Next, the most constraining of these minimum stage diameter estimates was selected and checked for compliance with the other minimum diameter constraints discussed in Section 7.3.5, where, if necessary, adjustments were made to come to a final diameter value. It was found that for most cases, the upper stage diameter proved to be the constraining factor for single-engine launch vehicle concepts, while the core stage diameter was the constraining factor for multi-engine launch vehicle concepts.

Following Equation 7.22, it was necessary to estimate the volume of the upper stage, which was variable for the second optimisation case. Therefore, the upper stage density, rho_{S2}, was introduced as a model constant. This term effectively considers the total sum of the core stage payload, this being the upper stage systems and the useful launch vehicle payload, with respect to its total volume. The value for the constant was derived from the Ariane 6(2) reference case. Although this would not ensure a high accuracy in the estimation, it allowed for a simple sizing method that could be used over a large range of inputs. The upper stage volume could thus be estimated using Equation 7.23. Subsequently, the upper stage length is found using Equation 7.24.

$$V_{S2} = \frac{M_{pay} + M_{S2}}{\rho_{S2}} \tag{7.23}$$

$$L_{S2} = \frac{4(M_{pay} + M_{S2})}{\pi \rho_{Upper} D^2} \tag{7.24}$$

Next, the lengths of the propellant tanks were calculated using Equation 7.25 and 7.26. As the propellant tanks were considered the most variable and, therefore, influential components for this study in terms of sizing, the core stage length was defined by Equation 7.27. Here, the terms D_f and D_{ox} are added to account for the length of the spherical end caps. L_0 is a constant, set to $7.09m$ based on the Ariane 6 reference vehicle, added to account for the collective length of all other systems, mostly related to propulsion, other than the propellant tanks. This was done to keep the model robust and simple.

$$L_f = \frac{4V_f}{\pi D^2} - \frac{2D}{3} \tag{7.25}$$

$$L_{ox} = \frac{4V_{ox}}{\pi D^2} - \frac{2D}{3} \tag{7.26}$$

$$L_{S1} = L_0 + L_f + L_{ox} + D_f + D_{ox} \tag{7.27}$$

Finally, the total launch vehicle length is found as the sum of the upper stage length and the core stage length. The final output of the sizing model is the total launch vehicle fineness ratio, which is based on the total launch vehicle length and diameter and is a measure of the aerodynamic efficiency of the launch vehicle design. Based on the setup of the sizing model, as presented in this section, a list of the main input and output variables for the sizing model could be compiled. This overview can be found in Table 7.11

Table 7.11: Sizing model variables

Variable	Symbol	Units	Type
Core stage propellant mass	M_p	kg	Input
Fuel density	ρ_f	kg/m^3	Input
Oxidiser density	ρ_{ox}	kg/m^3	Input
Oxidiser-to-fuel ratio	O/F	-	Input
Core stage fineness ratio	β_{S1}	-	Output
Core stage length	L_{S1}	m	Output
Fuel tank length	L_f	m	Output
Launch vehicle (stage) diameter	D	m	Output
Oxidiser tank length	L_{ox}	m	Output
Total launch vehicle fineness ratio	β_{tot}	-	Output
Total launch vehicle length	L_{tot}	m	Output
Total launch vehicle reference area	S_{tot}	m^2	Output
Upper stage fineness ratio	β_{S2}	-	Output
Upper stage length	L_{S2}	m	Output

7.3.4. Sizing model Sensitivity

Due to how the sizing model was set up, providing the exact inputs of the Ariane 6 launch vehicle would lead to an exact match with the component lengths of the vehicle found in literature, as shown in Table 7.12. Note that the total launch vehicle length found through the sizing model corresponds with the short fairing configuration, which is only available with Ariane 6(2). The sizing model was based on the short fairing because this was deemed more sensible for the given reference case i.e., a $4500kg$ payload to GTO.

Table 7.12: Sizing of Ariane 6 (with short fairing configuration) through the sizing model

Variable	Unit	Value	Type
Core stage propellant mass	kg	140000	Input
Payload (upper stage + useful payload)	kg	52000	Input
Oxidiser-to-fuel ratio	-	6.03	Input
Core stage length	m	27.5	Output
Upper stage length	m	29.5	Output
Total launch vehicle length	m	57	Output

Although the reference input variables led to a good match with the size of the reference launch vehicle, it was worth investigating the sensitivity of the sizing model with respect to its main input variables. From the setup of the sizing model in Section 7.3.3, it could be deduced that the main input variables are the core stage propellant mass and the core stage payload mass (upper stage mass + useful payload mass). Therefore, the behaviour of the model with respect to these input parameters was investigated by varying the relative mass distribution between these two input variables while maintaining a constant GLOM. The results of this analysis are visualised in Figure 7.3
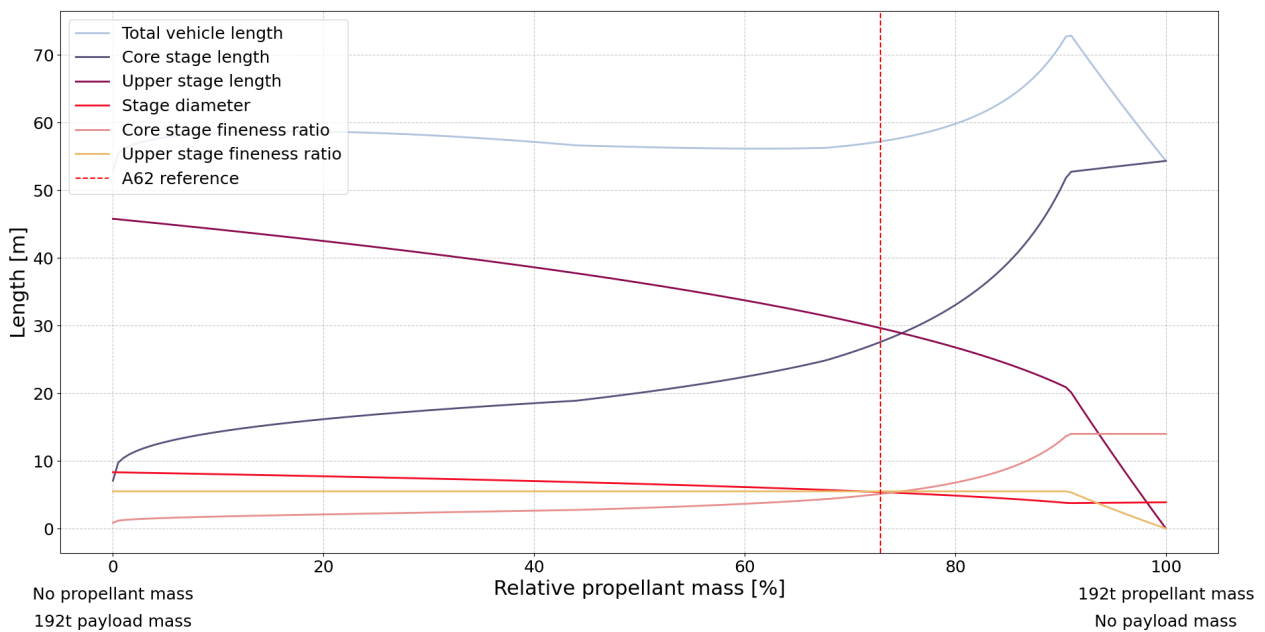
Figure 7.3: Sensitivity of the launch vehicle (stage) length with respect to the relative distribution of mass between the core stage propellant and the payload (upper stage + useful payload)

Several observations could be made. The stage lengths vary almost linearly on the left side of the figure, representing launch vehicle concepts with a high payload mass and a low propellant mass. In this part of the plot, the total launch vehicle length can also be observed to be near-constant. For launch vehicle concepts with a high propellant mass and a low payload mass, visualised on the right side of the plot, an exponential change in the stage lengths can be seen, especially for the core stage. This dynamic is especially noticeable just past the Ariane 6(2) reference point. The behaviour of the sizing model past this point can be explained due to the influence of the propellant tanks. As the propellant employed in this launch vehicle is LH2/LOX, the core stage length variations on the left side of the figure are determined almost exclusively by the liquid hydrogen fuel tank, while the liquid oxygen oxidiser tank is assumed to be spherical with no additional tank

length in between the spherical tank caps. The reason for this is the very low density of liquid hydrogen as compared to liquid oxygen. As the overall propellant mass increases, this oxidiser tank length becomes non-zero, and both the fuel tank and the oxidiser tank thus start contributing to the core stage length and, thereby, the total vehicle length.

It could also be observed that the maximum fineness ratio constraint of the upper stage is the predominant factor in determining the minimum stage diameter, as the maximum fineness ratio constraint of the core stage is only reached at a rather high propellant mass case. At that point, a more steep decrease in the upper stage length could logically be observed. A logical result of the sizing relations observed in the plot is the minimum length measured for both the core and upper stages. Due to how these sizing relations were set up, the minimum core stage length was found equal to the constant L_0, as this constant represented the collective length of all systems that were not dependent on the propellant mass. The minimum upper stage length was, however, observed to be zero as this corresponded to a case of zero mass, which effectively implied that there was no upper stage to be sized. This could again be considered a logical result with respect to the sizing relations used to set up the sizing model.

7.3.5. Mass and sizing model constraints
Several constraints were considered in setting up the mass and sizing model. The most important of these are discussed here.

Validity range of MERs
When using existing relations, it is important to consider the given validity ranges. Using the MERs outside of these validity ranges could introduce unknown errors in the result, which cannot be traced. Additionally, it is important to consider the fundamental parameters with which the MERs were created, such as the number of data points and the fitting of the MER to the data points. In the case of the MERs created by Zandbergen, not only the validity range but also the number of data points, the residual standard error (RSE), and the R^2 value were provided for each of the relations. An overview of these figures was provided in Table 7.8, and the stated validity ranges were imposed as a constraint in the mass and sizing model.

Minimum burn time
In the mass and sizing model, and by extent this study, Ariane 6(2) was used as a reference launch vehicle. As such, it was deemed important to transfer some of the inherent characteristics of this launch vehicle directly into the model to improve the comparative value of the results. One of these characteristics is the difference in burn time between the booster stage and the core stage. While both are ignited upon lift-off, booster stage burnout and separation are set to occur before burnout of the core stage, meaning that the core stage has an inherently longer burn time than the booster stage. Therefore, a minimum burn time constraint was imposed on the model to ensure a similar sequence of events. Here, the minimum burn time of the core stage was set equal to the burn time of the boosters, which was treated as a constant in this model.

Minimum diameter - Useful payload volume
From the aerodynamics model, it follows that the aerodynamic efficiency of a launch vehicle concept can be maximised by minimising the diameter, thereby minimising the reference area of the vehicle with respect to the incoming airflow. Minimising the diameter does, however, introduce certain difficulties in the design related to structural integrity, system capabilities, and spacing of essential systems. As such, several constraints were imposed on the model to ensure viable launch vehicle designs. The first of these constraints is related to the useful payload volume. While the main performance parameter considered in this study is the payload mass, it is worth considering that not only should a medium-lift launch vehicle have the capability to serve medium-weight payloads, but it should also allow for more voluminous structures to be taken on board. As such, in accordance with other medium-lift launch vehicles such as Ariane 5, Ariane 6, and Falcon 9, the minimum diameter for the upper stage was fixed at $5.4m$ for launch vehicle concepts for which the useful payload is between $2t$ and $20t$, which are labelled medium-lift launch vehicles by NASA classifications.[11][12][93]

Minimum diameter - Multi-engine configuration
While a single-engine configuration is sufficient to drive the Ariane 6 core stage, both single and multi-engine configurations were considered in this study for the proposed launch vehicle concepts. Sufficient spacing between engines is needed in a multi-engine configuration to avoid damage to the engines from impinging exhaust plumes from other engines. Therefore, a constraint was introduced on the minimum diameter to ensure sufficient spacing between engines for launch vehicle concepts with a multi-engine configuration. Although a dedicated CFD analysis and more complex design tools would be needed to find the optimum engine spacing, a $0.5m$ spacing was considered as a lower boundary for the sizing of the proposed launch vehicle concepts. A minimum diameter constraint could thus be derived as the sum of this spacing and the engine nozzle exit diameters. This value of $0.5m$ was deemed conservative based on the engine spacing found for Falcon 9.[11]

Minimum diameter - Maximum fineness ratio
The slenderness or fineness ratio of a launch vehicle (stage) is the ratio of its length to its diameter. A high fineness ratio is desirable as it leads to increased aerodynamic efficiency, as was derived from the RASAero II tables used in this study. Due to structural reasons, however, there is a limit to the extent to which the fineness ratio of a launch vehicle can be maximised. For a 2-stage vehicle, a fineness ratio of 14 for the first stage and a fineness ratio of 5.5 for the second stage are considered safe and conservative values.[141] Here, the booster stage was considered stage 0 as it runs parallel with the core stage. Based on the available Ariane 6 sizing data, it was found that a fineness ratio of almost 5.5 characterises the upper stage, which is thus agreeable with the imposed fineness ratio constraint. The sizing model was created to be dynamic, such that upon reaching the upper limit on the fineness ratio imposed on the model, the fineness ratio was fixed at this maximum value, while the diameter was made variable, therefore allowing for the overall structural integrity of the launch vehicle concepts to be preserved.

7.4. Flight mechanics
Upon describing the trajectory of a vehicle in a specific environment, it is important to make mention of the frameworks and supporting relations with which this trajectory was defined. As such, a brief overview of relevant reference frames and state variables will be provided in this section, after which the supporting equations of motion will be described.
For a more detailed and complete overview of flight mechanics and the existing frameworks to describe the behaviour of systems in specific environments, the reader is referred to relevant literature on this topic such as Mooij[142] and Mulder et al.[143].

7.4.1. Reference frames
A reference frame in the context of flight mechanics could be defined as a definition of the orientation and movement of the coordinate reference axes used to describe the motion of a system. The choice of reference frame is thus essential in describing the motion of a vehicle. Here, it is important to realise that depending on the specifics of the motion, some reference frames would allow for an easier definition than others. Therefore, it is often effective to describe the motion through multiple reference frames and employ frame transformations to translate this motion between reference frames. Below, the reference frames most relevant to this study will briefly be discussed.

- **Inertial reference frame:** An inertial reference frame is characteristically fixed in space. It is assumed to have no net force acting on it, and it does, as a result, not undergo any acceleration. Inertial reference frames are consistent with Newton's laws of motion and, therefore, essential in formulating fundamental principles and understanding the motion of bodies in cases for which no significant external forces need to be considered.
- **Body-fixed reference frame:** This reference frame is defined directly with respect to a system body. Here, the origin is often placed at the centre of mass of the body, with the coordinate axes aligning with the principal axes of the body. A body-fixed reference frame could be applied on celestial bodies but also on small vehicle bodies such as satellites and launch vehicles. It is especially effective in combination with an aerodynamic reference frame or the body-fixed reference frame of another body to make an effective comparison in the body states.

- **Aerodynamic reference frame:** While the origin of this reference frame often coincides with the origin of the body-centred reference frame, the aerodynamic reference frame is used to describe the orientation of the relevant aerodynamic forces, lift and drag, with respect to a vehicle body. In application to this study, this reference frame allows for the definition of the relevant attitude angles of the body needed to estimate the drag and lift forces at each integration step of the launch vehicle trajectory. This is visualised in Figure 7.4. As the aerodynamic reference frame is fixed to the airspeed vector along which the body moves, the angle of attack α, bank angle μ, and sideslip angle β can easily be defined between the body-fixed reference frame and the aerodynamic reference frame. Additionally, this also allows for a definition of the angular rotation rates relating to roll p, yaw r, and pitch q as a result of aerodynamic forces acting on the vehicle.
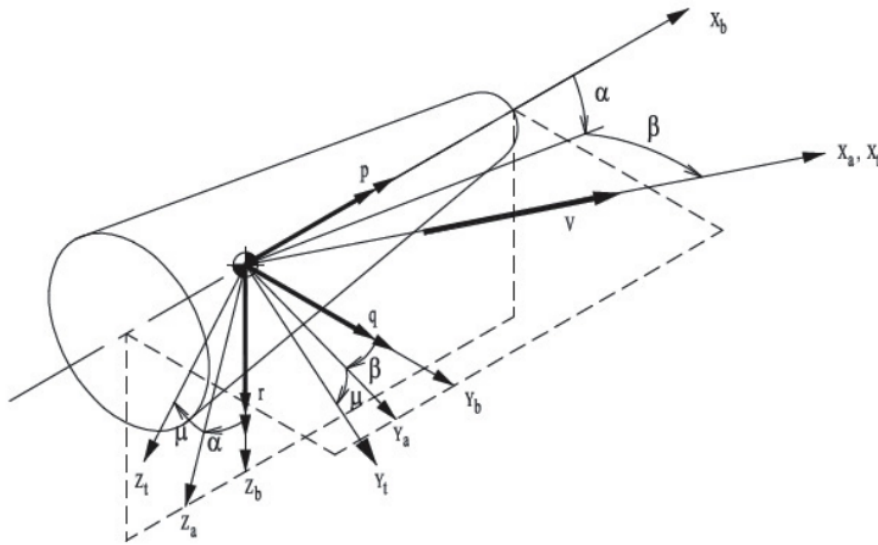
Figure 7.4: The aerodynamic reference frame for a vehicle body in comparison to the body-fixed reference frame[142]

Based on the above-stated reference frame type definitions, a reference frame specific to this study could be defined. Given the application that is central to this study, it was deemed essential to select an Earth-centered reference frame. Here, the plane defined by the X-axis and the Y-axis of the reference frame is set to coincide with the Earth's equatorial plane, while the origin of the frame, O, lies in the centre of the mass of Earth. The Z-axis of the system is described to coincide with the rotational axis of the planet, pointing North. Based on the current definition, one degree of freedom remains as the orientation of the X and Y-axes is not yet fixed. Two different relevant and commonly used reference frames could be defined, depending on how the orientation of these axes is defined, as can be seen in Figure 7.5a. The *Rotating Earth-centered reference frame (R)* is defined by fixing the X_R-axis to the equatorial plane and having it intersect with the Prime meridian at any point in time. The X_R-axis thus serves as a continuous indicator of zero longitude as it follows the rotation of Earth. The Y_R-axis completes the right-hand system. Contrary to the rotating Earth-centered reference system, the *Inertial Earth-centered reference system (I)* is fixed in space as per the aforementioned definition of inertial reference frames. Here, it is worth noting that as the reference frame is assumed to be fixed to Earth, it is not an actual inertial reference frame. Rather it can be assumed quasi-inertial when a relatively small period of time is considered for the motion to which the reference frame is descriptive. As argued by Vandamme[61], this assumption is valid for the ascending motion of launch vehicles. A commonly used inertial Earth-centered reference frame is the J2000 inertial reference frame, for which the X_I-axis is constrained by the equatorial plane of Earth and the ecliptic plane in which Earth rotates around the Sun. As visualised in Figure 7.5b,

the X_I-axis points in the direction of the Sun at the time of Vernal Equinox, which is a bi-yearly occurrence defined by the moment at which ecliptic plane and the equatorial plane intercept and the Sun is exactly above the equator. The Y_I-axis then completes the right-hand system. The J2000 inertial reference frame is a default setting for Tudat.[61][68]
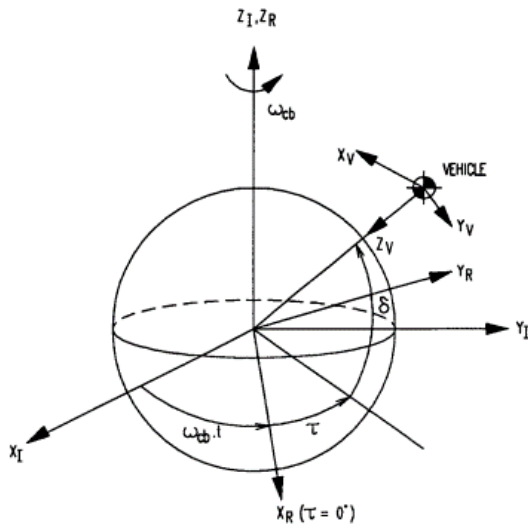
(a) An inertial planetocentric reference frame (I) in relation to a rotating planetocentric reference frame (R) and vertical vehicle-centered reference frame (V) [142]
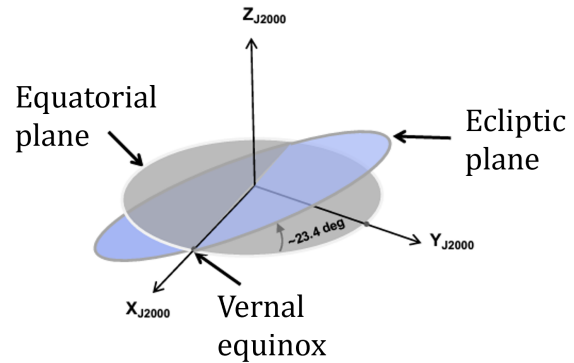
(b) J2000 inertial frame, used as a default setting for Tudat [144][68]

Figure 7.5: Earth-centered reference frames relevant to this study

7.4.2. State variables

Although important, a reference frame alone is not enough to describe the motion and behaviour of a system or, in this study, to describe the ascent trajectory of a launch vehicle in the Earth's atmosphere. State variables are used to define the position and behaviour of a system with respect to relevant reference frames. To describe the state progression of a system in a reference frame, different sets of state variables exist, the effectiveness of which highly depends on the application. A common approach to studying the motion of a spacecraft orbiting a celestial body is by describing the motion through Keplerian elements.
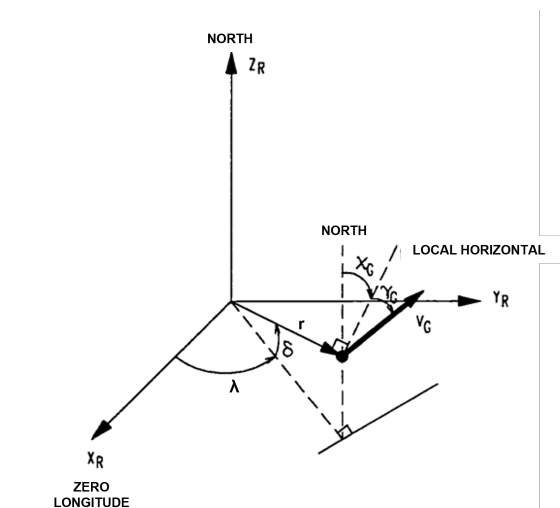
Figure 7.6: State of a vehicle in motion as expressed through spherical elements (adopted from Mooij[142])

State variable	Symbol	Applicable range
Distance from centre	r	NA
Longitude	λ	0/360 [°]
Latitude	δ	0/90 [°]
Relative velocity	V_G	NA
Flight path angle	γ	-90/90 [°]
Heading angle	χ	-180/180 [°]

Table 7.13: Definition of spherical coordinates and their applicable range

Other commonly used state variables are the spherical elements, which are especially applicable in the field of aeronautics and re-entry for describing the motion and behaviour of systems within the Earth's atmosphere. The relevant components to this coordinate definition are visualised in Figure 7.6 with respect to a rotating planetocentric reference frame. The meaning of these state variables and their applicable range i.e., the range for which they are valid in relevant applications, are stated in Figure 7.13. Here, r represents the distance from the centre of mass of the celestial body to the centre of mass of the vehicle body orbiting it. The relative velocity, V_G, is expressed with respect to the rotational velocity of the reference frame. For this study, the full range of applicability was considered for the longitude λ, latitude δ, and flight path γ, state angles. In practice, however, the flight path angle for viable trajectory solutions in this study did not go below -10°. As could be deduced from Figure 7.6, the heading angle, χ, is at 0°when the vehicle travels in the direction of the appointed North, while it is at 90°when the vehicle travels parallel with the equator in the direction of the appointed East.[142][143]

7.4.3. Equations of motion

Following the definition of relevant reference frames and state variables, the seven degrees of freedom equations of motion specific to this study could be formulated in terms of spherical elements. A full derivation of these equations will not be provided here, but can be found in relevant literature such as Mooij[142]. In Equation 7.28, the rate of change of the state variables is expressed in function of the current state. Through these relations, integration and propagation techniques can be used to predict the next vehicle state. The following variables were introduced, specific to this study:[51][142]

- R : Distance between the centre of mass of Earth and the centre of mass of the launch vehicle body.
- λ : Longitude position of the launch vehicle as compared to the point of zero longitude (X-axis, prime meridian).
- δ : Latitude position of the launch vehicle as compared to the point of zero latitude (X-Y plane, equatorial plane).
- V_G : Relative ground velocity of the launch vehicle with respect to Earth.
- γ : Flight path angle of the launch vehicle, expressing the angle between the velocity vector and the local horizontal.
- χ : Heading angle of the launch vehicle, expressing the angle between the velocity vector and the local North.
- M : Mass state of the launch vehicle, including all mass components.
- ω_E : Rotational rate of Earth around its rotational axis.
- q : Rate of change of mass of the launch vehicle, where positive values indicate mass loss.

For the state variables stated in Equation 7.28, the same applicability ranges apply as mentioned in Figure 7.13. Next to the variables introduced earlier, three force components were introduced, acting in the direction of the vehicle velocity, the flight path angle, and the heading angle, respectively. As can be deduced from Equation 7.29, these forces consist of influences of the propulsion system thrust, the atmospheric drag, the lift, and gravity effects. The thrust angle, θ, represents the angle between the thrust vector and the local horizontal. For this study, it was assumed that the thrust vector is aligned with the principal body axis of the launch vehicle, thus making the thrust vector equal to the pitch angle of the vehicle. A visualisation of the relation of the relevant force contributions and the relevant angles with the directions of interest can be found in Figure 7.7. Note that only a selection of the main forces acting on a launch vehicle in motion in the Earth's atmosphere was included here. Other forces, such as side forces caused by the wind, were ignored for this study. The equations of motion and the relevant forces could be implemented into the launch vehicle trajectory model through the Tudat toolbox.[51][68][142]

$$\begin{cases} \dot{R} = V \sin \gamma \\[2mm] \dot{\lambda} = \dfrac{V \cos \gamma \sin \chi}{R \cos \delta} \\[2mm] \dot{\delta} = \dfrac{V \cos \gamma \cos \chi}{R} \\[2mm] \dot{V} = \dfrac{F_V}{M} + \omega_E^2 R \cos \delta (\cos \delta \sin \gamma - \sin \delta \cos \gamma \cos \chi) \\[2mm] \dot{\gamma} = \dfrac{F_\gamma}{MV} + \dfrac{V \cos \gamma}{R} + 2\omega_E \cos \delta \sin \chi + \omega_E^2 R \cos \delta \dfrac{(\cos \delta \cos \gamma + \sin \delta \sin \gamma \cos \chi)}{V} \\[2mm] \dot{\chi} = \dfrac{F_\chi}{MV \cos \gamma} + \dfrac{V \cos \gamma}{R} \tan \delta \sin \chi + 2\omega_E (\sin \delta - \cos \delta \tan \gamma \cos \chi) + \omega_E^2 R \cos \delta \dfrac{\sin \delta \sin \chi}{V \cos \gamma} \\[2mm] \dot{M} = -q \end{cases} \tag{7.28}$$

$$\begin{cases} F_V = T \cos(\theta - \gamma) - D - Mg \sin \gamma \\[2mm] F_\gamma = [L + T \sin(\theta - \gamma)] \cos \mu - Mg \cos \gamma \\[2mm] F_\chi = [L + T \sin(\theta - \gamma)] \sin \mu \end{cases} \tag{7.29}$$

Figure 7.7: Representation of relevant state variables and forces in a rotating Earth-centered reference frame (Adopted from Balesdent[51])

7.5. Aerodynamics and trajectory model

To allow for *RQ-PERF-02* to be answered, it was deemed necessary to develop a model through which the different launch vehicle concepts constructed through the mass and sizing model could be assessed for their viability with respect to the reference mission. As such, the aerodynamics and trajectory model was created, through which the trajectory of launch vehicle concepts up to the point of core stage separation could be simulated. The setup and validation of these submodels will be discussed in this section.

Rather than to create a completely new model and perform extensive verification and validation efforts, the Tudat[68] python package was used to serve as a framework for the trajectory model created for this study. Tudat is a software platform originating from the Astrodynamics and Space Missions department at TU Delft that allows for computational support tasks in Python and C++ related to astrodynamics and space research. The advantage of using this package as a basis for the trajectory model is the fact that fundamental verification activities have already been performed and that several previous studies have already proven its effectiveness and accuracy for launch vehicle trajectory applications. Next to that, several publicly available example models exist that were used to aid in additional model verification efforts.

7.5.1. Aerodynamics model selection and variables

Upon setting up the vehicle performance model, it was found that accurate modelling of the aerodynamic forces acting on the proposed launch vehicle concepts during ascent is essential in setting up a representative trajectory model. Furthermore, it was argued in the setup of the sizing model that one of the major benefits of HTP-based storable bi-propellants is the relatively high specific impulse density as compared to conventional propellants. As this implied more aerodynamically efficient designs, it was essential to employ a reliable and accurate aerodynamics model in order to allow for an effective comparison of optimsied launch vehicle performances to be made.

As mentioned before, the Tudat Python environment was used as the main framework for setting up the aerodynamics and trajectory model. As such, use could be made of the built-in functions to model the aerodynamic acceleration of the launch vehicle concepts due to the aerodynamic forces experienced during the ascent trajectory. The aerodynamic acceleration can be estimated through Equation 7.30, where ρ is the atmospheric density, v_{air} is the airspeed, m is the mass of the launch vehicle body, and $\mathbf{R}^{(I/\,\mathrm{Aero}\,)}$ is the rotation matrix between the aerodynamic frame of the body and the inertial frame. These variables can be extracted from the vehicle state at every time step over the course of the trajectory. The aerodynamic coefficients C_D, C_L, and C_S, and the corresponding reference area S_ref are user-specified variables. Here, C_D is the drag coefficient, C_L is the lift coefficient, and C_S is the side force coefficient.[68] This last coefficient was ignored in the setup of the model for the sake of simplicity.

$$\mathbf{a} = -\frac{1}{m}\mathbf{R}^{(I/\,\mathrm{Aero}\,)}\left(\frac{1}{2}\rho v_{air}^2\, S_{ref}\begin{pmatrix} C_D \\ C_S \\ C_L \end{pmatrix}\right) \tag{7.30}$$

As no functionality is present in Tudat to analyse and estimate aerodynamic coefficients for specific launch vehicle geometries, an external model needed to be considered. Based on similar studies covering the topic of launch vehicle (trajectory) optimisation, two models were considered, these being RASAero II[86] and Missile DATCOM[69]. For the latter, only the 1997 version is publicly available due to International Traffic in Arms Regulations (ITAR). Ultimately, it was decided to make use of RASAero II, which was also used by Iyer[60] and Rozemeijer[70]. It also allows for the geometry of a launch vehicle concept to be visualised, thereby offering a variety of customisation options, including the selection of a specific nose cone geometry. Furthermore, it was argued that due to its more recent development and user support, the obtained models would be more representative of the design optimisation considered in this study, as it would be validated for more recent launch vehicle designs. The validity and the accuracy of the model were also considered. It is stated that the aerodynamic prediction methods used in the RASAero II software are of equivalent accuracy to professional aerodynamic analysis tools used for missiles, sounding rockets, and space launch vehicles. In Figure 7.8, the accuracy of the RASAero II aerodynamic coefficient prediction

model is visualised for a ballistic missile reference case. Furthermore, the accuracy of the RASAero II flight simulation functionalities is visualised in Figure 7.9. It shows an average altitude prediction error of 3.47%, with a reported error of less than 10% for 80.6% of flights.
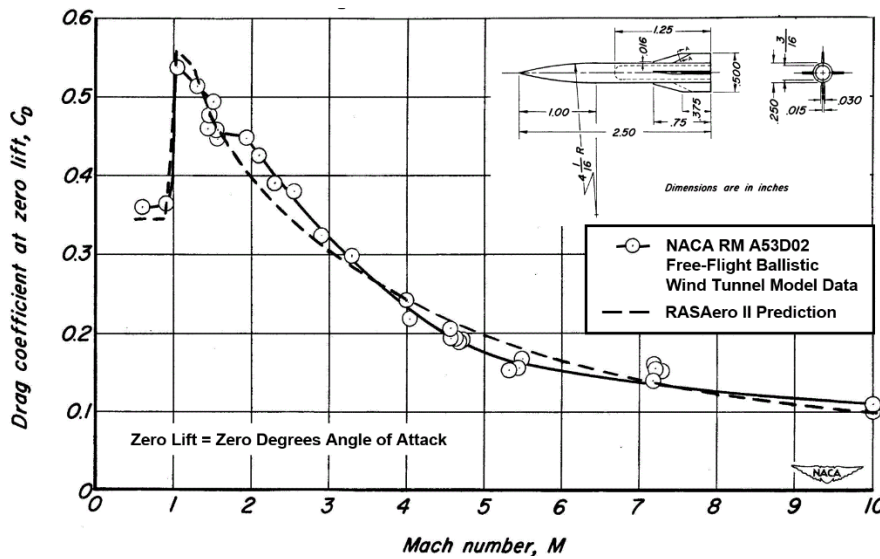
Figure 7.8: Accuracy of RASAero II for the prediction of NACA RM A53D02 drag coefficient [86]
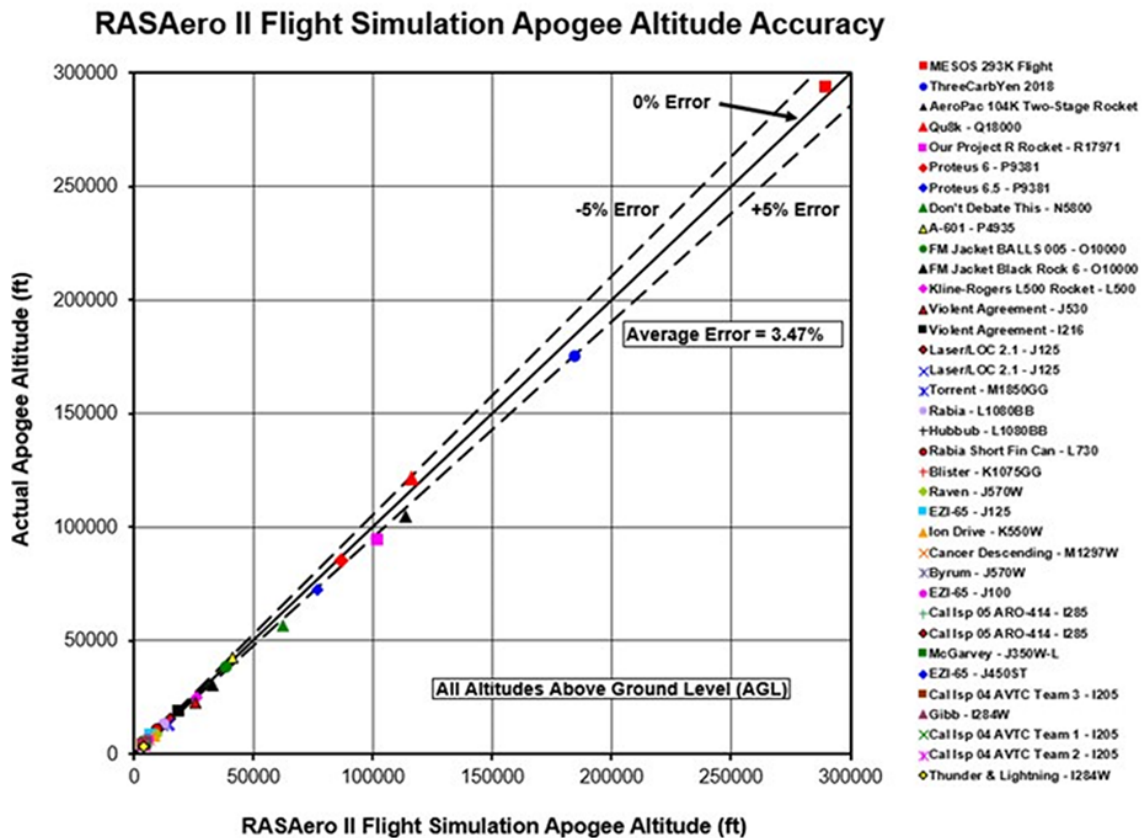
Figure 7.9: Accuracy of RASAero II flight simulation [86]

RASAero II allows for several vehicle-specific inputs to be entered to obtain aerodynamic coefficients. As mentioned before, the software allows for the geometry of the launch vehicle concepts to be

visualised, thereby specifying the diameter, length, and nose cone properties of the vehicles as the main input variables. Furthermore, it also allows for additional geometry components to be included in the model, such as drag-inducing perturbations and grid fins. For simplicity, these components were not considered for the setup of the aerodynamics model. Although the software allows for taper to be added, which refers to a varying diameter between launch vehicle stages, it was chosen to keep the stage diameter constant over the length of the launch vehicle for the sake of simplicity. Next to the launch vehicle geometry, the aerodynamic coefficients are dependent on the Mach number and the angle of attack of the vehicle during its ascent trajectory. Here, aerodynamic coefficient predictions can be obtained from RASAero II for a MACH number range of 0-25 and an angle of attack range of -15-15°. While the Mach number range was found to be efficient for the trajectories considered in this study, the angle of attack affects had to be extended by means of cubic interpolation. Based on the functionalities and the setup of the model discussed in this section, a list of the main input and output variables for the aerodynamics model could be compiled. This overview can be found in Table 7.14.

Table 7.14: Aerodynamics model variables

Variable	Symbol	Units	Type
Angle of attack	α	°	Input
Launch vehicle diameter	D	m	Input
Launch vehicle length	L_{tot}	m	Input
Mach number	M	$-$	Input
Aerodynamic acceleration	a	m/s^2	Output
Drag coefficient	C_D	$-$	Output
Lift coefficient	C_L	$-$	Output

7.5.2. Environment models

The environment in which a system operates is an influential factor in the behaviour and the subsequent performance of the system. Environment models allow for the physical properties of relevant environments to be simulated, therefore making it possible for the interaction of a system model with its relevant environments to be predicted. Tudat includes a variety of different models with different levels of complexity and accuracy based on the underlying assumptions. In selecting an environment model for this study it was thus important to find a balance between a sufficient level of accuracy in accordance with the requirements set for the study and a low level of complexity to ensure low computational time. The selection of the two most relevant environment models to this study, these being the atmospheric model and the gravitational model, will thus briefly be discussed here.

Atmospheric model

For the atmospheric model, two readily available models integrated into the Tudat module were considered, these being the US 1976 Standard Atmosphere Model (US76) and the NRLMSISE-00 atmosphere model. The US76 model is based on observational data from atmospheric measurements, which allowed for large tables of atmospheric data in function of altitude to be created. Between these altitude steps, atmospheric conditions were estimated in the Tudat module by means of cubic interpolation.[68] The data tables provided through the US76 models are valid from a range of -5km to 1000km. Here, it is worth mentioning that up to an altitude of 100km, data steps of 100m are taken, while thereafter, data steps of 1km are taken. Given that the end states for the Ariane 6(2) reference case considered in this study are taken at 209km altitude, the accuracy of the US76 atmospheric model could be questioned.[145]

Therefore, a second model was considered, this being the NRLMSISE-00 atmosphere model. This global reference model is more accurate than the US76 model and can also be made case-specific as it allows for time and coordinate positions to be provided as input variables. As such, this model has become very relevant for space research and is mostly used to support predictions of the orbital

decay of satellites due to atmospheric drag.[146]

Upon comparing the two proposed atmospheric models, it was found that the NRLMSISE-00 model requires significantly more computational effort, while the added functionalities are only partially relevant to this study, and the accuracy provided by the US76 model was deemed sufficient to make an accurate comparative analysis and to generate sufficiently accurate launch vehicle trajectory predictions. Additionally, it was found that similar studies on the topic of launch vehicle optimisation, such as Castellini[147], Dijkstra Hoefsloot[67], and van Kesteren[57] also opted for the US76 atmospheric model, which was thus also selected for this study.

Gravitational model

The gravity model is another essential environment model in simulating ascent trajectories for launch vehicles. It was deemed important to have a reliable and accurate gravitational model to effectively compare the mass performance of the proposed launch vehicle concepts. At the time of setting up this study, two different types of gravitational models were available through Tudat: the point mass gravity model and the spherical harmonics gravity model. Equation 7.31 is the central equation to the point mass gravity model, where the Earth is assumed to be perfectly spherical, and all the mass of the Earth is assumed to be concentrated at the centre of its body, as could be intuitively deduced. Following Equation 7.31, the gravity force acting on the launch vehicle body is thus a function of the universal gravitational constant, G, the mass of Earth, M_E, the gravitational parameter of Earth, μ_E, and the distance between the point mass representing Earth and the point mass representing the launch vehicle, $r_{LV,E}$. Here, the mass of the launch vehicle, M_{LV} can be assumed to be negligible.

$$\mathbf{F_G} = -\frac{GM_E M_{LV}}{|r_{LV,E}|^3} \mathbf{r}_{LV,E} = -\frac{\mu_E}{|r|^3} \mathbf{r} \tag{7.31}$$

In reality, the Earth is not a perfect sphere, but rather it has a more oblate shape, mostly due to the rotation around its axis. As a result, the mass of the Earth is not perfectly distributed, making the gravitational force dependent on the exact location of the attracted body. Spherical harmonics are mathematical functions used to describe these variations, which thus allows for the gravity environment to be more accurately modelled than through point mass models. The gravitational force on a launch vehicle can be found using spherical harmonic relations through Equation 7.32 and 7.32. Here, the mass of the launch vehicle is represented by M_{LV}, and ∇V is the gravitational potential. In Equation 7.33, the gravitational potential is described as a spherical harmonic series expansion of degree l and order m, where R_E is a constant representing the radius of Earth, r is the radial distance between the centre of Earth and the launch vehicle, and μ_E is the gravitational parameter of Earth. Y_{lm}^C and Y_{lm}^S are the normalised spherical harmonic Legendre functions, which are a function of r, but also of the spherical coordinates, θ and λ. C_{lm} and S_{lm} are the spherical harmonic coefficients, which are based on observational data. The GOCO05c model by Fecher et al.[148] is the spherical harmonic gravity field model integrated within Tudat with default order and degree settings of 200 and a possibility to increase the accuracy to a degree and order 720.[148][149]

$$\mathbf{F_G} = -M_{LV} \nabla V \tag{7.32}$$

$$V(\theta, \lambda, r) = \frac{\mu_E}{R_E} \sum_{l=1}^{\infty} \left(\frac{R_E}{r}\right)^{l+1} \sum_{m=1}^{l} \left[Y_{lm}^C(\theta, \lambda) C_{lm} + Y_{lm}^S(\theta, \lambda) + S_{lm}\right] \tag{7.33}$$

A gravity model based on spherical harmonics is overall a more accurate representation of the gravity environment as experienced by the launch vehicle during an ascent trajectory. Next to that, it also allows for the latitude and longitude of the launch pad to be accounted for, thus enabling a more accurate comparison with the reference case Ariane 6. Due to its increased functionality, the spherical harmonic gravity model was thus chosen over the point mass gravity model despite increased complexity and computational effort.

7.5.3. Trajectory model setup and variables

To ensure clarity in the explanation of the setup of this trajectory model, it is worth reiterating the final conditions relevant to this study. Rather than study the trajectory and the behaviour of the launch vehicle from launch up to the point of orbit insertion, the final conditions were set at the point of the core stage burnout and separation. The reasons for this were partially the lack of information on the Ariane 6 "projected" mission profile, but also the focus of this study on the core stage of the launch vehicle and the difficulties of modelling a multi-functional upper stage such as the Ariane 6 ULPM. As a result, the main stages between which a distinction was made in this study were the booster stage and the core stage, with the upper stage being considered part of the core stage "payload".

The Tudat package allowed for an effective distinction to be made between the flight of the core stage supported by the boosters and the flight of the core stage after booster separation. Here the end of the first flight phase, also referred to as the booster flight phase, was upon booster burnout, so at a time t=132.8s after lift-off. Thereafter, the booster dry mass was discounted from the vehicle model and the second flight phase, also referred to as the core stage flight phase, was modelled up to the end of core stage burnout. It is worth noting that the core stage actively provides thrust during both the first and the second flight phases.

Thrust modelling

Thrust is an essential parameter in modelling launch vehicle trajectories as it directly relates to the acceleration of the launch vehicle and, thus, its ability to lift off and overcome gravity. Therefore, accurate modelling of the thrust provided by the different launch vehicle stages was considered to be very important. The thrust of the core stage engine is estimated through the propulsion model and supplied as an input to the trajectory model. The atmosphere model is used to account for atmospheric pressure effects on the effective engine thrust at each integration step in accordance with Equation 7.1. Note that liquid propellant engines are often designed with some throttle settings to allow for the thrust output to be controlled and optimised. Incorporating this into the engine model was, however, deemed too complex for this study as it would have introduced an additional degree of freedom in the optimisation process. Furthermore, it would have required assumptions to be made with respect to the throttle capabilities of the conceptual HTP-based bi-propellant engines, for which little precedent exists.

Table 7.15: P120 C solid rocket motor characteristics as provided by the manufacturer (Avio)[101]

Characteristic	Value	Units
Propellant mass	143.7	t
Dry mass	11	t
Average thrust	4500	kN
Specific impulse	278.5	s
Burn time	132.8	s

It is worth noting that the majority of the thrust during the first flight phase is generated by the P120 C solid rocket boosters (SRB). This is necessary as this is the phase of flight during which the gravity and atmospheric drag forces that need to be counteracted are most severe. Data for the boosters was taken directly from the manufacturer, Avio, and was tabulated in Table 7.15. At first, the SRB thrust reported here was modelled to be constant over the full length of the SRB burn time. In reality, solid rockets seldom display a constant thrust profile as the surface burn area varies throughout flight depending on the grain geometry. It was thus found that this simplified approach led to an overestimation of the mass flow as this was estimated in the model at every integration step through Equation 7.3. As a result, the mass expelled by the SRB, as predicted by the model, was off by 150t. To obtain a more accurate model for the thrust of the SRB over time, a profile of the thrust variation over time in P-series solid rocket motors was obtained from a study by Dumont et al.[150]. As can be seen in Figure 7.10, the thrust of this type of solid rocket motor is indeed not constant over time but rather shows a peak in the first ten seconds, most likely to provide additional thrust and thereby a significant thrust-to-weight ratio at lift-off. This

thrust profile is imitated in the trajectory model for the SRB through a polynomial function, which is evaluated at every integration step. The result is visualised in Figure 7.11.
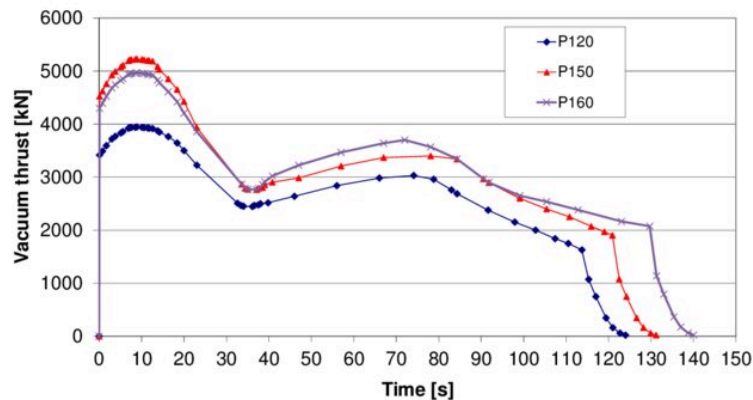
Figure 7.10: Thrust variation over time of P-series solid rocket boosters [150]
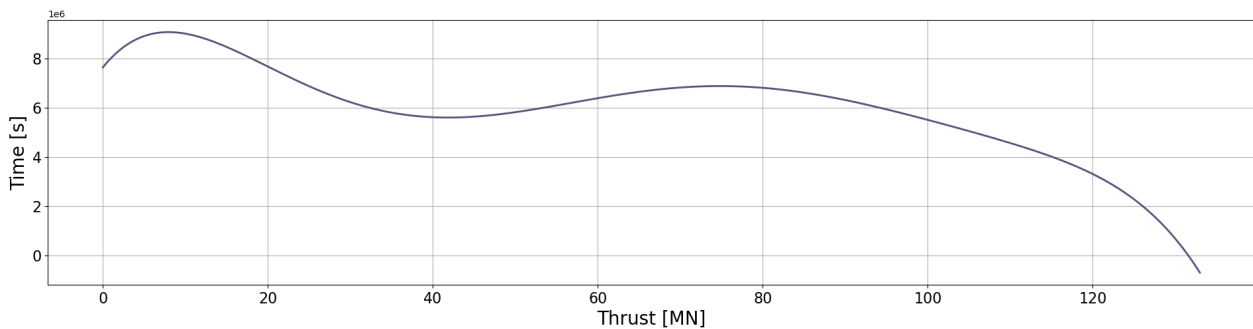
Figure 7.11: Estimate of the thrust profile of the P120C solid rocket booster

Guidance nodes

Guidance is a central part of any trajectory model as it allows for the vehicle to be controlled and steered towards its final state. In reality, launch vehicles are often controlled by means of active thrust vector control or steering through control surfaces. As a result of the redirection of forces, such as the thrust forces, and subsequent unalignment with the launch vehicle body axis, a moment is then imposed on the vehicle, which induces an attitude change. Although more realistic, the modelling of thrust vector control or passive control surfaces is a complex task that requires several additional variables and degrees of freedom to be considered. As such, it was deemed out of the scope of this study. Instead, an approach was considered in which the effects of these control vectors could be imitated by directly controlling the attitude change of the vehicle at every integration step. Thus, guidance was added to the model by assuming direct control of the aerodynamic angles of the vehicle. Here, specific constraints have to be introduced to realistically simulate the effects of active control vectors, as will be discussed in Section 7.5.6.

The specific guidance method considered in this study is known as pitch control law, which was also used and validated in similar studies by Dijkstra Hoefsloot[67], Vandamme[61], and van Kesteren[57]. The idea behind this method is to make use of the fundamental relation presented in Equation 7.34, where α is the angle of attack, γ is the flight path angle, and θ is the pitch angle. The specific meaning of these attitude angles within the vertical plane considered for this study is visualised in Figure 7.12. Sideslip forces and, subsequently, sideslip angles were considered to be negligible for this study, as was already mentioned in Section 7.5.1. To integrate pitch control law within the model, a set of pitch values or nodes had to be chosen, representing the pitch angle at specific time steps during the two flight phases. Here, the number of nodes is scaled with increasing flight time to ensure that the guidance method is dynamic. Between these nodes, values for the

pitch angles are defined through linear regression. Subsequently, a pitch angle could be defined at each integration step. By calling the flight angle at the current time step and subtracting it from the controlled pitch angle, a new angle of attack could be defined through Equation 7.34 and imposed on the vehicle model to enforce an attitude change and thereby control the translational motion of the launch vehicle throughout the flight.

$$\alpha = \theta - \gamma \tag{7.34}$$
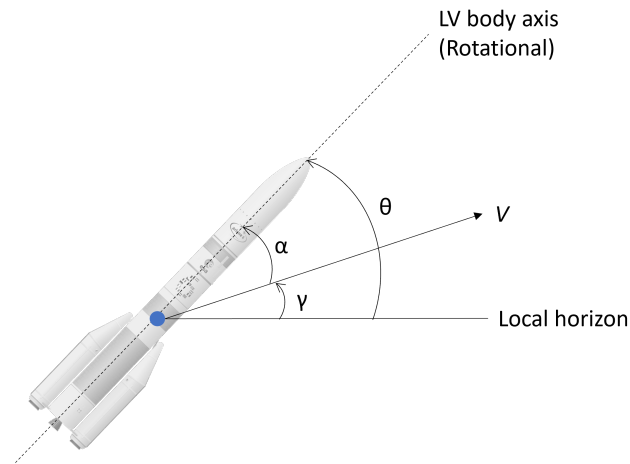
Figure 7.12: Representation of the aerodynamic angles for a launch vehicle in the vertical plane

An example of a use case for the pitch control law can be found in Figure 7.13. Here, the aerodynamic angles were plotted for the Ariane 6 reference case with respect to flight time. As can be seen, eleven pitch nodes were used to provide guidance to the vehicle model; three nodes for the booster phase, seven nodes for the core stage phase, and one node around the time of booster burnout and separation. It is clear from the behaviour of the aerodynamic angles that the pitch angle is directly controlled through the guidance inputs, while the angle of attack is shown to be reactive to those changes. The flight path angle, on the other hand, shows a more smooth behaviour as it is less sensitive to the control inputs.
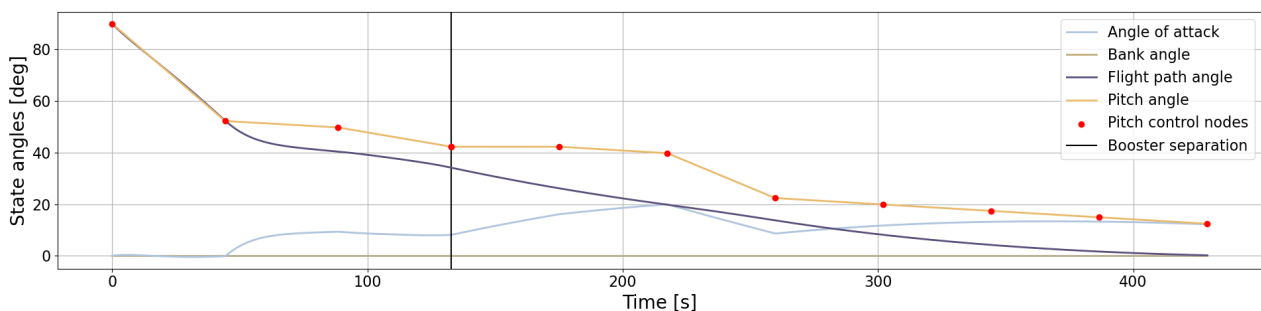
Figure 7.13: Predicted aerodynamic state angles with respect to time for the Ariane 6 reference case using pitch control law

Trajectory model variables

Based on the setup of the sizing model as presented in this section, a list of the main input and output variables for the sizing model could be compiled. This overview can be found in Table 7.16. Due to the nature of the trajectory model, several of the variables listed here are dynamic variables, which are set to change continuously as the flight of the vehicle is modelled. Note that as with the other models, not all inputs and outputs to the models were considered variables and were thus not included in Table 7.16. The most important among these are the initial and final states of the launch vehicles. For the Ariane 6(2) reference case, these states were listed in Table 7.17.

Table 7.16: Trajectory model variables

Variable	Symbol	Units	Type
Altitude states	H	m/s	Output
Angle of attack states	α	°	Output
Flight angle states	γ	°	Output
Mass states	M	kg	Output
Velocity states	V	m/s	Output
Booster specific impulse	$I_{sp,SRB}$	s	Input
Booster stage burn time	$t_{b,SRB}$	s	Input
Booster surface area	S_{SRB}	m_2	Input
Booster thrust profile	F_{SRB}	N	Input
Core stage burn time	$t_{b,Core}$	s	Input
Core stage specific impulse	$I_{sp,Core}$	s	Input
Core stage surface area	S_{Core}	m_2	Input
Core stage thrust profile	F_{Core}	N	Input
Drag coefficient	C_D	−	Input
Gross lift-off mass	$GLOM$	kg	Input
Lift coefficient	C_L	−	Input
Payload mass	M_{pay}	kg	Input
Pitch control nodes	θ	°	Input
Propellant mass	M_p	kg	Input
Upper stage surface area	S_{Upper}	$m2$	Input

Table 7.17: Initial and (target) final states for the Ariane 6(2) reference case
(*data based on the location of the Kourou launch site)

Initial state		
Launch altitude	0	m
Launch flight angle	90	°
Launch heading angle	0	°
Launch latitude*	5.2	°
Launch longitude*	-52.8	°
Launch velocity	0	m/s
GLOM	530	t
Target end state		
LLPM separation altitude	209.9	km
LLPM separation velocity	4.63	km/s

7.5.4. Trajectory optimisation

Reaching a specific set of final states such as those stated in Table 7.17 requires precise trajectory control so as to not overshoot or undershoot the target. This is especially important to allow for the upper stage to reach its intended orbit. Therefore, it was deemed necessary to optimise the trajectory for a specific set of objectives. Here, it was decided to provide trajectory optimisation in the model by optimising the pitch control nodes. It was identified that controlling and optimising the throttle setting of the core stage engines would also have been an effective method. As was mentioned in Section 7.5.3, however, it was decided not to incorporate any throttling capabilities in the engine model to reduce the complexity of the model as this would have introduced an addi-

tional degree of freedom.

To optimise the pitch control nodes over the trajectory of the launch vehicle, a genetic algorithm was developed. Genetic algorithms (GA) are numerical optimisation algorithms inspired by genetics and natural selection. While genetic algorithms are not as robust as compared to some other optimisation methods, their main advantages are found in the simplicity of the method and the fact that no exact initial solutions or gradient information are required, while extensive solution areas are explored to come to accurate solutions to the objective problem. This is possible as GA methods are centred around improving the initial population of solutions in accordance with the specified objective function.[54][56][81]

A general flowchart for the GA applied to the trajectory model can be found in Figure 7.14. The process is initiated by generating an initial population of random solutions, in this case a series of pitch control node sequences. Thereafter, the quality and fitness of these solutions are evaluated with respect to the objective function, and a fitness score is subsequently assigned to each solution. Next, the best solutions are selected to create a new solutions pool, which consists of the best solutions and crossovers of these best solutions, so-called child solutions. Additionally, an operator is used to add mutation to the solution selection process as to avoid a loss in diversity in the population of solutions. Each solution in the new solutions pool is then again evaluated, and this process is repeated for a pre-specified number of iterations, after which the most optimum solution is picked out.
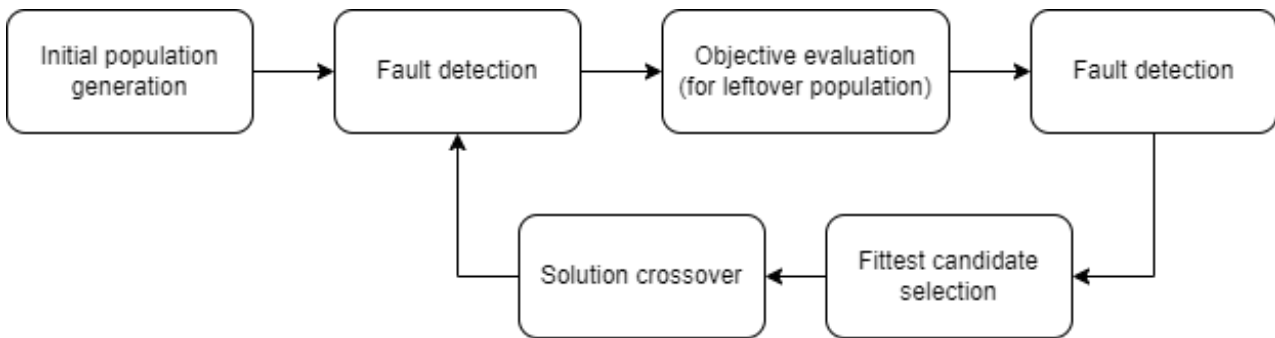
Figure 7.14: Generalised flowchart for the genetic algorithm used for trajectory optimisation

Upon implementing the GA in the trajectory model, several drawbacks of the method became evident, mostly related to a lack of efficiency and high computational effort. As such, several measures were added to increase the efficiency of the algorithm. A major obstacle to the efficiency of any optimisation method for this specific trajectory optimisation problem is the need to evaluate each solution by simulating the full flight of the launch vehicle with the proposed pitch node control sequences.

- **Pre-evaluation fault detection:** In this step, also indicated in Figure 7.14, the pitch node control sequences were assessed based on their shape and expected outcome. Significant spikes and sudden increases in the pitch angle between two subsequent nodes were deemed to lead to unrealistic trajectories. Therefore, all initial solutions were sorted in descending order. Later, newly created child solutions were once again evaluated, where solutions with a pitch angle increase of over 5°between subsequent nodes were removed from the solution pool. Additionally, already existing solutions were tagged and their scores preserved such that there was no need for these solutions to be reevaluated.

- **Intra-evaluation fault detection:** Indicators were implemented in the trajectory model to identify faulty solutions at any point during the simulation of the launch vehicle trajectory. These indicators were negative altitude values, altitude values of over 50% past the target altitude, velocity values of over 50% past the target velocity, and an altitude drop of more than $100km$. Here, large margins were applied to these indicators to ensure that no potentially correctable solutions were prematurely excluded from the solution space.

- **Post-evaluation fault detection:** Next to an evaluation through the objective function, additional factors were considered in determining a final score for each solution. These factors were mostly based on the trajectory constraints discussed in Section 7.5.6. The constraints considered here were the maximum pitch rate, the maximum dynamic pressure, and the maximum acceleration observed over the trajectory of the launch vehicle. So-called punishments were applied to the scores of the solutions violating these constraints.

- **Populaton regeneration:** Given that several solutions were excluded from the solution space or assigned a bad fitness score following the fault detection measures, a regeneration of the population was implemented after a specific number of iterations. Here, only a prespecified percentage of the population including the best solutions was recuperated, while the remaining solutions were replaced by new random pitch control node sequences. It was observed that implementing this measure brought more diversity into the population and allowed for an increased chance of successful and viable crossovers with the best solutions transferred from the previous population.

To allow for the proposed solutions for the trajectory optimisation problem to be evaluated, an objective function had to be defined. This objective function was based on a number of target states in the launch vehicle trajectory. To ensure the effectiveness of the objective function, a balance had to be found in selecting only a limited number of objective states while unambiguously representing the optimum trajectory. In the end, four objective states were considered, each of which was defined by a specific target value. The first three objective states are the core stage separation velocity (V_e), altitude (H_e), and flight angle (γ_e), with the fourth state being the maximum altitude (H_{max}) reached during the flight. Here, the first two objective states were included to ensure sufficient accuracy with respect to the initial conditions for the upper stage of the launch vehicle, while the latter two objective states were included to ensure that the trajectory is efficient and that the final state is stable. The objective function is stated in Equation 7.35.

$$O = f(\Delta V_e, \Delta H_e, \Delta \gamma_e, \Delta H_{max}) \tag{7.35}$$

To show the effectiveness of the GA method above applied to the trajectory model, a comparison was made based on Ariane 5 as a reference case. The fitness of the solutions before and after extensive optimisation is visualised in Figure 7.15 and 7.16 for the altitude and velocity states, respectively. It can be observed that an agreeable solution was already found without any regeneration of the solution population. After applying one regeneration cycle, however, it can be seen that the trajectory predicted by the model comes even closer to the trajectory based on data points from a real Ariane 5 flight. Next to the number of regeneration cycles, several other optimisation parameters were introduced as part of the GA method applied to the trajectory model. A sensitivity analysis on the main parameters will follow in Section 7.6.2 to show the effects of these parameters on the efficiency of the method and the accuracy of the results.
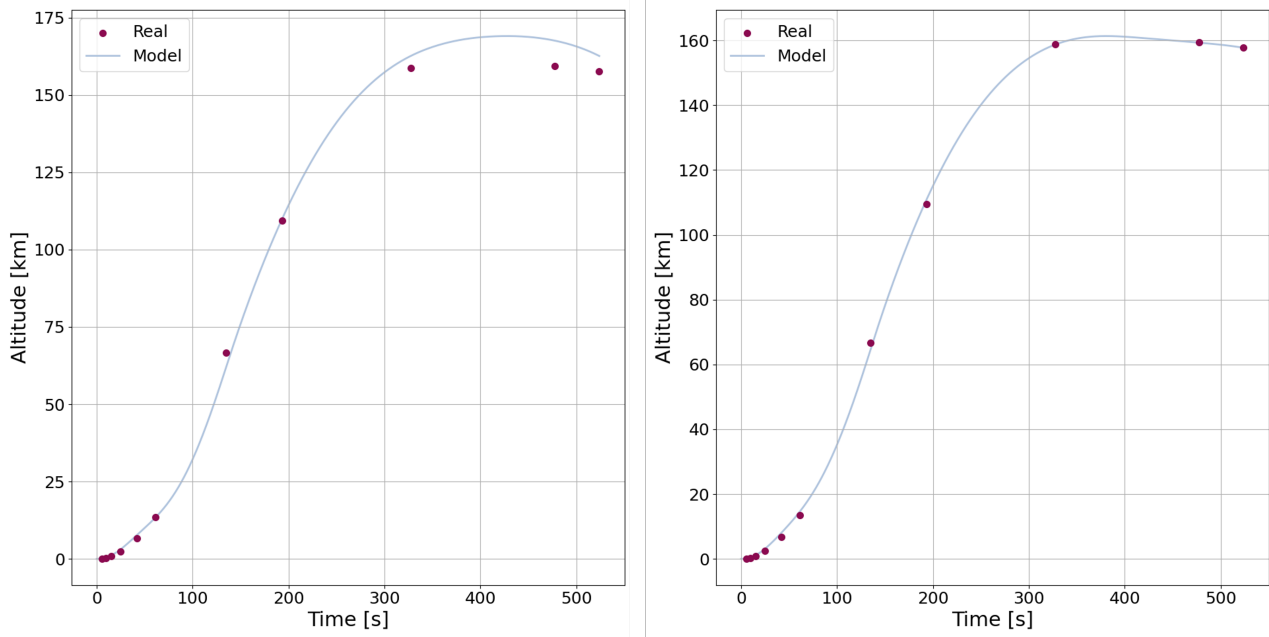
Figure 7.15: Fitness of the optimised pitch control node solution for the altitude state propagation of the Ariane 5 reference case. The solutions were generated for an initial population of 100 solutions without regeneration (left) and with one regeneration cycle (right).
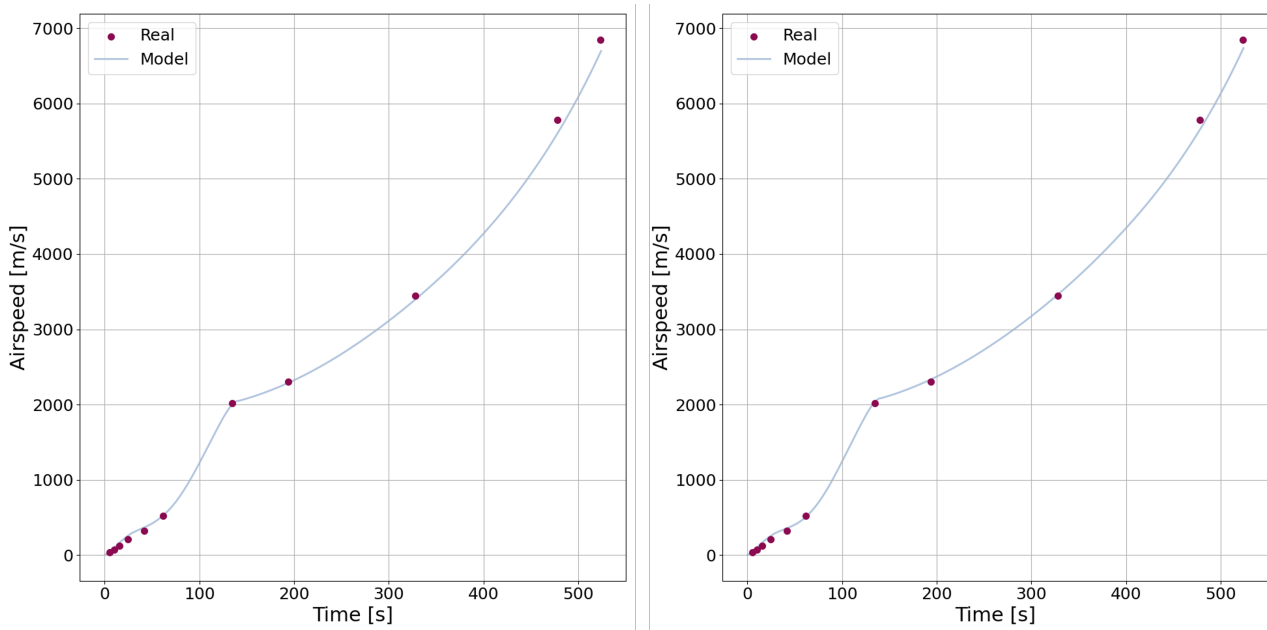
Figure 7.16: Fitness of the optimised pitch control node solution for the velocity state propagation of the Ariane 5 reference case. The solutions were generated for an initial population of 100 solutions without regeneration (left) and with one regeneration cycle (right).

7.5.5. Trajectory model validation

For the validation of the trajectory model and the trajectory optimisation methods, it was essential to compare predictions from the model to real flight data. Due to the absence of flight data specific to Ariane 6, the trajectory model could not be validated with the reference launch vehicle that was chosen for this study. However, given that the model was created based on the Ariane 6 as a reference case, it was preferable to select a similar flight case for the validation of the model. Here, Ariane 5 was deemed the most suitable candidate as it is a medium-lift launch vehicle, which also employs two P-series solid rocket boosters. More specifically, the VA-226 flight was selected as there was a good amount of available flight data and other vehicle-specific data available for this case. Flight VA-226 saw an ECA series Ariane 5 launch vehicle bring a 10.2t payload to a geostationary transfer orbit in 2015. Specifics to the mass, burn time, and propulsion performance of this vehicle were tabulated and can be found in Table 7.18. Here, it is worth noting that the thrust performance of the core stage engine is significantly larger than the thrust performance reported for the Ariane 5 engine reported in Table 7.3-7.5, the reason for this being the improved core stage engine motor that was integrated into the Ariane 5 ECA series launch vehicles. This more similar performance with the Ariane 6 core stage engine was another reason for considering VA-226 as a reference case.

Table 7.18: Characteristics specific to the Ariane 5 VA-226 flight important for the modelling of its trajectory[151]

Stage	Reported burn time [s]
Solid rocket boosters	141.9
Core stage	531
Mass components	**Reported mass [t]**
Fairing	2.4
Total payload	9.42
Vehicle equipment bay	0.97
Payload adaptor (ACU)	0.14
Ariane double launch structure (SYLDA)	0.53
Cryogenic upper stage (ESC-A)	19
Cryogenic main stage (EPC)	188
Solid rocket boosters (EAP)	554
Reported GLOM	780
Estimated GLOM	774.46
Propulsion components	**Reported performance [kN]**
Core stage engine vacuum thrust	1393
SRB engine vacuum thrust	2x7080
Objective states	**Reported state values**
Core stage separation velocity [km/s]	6.93
Core stage separation altitude [km]	157.7
Maximum altitude [km]	159.4

To verify the correct implementation of the propulsion and mass models in the trajectory (optimisation) model, the launch vehicle mass state over time was investigated. This dynamic is visualised in Figure 7.17, together with some reference points of interest representing the expected mass states at these time steps based on the mass budget presented in Table 7.18. From this figure, it can be concluded that the amount of mass expelled by the launch vehicle is slightly underestimated by the model as compared to the expected mass expulsion. Given that the error seems to grow at a steady rate throughout both the booster flight phase and the core stage flight phase, it can be deduced that this is the result of inaccuracies in the modelling of the core stage engine mass flow. Indeed, from

Table 7.5 it can be deduced that the mass flow is slightly underestimated for the Vulcain engines in the propulsion model. Apart from these small mass differences, it can be concluded that the mass state of the launch vehicle can be propagated quite accurately in the trajectory model.
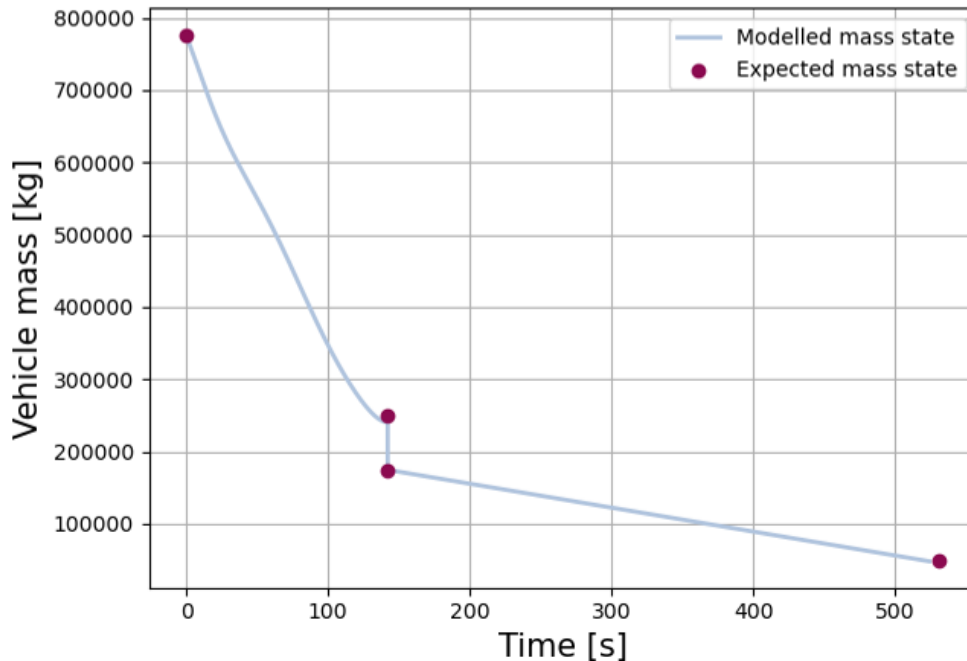
Figure 7.17: Comparison of the predicted to the expected launch vehicle mass over time for the Ariane 5 VA-226 flight

The optimised altitude and velocity profiles for the Ariane 5 VA-226 flight case were already shown in Figure 7.15 and 7.16, respectively. Some specific points of comparison from these figures are tabulated in Table 7.19, together with the corresponding errors.

Table 7.19: Comparison of the altitude and velocity state propagation for the Ariane 5 VA-226 flight as predicted by the trajectory optimisation model to real flight data

Time since launch [s]	Altitude			Velocity		
	Real [km]	Model [km]	Error [%]	Real [m/s]	Model [m/s]	Error [%]
5.5	0.09	0.13	44.4	36.2	51.6	42.5
9.8	0.32	0.45	40.6	72.2	98.5	36.4
15.3	0.87	1.14	31.0	123.1	156.1	26.8
24.8	2.41	3	24.5	209.9	235.4	12.1
41.7	6.69	7.5	12.1	322.3	318.6	-1.1
61.3	13.5	14	3.7	523.6	452.9	-13.5
134.6	66.7	63.5	-4.8	2020.2	1931.7	-4.4
193.7	109.4	111.2	1.6	2302.0	2228.1	-3.2
327.7	158.8	158.7	-0.1	3447.0	3381.2	-1.9
477.7	159.4	159.3	-0.1	5783.0	5655.0	-2.3
523.7	157.7	157.7	0.0	6901.0	6750.0	-2.2

For both the altitude and the velocity states, it can be observed that a large error is present at liftoff. A reason for this could be the point at which pitch control law is first imposed on the vehicle states, which in the model was set to occur after $30m$ of vertical flight. Next to that, the estimated

GLOM used for the vehicle model is lower than the GLOM reported for the real launch vehicle, as was stated in Table 7.18. This could have allowed the model to more quickly overcome gravity forces and thus accelerate and gain altitude at a quicker rate. Another conclusion that can be made based on the observed errors in the velocity profile is that a continuously lower velocity is predicted by the trajectory model after one minute of flight as compared to the real flight data. A reason for this could be the error in the thrust estimation in the propulsion model. As was shown in Table 7.5, the thrust estimated through the propulsion model is slightly lower than the actual thrust performance reported for the Vulcain engines. This could lead to slightly lower acceleration, most noticeable after the separation of the boosters, which is in part counteracted by the lower launch vehicle mass used for the trajectory model. It is also worth remarking that the trajectory of the launch vehicle is optimised for the objective states, these being the maximum altitude observed during the trajectory and the states of the launch vehicle at the time of core stage separation. Therefore, it was expected that the optimal trajectory proposed by the algorithm would result in slight errors throughout the trajectory of the vehicle and for minimum errors to be observed at its objective states. Additionally, taking into account the assumptions that were made in setting up the trajectory model, small variations should expected to occur as a result of the throttle setting used on the real core stage engine, as this was not considered in the model.

Overall, it was argued that while the errors observed in the trajectory model are noticeable, the errors observed for the objective states could be deemed acceptable for the model to be used for this study. The reason for this is that the trajectory model should allow for unrealistic launch vehicle concepts to be identified and thus for there to be a base framework for comparison of the payload capabilities of launch vehicle concepts shown to be within an acceptable range of the objective states.

7.5.6. Trajectory model constraints
To ensure the viability of simulated trajectories, several constraints were introduced into the trajectory model. The most relevant of these will be discussed here. Additional constraints, such as a maximum heat flux constraint, were considered but ultimately found to be less relevant for the study case.

Maximum dynamic pressure
The maximum dynamic pressure point, or Max Q point, occurs when aerodynamic forces are highest. At this point, the launch vehicle is expected to experience maximum structural stresses. To ensure that the structural integrity of the vehicle during flight is maintained and that risk is minimised, a constraint is commonly placed on the maximum dynamic pressure that should be experienced over the ascent trajectory. The dynamic pressure is a function of the atmospheric density ρ and the airspeed V, as can be deduced from Equation 7.36. Given the influence of the atmosphere, the Max Q point often occurs in the early stages of the flight, as is the case for Ariane 5 flight VA-226, for which the Max Q point was observed at $13km$ altitude.[151] An effective method for decreasing this maximum pressure point would be to throttle down the engines. In this study, a penalty was introduced to the objective score for pitch control node sequences resulting in a dynamic pressure of over $70kPa$. This is based on the Max Q point of $57kPa$ relevant for Ariane 5, including a margin to account for inaccuracies in the trajectory model.[57][147]

$$q = \frac{1}{2}\rho V^2 \tag{7.36}$$

Maximum acceleration
A commonly implemented constraint in launch vehicle (trajectory) optimisation studies is the maximum axial acceleration constraint. This constraint is not only important to ensure that the structural limitations of the launch vehicle are protected but also to ensure the safety of the payload. For Ariane 6, it is reported that the maximum acceleration loads that are to be taken into account for the payload structure are $3.6g$ during the SRB flight phase and up to $6g$ at SRB separation. Vandamme[61] mentions a maximum axial acceleration of $4.86g$ based on 6 launchers. As such, a maximum axial acceleration constraint of $5g$ was imposed for the trajectory model. It is worth mentioning that for the trajectory model used in this study, no throttling can be applied to reduce

aerodynamic loads. Furthermore, the loads caused by SRB separation are not explicitly mentioned. Therefore, a conservative value of $5g$ was imposed for the trajectory model for the maximum axial acceleration constraint experienced during the aerodynamic flight phase.[12][61]

Maximum pitch rate
Due to the alternative guidance control technique used in the trajectory model, an additional constraint was added to ensure a realistic depiction of guidance actuator systems. The pitch rate refers to the pitch angle change per second during the ascent trajectory. Based on similar studies, a maximum pitch rate constraint was set at $5°/s$ to ensure only viable pitch control node sequences are considered for trajectory optimisation.

7.6. Model optimisation

The construction of the vehicle performance model by connecting the various submodels allowed for a global optimisation function to be set up to evaluate the two optimisation cases defined to answer *RQ-PERF-02*. These cases were defined as follows:

- **Case I (GLOM):** For a fixed payload, upper stage, and boosters mass, what is the minimum gross-lift-off-weight needed for the conceptual launch vehicles to reach the required end state conditions?
- **Case II (Payload capability):** For a fixed gross-lift-off mass and boosters mass, what is the maximum payload (upper stage + useful payload) that can be brought on the conceptual launch vehicles while reaching the required end state conditions?

In this section, the methods that were needed to optimise for these two cases will be discussed. This will include a discussion on the selection of an optimiser and the variables selected for this optimisation effort, as well as a sensitivity analysis regarding some influential parameters of the underlying trajectory optimisation algorithm.

7.6.1. Optimiser selection and variables
First, the selection of an optimiser will be considered. Thereafter, a set of optimisation variables will be reviewed, and the relevant optimisation ranges will be stated.

Optimiser selection: Differential evolution
For the global optimisation problem in this study, the *scipy.optimize.differential_evolution()* optimiser was selected. Differential evolution is a heuristic algorithm method originally developed by Storn and Price[152] in 1996 and available in Python through the "scipy" package. Although it often requires a larger number of function evaluations than most conventional gradient-based optimisers, the differential evolution method allows for a larger solution space to be considered without the need for any initial solutions to be defined. As it requires fewer control variables, it is easy and robust to use. Furthermore, the specific Python implementation of this method allows for parallel computation, which was found to speed up the optimisation process significantly. *scipy.optimize.differential_evolution()* functions as a genetic algorithm, targeting the fittest solutions and performing crossover in search for solutions satisfying a minimised objective function. The "best1bin" crossover method was chosen for creating new child solutions. With this method, two random solutions of the population are chosen, after which the best solution is mutated using a mutation factor and the difference of both solutions. This method is expressed in Equation 7.37, where b' is the new child solution, $f_{mutation}$ is the mutation factor, and b_0 and b_1 are the best random solution and the other random solution from the population. The differential evolution function is supplied with boundary values for each optimisation variable, after which the initial population of solutions is systematically searched and generated through equally spaced solution values.[152][153]

$$b' = b_0 + f_{mutation}(b_0 - b_1) \tag{7.37}$$

Using the differential evolution optimisation method, different launch vehicle concepts are generated based on the solutions, represented through different combinations of the optimisation variables proposed by the algorithm. For each launch vehicle concept, the characteristic payload mass

or gross lift-off mass, depending on the optimisation case, is then estimated through the mass model. Trajectory optimisation is then performed on each unique solution to allow for the fitness of the solutions to be evaluated with respect to the optimisation objective function. This objective was set up to take into account both the mass performance of the launch vehicle concepts and its ability to reach the intended trajectory state. Thereby, adequate margins of uncertainty are taken into account, as will be discussed in Section 7.6.2.

Optimisation variables

An essential part of setting up the global optimisation function for the vehicle performance model was the choice of optimisation variables. Here, the number of optimisation variables was a key factor as a balance had to be found between the computational efficiency of the optimisation problem and the meaningfulness of the results. In choosing the optimisation variables, the inputs to the respective submodels described in the previous section were considered. Ultimately, the following variables were selected:

- **Core stage burn time** As was discussed in the setup of the mass model, the core stage engine burn time could be considered a crucial input variable as it allows for the core stage propellant mass to be calculated. This, in turn, allows for either the total GLOM or payload mass to be estimated, depending on the case being studied. Both these masses and the burn time itself are, in turn, very influential factors in the trajectory model. Finally, the core stage engine burn time is also an essential input in setting up the pitch control nodes for the guidance function. For this study, the lower bound of the core stage engine burn time was set at $230s$, approximately $100s$ after SRB burnout and $200s$ before core stage burnout for the Ariane 6(2) reference launch vehicle. The upper bound was set at $630s$, $200s$ after core stage burnout for the Ariane 6(2) reference launch vehicle.

- **Nozzle area ratio:** In the setup of the propulsion model, several engine-specific design variables were introduced. Here, both the nozzle area ratio and the nozzle throat area are variables related to the geometry of the engine nozzle. The nozzle area ratio is a crucial parameter as it regulates the expansion of exhaust gases. It, therefore, is a measure of the efficiency with which the gases can be expanded, and as such, it influences all two key performance factors of the engine, these being the thrust and the specific impulse. By allowing the nozzle area to vary, the point of ideal expansion, which depends on the ambient pressure, could indirectly be optimised. The upper and lower boundaries of the nozzle area ratio were set at 10 and 45, respectively, based on the constant value chosen for the nozzle throat area to keep the nozzle exit diameter between $1m$ and $2.1m$ based on other launch vehicle engines.

- **Chamber pressure:** Where the nozzle area ratio is a design factor regulating the expansion of the flow once it has passed through the nozzle throat, the chamber pressure is the design factor that influences the force with which the flow is pushed through the throat. The chamber pressure could thus be considered amongst the most crucial engine-specific design variables as it significantly influences the performance of the engine. As such, it was deemed essential to include this as a way to introduce effective engine thrust variation within the optimisation function. Based on initial optimisation efforts, it was found that setting the lower bound at $4MPa$ was most computationally efficient as lower chamber pressures led to too much performance loss to generate optimised designs in accordance with the optimisation objectives. The upper bound was set at $6MPa$, based on the Viking 5C and Vikas 4B engines. This constraint limited the performance potential of the proposed storable bi-propellant combinations significantly, especially in comparison the the Vulcain 2.1 reference engine, which has a chamber pressure of $11.8MPa$. The reason for setting the boundary at this relatively low value was the lack of existing storable propellant engine designs characterised by higher chamber pressures. Several possible explanations were given as to why this is. First of all, it should be realised that high-pressure engines need extensive and highly effective cooling mechanisms. Therefore, either the oxidiser or the propellant are used as cooling fluids. Most conventional storable propellants are exothermically decomposed at extremely high temperatures, meaning that there is a limit to the applications in which they can be used as coolants. An example of this is MMH, for which the maximum allowable chamber pressure at which it could be used as a coolant was estimated at $4MPa$ in a study by Palmnas and Sunden[154] Next to this,

rocket engines operating at a high chamber pressure require specialised materials which are suitable to withstand these high pressure and high-temperature environments. As storable propellants are often more reactive, compatibility with these specialised materials could be an issue. This a problem that was deemed especially relevant for hydrogen peroxide, as it displays bad compatibility with several materials commonly used in aerospace applications. The reactivity of these storable propellants could also impose additional risks when used as coolants in extreme conditions. Finally, it could be argued that there was never a need for the development of storable propellant engines operating at high pressures, as cryogenic propellant engines were long deemed the better alternative for high-thrust applications. This also means that any results generated for storable propellant engines operating at a high chamber pressure would imply an additional risk and cost aspect due to the need for extensive development efforts to investigate and test these new system conditions.

It is worth remarking that the bounds stated for the optimisation variables were iterated upon several times based on observations from initial optimisation simulations. While the above-mentioned variables were considered the most relevant and crucial for the global optimisation problem, it could be argued that several other variables could have been considered based on the inputs listed for the submodels introduced in this chapter. Below, a rationale is provided as to why these variables were considered less relevant optimisation variables as compared to those mentioned above.

- **Fuel choice:** The research objective set for this study states the intent to study HTP-based bi-propellants. As such, the fuel choice, assuming HTP as the oxidiser, could be assumed as one of the optimisation variables for the study as a whole. For the optimisation function, however, this was not considered as the launch vehicle concepts based on the proposed propellant combinations were all optimised separately from each other to allow for an effective analysis of the results.

- **Number of engines:** This was initially not considered an optimisation variable, keeping in mind the Ariane 6 reference launch vehicle, which employs only one engine on its core stage. It was, however, found that due to the decreased performance of the proposed storable bi-propellant combinations, the proposed launch vehicle concept required additional thrust to meet the trajectory state objectives. This was deemed to be partially the result of the upper boundary that was set for the chamber pressure. Rather than introducing it as an optimisation variable, however, the optimisation was simulated for a number of different constant values for the number of engines. After the optimal number was found, all launch vehicle concepts were optimised for this same constant.

- **Nozzle throat area:** The nozzle throat area was kept constant to add a constraint to the variation in the nozzle geometry and to avoid unrealistic geometries by varying both the nozzle area ratio and the nozzle throat area. Following similar engines, Vikas 4B and Viking 5C, the nozzle throat area was set at a constant of $0.075m$, based on which the boundary values for the nozzle area ratio were determined.

- **Oxidiser-to-fuel ratio:** For each bi-propellant, an optimum O/F exists at which complete combustion takes place, thus maximising the efficiency and the resulting performance of the combustion process. Another optimum O/F could be defined specifically for launch vehicle design based on maximising the specific impulse density. Rather than include it as an optimisation variable, it was decided to calculate the optimum O/F for each of the proposed bi-propellant combinations. These were then included as constants in the optimisation of the respective launch vehicle concepts. The optimum O/F for each propellant combination can be found in Table 8.3.

The boundary values specified for each of the proposed optimisation variables were tabulated in Table 7.20. Here, the constant values set for the other important model input variables, which were discussed above, were also included.

Table 7.20: Constants and boundary values defined for input variables of the global optimisation problem

Design variable	Optimisation variable?	Units	Boundary/constant value
Core stage burn time	Yes	s	230-630
Nozzle area ratio	Yes	–	10-45
Chamber pressure	Yes	MPa	4-6
Number of engines	No	–	3
Nozzle throat area	No	m^2	0.075
Oxidiser-to-fuel ratio	No	–	Propellant specific (Table 8.3)

7.6.2. Optimisation uncertainty

The main objective of this study is to perform a comparative analysis of the performance potential of several propellant combinations for a specific launch vehicle case. While this diminishes the need for a fully optimised and accurate set of results, it was still deemed important to have a rough measure of the uncertainty of the results due to the choice of parameters in setting up the various submodels. Therefore, some influential factors and main indicators of the uncertainty of the optimisation model will be discussed in this subsection. Next to that, an approach will be suggested to incorporate this uncertainty into the results presented in Chapter 8.

Trajectory optimisation GA parameters

In Section 7.5.4, the use and setup of a genetic algorithm for trajectory optimisation were discussed. Here, several parameters were introduced that could be adjusted to find a balance between computational efficiency and certainty of the optimisation results. Below, a brief rundown of the most influential parameters will be given. Thereafter, a sensitivity analysis based on these parameters will follow to provide reasoning for the exact settings of the trajectory optimisation algorithm parameters that were decided upon.

- **Population size:** This is the number of unique solutions, in this context pitch control node sequences, initially provided to the algorithm. As the population size is maintained between generations, this is also the total number of solutions, not necessarily unique, considered in subsequent generations.
- **Number of iterations:** As all solutions of the population have been evaluated with respect to the objective function, the best solutions are selected and modified to generate so-called child solutions for the next generation, which is subsequently also evaluated. Each repetition of this process is referred to as an iteration.
- **Number of regeneration cycles:** Rather than iterate and create new generations with existing solutions, the best solution could also be transferred to a new population which is then filled with new randomly generated unique solutions. This process was described as regeneration.

It is worth noting that there were other parameters that could be adjusted in setting up the algorithm. It was, however, found that these were not as influential as the three parameters introduced above. To determine the exact values to which the parameters were set for this study, a sensitivity analysis was performed in which the computational time and accuracy of the optimisation results were compared for different settings. In Figure 7.18 and 7.19, the average and the standard deviation of the trajectory optimisation objective scores are visualised for different settings of the GA. Here, the objective scores were found through the objective function expressed in Equation 7.35, as a function of the altitude, flight angle, and velocity end states of the concept launch vehicle, and as a function of the maximum altitude observed during the trajectory. To illustrate the meaning of these scores, a comparison can be made with the optimised trajectory that was shown in Figure 7.15 and which was awarded a score of 2.
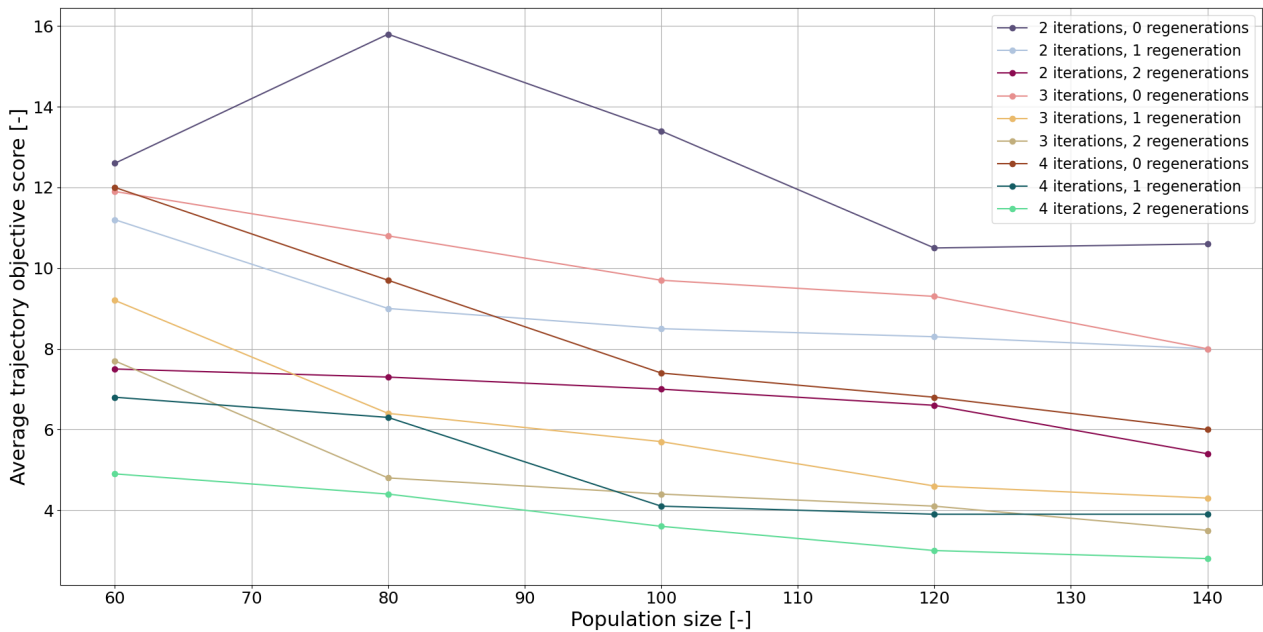
Figure 7.18: The average of the objective scores obtained for the optimised trajectory of a proposed launch vehicle concept, compared for different settings of the optimisation algorithm (GA)
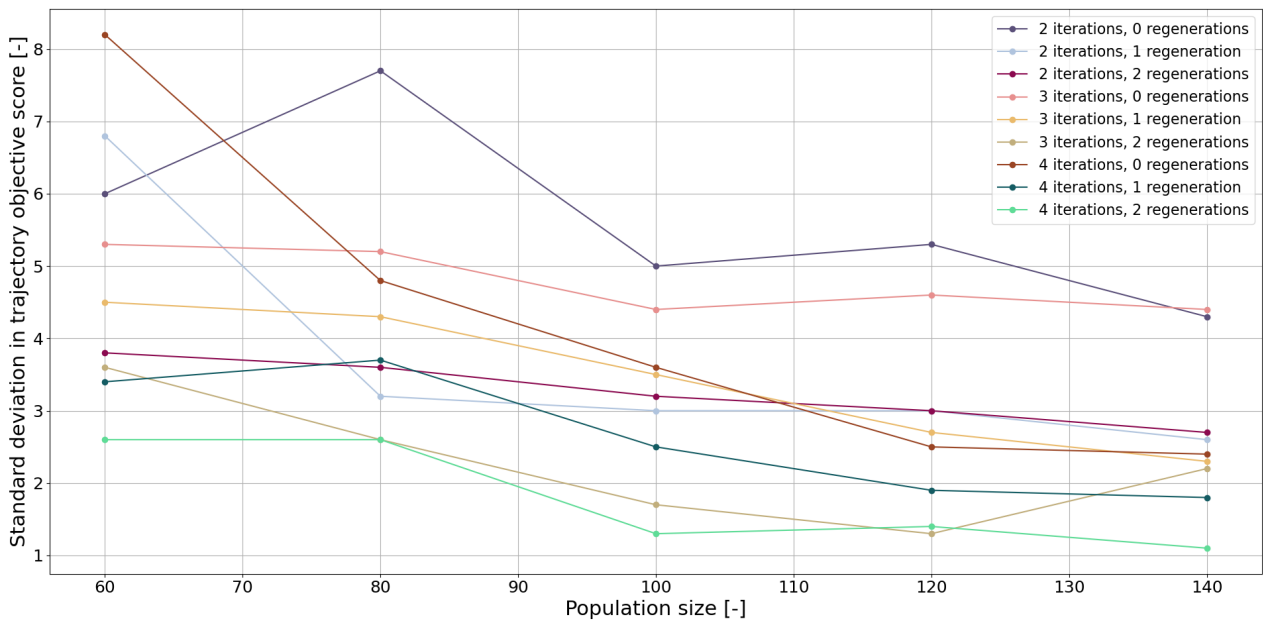
Figure 7.19: The standard deviation of the objective scores obtained for the optimised trajectory of a proposed launch vehicle concept, compared for different settings of the optimisation algorithm (GA)

Due to the fault detection methods introduced in the algorithm, several "faulty" solutions are discarded, and the number of unique solutions is decreased, as well as the level of variation in new generations. Therefore, it was found that a large number of iterations is not as effective for this specific optimisation algorithm. As can be observed in Figure 7.18, the regeneration method proves to be more effective as it increases the chance of new solutions with a high fitness to the objective solution being introduced. Similarly, a large population size is shown to be important in obtaining accurate and consistent scores. It was found that this was especially effective in combination with several regeneration cycles to maximise the amount of fresh solutions.

Next to the accuracy of the optimisation algorithm through the selected parameters, it was also deemed important to take into account the computation time needed for each trajectory optimisation effort. As a trajectory optimisation sequence is performed for each unique solution of the global optimisation model, the total time needed for a convergent solution to be found through the global optimisation model is effectively the sum of the computational times needed for each trajectory optimisation effort. In Figure 7.20, the average of the trajectory optimisation computation times are visualised for different settings of the GA. It can be observed that the computational time progresses linearly with population size. Similarly, a quasi-linear increase can be observed for increasing iteration and regeneration cycles. It is worth noting that the absolute values found for the computational time are a result of the computer on which the simulation is run, yet it is a good indicator for a comparative analysis.
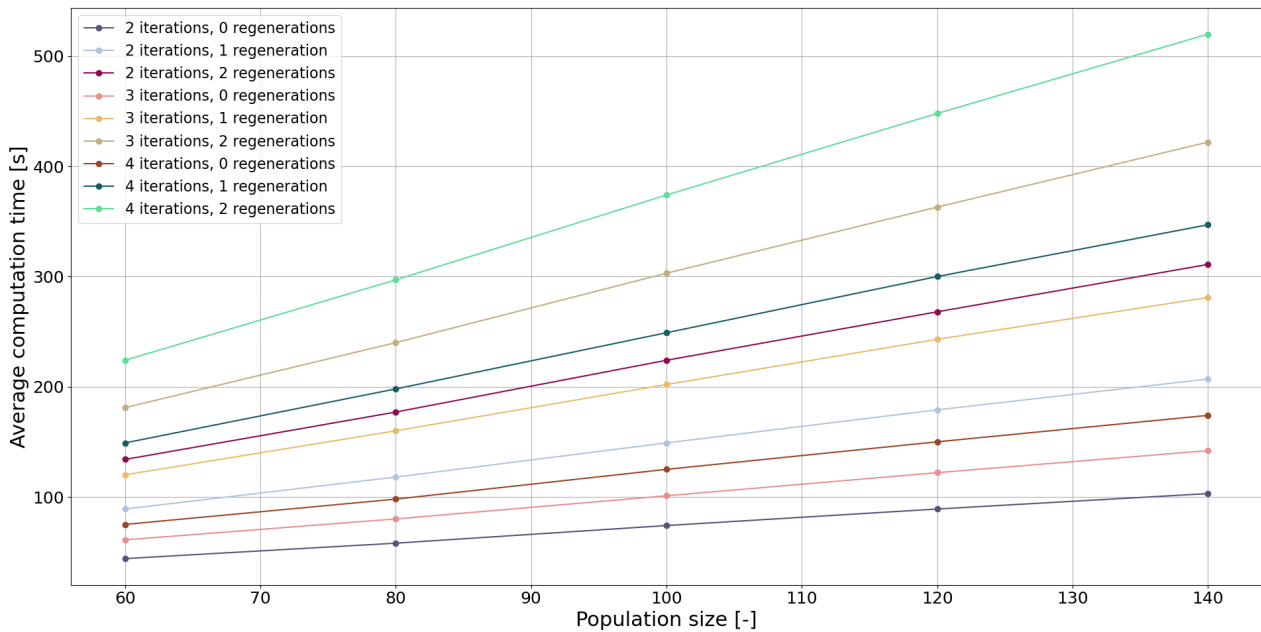
Figure 7.20: The average of the computational time needed to optimise the trajectory of a proposed launch vehicle concept, compared for different settings of the optimisation algorithm (GA)

Based on the analysis presented above, it was decided to adjust the population size parameter to 100, the number of iterations to 3, and the number of regeneration cycles to 1. These settings correspond to an average computation time of 200s, while maintaining an average objective score of 5.7. Choosing these settings allowed for the computational time per trajectory optimisation effort to be lowered significantly, thereby also guaranteeing a reasonable average objective score of 5.7±3.5. It was realised, however, that the increased deviation in the objective scores as compared to more accurate settings could potentially introduce inaccuracies in the result. Given that the standard deviation on the objective score for these settings was found to be 3.5, trajectory optimisation applied to the same launch vehicle concept could have led to trajectory objective scores between 2.2 and 9.2. As such, it was found that it would be hard to distinguish between good solutions for which a bad trajectory score was obtained and bad solutions for which already the best possible trajectory objective score was obtained. At first, it was attempted to solve this problem by performing additional trajectory optimisation on these border cases, thereby using more accurate settings for the algorithm. It was found, however, that increasingly more of these border cases were found as the global optimisation model converged, making this approach very complex and computationally expensive.

Instead, it was decided to apply a margin of uncertainty on the results, thereby expressing the global optimisation results, either the payload capability or the gross lift-off mass, as a range rather than one definitive set of values. This range was effectively determined by including all solutions for which a trajectory objective score of 5.7±3.5 was found. Here, the centre point of this range was

set at the highest payload solution for which a trajectory objective score between 0 and 5.7 was obtained.

Chamber pressure boundary constraint
Upon discussing the upper boundary value for the chamber pressure in the context of the global optimisation setup, a lack of existing storable propellant engines operating at high chamber pressure was argued. Here, the Vikas 4B and the Viking 5C were pointed out to be the storable propellant engines operating at the highest chamber pressure. This is, however, not strictly true as the RD-253 family of rocket engines operate at a reported chamber pressure of up to $16MPa$. Subsequently, the strongest engines in this family are characterised by a reported vacuum thrust of just below $1.9MN$. This thus contradicts the conclusions drawn in Section 7.6.1 and the subsequent boundary values set for the chamber pressure as an optimisation variable. Yet, it was noted that this series of high-performance storable propellant engines could be considered an exception rather than the norm, and the aforementioned problems related to the development of storable propellant engines operating at a high chamber pressure are still relevant. Therefore, it was deemed essential to investigate the potential effects of the imposed upper boundary for the chamber pressure on the performance of the design concepts. In Figure 7.21, using the propulsion model set up for this study, the three key engine performance characteristics of thrust, specific impulse, and mass flow were calculated for a range of chamber pressure values. The relative increase of these parameters was measured with increasing chamber pressure as compared to a reference point set at the upper boundary value of $6MPa$, which was considered for the global optimisation study. Here, it could be observed that all performance parameters have a quasi-linear relation with the chamber pressure. Furthermore, while a noticeable increase was observed in the mass flow, vacuum thrust, and sea-level specific impulse for increasing chamber pressure, the most significant increase was observed for the sea-level thrust. Here, a relative increase of 250% was observed at the chamber pressure with which the RD-275M rocket engine is operated as compared to the reference point. The effect of an increasing chamber pressure could be seen to be most significant for sea-level terms. Looking at Equation 7.9, this does indeed make sense as the chamber pressure is included in the atmospheric pressure term that is part of the thrust coefficient equation.
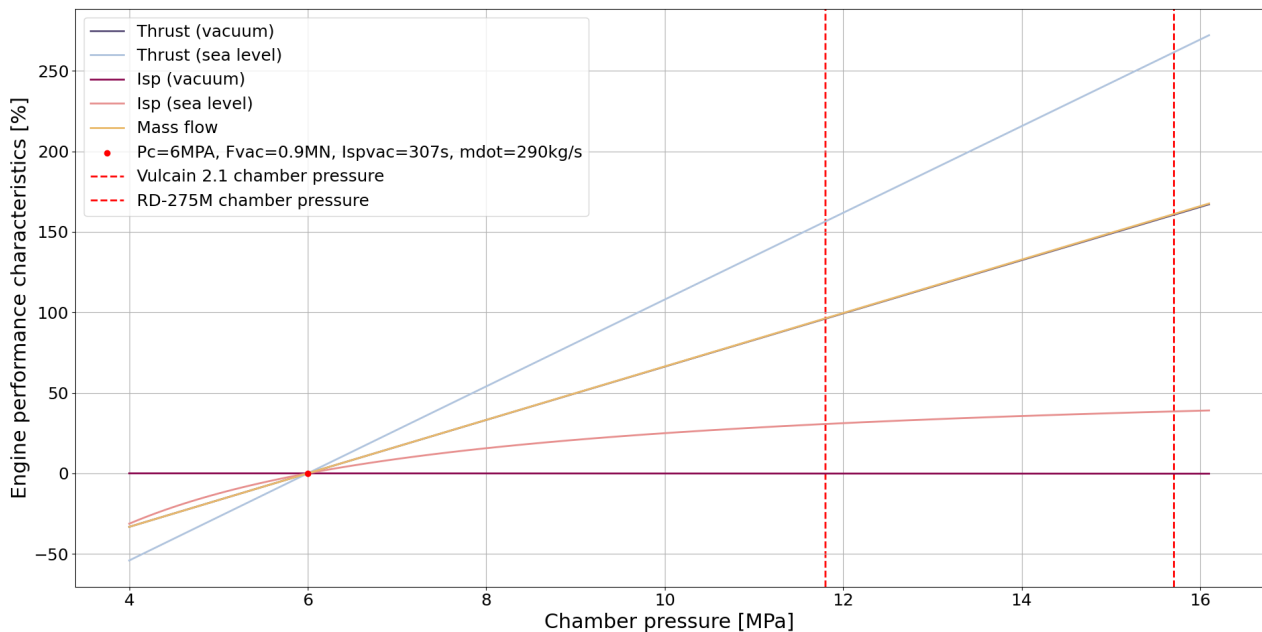
Figure 7.21: The sensitivity of key engine performance characteristics (thrust, specific impulse, mass flow) to an increase in chamber pressure. The data was gathered for a RP-1/HTP engine with a nozzle ratio of 45, an O/F of 6, and a nozzle throat area of $0.075m^2$.

Following the significant effects of the chamber pressure on the engine performance, it was realised that due to the precedent set by the RD-253 series rocket engines, the consideration of high cham-

ber pressures for optimisation purposes was required to ensure a wider range of applications was covered in this study. Yet, it was also noted that since the RD-253 rocket engine family could be considered outliers amongst the storable propellant engines in terms of operating chamber pressure, simply setting the upper boundary for the chamber pressure to a higher value of $16MPa$ could also introduce an undesired bias into the results. Here, it is also important to note that the storable propellant used in the RD-253 series rocket engines was MMH/NTO rather than an HTP-based bi-propellant. As such, any additional difficulties with respect to the future development of such a high-pressure rocket engine employing hydrogen peroxide would not be accounted for. Therefore, it was decided to investigate the effects and the potential of increased chamber pressures by means of a sensitivity analysis rather than to make changes to the original optimisation case. In this sensitivity analysis, a revised boundary value for the chamber pressure of $16MPa$ would be considered for the optimisation of a single bi-propellant combination based on the performance potential observed in the original optimisation study. The boundary values for this additional optimisation study case were tabulated in Table 7.21. Note that the core stage burn time boundaries were also adjusted to give more insight into the range of the results.

Table 7.21: Constants and boundary values defined for input variables of the additional global optimisation problem (revised chamber pressure boundary)

Design variable	Optimisation variable?	Units	Boundary/constant value
Core stage burn time	Yes	s	132.8-1132.8
Nozzle area ratio	Yes	–	10-45
Chamber pressure	Yes	MPa	4-16
Number of engines	No	–	3
Nozzle throat area	No	m^2	0.075
Oxidiser-to-fuel ratio	No	–	Propellant specific (Table 8.3)

7.7. Chapter summary

In this chapter, the setup of the second research segment was described, central to which is the vehicle performance model. This mostly analytical model was created to allow for an answer to RQ-PERF-01 and RQ-PERF-02 to be provided regarding the propulsion and mass performance potential of proposed launch vehicle concepts employing HTP. To this extent, five (sub)models were introduced. The *propulsion model* was needed to estimate the performance of engines for different propellants and engine settings. Therefore, data was extracted from NASA's CEA program to model the combustion process in the engine, after which ideal rocket theory was used to predict the performance of the engine. To account for inefficiencies in the engine that are not considered through ideal rocket theory, correction factors were introduced in the model based on data from existing engines.

To set up the *mass model*, existing MERs by Zandbergen were implemented and validated. Upon validating the resulting model with existing launch vehicles, a mean error of 6.41% was observed. Furthermore, the model proved to be very accurate in predicting the mass of the Ariane 6(2) reference launch vehicle. A major advantage of HTP-based propellants is their high density. Therefore, a *sizing model* was deemed essential to capture and effectively compare the effect of this density advantage on the resulting launch vehicle geometry. The sizing model was set up using simple geometric relations and relevant structural constraints, the most influential of which was the fineness ratio constraint. By imposing this constraint, the resulting launch vehicle geometries are made aerodynamically efficient while ensuring structural integrity. Another relevant assumption to be introduced was the no-taper assumption, which effectively means that the stage diameter is kept constant over the whole launch vehicle length, similar to Ariane 5 and Ariane 6.

The vehicle geometry found in the sizing model was used as an input for the *aerodynamics model*, together with the Mach number and the angle of attack at a given state. Using the RASAero II software, these inputs could be combined to predict the aerodynamic coefficients, C_D and C_L, of the

launch vehicle at the given state. The side force coefficient C_S was assumed to be negligible. Using the inputs from the other models, the trajectory of the launch vehicle concepts was predicted by making use of the Tudat Python module. To provide guidance to the vehicle, a pitch control law method was employed, which enforces pitch angles to the vehicle at every time step of the trajectory based on prespecified nodes. Trajectory optimisation was added to the model, where a genetic algorithm is used to find the optimal sequence of pitch nodes needed to reach an objective state. This objective state was defined as a function of the final velocity, altitude, and flight path angle states, as well as the maximum altitude state over the course of the trajectory. This model was effectively validated using data from an Ariane 5 mission.

Finally, *global optimisation* was introduced to the vehicle performance model, thereby connecting all (sub)models. Two optimisation cases were described, the first focusing on the optimisation of the launch vehicle GLOM, and the second focusing on the optimisation of the launch vehicle payload capability. A genetic algorithm was introduced to optimise based on four input variables: core stage burn time, nozzle area ratio, chamber pressure, and number of core stage engines. The boundaries for these inputs can be found in Table 7.20. A factor of uncertainty was introduced based on the accuracy of the trajectory optimisation model. The optimisation point is defined as the maximum mass state for which a trajectory score of at least 5.7 is found. Other viable trajectories were considered to be those up to 9.2. The results of this optimisation effort and a subsequent sensitivity analysis will follow in Chapter 8.

8.Vehicle performance model results

In Chapter 4, it was explained that this study consisted of two main research segments, corresponding to subdivision made to the main research objective in Chapter 3. Here, the second research objective was aimed at *investigating the performance potential of employing storable propellants based on hydrogen peroxide as an oxidiser on the core stage of a medium-weight launch vehicle with respect to overall launch vehicle propulsion and mass performance definitions*. A further subdivision was made in this research segment to set up two main research questions, thereby making a distinction between the propulsive performance and mass performance of the launch vehicle concepts. The two main research questions for the second research segment were defined as:

- RQ-PERF-01: What is the propulsion performance potential of storable non-toxic fuels combined with hydrogen peroxide?
- RQ-PERF-02: How does the integration of selected green bi-propellants in the core stage of a medium-lift expendable launch vehicle affect the payload capability of the vehicle?

In Chapter 7, the setup of the *vehicle performance model* was described. This numerical model allowed for answers to be provided to the research questions of the second research segment. Here, *RQ-PERF-01* was addressed through the propulsion model. The subsequent answers to this research question will be provided in Section 8.1. A mass and sizing model and an aerodynamics and trajectory model were connected to the propulsion model to allow for global optimisation with respect to mass performance as to answer *RQ-PERF-02*. The results of this optimisation study will be presented and analysed in Section 8.2. Furthermore, a brief sensitivity analysis will be presented in Section 8.2.3, in which the sensitivity of the payload capability optimisation results to the optimisation model inputs will be discussed.

The first research segment of this study concerned a *baseline fuel assessment* in which a large number of HTP-based bi-propellants were evaluated based on non-performance related characteristics. After a preliminary feasibility assessment, only a small selection of these propellants was considered for a detailed assessment and suggested for a further numerical comparison through the vehicle performance model. In Chapter 6, four additional propellants were added to this list for which a high performance was predicted and which were deemed interesting for further study despite not being included in the final assessment of the first research segment. An overview of the propellants considered for the vehicle performance model can be found inTable 8.1.

Table 8.1: Fuels considered for the PICE assessment and additional fuels considered for the vehicle performance model

PICE assessment	Vehicle performance model only
Ethanol	DMAZ
Isooctane	Jet-A
Isopropanol	JP-10
Methanol	Methane
RP-1/Kerosene	
TMPDA	
Toluene	
Turpentine	

8.1. Propellant propulsion potential

The capabilities of a launch vehicle are predominantly the result of the performance capabilities of its engines, as these provide the propulsion needed for the launch vehicle to reach its intended

state. The most important factors contributing to the performance of rocket engines are the design of the engine and the choice of propellant. Therefore, when making a comparative study on rocket propellants, it is important to understand the propulsive potential that is characteristic of each of these propellants. An effective parameter used to express the propulsive potential of rocket propellants is the specific impulse. It is, in essence, a measure of the efficiency with which the available propellant mass is used to provide a velocity increment to the system, i.e., a measure of how efficiently the propellant is converted to workable impulse. Although this performance parameter is also affected by the general engine design, it is mostly determined by the selected propellant and is, therefore, a relevant measure for the propulsive potential of the propellant.

For this study, a propulsion model was developed to predict the propulsive performance of specific engine designs. As per the setup of this model explained in Section 7.2, CEA was used to model the combustion of the selected propellants. Relevant outputs were then processed and combined with inputs of the engine design to predict the performance of the engine through ideal rocket theory. It is thus important to realise that the predictions for the specific impulse obtained through this model are, to some extent, dependent on specific engine design parameters. As the specific impulse is mostly dependent on the choice of propellant, however, it could be argued that the comparative value of this analysis was mostly maintained if the same engine design was assumed for all propellant combinations. Therefore, it should be noted that all of the results presented in this section were obtained for the same engine design inputs. These inputs were tabulated in Table 8.2 and were based on the boundary values set for these variables in Section 7.6.1 in the context of the global optimisation study. Additionally, vacuum conditions were assumed as to neglect the effect of the atmosphere on the results.

Table 8.2: Engine design parameters used to generate the results for the analysis of the propellant propulsion potential

Engine Design variable	Units	Value
Chamber pressure	MPa	6
Nozzle area ratio	–	0.075
Nozzle throat area	m^2	45

8.1.1. Optimum oxidiser-to-fuel ratio

The oxidiser-to-fuel ratio is an expression indicating the mass-specific proportions between the oxidiser and the fuel in a bi-propellant mixture. Controlling this ratio is crucial in realising an effective and energy-rich combustion process. For each specific bi-propellant combination, an optimum O/F exists, signifying complete and thus efficient combustion. Not coincidentally, this point of optimum O/F coincides with the maximum value of specific impulse for the specific propellant. After all, the specific impulse is a measure of the efficiency of the propellant, meaning that incomplete combustion as a result of a non-optimum O/F is bound to negatively affect the specific impulse. In accordance with the definition of optimum O/F presented here, the optimum O/F values for the propellants studied in this research segment could be deduced from Figure 8.1. Here, LH2/LOX (hydrolox, cryogenic) and UDMH/NTO (storable) were included to serve as a reference for conventional propellants used in launch vehicles. From this figure, it can be observed that most HTP-based propellant combinations are characterised by a rather high O/F between 6 and 8. This means that the relative amount of HTP needed to ensure efficient combustion in these cases is quite high. Exceptions to this are methanol, ethanol, isopropanol, and DMAZ, for which an optimum O/F between 3 and 5 was found, similar to that of hydrolox. It is worth noting that reference propellant UDMH/NTO is characterised by a rather low optimum O/F, meaning that a relatively high amount of UDMH is needed for efficient combustion to take place. This is especially problematic given the high level of toxicity for which this fuel is known.
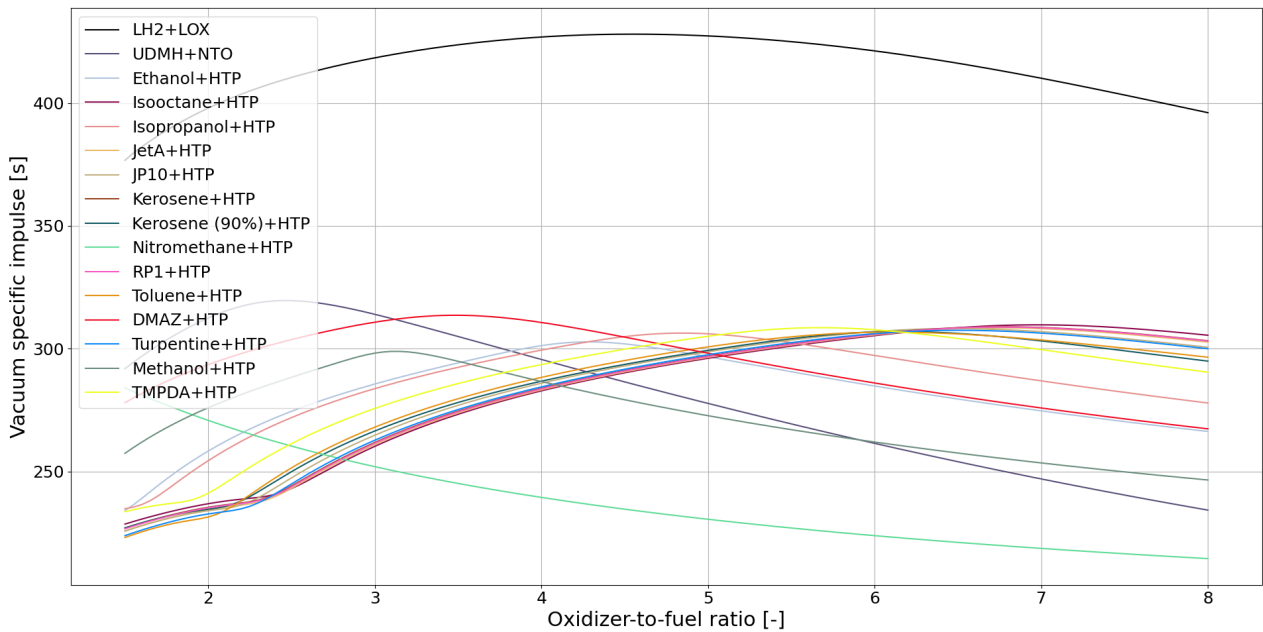
Figure 8.1: The optimum oxidiser-to-fuel for the proposed bi-propellant combinations ($eta = 45$, $A_t = 0.075m^2$, $P_c = 6MPa$)
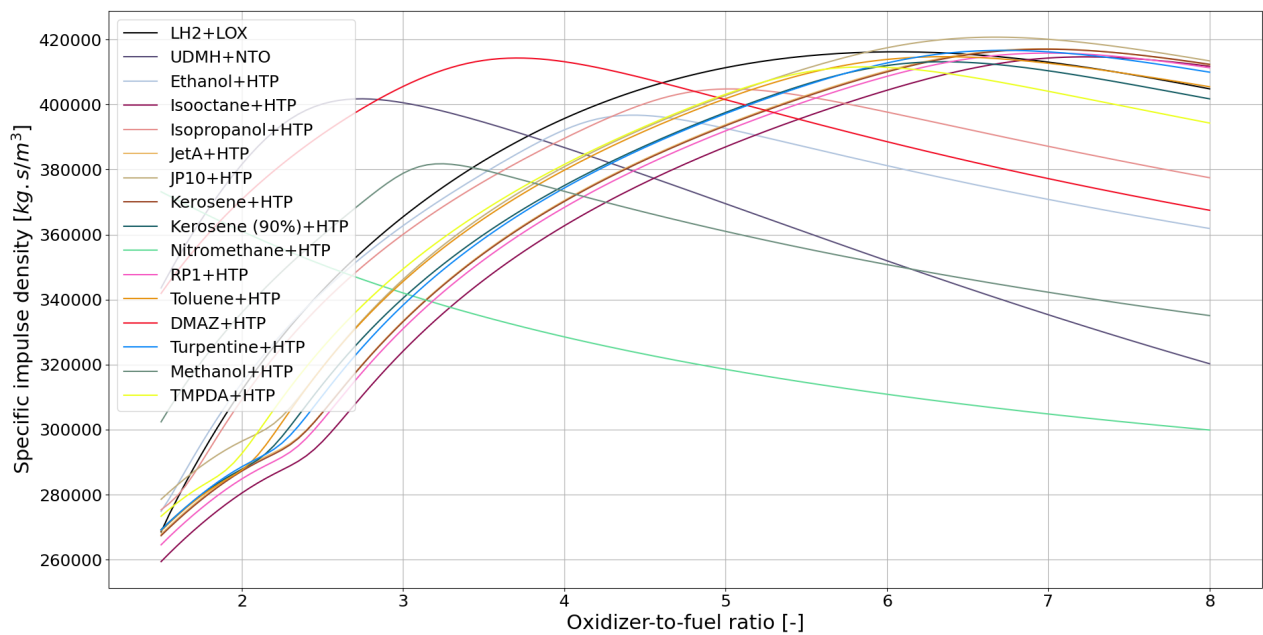
Figure 8.2: Specific impulse density versus oxidiser-to-fuel for the proposed bi-propellant combinations ($eta = 45$, $A_t = 0.075m^2$, $P_c = 6MPa$)

In Section 7.6.1, it was discussed that the O/F would be assumed constant during the global optimisation study, hereby taking on the optimum value for each specific propellant. That optimum O/F is not the same as the one referred to above, but rather it is based on a definition more applicable to launch vehicle design. As stated earlier, O/F is a measure of the amount of oxidiser mass to the amount of fuel mass used in a combustion reaction. The O/F setting for the main engine thus directly affects the ratio of oxidiser mass to fuel mass taken on board the launch vehicle. From the setup of the sizing model in Section 7.3.3, it could be deduced that the propellant volume is a very influential factor in the total size of the launch vehicle. As such, a high propellant density is considered desirable to limit the overall dimensions of the launch vehicle and thereby

improve the aerodynamic efficiency of the design. In Figure 8.2, the distribution of optimum O/F values for the selected propellants was visualised as per the revised definition for optimum O/F. The different optimum O/F found for the considered propellant combinations with both definitions of the optimum value were tabulated in Table 8.3. For the majority of the propellants, a shift in the optimum O/F value can be observed, albeit not very significant in most cases. Most noticeably, the optimum O/F for the conventional propellant hydrolox has shifted from 4.55 to 6.05. The latter value matches well with the O/F of 6.03 reported for the Vulcain 2.1 rocket engine, which employs hydrolox and was considered the reference engine for this study. As such, the validity of this approach for launch vehicle design was confirmed.

Table 8.3: Optimum oxidiser-to-fuel ratio for proposed bi-propellants and the oxidiser-to-fuel ratio selected for the optimisation model based on specific impulse density

Fuel Oxidiser	LH2 LOX	UDMH NTO	Ethanol HTP	Isooctane HTP	Isopropanol HTP	Jet-A HTP
Optimum O/F (Isp, vac)	4.55	2.45	4.3	6.95	4.85	6.75
Optimum O/F ($\rho - Isp, vac$)	6.05	2.75	4.45	7.25	5.05	6.95

Fuel Oxidiser	JP-10 HTP	Kerosene HTP	Kerosene 90% HTP	Nitromethane HTP	RP-1 HTP	Toluene HTP
Optimum O/F (Isp, vac)	6.75	6.75	6.15	1.5	6.75	6.1
Optimum O/F ($\rho - Isp, vac$)	6.65	7	6.35	1.5	7	6.35

Fuel Oxidiser	DMAZ HTP	Turpentine HTP	Methanol HTP	TMPDA HTP
Optimum O/F (Isp, vac)	3.5	6.5	3.15	5.65
Optimum O/F ($\rho - Isp, vac$)	3.7	6.7	3.25	5.85

8.1.2. Performance comparison

As a result of the prior analysis, an additional measure of the propulsive potential was identified to accommodate a comparative performance analysis of the considered bi-propellants. Next to the specific impulse at vacuum conditions, the specific impulse density for each of these propellants was thus predicted through the propulsion model, thereby respecting the optimum O/F values stated in Table 8.3. The results of this simulation were visualised in Figure 8.3. Some important observations can be made that were already visible in Figure 8.1 and Figure 8.2. First of all, it can be seen that in terms of the pure specific impulse performance, the cryogenic reference propellant hydrolox outperforms all of the storable propellants considered for this analysis by at least 109s or 25%. Additionally, the other reference propellant included in this analysis, UDMH/NTO, also shows better performance than the HTP-based propellants. Here, it is important to realise that the difference with the best-performing HTP-based propellant is significantly smaller at only 5s or 2%. Amongst the HTP-based bi-propellants, most of the performance predictions show to be within a range of 300-310s for the vacuum specific impulse, with only DMAZ/HTP being a top outlier at 314s and nitromethane/HTP being a bottom outlier at 284s. A clear shift in performance can be observed when taking into consideration the reported values for the specific impulse density. Here

hydrolox, as a result of the low density of liquid hydrogen, is predicted to have a similar or lower specific impulse density than the kerosene derivative fuels. Amongst these, RP-1 shows the highest performance in terms of specific impulse density. Furthermore, high performance can also be observed for isooctane, turpentine, and DMAZ. Also interesting is the noticeably lower performance of some fuels, including ethanol and methanol, but also UDMH/NTO, which outperforms the HTP-based propellants in terms of pure specific impulse. These results could be considered unsurprising given the high optimum O/F found for the HTP-based bi-propellants and the high density of hydrogen peroxide in its concentrated state. It is worth pointing out that the density figures used for setting up the analysis were derived from CEA. Values found at other sources could lead to slightly different relative proportions.
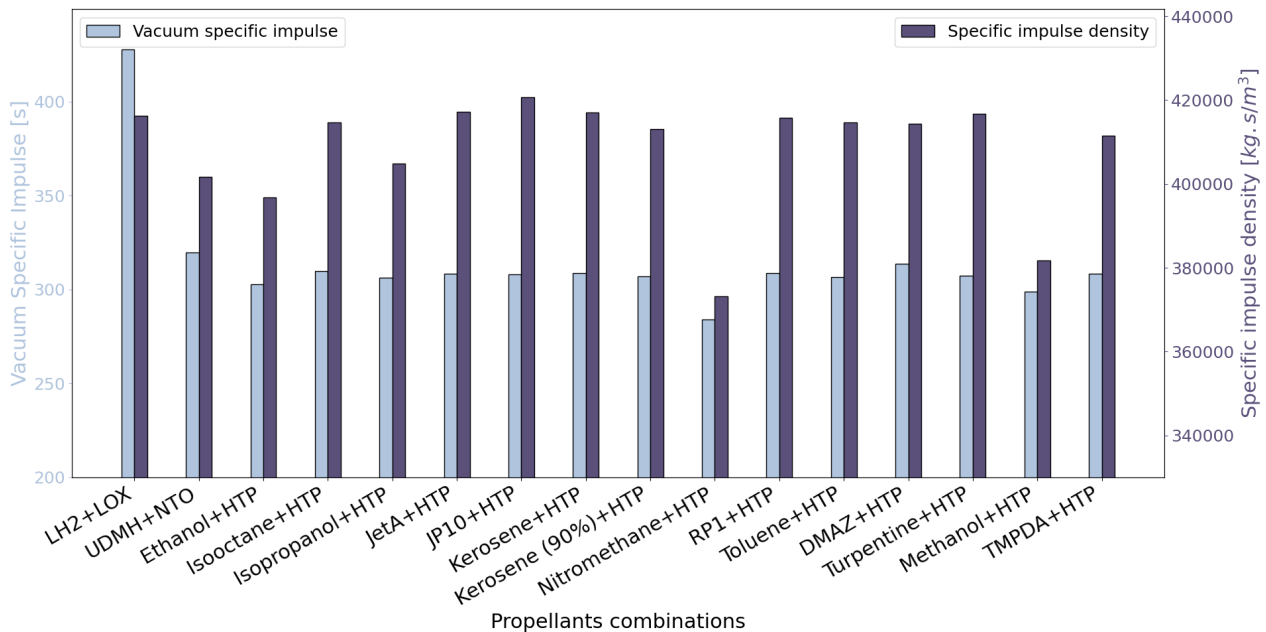
Figure 8.3: Comparison of the propulsion potential of the proposed bi-propellants through the vacuum specific impulse and the specific impulse density ($eta = 45$, $A_t = 0.075m^2$, $P_c = 6MPa$)

Based on the observations made through this comparative analysis of the propulsion performance of the considered propellants, an answer could be formulated to research question **RQ-PERF-01** and its corresponding subquestions. In terms of specific impulse, the HTP-based bi-propellants considered for this study were shown to have significantly lower performance than the cryogenic reference propellant hydrolox and slightly lower performance than the conventional storable bi-propellant UDMH/NTO. Hereby, the highest specific impulse amongst HTP-based bi-propellants was found for DMAZ/HTP. In terms of specific impulse density, a similar or better performance was found for kerosene-derivative fuels as compared to hydrolox, while also for isooctane, DMAZ, and turpentine, a high performance was found. These fuels all performed better than UDMH/NTO in terms of specific impulse density. The results from the propulsion potential analysis closely match the hypotheses which were formulated in Section 4.3 based on findings from literature. The specific impulse values predicted through the propulsion model were within the expected range for both the cryogenic reference propellant hydrolox and the HTP-based propellants. As expected, slight deviations could be attributed to the choice of engine parameter inputs and experimental conditions. Furthermore, the difference in specific impulse between the HTP-based propellants and hydrolox was observed to be 25%, which exactly matched the predictions stated in the hypotheses.

8.2. Global mass optimisaton

In launch vehicle design, mass is arguably one of the most important design drivers as not only is it a good indicator of the capabilities of a vehicle, but it also influences other design factors such as cost and development needs. As a launch vehicle consists of several mass components, the study

of mass optimisation in launch vehicle design could cover many different aspects of the design and is not limited to one optimisation point. As such, two main optimisation cases were defined in this study.

- **Case I (GLOM):** For a fixed payload, upper stage, and boosters mass, what is the minimum gross-lift-off-weight needed for the conceptual launch vehicles to reach the required end state conditions?
- **Case II (Payload capability):** For a fixed gross-lift-off mass and boosters mass, what is the maximum payload (upper stage + useful payload) that can be brought on the conceptual launch vehicles while reaching the required end state conditions?

As explained in Section 8.2, a global optimisation model was set up using a heuristic method to search a constrained solution space. These solutions were then subjected to trajectory optimisation and subsequently evaluated with respect to the objective function. New solutions were constructed based on the fittest solutions found in previous iterations and this process was repeated until an optimum solution was found. Due to the limited accuracy of the trajectory optimisation algorithm, a margin of uncertainty was applied to the results, specific for each optimisation run. As stated before, the focus of this study is to provide a comparative analysis of launch vehicle concepts based on different HTP-based bi-propellants. The objective was to compare the mass performance potential of these launch vehicle concepts, both with respect to each other and with respect to a reference launch vehicle, this being Ariane 6 in a 2-booster configuration. As such, the results presented in this section will be analysed with a focus on comparison rather than definitive prediction value.

8.2.1. Global GLOM optimisation

As stated above, case I was centred around the optimisation of the gross lift-off mass of the launch vehicle concepts. Here, a fixed payload mass was assumed based on the Ariane 6(2) launch vehicle. The goal of this optimisation was thus to find the minimum GLOM needed to get a specific payload mass to a prespecified orbit. Upon starting the optimisation process, it was found that the thrust generated by the proposed storable engines was insufficient to bring the payload to the required trajectory states in a 1-engine configuration. As such, the optimisation model was run for different engine configurations until convergent solutions were found for a launch vehicle concept using two core stage engines. It is worth noting that increasing the number of engines also implies an increase in mass flow rate and, thus, an increase in the total propellant mass. It was found, however, that by using a 2-engine configuration, the observed thrust-to-weight ratio (T/W) is sufficient to provide the acceleration required to reach the objective trajectory states within a reasonable amount of time. It is worth mentioning that while increasing the number of engines solved the problem as it allowed for a reasonable optimised solution to be found, it could lead to other complications. As more systems are used and need to be interconnected, the overall complexity of the launch vehicle design increases, thus decreasing the reliability of the system. Furthermore, sufficient space needs to be available for the engines and the additional system structures to be placed on the core stage. Due to the minimum stage diameter constraints imposed when setting up the sizing model in Section 7.3.3, this did not turn out to be a problem in this study. Also, while it is important to mention the added complexity of a 2-engine configuration, no further quantification of this design choice on the overall reliability of the launch vehicle was performed given that the focus of this study was purely on launch vehicle mass optimisation.

The results of the GLOM optimisation model can be found in Figure 8.4 and 8.5. Here, it can be seen that all optimised launch vehicle concepts were found to have a GLOM in the same range of 750-850t. This corresponds to a 42-61% difference as compared to the reference mass of Ariane 6(2) as reported in literature. It can also be observed that the Ariane 6(2) GLOM predicted through the optimisation model is 3% lower than this value reported in literature. It should be mentioned that while it is likely that a similar level of "underestimation" of the GLOM could be assumed for the HTP-based launch vehicle concepts, this can not be confirmed with certainty. A plausible explanation for this underestimation is the slight performance differences observed between cryogenic propellant designs and storable propellant designs in the propulsion model and in the mass and sizing model. While small, it is not unreasonable to think that this could have led to a difference in the optimised

GLOM of up to 3% or 15t. Furthermore, it is reasonable to assume that assumptions made in the trajectory model, such as the absence of sideslip forces and the constant heading angle, have similarly influenced the mass optimisation results predicted through the model.
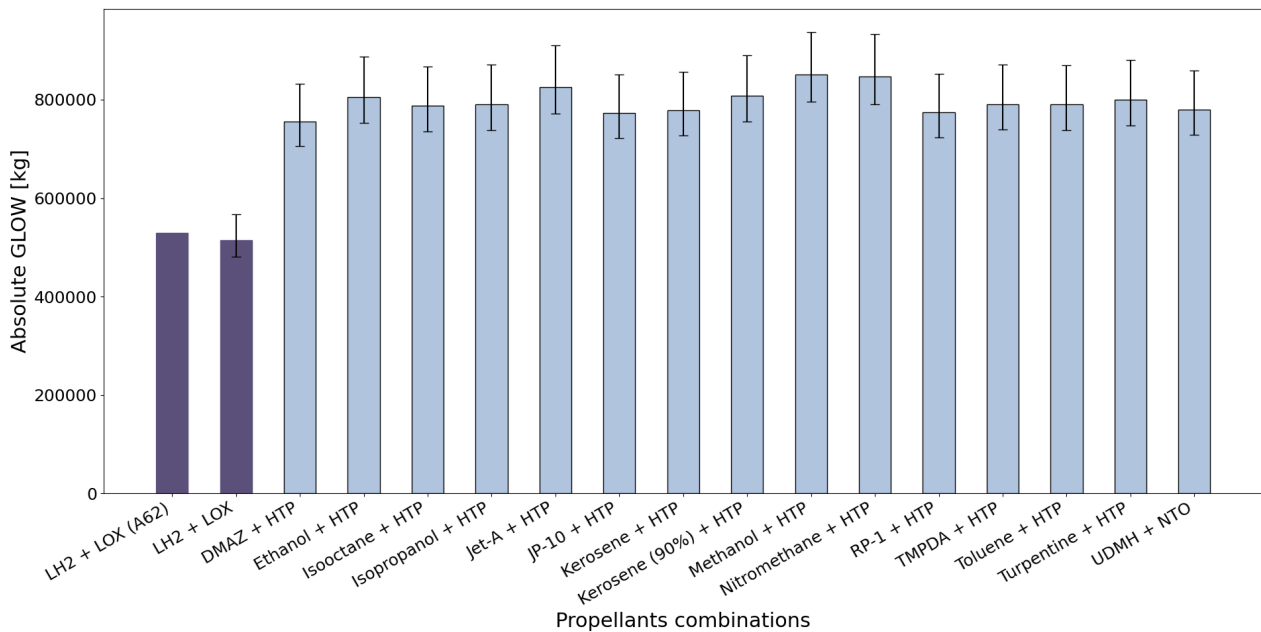
Figure 8.4: Comparison of the optimised absolute GLOM for the considered bi-propellant combinations with respect to the real and model-optimised GLOM of Ariane 6(2)
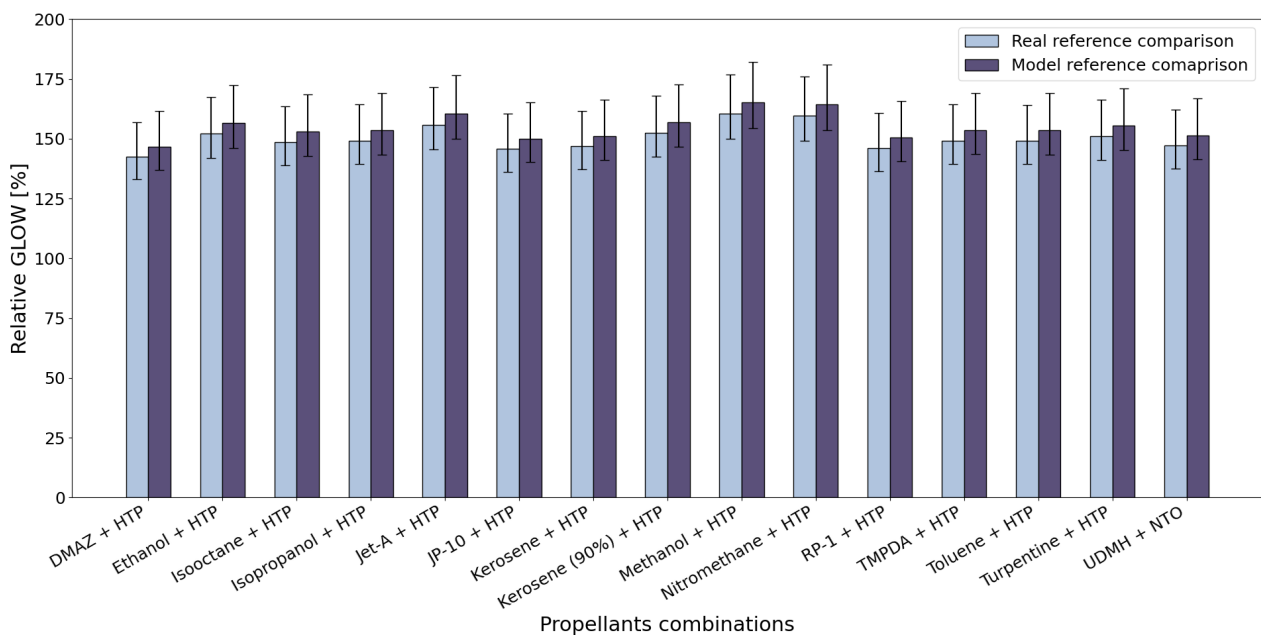
Figure 8.5: Comparison of the optimised relative GLOM for the considered bi-propellant combinations with respect to the real and model-optimised GLOM of Ariane 6(2)

Overall, the kerosene-derivative fuels seem to have the best i.e., lowest, GLOM performance amongst the HTP-based storable bi-propellants. Here, the minimum GLOM was found for RP-1 fuel at 755t or a 42% increase in mass as compared to the Ariane 6(2) mass predicted through the optimisation model. Similar GLOM results were found for DMAZ and isooctane. These results match the

results found through the propulsion potential analysis performed in Section 8.1. Finally, it can be observed that the best-performing HTP-based bi-propellants were found to have a lower value for the optimised GLOM than the conventional storable propellant UDMH/NTO. Here, the optimised launch vehicle concept employing UDMH/NTO showed to be $25t$ or 3% heavier than the optimised launch vehicle concept employing RP-1/HTP. This again matches the results found through the propulsion potential analysis.

8.2.2. Global payload capability optimisation

For the second optimisation case, a constraint was placed on the GLOM as it was set to a constant value of $530t$, equal to that of Ariane 6(2) as reported in literature. Instead, the payload capability of the launch vehicle concepts was subject to optimisation. In the vehicle performance model, the trajectory state that is considered for trajectory optimisation is the state at the core stage burnout and separation. As such, the payload capability referred to here is the payload capability of the combined boosters and core stage, consisting of the upper stage mass and the useful launch vehicle payload. Unlike the GLOM optimisation case, it was found that solutions converged for a 3-engine configuration.

The results of the payload capability optimisation case can be found in Figure 8.6, 8.7, and 8.8. Although the core stage payload mass is the value directly obtained through the optimisation model, a reference figure was created for the optimised useful payload mass to GTO based on the fraction of the useful payload to the upper stage mass derived from the Ariane 6(2) reference launch vehicle. As for the GLOM optimisation case, it can be found that the Ariane 6(2) payload capability predicted through the optimisation model is slightly more optimistic, with a difference of $0.2t$ or 5% more payload to GTO. For the storable propellants, the useful payload capability could be found to be in the range of 2.3-3t. As such, the storable bi-propellant for which the highest useful payload capability was found, RP-1/HTP, can bring 38% less payload to GTO than the model-optimised Ariane 6(2) launch vehicle, which can bring $4.7t$ of useful payload to GTO. Another repeating observation to be made is the excellent performance of the kerosene-derivative fuels and DMAZ. While the results for the conventional storable propellant UDMH/NTO are better than for the GLOM optimisation case, all the kerosene-derivative fuels, DMAZ, and isooctane perform 1-5% better.
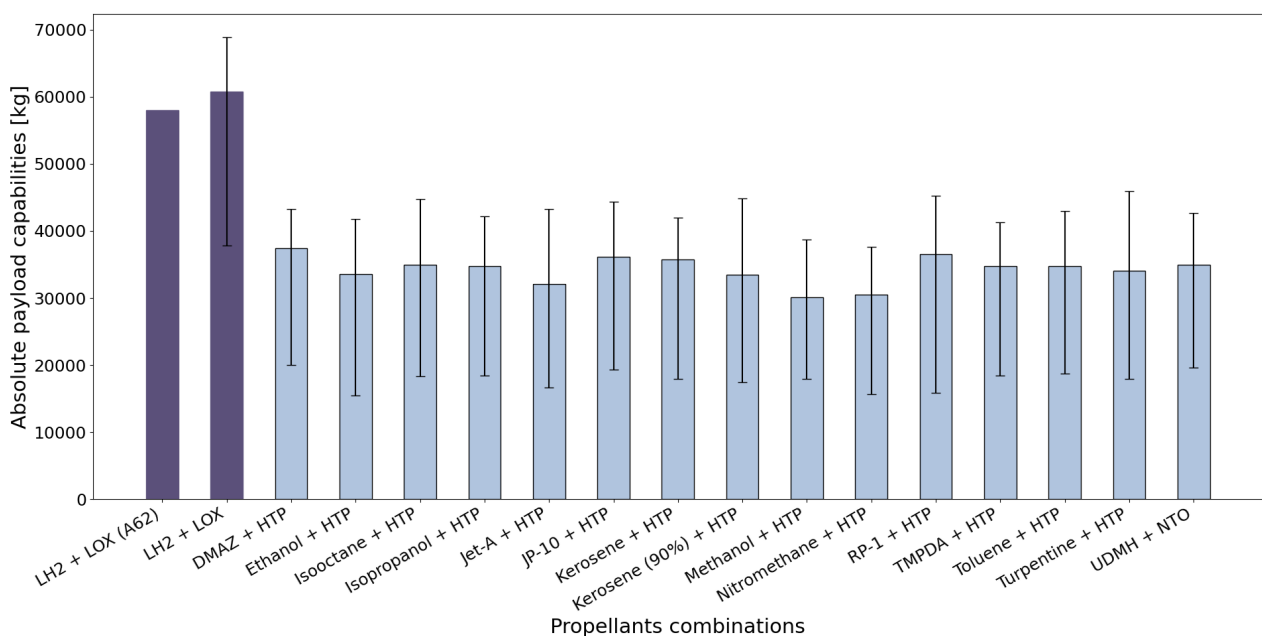
Figure 8.6: Comparison of the optimised absolute payload (upper stage + GTO useful payload) capability for the considered bi-propellant combinations with respect to the real and model-optimised payload capability of Ariane 6(2)
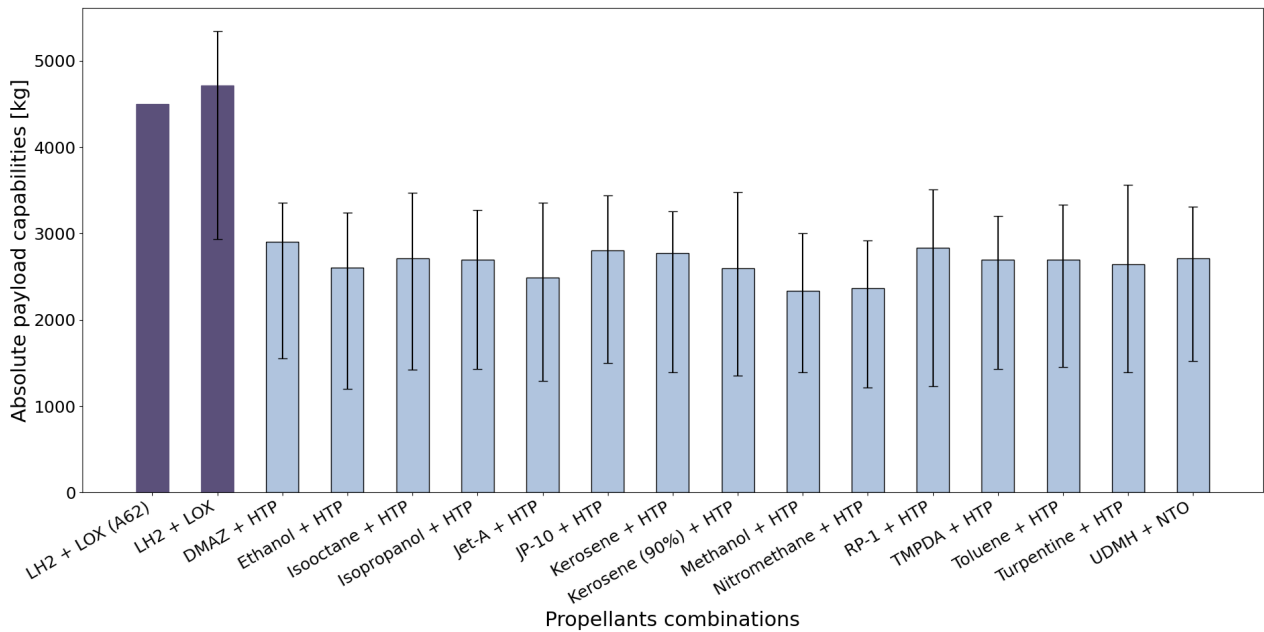
Figure 8.7: Comparison of the optimised absolute payload (GTO useful payload) capability for the considered bi-propellant combinations with respect to the real and model-optimised payload capability of Ariane 6(2)
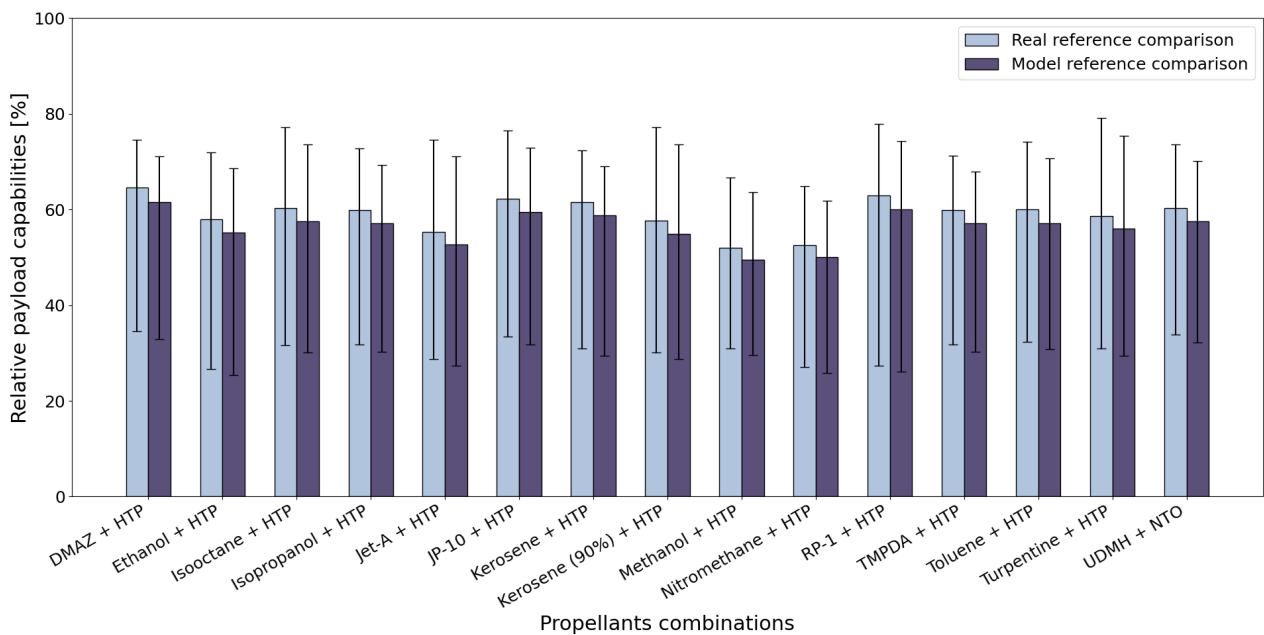
Figure 8.8: Comparison of the optimised relative payload capability for the considered bi-propellant combinations with respect to the real and model-optimised payload capability of Ariane 6(2)

Although the GLOM and the payload capability were treated as two separate optimisation cases, it was expected that similar relative proportions would be found between the different propellant combinations considered for this study. Similarly, it was expected that these findings would match with those found in the comparative analysis of the propulsion potential. This is because the difference in optimised mass performance, regardless of whether this is GLOM or payload capability, in this study is largely the result of the choice of propellant and thus inherently linked to the propulsion potential of the selected propellants. Overall, both the propulsion potential analysis and the dual mass performance analysis led to the conclusion that kerosene-derivative fuels,

DMAZ, and isooctane are the most promising fuel options for HTP-based storable bi-propellants in launch vehicle applications. This matches the hypotheses formulated in Section 4.3 regarding the mass performance potential of HTP-based propellants as compared to conventional cryogenic propellants. Overall, a payload capability similar to the expected 50% of the cryogenic reference propellant was found for all of the proposed propellant combinations. The best-performing combination, RP-1/HTP, proved to be 12% better than expected in terms of the payload capability.

Based on the observations made through this comparative analysis of the mass performance of the considered propellants, an answer could be formulated to research question **RQ-PERF-02** and its corresponding subquestions. The useful payload capability of the HTP-based storable bi-propellants considered in this study was found to be less than that of the Ariane 6(2) reference launch vehicle employing a conventional cryogenic propellant. Yet, the results show that these propellants do have the capability to bring payload to orbit. While the propulsion potential analysis showed promising results for the performance and use of these propellants, a major limiting factor in the payload capability optimisation case was the upper boundary set for the chamber pressure at which the storable propellant engines could be operated. As the sensitivity analysis in Section 7.6.2 showed, greater thrust potential could be unlocked if the boundaries of this limiting factor could be pushed. Therefore, the influence of the chamber pressure and the other input parameters considered for the optimisation problem will be investigated in Section 8.2.3.

Another interesting conclusion to be drawn from the results is the promising performance potential of the HTP-based storable bipropellants as compared to the conventional but highly toxic storable propellant UDMH/NTO. Increased development efforts towards HTP-based storable bi-propellant rocket engines could thus not only lead to a promising alternative to cryogenic propellants, but it could also allow for the complete replacement of toxic hydrazine-derivative fuels.

8.2.3. Global payload capability optimisation sensitivity

An important aspect of launch vehicle design and optimisation efforts is a comprehensive understanding of the interrelations between various parameters driving the design. In Section 8.2, the setup of the global optimisation model was described. There, a set of input variables was defined, which were used to optimise the GLOM and the payload capability of the proposed launch vehicle concepts. To validate and contextualise these results for future design efforts on this topic, it was deemed imperative to investigate the sensitivity of the optimisation results to these key parameters. The sensitivity analysis was limited to the global payload capability optimisation results because this was the main study case highlighted in RQ-PERF-02. Similar conclusions could be expected for the sensitivity of the global GLOM optimisation, given the similarity between the two optimisation cases observed in Section 8.2.1 and 8.2.2.

For this sensitivity analysis, the influence of five input variables was considered on the payload mass and trajectory objective score of a launch vehicle concept employing RP-1/HTP. This propellant was selected as it was found to be the best-performing propellant, in terms of optimised payload capability, amongst the HTP-based propellant combinations considered in this study. In setting up the sensitivity analysis, the three main optimisation variables for the optimisation model were considered: core stage burn time, nozzle area ratio, and chamber pressure. On top of that, two more adjacent parameters were considered, these being the number of engines and the nozzle throat area. The boundary constraints treated for this analysis are tabulated in Table 8.4. For the chamber pressure, the boundary range was increased as compared to the regular optimisation problem as a result of the discussion in Section 7.6.2. Furthermore, boundaries for the number of engines were determined by trial and error in accordance with the other parameters. The nozzle throat area was determined based on existing engines introduced in Section 7.2. Finally, the optimum O/F was used throughout all of the results in this sensitivity analysis.

Table 8.4: Constants and boundary values defined for input variables of the sensitivity analysis of the global payload capability optimisation of a launch vehicle concept employing RP-1/HTP

Design variable	Optimisation variable?	Units	Boundary/constant value
Core stage burn time	Yes	s	132.8-1132.8
Nozzle area ratio	Yes	–	10-45
Chamber pressure	Yes	MPa	2-16
Number of engines	No	–	1-3
Nozzle throat area	No	m^2	0.05-0.075
Oxidiser-to-fuel ratio	No	–	7 (Table 8.3)

Chamber pressure vs burn time

The sensitivity of the payload mass and the trajectory objective score with respect to the chamber pressure and the core stage burn time is visualised in Figure 8.9-8.11 for a 1-3 core stage engine configuration, respectively. For the setup of this sensitivity analysis, a launch vehicle concept employing RP-1/HTP was considered. Note that the burn time in these plots refers to the time from separation of the booster stage to burnout of the core stage. As such, zero burn time corresponds to cases where the core stage burnout and separation coincide with that of the booster stage. Also note that the region of viable trajectories represents the launch vehicle concepts for which a trajectory objective score of 5.7±3.5 could be found, as per the discussion concerning the trajectory optimisation uncertainty in Section 7.6.2. The optimised payload capability case is, however, defined by the maximum payload configuration for which a trajectory objective score of 0-5.7 could be found.

From the sensitivity figures, it can be deduced that the smallest payload mass is found for a combination of maximum burn time and maximum chamber pressure. This thus indicates that the mass flow rate of the engine increases with an increase in chamber pressure. In fact, it can be observed that the top right part of the grid represents negative payload cases, which correspond to the propellant mass surpassing the constant GLOM constraint. This effect is magnified when the number of engines is increased. As such, it can be observed that the maximum burn time for which valid launch vehicle concepts are found decreases to $850s$ and $500s$ for a 2-engine and a 3-engine configuration, respectively.

With an increasing number of engines, there is a noticeable shift of the region of viable trajectories to the left, to smaller chamber pressure values. As a result, the point representing the optimised payload capability is also shifted to smaller chamber pressure values. As per the discussion in Section 8.2 on the difficulties and increased complexity of elevated chamber pressures, this could be seen as a positive observation. It should, however, be mentioned that increasing the number of engines also leads to an increase in complexity and a decrease in the system reliability, which are considerations that are not visualised in the sensitivity figures. Next to that, as indicated by the contour lines on the payload mass plots, a decrease in the predicted payload capability of the proposed launch vehicle concepts can be related to an increase in the number of engines and a subsequent decrease in the optimum chamber pressure. This difference is as much as $3.5t$ between the single-engine configuration and the 3-engine configuration, which can be translated to approximately $270kg$ of useful payload to GTO as per the conversion factor applied in Section 8.2.2.

The optimised payload capability reported in Section 8.2.2 was found for a 2-engine configuration. Given that the upper boundary considered for the global payload capability optimisation problem was set at $6MPa$, this is sensible. Upon inspecting Figure 8.9, it can be observed that no viable trajectories were found for chamber pressure values below $6MPa$. Similarly, however, no viable trajectories were found for chamber pressure values above $13MPa$, with the optimisation point sitting at $9MPa$. While it was deduced from Figure 7.21 that the thrust performance of an engine scales linearly with its chamber pressure, it can be argued that engines with a chamber pressure beyond $9MPa$ would be more suitable for launch vehicles with a higher GLOM. This is because, due

to the setup of the vehicle performance model, the core stage burn time and the total propellant mass were both connected to the fixed GLOM and the engine mass flow rate, which also scales linearly with the chamber pressure of the engine. As such, the burn time available for engines with a high chamber pressure is not long enough to provide sufficient acceleration to make the payload reach its required end state at core stage burnout. This effectively shows that the vehicle performance model is rather limited for pure launch vehicle design problems. It is, however, a suitable model for this study as it allows for an effective comparison analysis to be made between different launch vehicle concepts for similar constraints.
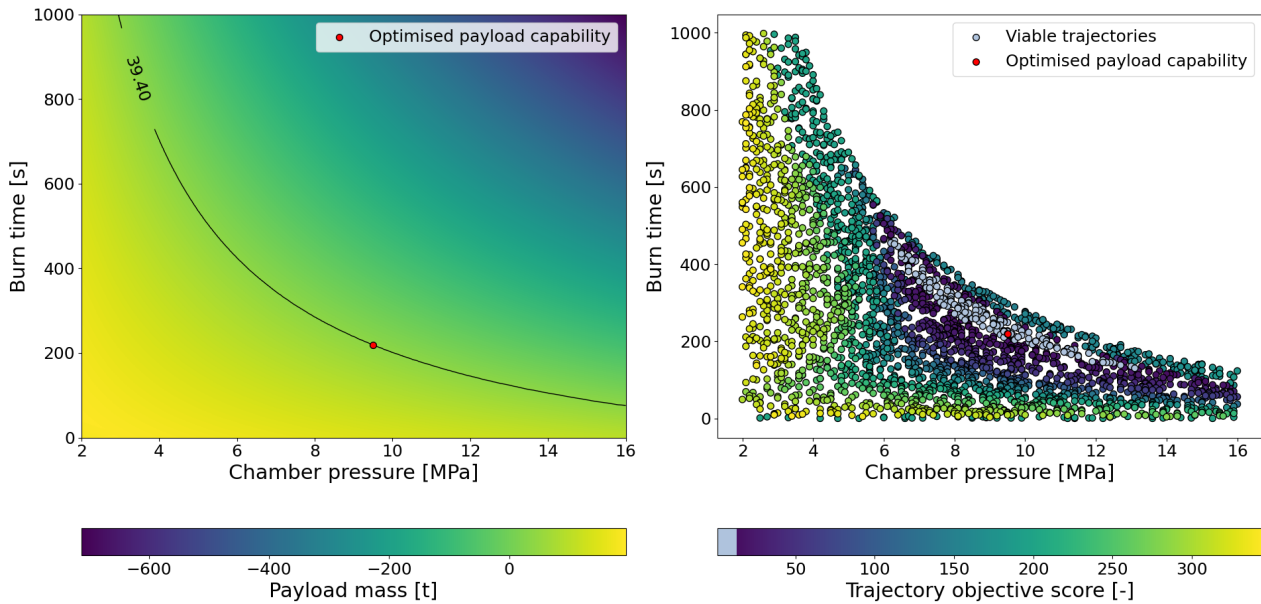
Figure 8.9: Spread of the payload masses (left) and trajectory objective scores (right) as a function of chamber pressure and core stage burn time after SRB separation, for global payload capability optimisation ($A_t = 0.075m$, $\epsilon = 45$, $N_{eng} = 1$)
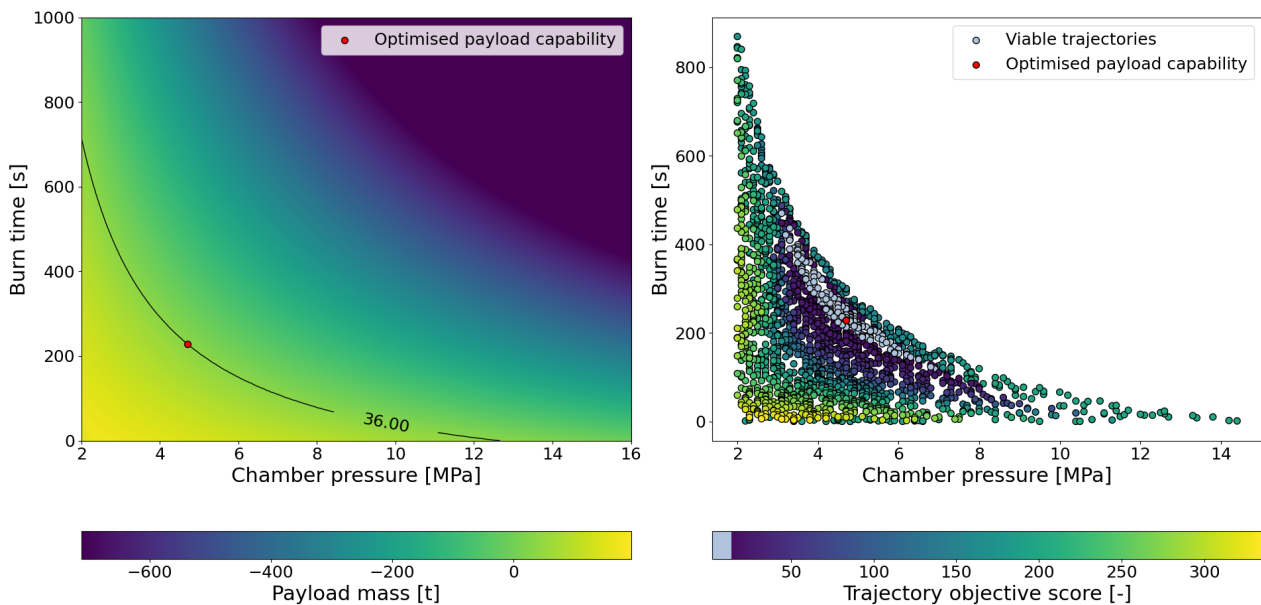
Figure 8.10: Spread of the payload masses (left) and trajectory objective scores (right) as a function of chamber pressure and core stage burn time after SRB separation, for global payload capability optimisation ($A_t = 0.075m$, $\epsilon = 45$, $N_{eng} = 2$)
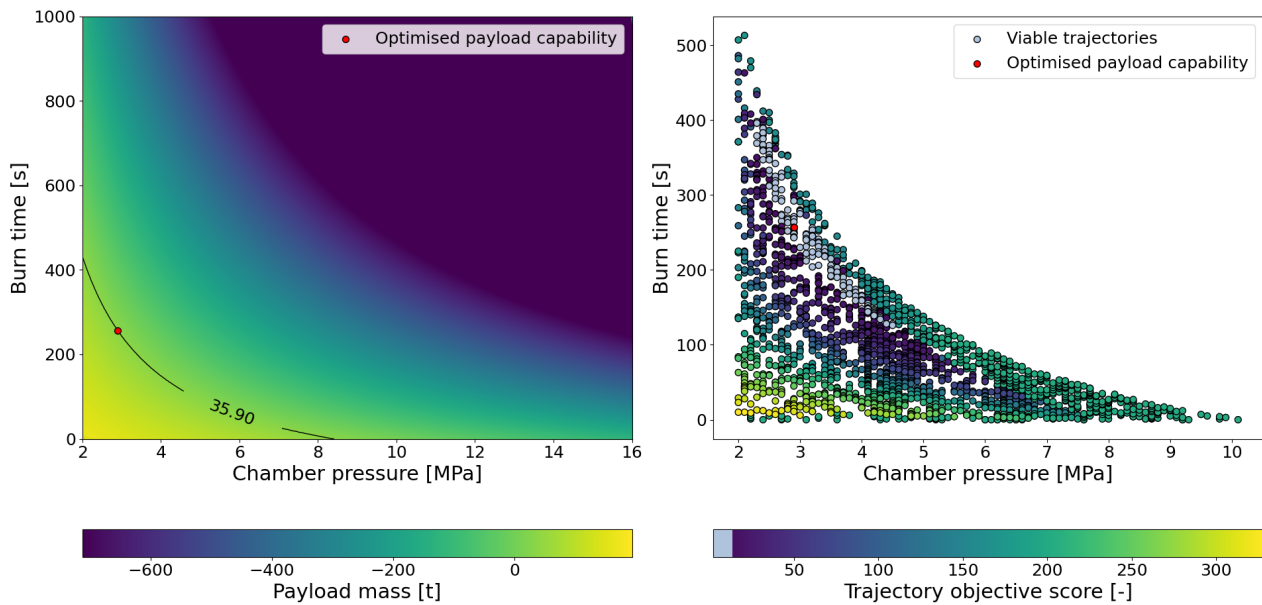
Figure 8.11: Spread of the payload masses (left) and trajectory objective scores (right) as a function of chamber pressure and core stage burn time after SRB separation, for global payload capability optimisation ($A_t = 0.075m$, $\epsilon = 45$, $N_{eng} = 3$)

Nozzle area ratio vs burn time

The sensitivity of the payload mass and the trajectory objective score with respect to the nozzle area ratio and the core stage burn time is visualised in Figure 8.9-8.11 for a 1-3 core stage engine configuration, respectively. The setup of this sensitivity analysis was similar to the setup considered in Section 8.2.3, except that the influence of the nozzle area was investigated. As such, a constant value of $4.5MPa$ was assigned to the chamber pressure, the input for which the optimised payload capability was found in Section 8.2.2. From these sensitivity plots, it can immediately be observed that the influence of the nozzle area ratio on the payload mass is almost negligible as the payload mass decreases almost linearly with the burn time. Indeed, based on Figure 7.2, it was concluded that for a constant nozzle throat area, the mass flow rate of the engine is not affected by a varying nozzle area ratio.

From Figure 8.12, it can be observed that no optimisation point was found for the launch vehicle concepts with a single-engine configuration. This means that no viable trajectories were found through the trajectory optimisation algorithm. From the chamber pressure sensitivity plot in Figure 8.9, it can be seen that no viable trajectories were found for a chamber pressure of $4.5MPa$. This would explain why no viable trajectories could be found in the nozzle area ratio sensitivity plot for the single-engine configuration, for which a constant chamber pressure of $4.5MPa$ was assumed. It does, however, also show that the chamber pressure is a more influential parameter in terms of the launch vehicle performance as compared to the nozzle area ratio.

In Figure 8.13 and 8.14, where the nozzle area ratio sensitivity plots for the 2-engine and the 3-engine configuration are visualised, an optimisation point was found. It can be observed that for both configurations, this point was found as larger values for the nozzle area ratio. From ideal rocket theory, more specifically Equation 7.1, it follows that the effect of the nozzle exit area on the thrust performance of the engine is mostly introduced through the atmospheric pressure term. Therefore, a small nozzle exit area is preferred at low altitudes, where the atmospheric pressure is high, while a larger nozzle exit area is preferred at higher altitudes, where the atmospheric pressure becomes very small. Given that for this sensitivity analysis, the nozzle throat area was set to be constant, the nozzle exit area is varied as a function of the nozzle area ratio. As a result, this same effect on the thrust can be extrapolated to the nozzle area ratio. Due to the design of the launch vehicle concepts, most of the thrust during the booster phase of the ascent is provided by the SRB. As a result, the atmospheric pressure will be almost negligible by the time the SRB

have separated, and the vehicle is solely propelled by the core stage engine(s). Therefore, it could be argued that a larger nozzle exit area, and thus a larger nozzle area ratio, are desirable for these launch vehicle concepts. This thus explains the tendency of the optimisation points in the nozzle area ratio sensitivity plots towards larger values for the area ratio.

Finally, a repeated observation from the chamber pressure sensitivity analysis is the higher payload capability found for launch vehicle concepts with a lower number of core stage engines. In this case, the optimised payload capability of the 2-engine configuration was found to be $5.7t$ better than that of the 3-engine configuration. This can be translated to approximately $440kg$ of useful payload to GTO. It could be argued that this is largely the result of the constant value set for the chamber pressure, which was closer to the optimal chamber pressure for a 2-engine configuration than to the optimal chamber pressure for a 3-engine configuration. This confirms that the engine nozzle area ratio is a significantly less influential parameter in the performance of the launch vehicle concepts than the engine chamber pressure.
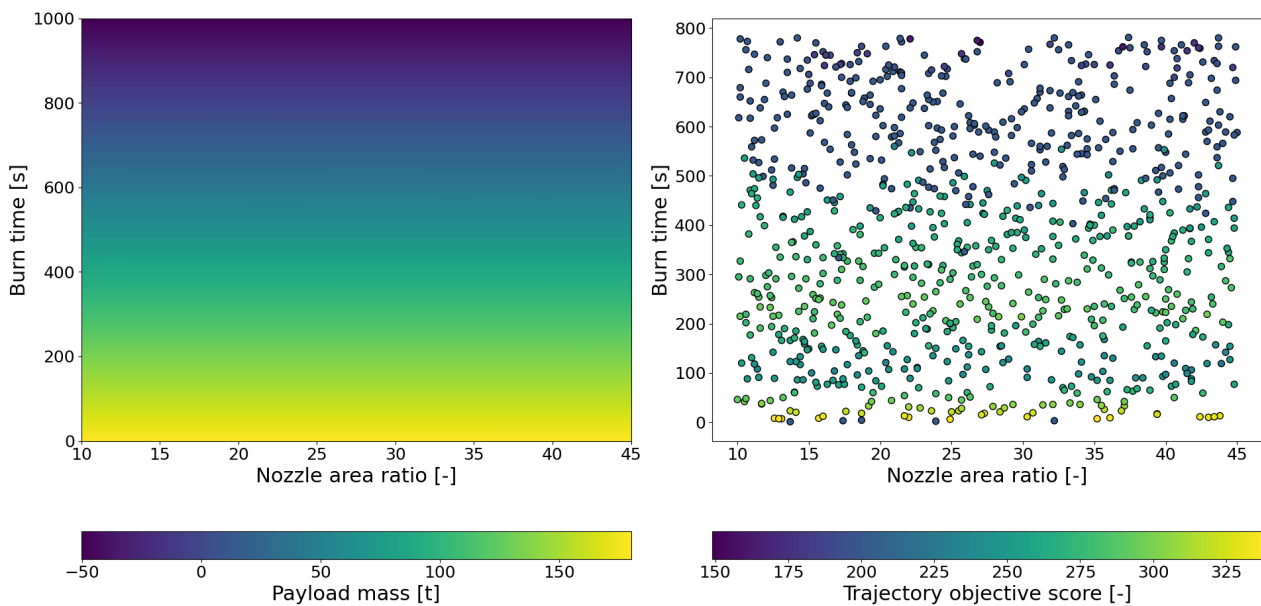
Figure 8.12: Spread of the payload masses (left) and trajectory objective scores (right) as a function of nozzle area ratio and core stage burn time after SRB separation, for global payload capability optimisation ($A_t = 0.075m$, $P_c = 4.5MPa$, $N_{eng} = 1$)
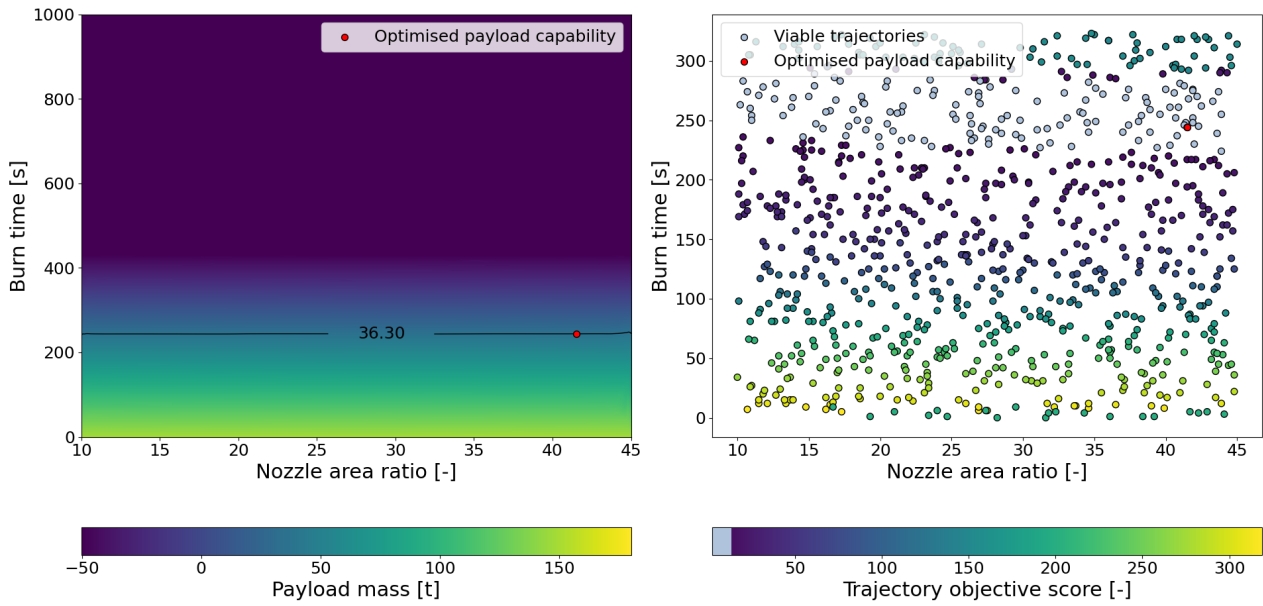
Figure 8.13: Spread of the payload masses (left) and trajectory objective scores (right) as a function of nozzle area ratio and core stage burn time after SRB separation, for global payload capability optimisation ($A_t = 0.075m$, $P_c = 4.5MPa$, $N_{eng} = 2$)
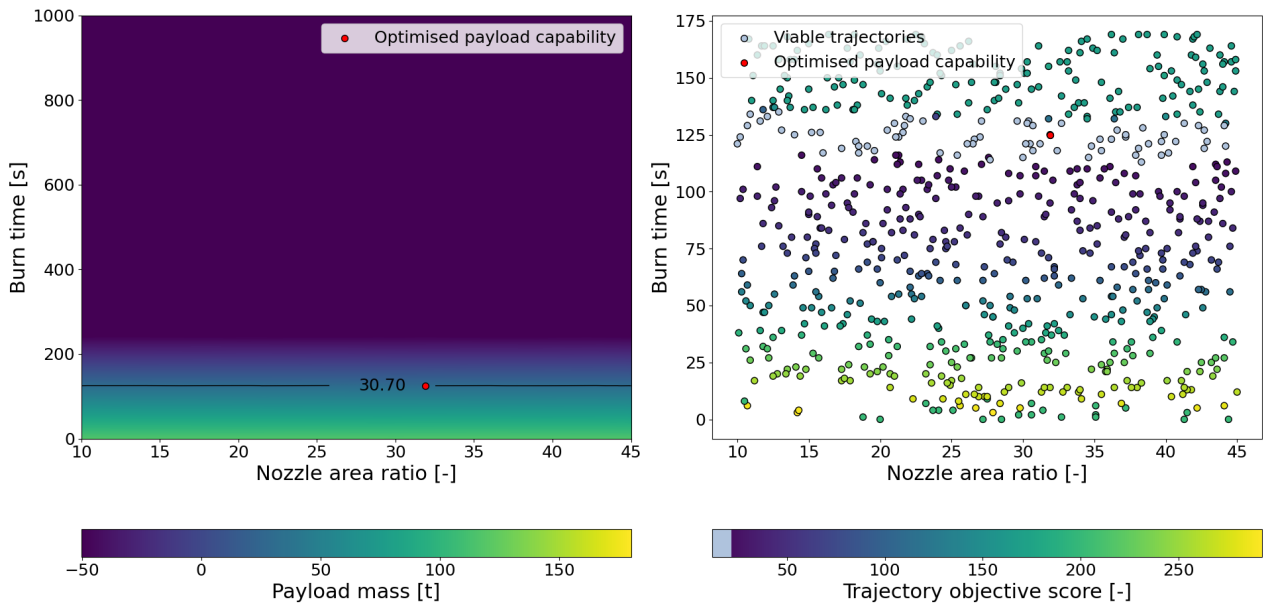
Figure 8.14: Spread of the payload masses (left) and trajectory objective scores (right) as a function of nozzle area ratio and core stage burn time after SRB separation, for global payload capability optimisation ($A_t = 0.075m$, $P_c = 4.5MPa$, $N_{eng} = 3$)

Nozzle throat area vs burn time

In addition to the nozzle area ratio and the chamber pressure, which were both variables for the global optimisation model, the nozzle throat area was also considered in this sensitivity analysis. The sensitivity of the payload mass and the trajectory objective score with respect to the chamber pressure and the core stage burn time is visualised in Figure 8.9-8.11 for a 1-3 core stage engine configuration, respectively. The nozzle area ratio was set at a constant value of 45, while the chamber pressure was set at a constant value of $4.5MPa$. From the sensitivity plots, it can be observed

that the size of the nozzle throat area affects the payload mass to some extent. This could indeed be expected following the relation between the engine mass flow rate and the nozzle throat area described in Equation 7.8.

As was the case for the nozzle area ratio, no viable trajectories could be found in Figure 8.15, which represents the nozzle throat area sensitivity plot for a single-engine configuration. This can once again be explained through the choice of constant value for the chamber pressure, which means that the engine does not deliver enough thrust for the required end states to be reached with a single core stage engine. Therefore, it can be concluded that the chamber pressure is a more influential parameter in terms of the launch vehicle performance as compared to the nozzle throat area.

The payload capability optimisation point was found at a high value for the throat area in Figure 8.16 for the 2-engine configuration. In Figure 8.17, a shift can be observed for this optimisation point and the region of viable trajectories towards lower values of the nozzle throat area. It could be argued that the increased thrust for engines with a larger nozzle throat area is not enough to provide the required acceleration to the same payload mass that can be serviced with a smaller throat area. The reason for this is the same as was discussed in Section 8.2.3 concerning the fixed constant GLOM and the setup of the vehicle performance model, which connects the propellant and the payload mass to the core stage mass flow rate and the core stage burn time.
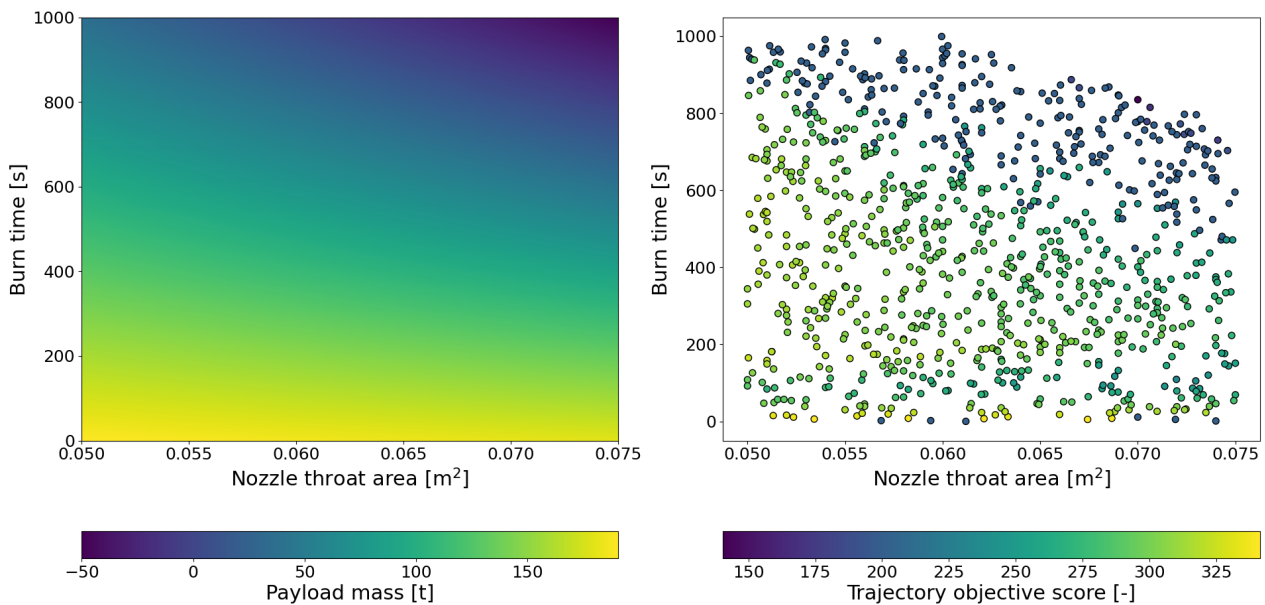
Figure 8.15: Spread of the payload masses (left) and trajectory objective scores (right) as a function of nozzle throat area and core stage burn time after SRB separation, for global payload capability optimisation ($P_c = 4.5 MPa$, $\epsilon = 45$, $N_{eng} = 1$)
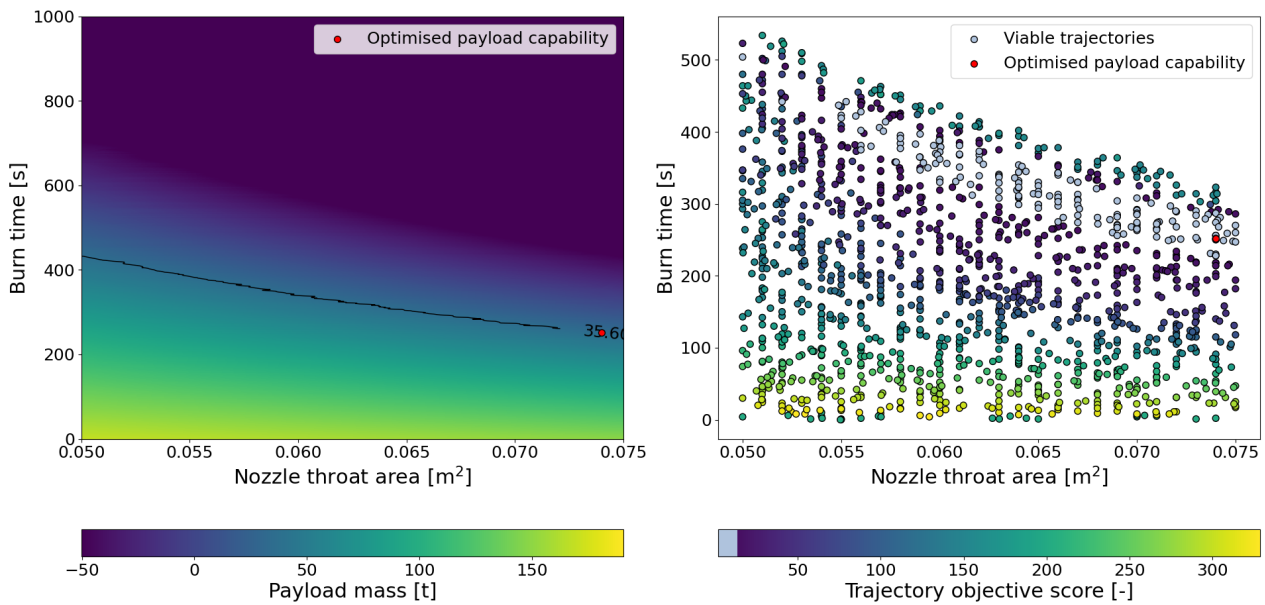
Figure 8.16: Spread of the payload masses (left) and trajectory objective scores (right) as a function of nozzle throat area and core stage burn time after SRB separation, for global payload capability optimisation ($P_c = 4.5MPa$, $\epsilon = 45$, $N_{eng} = 2$)
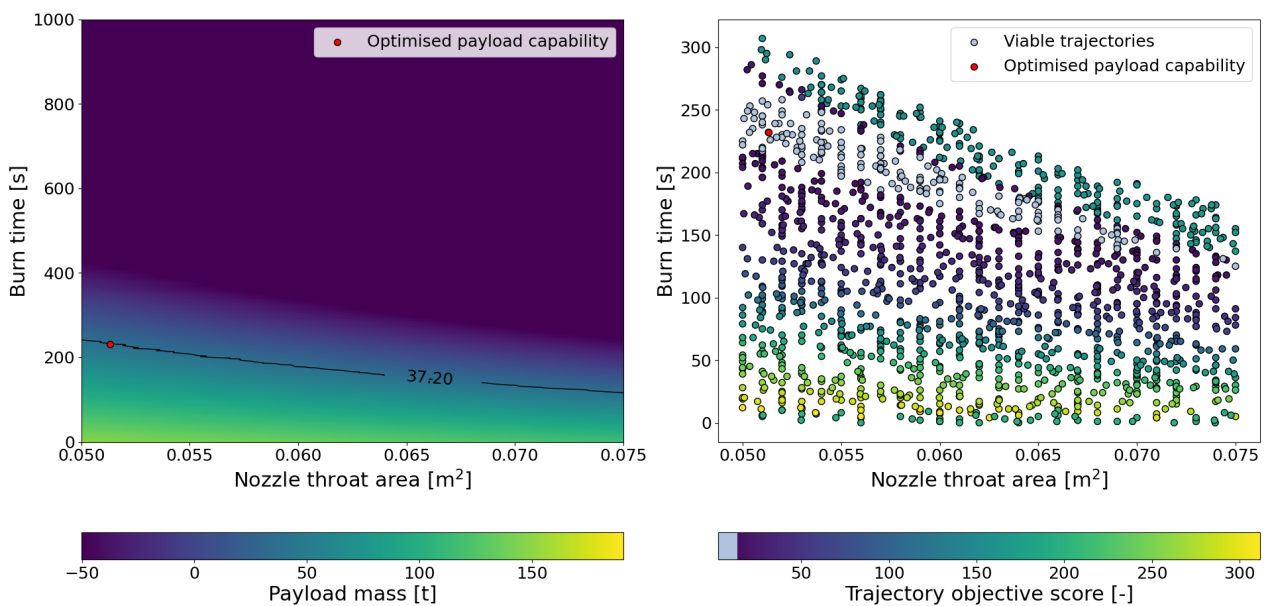
Figure 8.17: Spread of the payload masses (left) and trajectory objective scores (right) as a function of nozzle throat area and core stage burn time after SRB separation, for global payload capability optimisation ($P_c = 4.5MPa$, $\epsilon = 45$, $N_{eng} = 3$)

8.3. Chapter summary

In this chapter, the results of the second research segment were presented and discussed. Thereby, an answer was provided to *RQ-PERF-01* and *RQ-PERF-02*. The *vehicle performance model* was central to this effort, as it allowed for the propulsion and mass performance of the proposed launch vehicle concepts to be calculated. The propulsion performance propulsion was investigated by comparing the proposed propellant combinations through their maximum specific impulse at vacuum conditions and through their maximum specific impulse density for the same set of engine input parameters. Based on these measures, two definitions for the optimum O/F were proposed. It

was found that the HTP-based propellants showed a more than 25% lower performance compared to the cryogenic reference propellant hydrolox in terms of the specific impulse, as well as slightly lower performance compared to UDMH/NTO. The highest specific impulse amongst the HTP-based propellants was found for DMAZ. In terms of specific impulse density, RP-1 and other kerosene derivative fuels were found to show the highest performance, while similarly good performance was reported for DMAZ, isooctane, and turpentine. Furthermore, these HTP-based propellants also outperformed both hydrolox and UDMH/NTO, which thus shows the propulsion performance potential of HTP.

To assess the mass performance potential of the proposed launch vehicle concepts, both the GLOM and the payload capability were subject to optimisation. The optimised GLOM for the Ariane 6(2) reference vehicle was found to be within 3% of the GLOM reported for this vehicle in literature. It was found that the best-performing HTP-based propellant was RP-1 at a 42% higher GLOM compared to the optimised reference vehicle. Furthermore, DMAZ and isooctane, but also UDMH/NTO, showed to have a similar performance. Similar results were found for the payload capability optimisation case, as the Ariane 6(2) payload capability was 5% higher than the value reported in literature and 38% higher than the prediction for the best-performing HTP-based propellant RP-1. Other kerosene derivatives, as well as DMAZ and isooctane, were all found to have similar payload capability, which was also 1-5% better than that of UDMH/NTO. A sensitivity analysis was performed to validate and contextualise these results for future design efforts on this topic. It was found that the most influential design parameter is the engine chamber pressure. Furthermore, while the aforementioned optimisation results were found using a 2-engine configuration for the core stage, the sensitivity analysis showed that elevated chamber pressures would allow for a single-engine core stage design to be used and for the payload capability to be increased. It is, therefore, possible that further development efforts and studies regarding the design and capabilities of HTP-based storable bi-propellant rocket engines could further improve the mass performance potential of these launch vehicle concepts.

9.Conclusion

Cryogenic and semi-cryogenic propellants are the most commonly used liquid propellants for applications in medium-lift launch vehicles. Despite their high performance, the storage requirements for these propellants often lead to complex, heavy, and voluminous structures. The only storable propellant used in medium-lift launch vehicles, UDMH/NTO, comes with its own problems of high toxicity and reduced performance. A promising alternative to this could be storable fuels with highly concentrated hydrogen peroxide (HTP) as an oxidiser. Despite a shorter history of dedicated development, HTP has proved itself an effective oxidiser for in-space applications and small-lift launch vehicles. Therefore, the question could be raised towards the potential of this oxidiser for applications in medium-lift launch vehicles. In this study, a research goal was formulated in response to this question:

> *To further map the potential of hydrogen peroxide in space applications by assessing the performance and integration potential of a low-toxicity storable bi-propellant employing highly concentrated hydrogen peroxide as an oxidiser in the core stage of a medium-lift launch vehicle.*

In working towards the above-stated research goal and answering the research questions corresponding to it, this study was divided into two main research segments. The first of these research segments was referred to as the *baseline fuel assessment* and was focused on evaluating a large selection of potential fuels for their compatibility and integration potential with hydrogen peroxide. In this segment, a *preliminary feasibility assessment* and an *availability assessment* were introduced to reduce the number of potential fuel candidates by selecting those that were deemed most feasible and interesting for further study with respect to the stated research goal and intended application. The preliminary feasibility assessment consisted of surface-level evaluations of the candidate fuels with respect to minimum performance, combustion stability, storage state, and an overall toxicity threshold. The availability assessment was aimed at evaluating both the availability of the fuel sources and the availability of data for further study. Following these first phases of the baseline fuel assessment, the initial list of 86 potential fuels was narrowed down to just 12 fuels to be considered for further study in the second research segment. These were listed in Table 6.1. It was found that especially toxicity and storage state are suitable criteria for a decisive surface-level evaluation.

Out of these 12 fuels, eight were selected for a detailed assessment in the last phase of the first research segment, which was referred to as the *propellant integration and compatibility evaluation or PICE*. Through PICE the fuels were assessed based on six criteria that were not directly related to performance, these being handling toxicity, environmental toxicity, material compatibility, handling and storage, development level, and coolant qualities. A numerical comparison was made between the fuels based on these criteria by means of an analytical hierarchy process. It was found that RP-1 (and by extension other kerosene derivatives) could be considered the most suitable fuel for combination with highly concentrated hydrogen peroxide in launch vehicle propulsion applications on the basis of the non-performance-related design drivers considered in this study. Furthermore, ethanol, methanol, isooctane, and isopropanol all showed to be promising alternatives. The deciding factors in this analysis were the development level and the materials compatibility, as similar scores were found for all fuels for the other assessment criteria.

In the second research segment, the 12 remaining fuels were evaluated based on their performance potential in combination with HTP. Here, a distinction was made between pure propulsive potential and mass performance potential. The former refers to the characteristic propulsive performance of the propellants, and the latter treats the performance potential of the propellants as integrated in a reference launch vehicle. To compare the propulsive potential of the proposed propellants,

the maximum values for the specific impulse and the specific impulse density were calculated at vacuum conditions for a fixed set of engine parameters at the optimum oxidiser-to-fuel ratio for each propellant. It was concluded that in terms of the vacuum specific impulse, the cryogenic reference propellant showed significantly better performance, with the predicted specific impulse for hydrolox being at least 25% higher than that of the considered storable propellants. Next to that, it was also found that UDMH/NTO outperformed the HTP-based propellants, with a 2% higher specific impulse than DMAZ/HTP. When considering specific impulse density, it was found that hydrolox was predicted to have a similar or lower specific impulse density than the HTP-kerosene derivative propellants. Furthermore, a high performance could also be observed for isooctane, turpentine, and DMAZ, while noticeably lower performance was reported for UDMH/NTO. Due to their high density in combination with an average specific impulse performance, HTP-based propellants could be concluded to have a high propulsive potential, displaying specific impulse density values comparable to that of conventional cryogenic propellants used in medium-lift launch vehicles.

A model was created, referred to as the *vehicle performance model*, to allow for the mass performance of the proposed HTP-based propellants to be assessed in the context of a launch vehicle application. Next to the aforementioned propulsion model, a mass and sizing model, and an aerodynamics and trajectory model were set up. A global optimisation model was then created to connect these models and to optimise the mass performance of launch vehicle concepts, employing the proposed propellants, for two mass optimising cases: minimised *gross lift-off mass (GLOM)* and *maximised payload capability*. It was found that the optimised GLOM for these launch vehicle concepts were 42-61% higher than that of the Ariane 6(2), which was used as a reference launch vehicle for this study. Similarly, following optimisation of the payload capability, it was found that the launch vehicle concepts between 2.3t and 2.9t of useful payload to GTO, as compared to the 4.6t found when applying the same optimisation model to the Ariane 6(2) case. Overall, the best-performing fuels in combination with HTP were found to be RP-1 and other kerosene derivatives. DMAZ and isooctane were also found to have a similar payload capability, which was 1-5% better than that of UDMH/NTO. These findings matched up with those of the propulsion potential analysis.

Overall, the useful payload capability of the HTP-based storable bi-propellants considered in this study was found to be less than that of the Ariane 6(2) reference launch vehicle employing a conventional cryogenic propellant. Yet, the results show that these propellants do have the capability to bring payload to orbit. It is also believed that advances in the design of HTP-based storable bi-propellant rocket engines could further improve this payload capability. While the propulsion potential analysis showed promising results for the performance and use of these propellants, improvements could still be made. This was supported by the results of the sensitivity analysis, where is was shown that elevated chamber pressures could allow for a single-engine core stage design and an effective increase in payload capability. Greater thrust potential for HTP-based storable propellant engines could be unlocked if the boundaries of these engine designs could be pushed. Another conclusion to be drawn from the results is the promising performance potential of the HTP-based storable bipropellants as compared to the conventional but highly toxic storable propellant UDMH/NTO. Increased development efforts towards HTP-based storable bi-propellant rocket engines could thus not only lead to a promising alternative to cryogenic propellants, but it could also allow for the complete replacement of toxic hydrazine-derivative fuels.

10.Recommendations

The main goal of this study was to further map the potential of HTP-based propellants for applications in the space industry. In reaching this goal, several promising findings were made that could prove to be interesting for further study. Additionally, the limitations of this research were highlighted several times throughout this report. As such, a set of recommendations could be proposed to improve the results of this study and to further expand on the topic of hydrogen peroxide for space applications.

- **Experimental testing of promising fuels:** In Chapter 5, it became evident that for many of the proposed fuels, little data is available needed to properly evaluate the suitability of the fuels for launch vehicle design. Furthermore, experimental data on fuels with hydrogen peroxide proved to be even more scarce. Most of the sources covering this topic are outdated or incomplete. Therefore, it is recommended that a new series of experiments should be conducted. Experimental data should provide a more developed insight into the properties of proposed propellant combinations and their behaviour in more representative settings that go beyond the predicting capabilities of pure theoretical models. Suggested experiments could be focused on material compatibility, toxicity, combustion stability, hypergolicity, energy release with hydrogen peroxide, and shelf life testing.

- **Ignition delay time:** As an additional point to the first recommendation, experiments should be conducted with respect to the ignition delay time of the proposed fuels with HTP. An important factor that is specific to hypergolic propellant combinations is the ignition delay time (IDT), which refers to the time between fluid contact and ignition.[155] The ignition delay time is directly dependent on several characteristic factors, both physical and chemical. The most important of these are O/F ratio, spray pressure, local mixing conditions, injector size, and the general reactivity potential between oxidiser and fuel. Small values for the IDT allow for a shorter combustion chamber and thus further weight reduction of the propulsion system.[104] Exceedingly high values for IDT, however, may lead to the accumulation of propellant in the combustion chamber and an uncontrolled ignition sequence.[155] This could result in a catastrophically hard start and destruction of the engine if not terminated timely.[104] It was approximated that for acceptable and reliable ignition performance, the IDT observed in the combustion chamber should be below 100ms.[155] Certain chemicals could be added to decrease the ignition delay time. Research into these so-called additives for the proposed propellant combinations could be very valuable as it would broaden the range of potential fuels that could be combined with hydrogen peroxide.

- **Reusability:** This study covered the application of HTP-based storable bi-propellants in expendable launch vehicles with a specific focus on medium-lift launch vehicles. Currently, small-lift expendable launch vehicles exist which are operating with HTP. Therefore, a logical next step would be to start looking into the application of hydrogen peroxide for reusable launch vehicles. Elferink[5] argued a similar path as he stated the shift in the launch vehicle market to a higher level of reusability. Therefore, it would be interesting to investigate the potential of HTP-based propellants for this application. It is worth noting that this shifted focus will also require a revision of the proposed trade-off criteria, as the relative importance of these criteria is dependent on the intended application.

- **Cost analysis:** Due to the already wide scope of this study, there was no time to look into the cost aspect regarding the use of an HTP-based storable bi-propellant for launch vehicle applications. Yet, this is a very important design driver in the space industry, especially with the increasing level of commercialisation. A surface-level cost analysis for upper stages was already performed by ELferink[5], but his results included very high margins of uncertainty. Therefore, a more detailed and decisive cost study applied to the whole launch vehicle could be very interesting to further stimulate the use of hydrogen peroxide.

- **High chamber pressure designs for HTP-based rocket engines:** As mentioned in the conclusions, a limiting factor to the performance of the proposed launch vehicle concepts was the upper boundary constraint placed on the chamber pressure for optimisation purposes due to the lack of existing storable propellant rocket engines operating at these high chamber pressures and due to the expected problems with HTP in such high pressure/high-temperature environments. In Section 8.2.3, the performance potential of elevated chamber pressures was proved, as a single-engine core stage design was made possible, and a significant increase in the payload capability was reported. A theoretical study into the possibility of creating such engines, or even dedicated development efforts, would be crucial in exploring and benefitting from the full potential of hydrogen peroxide. Development efforts focusing on other parts of the engine or propulsion system design could also be recommended, as this could lead to further mapping of the potential of hydrogen peroxide for space applications.

- **Multi-engine design:** In contrast to the previous recommendation, an effort could be made to reduce the complexity of the HTP-based engines. By increasing the number of engines, the overall performance of the complete system could be increased to the extent that the individual performance of each of the engines is less important. This is already the case with the Skyrora XL launch vehicle, which makes use of nine small HTP-based rocket engines for its first stage.[45] Furthermore, it was also illustrated in the sensitivity analysis in Section 8.2.3, as it was observed that a similar payload capability could be realised by increasing the number of engines and thereby decreasing the chamber pressure.

- **No-SRB configuration:** Subject to the reference vehicle selected for this study, a launch vehicle design was considered that included two high-thrust solid rocket boosters. Furthermore, the upper stage, although not specifically considered, was assumed to be propelled by hydrolox rather than a HTP-based propellant. For future studies on this topic, it would be interesting to consider a setup for which the dependency on other propellants is taken out i.e., a launch vehicle design fully propelled by hydrogen peroxide engines. To this extent, the option of an HTP-based (reusable) booster stage could also be investigated.

References

[1] ArianeGroup. *Ariane 6 revealed on its launch pad in preparation for hot-firing tests*. June 2023. URL: https://press.ariane.group/strongariane-6-seule-sur-son-pas-de-tir-pour-preparer-les-essais-a-feu-strong-8768/.

[2] Our World In Data and United Nations Office for Outer Space Affairs. *Annual number of objects launched into space*. 2022. URL: https://ourworldindata.org/grapher/yearly-number-of-objects-launched-into-outer-space.

[3] European Commission. *REACH Restrictions*. 2023. URL: https://single-market-economy.ec.europa.eu/sectors/chemicals/reach/restrictions_en.

[4] Tereza Pultarova. *Hydrazine ban could cost Europe's space industry billions*. Oct. 2017. URL: https://spacenews.com/hydrazine-ban-could-cost-europes-space-industry-billions/.

[5] Pepijn Elferink. "Prototype X: A Cost-Based Design Optimization of an Upper Stage Liquid Propulsion Module with Green-Storable Propellants". PhD thesis. Delft: Delft University of Technology, May 2022. URL: http://repository.tudelft.nl/..

[6] Harry W. Jones. "The Recent Large Reduction in Space Launch Cost". In: *International Conference on Environmental Systems (ICES)*. Albuquerque, New Mexico, July 2018.

[7] Jinhyun Bae, Jaye Koo, and Youngbin Yoon. "Development Trend of Low Cost Space Launch Vehicle and Consideration of Next Generation Fuel". In: *Journal of the Korean Society for Aeronautical & Space Sciences* 45.10 (Oct. 2017), pp. 855–862. ISSN: 1225-1348. DOI: 10.5139/jksas.2017.45.10.855.

[8] Timo Wekerle et al. "Status and trends of smallsats and their launch vehicles - An up-to-date review". In: *Journal of Aerospace Technology and Management* 9.3 (Sept. 2017), pp. 269–286. ISSN: 21759146. DOI: 10.5028/jatm.v9i3.853.

[9] Gordon Briggs and John Milthorpe. "Strategic Propellant Choices for an Australian Medium Launch Vehicle". In: *7th Australian Space Science Conference*. Sydney, Australia, Sept. 2007. URL: https://www.researchgate.net/publication/270158216.

[10] Bhavya Lal et al. *Global Trends in Small Satellites*. Tech. rep. Alexandria, Egypt: IDA Science and Technology Policy Institute Alexandria, July 2017. URL: https://www.researchgate.net/publication/335429689.

[11] SpaceX. *Falcon User's Guide*. Sept. 2021.

[12] Arianespace. *Ariane 6 User's Manual for Multi-Launch Service (MLS)*. June 2021. URL: www.arianespace.com.

[13] James Richard Wertz and Wiley J. Larson. *Reducing space mission cost*. Kluwer Academic Publishers, July 1996.

[14] European Chemical Agency (ECHA). *Candidate List of substances of very high concern for Authorisation*. 2023. URL: https://echa.europa.eu/candidate-list-table/-/dislist/details/0b0236e1874bc9ff.

[15] Ishan Patel, P. B. Sharma, and Rupesh Aggarwal. "Green Propellant: A Study". In: *International Journal of Latest Trends in Engineering and Technology* 6.1 (Sept. 2015), pp. 83–87. URL: https://www.researchgate.net/publication/290429002.

[16] George P. Sutton and Oscar Biblarz. *Rocket propulsion elements*. 9th. John Wiley & Sons, Feb. 2016.

[17] Marcos A Kettner and Thomas M Klapötke. "Synthesis of new oxidizers for potential use in chemical rocket propulsion". In: *Chemical rocket propulsion: A comprehensive survey of energetic materials*. Springer, 2017, pp. 63–88. DOI: http://dx.doi.org/10.1007/978-3-319-27748-6{_}2.

[18] Barry T. C. Zandbergen. *AE4-S01 Thermal Rocket Propulsion (version 2.08)*. Tech. rep. Delft University of Technology (TU Delft), 2020.

[19] David H. Huang and Dieter K. Huzel. *Modern Engineering for Design of Liquid-Propellant Rocket Engines*. Vol. 147. Washington DC: American Institute of Aeronautics and Astronautics (AIAA), Jan. 1992. ISBN: 978-1-56347-013-4. DOI: 10.2514/4.866197. URL: https://arc.aiaa.org/doi/book/10.2514/4.866197.

[20] Bruce Chehroudi, Doug Talley, and Vigor Yang. "Liquid Propellants and Combustion: Fundamentals and Classifications". In: *Encyclopedia of Aerospace Engineering*. Vol. 2. Wiley, Dec. 2010. DOI: 10.1002/9780470686652.eae108.

[21] ChemSafetyPro. *EU REACH Regulation (EC) No 1907/2006*. Dec. 2015. URL: https://www.chemsafetypro.com/Topics/EU/REACH_Regulation_EC_No_1907_2006.html.

[22] Amir S. Gohardani et al. "Green space propulsion: Opportunities and prospects". In: *Progress in Aerospace Sciences* 71 (Nov. 2014), pp. 128–149. ISSN: 03760421. DOI: 10.1016/j.paerosci.2014.08.001.

[23] Walter Cecil Schumb, Charles N Satterfield, and Ralph L Wentworth. *Hydrogen Peroxide*. New York: Reinhold Pub. Corp.; London: Chapman and Hall, 1955.

[24] C. N. Hill. *Vertical Empire, A: The History of the UK Rocket and Space Programme, 1950-1971*. WORLD SCIENTIFIC PUB CO INC, 2001.

[25] E Wernimont et al. *Past and present uses of rocket grade hydrogen peroxide*. Tech. rep. LLC Aliso Viejo, CA: General Kinetics, 1999.

[26] John Drury Clark. *Ignition!: An informal history of liquid rocket propellants*. Rutgers University Press, 1972.

[27] Steven C Williams. *Hydrogen Peroxide Material Compatibility Chart from ISM and IS Med Specialties*. Tech. rep. 2020.

[28] Hellmuth Walter. "Experience with the Application of Hydrogen Peroxide for Production of Power". In: *Journal of Jet Propulsion* 24.3 (May 1954), pp. 166–171. ISSN: 1936-9980. DOI: 10.2514/8.6484. URL: https://arc.aiaa.org/doi/10.2514/8.6484.

[29] A J Musker et al. "Hydrogen peroxide-From bridesmaid to bride". In: *3rd ESA International Conference on Green Propellants for Space Propulsion*. Dec. 2006. URL: https://www.researchgate.net/publication/265868341.

[30] ECHA. *https://echa.europa.eu/*. 2023.

[31] M. T. Constantine and E. F. C. Cain. *Hydrogen peroxide handbook*. Air Force Rocket Propulsion Laboratory, US Air Force Systems Command, 1967.

[32] Mark Ventura. "Long Term Storability of Hydrogen Peroxide". In: *41st AIAA/ASME/SAE/ASEE Joint Propulsion Conference & Exhibit*. Reston, Virigina: American Institute of Aeronautics and Astronautics, July 2005. ISBN: 978-1-62410-063-5. DOI: 10.2514/6.2005-4551. URL: http://arc.aiaa.org/doi/abs/10.2514/6.2005-4551.

[33] Wioleta Kopacz et al. "Hydrogen peroxide – A promising oxidizer for rocket propulsion and its application in solid rocket propellants". In: *FirePhysChem* 2.1 (Mar. 2022), pp. 56–66. ISSN: 26671344. DOI: 10.1016/j.fpc.2022.03.009.

[34] K. A. Cooper and J. G. Watkinson. "The supercooling of aqueous hydrogen peroxide". In: *Transactions of the Faraday Society* 53 (1957), p. 635. ISSN: 0014-7672. DOI: 10.1039/tf9575300635.

[35] C. W. Jones. "Applications of Hydrogen Peroxide and Derivatives". In: *Organic Process Research & Development* 4.3 (1999), pp. 232–233. ISSN: 1083-6160. DOI: 10.1021/op000003w.

[36] Dylan Desantis. *Satellite Thruster Propulsion-H2O2 Bipropellant Comparison with Existing Alternatives*. Tech. rep. Warsaw, Poland: Institute of Aviation, Mar. 2014. URL: https://www.researchgate.net/publication/261288210.

[37] Grzegorz Rarata, Karolina Rokicka, and Paweł Surmacz. "Hydrogen peroxide as a high energy compound optimal for propulsive applications". In: *Central European Journal of Energetic Materials* 13.3 (2016), pp. 778–790. ISSN: 17337178. DOI: 10.22211/cejem/65005.

[38] Ersin Yener Yazici and Haci Deveci. "Factors Affecting Decomposition of Hydrogen Peroxide". In: *Proceedings of the XIIth. International Mineral Processing Symposium, Gülsoy*. 2010. DOI: `10.13140/RG.2.1.1530.0648`.

[39] Lester P. Kuhn and Carl Wellman. *The Metal Ion Catalyzed Oxidation of Hydrazine with Hydrogen Peroxide*. Tech. rep. ARMY BALLISTIC RESEARCH LAB ABERDEEN PROVING GROUND MD, 1972. URL: `https://apps.dtic.mil/sti/citations/AD0746956`.

[40] Guohua Gao et al. "Advances in the production technology of hydrogen peroxide". In: *Chinese Journal of Catalysis* 41.7 (July 2020), pp. 1039–1047. ISSN: 18722067. DOI: `10.1016/S1872-2067(20)63562-8`.

[41] Cui-e Zhao et al. "Nanostructured material-based biofuel cells: recent advances and future prospects". In: *Chemical Society Reviews* 46.5 (2017), pp. 1545–1564. ISSN: 0306-0012. DOI: `10.1039/C6CS00044D`.

[42] Rosa Arrigo et al. "Pd Supported on Carbon Nitride Boosts the Direct Hydrogen Peroxide Synthesis". In: *ACS Catalysis* 6.10 (Oct. 2016), pp. 6959–6966. ISSN: 2155-5435. DOI: `10.1021/acscatal.6b01889`.

[43] Chris Winder, Rola Azzi, and Drew Wagner. "The development of the globally harmonized system (GHS) of classification and labelling of hazardous chemicals". In: *Journal of Hazardous Materials* 125.1-3 (Oct. 2005), pp. 29–44. ISSN: 03043894. DOI: `10.1016/j.jhazmat.2005.05.035`.

[44] David M. Harland and Ralph D. Lorenz. "Black Arrow". In: *Space Systems Failures: Disasters and Rescues of Satellites, Rockets and Space Probes*. Springer Science & Business Media, 2007, pp. 97–98.

[45] Skyrora Ltd. *Skyrora XL orbital launch vehicle*. 2023. URL: `https://www.skyrora.com/skyrora-xl/`.

[46] Daduí C. Guerrieri et al. "Selection and Characterization of Green Propellants for Micro-Resistojets". In: *Journal of Heat Transfer* 139.10 (Oct. 2017). ISSN: 15288943. DOI: `10.1115/1.4036619`.

[47] Y. Batonneau et al. "Green propulsion: Catalysts for the european FP7 project GRASP". In: *Topics in Catalysis*. Vol. 57. 6-9. Kluwer Academic Publishers, 2014, pp. 656–667. DOI: `10.1007/s11244-013-0223-y`.

[48] European Commission. *GRASP project information*. 2013. URL: `https://cordis.europa.eu/project/id/244725`.

[49] Carsten Scharlemann. "Green advanced space propulsion - A project status". In: *47th AIAA/ASME/SAE/ASEE Joint Propulsion Conference and Exhibit 2011*. American Institute of Aeronautics and Astronautics Inc., 2011. ISBN: 9781600869495. DOI: `10.2514/6.2011-5630`.

[50] Carsten Scharlemann. "Green Propellants: Global Assessment of Suitability and Applicability". In: *3rd European Conference for Aero-Space Sciences (EUCASS'09)*. Seibersdorf, Austria: Austrian Research Centers GmbH - ARC, 2009.

[51] Mathieu Balesdent. "Multidisciplinary design optimization of launch vehicles". PhD thesis. Nantes: Ecole Centrale de Nantes (ECN), 2011.

[52] Cédric Dupont, Sylvain Pernon, and Jean Oswald. "ARES Rockets Demonstrators of French Space Agency Project PERSEUS". In: *20th Symposium on European Rocket and Balloon Programmes and Related Research*. Hyére, France, Oct. 2011.

[53] Wiley J Larson, Gary N Henry, and Ronald W Humble. *Space propulsion analysis and design*. McGraw-Hill, 1995.

[54] Douglas J. Bayley et al. "Design Optimization of a Space Launch Vehicle Using a Genetic Algorithm". In: *Journal of Spacecraft and Rockets* 45.4 (July 2008), pp. 733–740. ISSN: 0022-4650. DOI: `10.2514/1.35318`.

[55] R. Braun, A. Moore, and I. Kroo. "Use of the collaborative optimization architecture for launch vehicle design". In: *6th Symposium on Multidisciplinary Analysis and Optimization*. Reston, Virigina: American Institute of Aeronautics and Astronautics, Sept. 1996. DOI: `10.2514/6.1996-4018`. URL: `https://arc.aiaa.org/doi/10.2514/6.1996-4018`.

[56]   Kai Dresia et al. "Multidisciplinary design optimization of reusable launch vehicles for different propellants and objectives". In: *Journal of Spacecraft and Rockets* 58.4 (2021), pp. 1017–1029. ISSN: 15336794. DOI: 10.2514/1.A34944.

[57]   M W. Van Kesteren. *Air Launch versus Ground Launch: a Multidisciplinary Design Optimization Study of Expendable Launch Vehicles on Cost and Performance*. Delft, Nov. 2013. URL: http://repository.tudelft.nl/.

[58]   Eleonoor Van Beers. *The Mars Shuttle An investigation into the feasibility of a shuttle vehicle between the Martian surface and an orbital node to support the continued presence of humans on Mars*. Delft, Aug. 2021. URL: http://repository.tudelft.nl/..

[59]   Ruwan R. L. Ernst. *Liquid Rocket Analysis (LiRA) Development of a Liquid Bi-Propellant Rocket Engine Design, Analysis and Optimization Tool*. Delft, May 2014.

[60]   Swati Shridhar Iyer. *Methalox Propellant for Future Launch Vehicles A comparative study of methalox, hydrolox and kerolox propellants for future launch vehicles*. Delft, June 2022. URL: https://repository.tudelft.nl/islandora/object/uuid%3Aba92d788-a566-43f5-82f8-959d3b7e38b5?collection=education.

[61]   Jan Vandamme. *Assisted-Launch Performance Analysis Using Trajectory and Vehicle Optimization*. Delft, Dec. 2012. URL: http://repository.tudelft.nl/.

[62]   Wiegand A, Cremaschi F, and al. *Design Optimisation and Performance Analysis of Launch Vehicles with ASTOS*. Tech. rep. 2014.

[63]   NASA. *Chemical Equilibrium Applications (CEA)*. 2002.

[64]   Alexander Ponomarenko. *Rocket Propulsion Analysis (RPA)*. 2015.

[65]   NASA. *Program to Optimize Simulated Trajectories II (POST2)*. 2022.

[66]   G. L. Brauer, D. Ej Cornick, and Richard Stevenson. *Capabilities and applications of the Program to Optimize Simulated Trajectories (POST). Program summary document*. Tech. rep. NASA, 1977. URL: https://ntrs.nasa.gov/citations/19770012832.

[67]   Stijn Dijkstra Hoefsloot. *A feasibility study on the recovery of Electron's srst stage using a vertical landing approach*. Delft, June 2022.

[68]   TU Delft. *TU Delft Astrodynamics Toolbox*. 2012. URL: https://docs.tudat.space/en.

[69]   United States Airforce. *Missile Datcom*. 1997.

[70]   Mark D. Rozemeijer. *Launch Vehicle First Stage Reusability Launch Vehicle First Stage Reusability a study to compare different recovery options for a reusable launch vehicle*. Delft, Dec. 2020. URL: http://repository.tudelft.nl/..

[71]   Stephane Contant. *Design and Optimization of a Small Reusable Launch Vehicle Using Vertical Landing Techniques*. Delft, Nov. 2019. URL: http://repository.tudelft.nl/..

[72]   Charles E. Rogers and David Cooper. *Rogers Aeroscience RASAero Aerodynamic Analysis and Flight Simulation Software*. 2008.

[73]   Barry T. C. Zandbergen. *AE1222-II: Launch Vehicle design and sizing (version 1.06.1)*. Delft: TU Delft, Faculty of Aerospace Engineering, 2017.

[74]   Marcel Barrere et al. *Rocket propulsion*. Tech. rep. Liège, Belgium: LTAS, Jan. 1960.

[75]   Jeff Cerro et al. *Structural Weight Estimation for Launch Vehicles*. Tech. rep. NASA, 2002.

[76]   Nicolas Duranté et al. "Multi-disciplinary Analysis and Optimisation Approach for the Design of Expendable Launchers". In: *10th AIAA/ISSMO Multidisciplinary Analysis and Optimization Conference*. Reston, Virigina: American Institute of Aeronautics and Astronautics, Aug. 2004. ISBN: 978-1-62410-019-2. DOI: 10.2514/6.2004-4441.

[77]   Jaroslaw Sobieszczanski-Sobieski, Jeremy Agte, and Robert Sandusky Jr. "Bi-level integrated system synthesis (BLISS)". In: *7th AIAA/USAF/NASA/ISSMO Symposium on Multidisciplinary Analysis and Optimization*. Reston, Virigina: American Institute of Aeronautics and Astronautics, Sept. 1998. DOI: 10.2514/6.1998-4916.

[78] Peter Friedrich Gath. "CAMTOS-a software suite combining direct and indirect trajectory optimization methods". PhD thesis. University of Stuttgart, 2002.

[79] Christof Büskens and Dennis Wassel. "The ESA NLP Solver WORHP". In: *Modeling and Optimization in Space Engineering*. 2012, pp. 85–110. DOI: 10.1007/978-1-4614-4469-5{_}4.

[80] Antony Jameson. *Gradient Based Optimization Methods*. Tech. rep. Princeton University, 1995.

[81] David Alexander Coley. *An introduction to genetic algorithms for scientists and engineers*. World Scientific Publishing Company, Jan. 1999. ISBN: 9810236026.

[82] Marc Parizeau et al. "DEAP: Evolutionary Algorithms Made Easy". In: *Journal of Machine Learning Research* 13 (2012), pp. 2171–2175. URL: https://www.jmlr.org/papers/v13/fortin12a.html.

[83] Guido van Rossum. *Python*. 2022.

[84] David L. Akin. *Mass Estimating Relations*. Maryland, 2016. URL: https://spacecraft.ssl.umd.edu/academics/791S16/791S16L08.MERsx.pdf.

[85] Barry T. C. Zandbergen. "Simple mass and size estimation relationships of pump fed rocket engines for launch vehicle conceptual design". In: *6th European Conference for Aeronautics and Space Sciences (EUCASS)*. Krakow, Poland, July 2015. URL: https://www.researchgate.net/publication/279711349.

[86] Charles E Rogers, David Cooper, and Rogers Aeroscience. *Rogers Aeroscience RASAero II Aerodynamic Analysis and Flight Simulation Program Users Manual*. Lancaster, CA, 2019. URL: www.rasaero.comwww.rasaero.com.

[87] Adam Okninski et al. "Development of a small green bipropellant rocket engine using hydrogen peroxide as oxidizer". In: *50th AIAA/ASME/SAE/ASEE Joint Propulsion Conference 2014*. American Institute of Aeronautics and Astronautics Inc., 2014. ISBN: 9781624103032. DOI: 10.2514/6.2014-3592.

[88] Wojciech Florczuk and Grzegorz Rarata. "Performance evaluation of the hypergolic green propellants based on the HTP for a future next-generation space crafts". In: *53rd AIAA/SAE/ASEE Joint Propulsion Conference, 2017*. American Institute of Aeronautics and Astronautics Inc, AIAA, 2017. ISBN: 9781624105111. DOI: 10.2514/6.2017-4849.

[89] ArianeGroup. *VULCAIN® 2. 1 engine space propulsion*. Vernon Cedex, France, 2019. URL: www.ariane.group.

[90] Aerojet Rocketdyne. *RS-68A PROPULSION SYTEM*. Mar. 2019. URL: www.rocket.com.

[91] Centre National d'Études Spatiales (CNES). *ARIANE 6*. Nov. 2022. URL: https://ariane6.cnes.fr/en/ariane-6-2.

[92] Arianespace. *Ariane 6 User's Manual*. Feb. 2021. URL: www.arianespace.com.

[93] Paul K. Mcconnaughey et al. *Launch propulsion systems roadmap (technology area 01)*. Tech. rep. Washington DC, United States of America: National Aeronautics and Space Administration (NASA), 2012. URL: https://ntrs.nasa.gov/citations/20120014957.

[94] European Space Agency (ESA). *Media backgrounder for ESA Council at Ministerial Level*. Nov. 2014. URL: https://www.esa.int/Newsroom/Press_Releases/Media_backgrounder_for_ESA_Council_at_Ministerial_Level.

[95] D. Gallois. *Ariane 6, un chantier européen pour rester dans la course spatiale*. Dec. 2014. URL: https://www.lemonde.fr/economie/article/2014/12/01/les-europeens-s-appretent-a-mettre-ariane-6-en-chantier_4532259_3234.html.

[96] J. Posaner. *Europe's lack of rocket 'audacity' leaves it scrambling in the space race*. 2021. URL: https://www.politico.eu/article/europe-arianespace-rocket-space-race/.

[97] Arianespace. *ARIANE 62 - MISSION PROFILE*. 2023. URL: https://www.arianespace.com/vehicle/ariane-6/mission-profile-ariane-62/.

[98] Spaceflight101. *Ariane 5 ES*. 2022. URL: https://spaceflight101.com/spacerockets/ariane-5-es-2/.

[99] Jeff Foust. *Ariane 6 first launch slips to late 2023*. Oct. 2022. URL: https://spacenews.com/ariane-6-first-launch-slips-to-late-2023/.

[100] European Space Agency (ESA). *Vega-C successfully completes inaugural flight*. July 2022. URL: https://www.esa.int/Enabling_Support/Space_Transportation/Vega/Vega-C_successfully_completes_inaugural_flight#:~:text=The%20launch%20caps%20a%20multi,10%3A13%20local%20time)..

[101] Avio. *P120 C MOTOR MAIN CHARACTERISTICS*. 2023. URL: https://www.avio.com/vega-c.

[102] Arianespace. *Ariane 6*. 2023. URL: https://www.arianespace.com/vehicle/ariane-6/.

[103] J. Merino et al. "ARIANE 6 - Tanks and Structures for the New European Launcher". In: *Deutscher Luft- und Raumfahrtkongress*. 2017.

[104] Sh. L. Guseinov et al. "Hypergolic propellants based on hydrogen peroxide and organic compounds: historical aspect and current state". In: *Russian Chemical Bulletin* 67.11 (Nov. 2018), pp. 1943–1954. ISSN: 1066-5285. DOI: 10.1007/s11172-018-2314-1. URL: http://link.springer.com/10.1007/s11172-018-2314-1.

[105] John W. Bennewitz and Robert A. Frederick. "Overview of Combustion Instabilities in Liquid Rocket Engines - Coupling Mechanisms & Control Techniques". In: *49th AIAA/ASME/SAE/ASEE Joint Propulsion Conference*. Reston, Virginia: American Institute of Aeronautics and Astronautics, July 2013. ISBN: 978-1-62410-222-6. DOI: 10.2514/6.2013-4106.

[106] R. W. Humble, G. N. Henry, and W. J. Larson. *Space propulsion analysis and design*. New York: McGraw-Hill, 1995.

[107] Shamim Rahman and Bartt Hebert. "Large Liquid Rocket Development Testing – Strategies and Challenges". In: *41st AIAA/ASME/SAE/ASEE Joint Propulsion Conference & Exhibit*. Reston, Viragina: American Institute of Aeronautics and Astronautics, July 2005. ISBN: 978-1-62410-063-5. DOI: 10.2514/6.2005-3564.

[108] Vittorio Bombelli, Ton Marée, and Fabio Caramelli. "Non-toxic liquid propellant selection method a requirement-oriented approach". In: *41st AIAA/ASME/SAE/ASEE Joint Propulsion Conference and Exhibit*. 2005. DOI: 10.2514/6.2005-4453.

[109] Stefania Carlotti and Filippo Maggi. "Evaluating New Liquid Storable Bipropellants: Safety and Performance Assessments". In: *Aerospace* 9.10 (Oct. 2022). ISSN: 22264310. DOI: 10.3390/aerospace9100561.

[110] Maxim Kurilov et al. "A method for screening and identification of green hypergolic bipropellants". In: *International Journal of Energetic Materials and Chemical Propulsion* 17.3 (2018), pp. 183–203. ISSN: 21507678. DOI: 10.1615/IntJEnergeticMaterialsChemProp.2018028057.

[111] S. McClendon, W. Miller, and C. Herty III. "Fuel selection criteria for ducted rocket application". In: *16th Joint Propulsion Conference*. Reston, Viragina: American Institute of Aeronautics and Astronautics, June 1980. DOI: 10.2514/6.1980-1120.

[112] N. T. Drenthe et al. "Cost estimating of commercial smallsat launch vehicles". In: *Acta Astronautica* 155 (Feb. 2019), pp. 160–169. ISSN: 00945765. DOI: 10.1016/j.actaastro.2018.11.054.

[113] Canadian Centre for Occupational Health and Safety (CCOHS). *Globally Harmonized System (GHS)*. 2023. URL: https://www.ccohs.ca/oshanswers/chemicals/ghs.html.

[114] W. H. L. Dornette and Miles E. Woodworth. *Report of Committee on Fire Hazards of Materials*. Tech. rep. National Fire Protection Agency (NFPA), 1969.

[115] Jonathan Hart. *Hazardous Materials Identification*. Nov. 2021. URL: https://www.nfpa.org/news-blogs-and-articles/blogs/2021/11/05/hazardous-materials-identification.

[116] William Popendorf. "Vapor Pressure and Solvent Vapor Hazards". In: *American Industrial Hygiene Association Journal* 45.10 (Oct. 1984), pp. 719–726. ISSN: 0002-8894. DOI: 10.1080/15298668491400494.

[117] Martin John Pitt and Martin J Pitt. "A Vapour Hazard Index for COSHH and DSEAR". In: *Hazards XIX*. Manchester, Mar. 2006. URL: https://www.researchgate.net/publication/290392937.

[118] B. Nufer. "A summary of NASA and USAF hypergolic propellant related spills and fires". In: *SpaceOps 2010 Conference*. 2010. ISBN: 9781624101649. DOI: 10.2514/6.2010-1994.

[119] John A. Halchak, James L. Cannon, and Corey Brown. "Materials for Liquid Propulsion Systems". In: *Aerospace Materials and Applications*. Reston ,VA: American Institute of Aeronautics and Astronautics, Inc., Jan. 2018, pp. 641–698. DOI: 10.2514/5.9781624104893.0641.0698. URL: https://arc.aiaa.org/doi/10.2514/5.9781624104893.0641.0698.

[120] Grant Henson. "Materials for Launch Vehicle Structures". In: *Aerospace Materials and Applications*. Reston ,VA: American Institute of Aeronautics and Astronautics, Inc., Jan. 2018, pp. 435–504. DOI: 10.2514/5.9781624104893.0435.0504. URL: https://arc.aiaa.org/doi/10.2514/5.9781624104893.0435.0504.

[121] Graco Incorporated. *Chemicial Compatibility Guide*. Tech. rep. Graco Incorporated, Feb. 2013.

[122] Forrest S Forbes and Peter A Van Splinter. "Liquid rocket propellants". In: *Encyclopedia of Physical Science and Technology*. Ed. by Robert A. Meyers. 3rd ed. 2003. ISBN: 978-0-12-227410-7.

[123] European Space Agency (ESA). *Technology Readiness Levels (TRL)*. 2023. URL: https://www.esa.int/Enabling_Support/Space_Engineering_Technology/Shaping_the_Future/Technology_Readiness_Levels_TRL#:~:text=The%20scale%20ranges%20from%201,a%20flight%20mission%20in%20space..

[124] Chuang Zhou et al. "The Influence of Thrust Chamber Structure Parameters on Regenerative Cooling Effect with Hydrogen Peroxide as Coolant in Liquid Rocket Engines". In: *Aerospace* 10.1 (Jan. 2023). ISSN: 22264310. DOI: 10.3390/aerospace10010065.

[125] Fabio Kerstens. *Preliminary Design of a Small Hydro-gen Peroxide Cooled Thrust Chamber for Additive Manufacturing*. Delft, May 2021. URL: http://repository.tudelft.nl/..

[126] Rui Serra-Maia et al. "Mechanism and Kinetics of Hydrogen Peroxide Decomposition on Platinum Nanocatalysts". In: *ACS Applied Materials & Interfaces* 10.25 (June 2018), pp. 21224–21234. ISSN: 1944-8244. DOI: 10.1021/acsami.8b02345.

[127] E. N. Sieder and G. E. Tate. "Heat transfer and pressure drop of liquids in tubes". In: *Industrial & Engineering Chemistry* 28.12 (1936), pp. 1429–1435. URL: https://pubs.acs.org/sharingguidelines.

[128] Maynard F Taylor. *Correlation of local heat-transfer coefficients for single-phase turbulent flow of hydrogen in tubes with temperature ratios to 23*. National Aeronautics and Space Administration (NASA), Jan. 1968. URL: https://ntrs.nasa.gov/citations/19680004771.

[129] R. W. Saaty. "The analytic hierarchy process-what it is and how it is used". In: *Mathematical Modelling* 9.3-5 (1987), pp. 161–176. ISSN: 02700255. DOI: 10.1016/0270-0255(87)90473-8.

[130] Thomas L. Saaty. "Decision making with the analytic hierarchy process". In: *International Journal of Services Sciences* 1.1 (Jan. 2008), p. 83. ISSN: 1753-1446. DOI: 10.1504/IJSSCI.2008.017590. URL: http://www.inderscience.com/link.php?id=17590.

[131] Thijs Mathot. *Analytical Hierarchy Process Trade-off Tool Users Manual v2.7*. Tech. rep. Dutch Space B.V., 2012.

[132] John J Rusek, T L Pourpoint, and J J Rusek. *Novel organometallic propellants for hypergolic applications*. Tech. rep. West Lafayette, Indiana, USA: Swift Enterprises, Ltd., 2002.

[133] Felix Lauck et al. "Green bipropellant development – A study on the hypergolicity of imidazole thiocyanate ionic liquids with hydrogen peroxide in an automated drop test setup". In: *Combustion and Flame* 226 (Apr. 2021), pp. 87–97. ISSN: 15562921. DOI: 10.1016/j.combustflame.2020.11.033.

[134] Brian Melof and Mark Grubelich. "Investigation of hypergolic fuels with hydrogen peroxide". In: *37th Joint Propulsion Conference and Exhibit*. Reston, Virigina: American Institute of Aeronautics and Astronautics, July 2001. DOI: 10.2514/6.2001-3837. URL: https://arc.aiaa.org/doi/10.2514/6.2001-3837.

[135] Barrie Mellor. *A Preliminary Technical Review of DMAZ: A Low-Toxicity Hypergolic Fuel.* Tech. rep. Westcott, England: Edotek Ltd., Sept. 2004. URL: https://www.researchgate.net/publication/234310816.

[136] Hongjae Kang, Dongwook Jang, and Sejin Kwon. "Demonstration of 500 N scale bipropellant thruster using non-toxic hypergolic fuel and hydrogen peroxide". In: *Aerospace Science and Technology* 49 (2016), pp. 209–214. ISSN: 12709638. DOI: 10.1016/j.ast.2015.11.038.

[137] Rohit Mahakali et al. "Development of Reduced Toxicity Hypergolic Propellants". In: *47th AIAA/ASME/SAE/ASEE Joint Propulsion Conference & Exhibit.* Reston, Viriginia: American Institute of Aeronautics and Astronautics, July 2011. ISBN: 978-1-60086-949-5. DOI: 10.2514/6.2011-5631.

[138] Hongjae Kang and Sejin Kwon. "Green hypergolic combination: Diethylenetriamine-based fuel and hydrogen peroxide". In: *Acta Astronautica* 137 (Aug. 2017), pp. 25–30. ISSN: 00945765. DOI: 10.1016/j.actaastro.2017.04.009.

[139] Peter Fortescue, John Stark, and Graham Swinerd. *Spacecraft Systems Engineering, Third Edition.* 3rd ed. John Wiley & Sons, Jan. 2003. URL: www.wileyeurope.cam.

[140] P. Bose and K.M. Pandey. "Analysis of Thrust Coefficient in a Rocket Motor coefficient and important criteria for nozzle design". In: *International Journal of Engineering and Advanced Technology (IJEAT)* 1.3 (Feb. 2012). URL: https://www.researchgate.net/publication/271907332_Analysis_of_Thrust_Coefficient_in_a_Rocket_Motor.

[141] Majid Hosseini et al. "Multidisciplinary design optimization of an expendable launch vehicle". In: *Proceedings of 5th International Conference on Recent Advances in Space Technologies - RAST2011.* IEEE, June 2011, pp. 702–707. ISBN: 978-1-4244-9617-4. DOI: 10.1109/RAST.2011.5966932. URL: http://ieeexplore.ieee.org/document/5966932/.

[142] Erwin Mooij. *The motion of a vehicle in a planetary atmosphere.* Tech. rep. Delft: TU Delft, Faculty of Aerospace Engineering, Dec. 1994.

[143] J.A. Mulder et al. *Flight dynamics lecture notes ae3202.* Delft, 2013.

[144] Navigation and Ancillary Information Facility (NAIF). *An overview of reference frames and coordinate systems in the SPICE context.* Tech. rep. NAIF, Apr. 2023.

[145] National Oceanic and Atmospheric Administration (NOAA), National Aeronautics and Space Administration (NASA), and United States Air Force. *U.S. STANDARD ATMOSPHERE, 1976.* Tech. rep. Washington D.C., Oct. 1976.

[146] J. M. Picone et al. "NRLMSISE-00 empirical model of the atmosphere: Statistical comparisons and scientific issues". In: *Journal of Geophysical Research: Space Physics* 107.A12 (2002). ISSN: 21699402. DOI: 10.1029/2002JA009430.

[147] Francesco Castellini, Luciano Galfetti, and Sergio Ricci. "Multidisciplinary Design Optimization For Expendable Launch Vehicles". PhD thesis. Milan: Politecnico di Milano, 2012.

[148] T. Fecher et al. *GOCO05c: A New Combined Gravity Field Model Based on Full Normal Equations and Regionally Varying Weighting.* May 2017. DOI: 10.1007/s10712-016-9406-y.

[149] Henry N. Pollack. "Spherical harmonic representation of the gravitational potential of a point mass, a spherical cap, and a spherical rectangle". In: *Journal of Geophysical Research* 78.11 (Apr. 1973), pp. 1760–1768. DOI: 10.1029/jb078i011p01760.

[150] Etienne Dumont et al. "Advanced TSTO launch vehicles". In: *4th European Conference for Aerospace Sciences (EUCASS).* DLR, June 2011. URL: https://www.researchgate.net/publication/225021406.

[151] Arianespace. *VA226.* Tech. rep. ArianeGroup, Sept. 2015.

[152] Rainer Storn and Kenneth Price. "Differential Evolution-A Simple and Efficient Heuristic for Global Optimization over Continuous Spaces". In: *Journal of Global Optimization* 11 (Jan. 1997), pp. 341–359. DOI: http://dx.doi.org/10.1023/A:1008202821328.

[153] Scipy. *scipy.optimize.differential_evolution.* 2023. URL: https://docs.scipy.org/doc/scipy/reference/generated/scipy.optimize.differential_evolution.html#scipy-optimize-differential-evolution.

[154] U. Palmns and R. Sundi. "Parametric performance design study of a 20 kN high storable propellant pump-fed engine". In: *Acta Astronautica* 17.8 (Jan. 1988), pp. 837–852.

[155] Stephen M. Davis and Nadir Yilmaz. "Advances in Hypergolic Propellants: Ignition, Hydrazine, and Hydrogen Peroxide Research". In: *Advances in Aerospace Engineering* 2014.1 (Sept. 2014), pp. 1–9. ISSN: 2356-6531. DOI: 10.1155/2014/729313.

A. Hydrogen peroxide material compatibility chart

Hydrogen Peroxide Material Compatibility Chart

All wetted surfaces should be made of materials that are compatible with hydrogen peroxide. The wetted area or surface of a part, component, vessel or piping is a surface which is in permanent contact with or is permanently exposed to the process fluid (liquid or gas).

Less than 8% concentration H2O2 is considered a non-hazardous substance. Typically encountered versions are baking soda-peroxide toothpaste (0.5%), contact lens sterilizer (2%), over-the-counter drug store Hydrogen Peroxide (3%), liquid detergent non-chlorine bleach (5%) and hair bleach (7.5%).

At 8% to 28% H2O2 is rated as a Class 1 Oxidizer. At these concentrations H2O2 is usually encountered as a swimming pool chemical used for pool shock treatments.

In the range of 28.1% to 52% concentrations, H2O2 is rated as a Class 2 Oxidizer, a Corrosive and a Class 1 Unstable (reactive) substance. At these concentrations, H2O2 is considered industrial strength grade.

Concentrations from 52.1% to 91% are rated as Class 3 Oxidizers, Corrosive and Class 3 Unstable (reactive) substances. H2O2 at these concentrations are used for specialty chemical processes. At concentrations above 70%, H2O2 is usually designated as high-test peroxide (HTP).

Concentrations of H2O2 greater than 91% are currently used as rocket propellant. At these concentrations, H2O2 is rated as a Class 4 Oxidizer, Corrosive and a Class 3 Unstable (reactive) substance.

Material	Compatibility 10% H_2O_2	Compatibility 30% H_2O_2	Compatibility 50% H_2O_2	Compatibility 100% H_2O_2 (HTC)

Chemical resistance data is based on 72° F (22° C) unless otherwise noted
A- Suitable
B - Good, minor effect, slight corrosion or discoloration
F - Fair, moderate effect, not recommended for continuous use;
softening, loss of strength, and/or swelling may occur
X - Do Not Use - severe effect, not recommended for ANY use
NA - Information Not Available

1 - Satisfactory to 120°F (48° C)
2 - Satisfactory for O-rings, diaphragms or gaskets
3 - Temporary use only

Material	10%	30%	50%	100%
304 stainless steel	B[1]	B[1]	B[1]	B[1]
316 stainless steel	B	B	A[1]	A[1]
416 stainless steel	B	B	F	X
440C stainless steel	B	B	A	X
ABS plastic	A	A	A	A

It is the sole responsibility of the system designer and user to select products suitable for their specific application requirements and to ensure proper installation, operation, and maintenance of these products. Material compatibility, product ratings and application details should be considered in the selection. Improper selection or use of products described herein can cause personal injury or product damage. In applications where exposure to harmful chemicals is frequent, of long duration or in high concentrations, additional testing is recommended.

IS MED
SPECIALTIES

End your search, simplify your supply chain
ISO 9001:2015 Certified Companies

Hydrogen Peroxide Material Compatibility Chart

ver 09-Jul-2020

Material	Compatibility 10% H_2O_2	Compatibility 30% H_2O_2	Compatibility 50% H_2O_2	Compatibility 100% H_2O_2 (HTC)

Chemical resistance data is based on 72° F (22° C) unless otherwise noted

A- Suitable
B - Good, minor effect, slight corrosion or discoloration
F - Fair, moderate effect, not recommended for continuous use;
softening, loss of strength, and/or swelling may occur
X - Do Not Use - severe effect, not recommended for ANY use
NA - Information Not Available

1 - Satisfactory to 120°F (48° C)
2 - Satisfactory for O-rings, diaphragms or gaskets
3 - Temporary use only

Material	Compatibility 10% H_2O_2	Compatibility 30% H_2O_2	Compatibility 50% H_2O_2	Compatibility 100% H_2O_2 (HTC)
Acetal (Delrin®)	X	X	X	X
Acrylic (PMMA)	B	F	NA	X
Alloy 20 (Carpenter 20)	F	B	B	X
Aluminum	A	A	A	A
Brass	X	X	X	X
Bronze	B	B	B	B
Buna N (Nitrile)	X	X	X	X
Carbon graphite	F	F	F	F
Carbon steel	X	X	X	X
Cast iron	F	X	X	X
Ceramic Al_2O_3	A	A	A	A
Ceramic magnet	A	A	A	A
Copper	X	X	X	X
CPVC	A	A	A	A
EPDM	A	B	B	X
Epoxy (epoxide polymers)	F	B	B	X
FKM (fluoroelastomers, Viton®)	A	A	A	A
Hastelloy-C®	A	A	A	A
HDPE	A	A	A	X
Hypalon®	X	X	X	X
Hytrel® (polyester elastomer)	X	X	X	X
LDPE	A	F[1]	F[1]	F[1]
Natural rubber	B	F	F	F
Neoprene	X	X	X	X
NORYL®	A[1]	A[1]	A	A

It is the sole responsibility of the system designer and user to select products suitable for their specific application requirements and to ensure proper installation, operation, and maintenance of these products. Material compatibility, product ratings and application details should be considered in the selection. Improper selection or use of products described herein can cause personal injury or product damage. In applications where exposure to harmful chemicals is frequent, of long duration or in high concentrations, additional testing is recommended.

IS MED SPECIALTIES

End your search, simplify your supply chain
ISO 9001:2015 Certified Companies

4091 S. Eliot St., Englewood, CO 80110-4396
Phone 303-781-8486 I Fax 303-761-7939
Ismedspec.com

© Copyright 2020 IS MED Specialties

Hydrogen Peroxide Material Compatibility Chart

ver 09-Jul-2020

Material	Compatibility 10% H$_2$O$_2$	Compatibility 30% H$_2$O$_2$	Compatibility 50% H$_2$O$_2$	Compatibility 100% H$_2$O$_2$ (HTC)

Chemical resistance data is based on 72° F (22° C) unless otherwise noted

A- Suitable

B - Good, minor effect, slight corrosion or discoloration

F - Fair, moderate effect, not recommended for continuous use;

softening, loss of strength, and/or swelling may occur

X - Do Not Use - severe effect, not recommended for ANY use

NA - Information Not Available

1 - Satisfactory to 120°F (48° C)

2 - Satisfactory for O-rings, diaphragms or gaskets

3 - Temporary use only

Material	Compatibility 10% H$_2$O$_2$	Compatibility 30% H$_2$O$_2$	Compatibility 50% H$_2$O$_2$	Compatibility 100% H$_2$O$_2$ (HTC)
Nylon (polyamides)	F	X	X	X
PCTFE (Kel-F® and Neoflon®)	A[1]	A[1]	A[1]	X
PFA (perfluoroalkoxy alkanes)	A	A	A	A
Polycarbonate	A[1]	A[1]	A[1]	A
Polypropylene	A	B	B	B
PP-363 (plasticized vinyl)[2]	A	A	A	X
PPS (Ryton®)	A	A	F	F
PTFE (Garlock Glyon® 3500)[2]	A	A	A	X
PTFE (Teflon®), virgin[2]	A	A	A	A
PVC	A	A	A	A
PVDF (Hylar®)	A[1]	A[1]	X	X
PVDF (Kynar®)	A	A	A	A
PVDF (Solef®)	A[1]	A[1]	X	X
Silicone	A	B	B	B
SPR (styrene butadiene rubber)	X	X	X	X
Thiokol™ (polysulfide polymers)	X	X	X	X
Titanium[3]	A	B	B	B
TPE (thermoplastic elastomers)	X	X	X	X
TPU (thermoplastic polyurethanes)	X	X	X	X
Tygon®	B	B	B	B
Tungsten carbide	X	X	X	X
Viton® A[2]	A	A	A	A

It is the sole responsibility of the system designer and user to select products suitable for their specific application requirements and to ensure proper installation, operation, and maintenance of these products. Material compatibility, product ratings and application details should be considered in the selection. Improper selection or use of products described herein can cause personal injury or product damage. In applications where exposure to harmful chemicals is frequent, of long duration or in high concentrations, additional testing is recommended.

IS MED SPECIALTIES

End your search, simplify your supply chain
ISO 9001:2015 Certified Companies

B.AHP criteria overview document

Trade-off criteria weight assessment

A weight assessment of the trade-off criteria needed for the selection of a fuel for launch vehicle applications

by

Michaël Staelens

Student number	4796969
Supervisor	Dr. ir. B.V.S. Jyoti TU Delft, supervisor, Ast. Prof. Tu Delft
Institution:	Delft University of Technology
Study period:	2023

TUDelft

Preface

This document was written to give the reader a basic idea of the objective of this study and the method proposed for the fuel selection process. Next to that, it contains an overview of all criteria relevant to the trade-off, such that a clear and unambiguous interpretation of these criteria is available for all experts who will provide input in determining relative weights for these criteria.
The relative weighting can be registered in the excel sheet that came together with this document. This excel sheet is to be sent back to me (M.Staelens@student.tudelft.nl).

Thank you very much for providing me with your expertise and input!

Contents

1.Methodology

This document was written to give the reader a basic idea of the objective of this study and the method proposed for the fuel selection process. Next to that, it contains an overview of all criteria relevant to the trade-off, such that a clear and unambiguous interpretation of these criteria is available for all experts who will provide input in determining relative weights for these criteria.

The main objective of this study is to perform a cost and performance analysis for the integration of a hydrogen peroxide based bi-propellant into the main stage of a medium-weight expendable launch vehicle to further map the potential of hydrogen peroxide for space applications. A crucial aspect of this is the selection of a fuel that displays both favourable usage properties and good performance characteristics in combination with hydrogen peroxide.

Given the high number of potential fuel combinations with highly concentrated hydrogen peroxide (HTP) proposed in literature, an efficient fuel selection process is crucial. The following process has been proposed (here, mostly step 2 is relevant for this document):

- **Step 1 - Preliminary feasibility assessment**: all fuels will be subjected to a surface-level assessment regarding the minimum requirements for certain fuel characteristics. These are related to combustion stability with HTP, state at expected storage conditions, overall (maximum) toxicity levels, and minimum performance levels. Based on this assessment, a selection of promising fuels will be made and the leftover options will be discarded. Although not specifically mentioned as a criterion, the extent of available literature or research on the proposed fuels will also be considered as a factor in the selection process.
- **Step 1.5 - Availability assessment**: The availability of all selected fuels will be checked as this is considered to be a killer criterion due to its implications with respect to cost and transportation needs. It is also important to determine that the selected fuels are not at risk of becoming scarce in the future, so as to not waste resources on research and development efforts for a fuel that is only interesting for short-term use.
- **Step 2 - AHP trade-off**: the fuels selected in step 1 will be subjected to a trade-off, for which an Analytical Hierarchy Process (AHP) tool will be employed to make a more narrow selection for promising fuels for the research intend. This trade-off aims to further explore the potential of the fuels with respect to integration and compatibility in the launch vehicle propulsion system regarding other characteristics than pure performance. The relevant criteria can be deduced from the schematic included in Figure 1.2: Handling toxicity, environmental toxicity, handling and storage, material compatibility, development level, and cooling quality. Assigning suitable relative weights to these criteria is the main purpose of this document.
- **Step 3 - Performance assessment**: An analytical/numerical model will be set up to estimate the effects of propellant choice on the payload capability and the cost of a reference launch vehicle. This will thus allow for the performance of these propellants to be assessed. The most promising fuels will then be selected for further review. If needed, an iteration will be performed in which previous steps will be revisited.

The tool that will be used for the trade-off needed in step 2 is the AHP trade-off tool based on Dr Saaty. An important aspect of this tool is determining the relative importance weights assigned to the different criteria. This is done by assessing the relative importance between pairs of criteria. In order to provide a level of objectivity to this otherwise rather subjective process, this weight assignment should be performed by multiple experts before resulting in a final weight score for all of the criteria. For reference, the manual specific to this tool was attached to this document and can be found in Appendix B[1].

---

[1]This appendix was left out for the version of this document included in the appendices of the MSc thesis document

The relative weighting can be registered in the Excel sheet that came with this document. Criteria are evaluated by putting an x underneath the scale from 9 to 1 to 9. The x is put closer towards the criterion that is expected to be more relevant or more important concerning the indicated performance parameter. The more pronounced the difference, the closer the x has to be put to the best or more important criterion. To understand the intended meaning of the different scaling values proposed in the AHP trade-off tool manual, Figure 1.1 can be referred to.

Intensity	Definition	Explanation
1	Equal	Two items contribute equally to the objective
3	Moderate	Experience and judgment slightly favor one item over another
5	Strong	Experience and judgment strongly favor one item over another
7	Very strong	An item is strongly favored and its dominance demonstrated in practice
9	Extreme	The evidence favoring one activity over another is of the highest possible order of affirmation
2,4,6,8	Intermediate values	When compromise is needed

Figure 1.1: Meaning of the different scaling values as proposed in the AHP trade-off tool manual
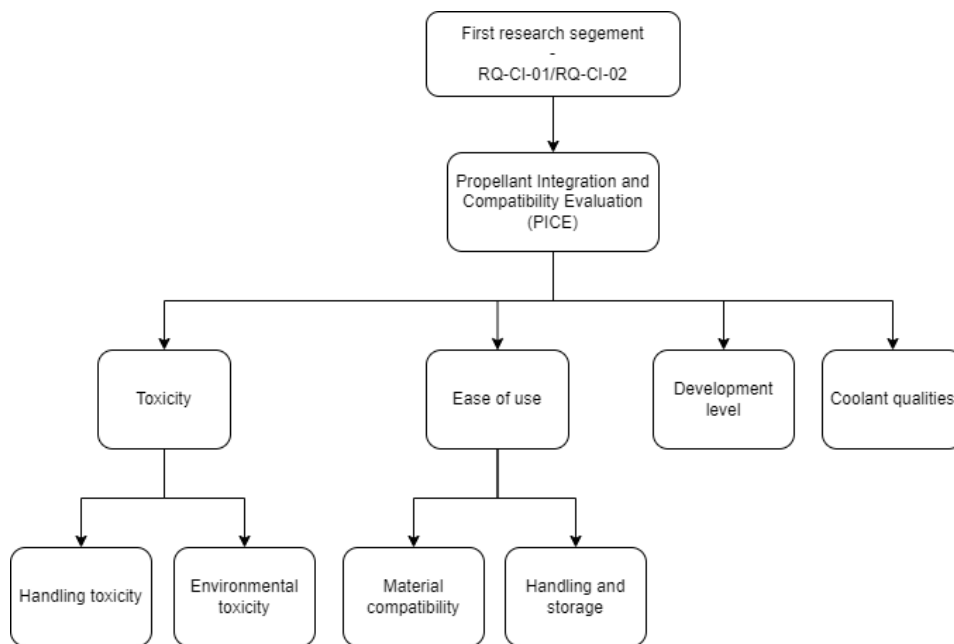
Figure 1.2: Criteria and subcriteria considered for the AHP trade-off assessment

2

2.Criteria overview

Below, all relevant criteria belonging to the propellant integration potential assessment will briefly be described to ensure that all experts assessing the criteria weights are given a clear and unambiguous interpretation for each of the proposed criteria. Note that these criteria will be specific to the fuel selection, as the oxidiser for this study was already determined.

PICE-C01: Toxicity
PICE-C01.1: Environmental toxicity (Toxicity): Since environmental concerns are becoming increasingly important to the space industry and its partners, this criterion should allow for anticipating future propellant bans. In this case, mostly the direct environmental safety codes for the proposed fuels, rather than the propellant combinations with HTP, will be considered. To be able to make an effective comparison between fuels, the base products of the bi-propellant systems will be measured on the GHS scale. This "Global Harmonised System of Classification and Labelling of Chemicals" includes nine main classes that are concerned with different kinds of toxicity and hazards, including a class specifying environmental hazards.

PICE-C01.2: Handling toxicity (Toxicity):
Another criterion derived from fuel safety addresses the hazards related to the handling and transportation of the fuels. This is not only important for the overall cost of the fuel, but also for the support from funding sources. Similar to the environmental hazards criterion, the GHS scale will also be employed for scoring the fuels according to this criterion. Next to this, the stability and ease of transportation will also be addressed. This is of importance as it is directly related to the transportation range and thus the cost of manufacturing.

PICE-C02: Ease of use
PICE-C02.1: Material compatibility (Ease of use): The choice of materials is an important factor in obtaining structural modifications, weight reductions, effective cooling mechanisms and other launch vehicle system improvements. This is expected to remain an important factor in future optimisation efforts for launch vehicle design. Therefore, the material compatibility criterion should allow for the potential fuels to be assessed for their overall compatibility and reactivity, or lack thereof, with respect to current and potential future aerospace materials.

PICE-C02.2: Handling and storage: When considering a fuel for rocket propellants, it is important that it can be stored under the required conditions without showing signs of decomposition or other unstable behaviour. The storage criterion for this trade-off is defined as a focus on the behaviour of potential fuels in the expected storage conditions regarding storage temperature, pressure, and time. Here, it will be assessed whether how the fuels would perform in these storage conditions with respect to stability, decomposition rate, explosion risk, and state transition, i.e., whether a liquid state is maintained. This ties into the handling of the fuels as the flammability and reactivity of the fuel are considered.

PICE-C03: Development level
A consideration in selecting a novel propellant combination for application in launch vehicles is the relative lack of development with respect to established propellants. It should be noted that for some HTP-based propellant combinations, a fair amount of studies and systems development efforts have already been conducted. Following development cost and time arguments, it might thus be more interesting to select such propellant combinations over options for which a lower research development progress has been reported. Therefore, the development level criterion will focus on assessing the overall research study and systems development level of the potential fuels, both as separate chemicals and in combination with hydrogen peroxide.

PICE-C04: Cooling qualities

Although debated, it could be derived from recent research studies that hydrogen peroxide can not effectively be used as a coolant for large-scale regenerative cooling efforts in propulsion systems. To account for this, the coolant capabilities of the proposed fuels should be assessed. The cooling qualities criterion is thus deemed important as this will be a non-negligible influence on the overall safety, reliability, and performance of the propulsion system.

C.Preliminary fuel selection evaluations

Table C.1: Criteria evaluations from the preliminary fuel selection involving 86 fuels - Part 1
(GREEN=Selected for PICE , YELLOW=Rejected for PICE/Accepted for reference , RED=Rejected for PICE)
(*Final evaluation made after preliminary feasibility assessment, **Liquid storage state*)

Fuel	Performance evaluation	Combustion evaluation	Toxicity evaluation	Storage evaluation
1,2,4-Triazole	NA	NA	Low	Solid
1,2-diaminocyclohexane	NA	NA	Medium/High	Liquid
1,3-diaminopropane	NA	NA	Medium/High	Liquid
1,5-hexadiyne	NA	NA	Low	High melting point**
Acetaldehyd	LOW	NA	Low	Low boiling point**
Acythelene	High	Low	Low/Medium	Unstable
Alpha-terpineol	NA	NA	None	Solid
Ammonia	Low/Medium	NA	Low	Gaseous
Benzaldehyde	Low/Medium	High	Low	Liquid
Block O*	Medium	High	None	Unknown transition temperatures** Poor storage
BMIM SCN*	High	High	Low/Medium	Unknown boiling point**
Butane	Medium/High	NA	Low	Gaseous
Cyclopropane	Medium/High	NA	Medium	Gaseous
Decaborane	NA	NA	NA	Solid
DETA*	High	High	Medium	Liquid
Dibutyl ether	Medium/High	NA	Medium/High	Liquid
Diglyme	Low	NA	High	Liquid
Dimethylether	Medium	NA	Low/Medium	Gaseous
d-limonene	Low/Medium	NA	Low	Liquid
DMA	Medium	NA	Low	Gaseous
DMAZ	High	High	Low	Liquid
DMEA/DMAE*	Medium/High	High	None/Low	Liquid
DMF	NA	NA	Low	Liquid
DMSO	NA	NA	Low	Solid
EDA	NA	NA	Low	High melting point**
EMIM SCN*	High	High	Low/Medium	Unknown boiling point**

Table C.2: Criteria evaluations from the preliminary fuel selection involving 86 fuels - Part 2
(GREEN=Selected for PICE , YELLOW=Rejected for PICE/Accepted for reference , RED=Rejected for PICE)
(*Final evaluation made after preliminary feasibility assessment, **Liquid storage state*)

Fuel	Performance evaluation	Combustion evaluation	Toxicity evaluation	Storage evaluation
Ethane	Medium/High	NA	Medium/High	Gaseous
Ethanol	High	High	None	Liquid
Ethyl methyl ether	High	NA	Medium/High	Gaseous
Ethylene	High	NA	None	Gaseous
Ethylene glycol	NA	NA	NA	Liquid
Ethylenediamine	NA	NA	Medium/High	High melting point**
Furaldehyde	NA	NA	NA	Liquid
Furfuryl alcohol	Low	Low	Low	Liquid
Furfuryl amine	NA	NA	NA	Liquid
Heptane	High	NA	Medium/High	Liquid
Hydrogen	High	High	Low	Gaseous
Isoamyl alcohol*	Medium/High	High	NA	Liquid
Isooctane	Medium/High	High	Low/Medium	Liquid
Isopropyl alcohol	Medium/High	NA	Low	Liquid
Jet-A	High	High	Low	Liquid
JP-10	High	High	Low	Liquid
JP-4*	Medium/High	High	Low	Liquid
JP-5*	Medium/High	High	Low	Liquid
JP-8*	Medium/High	High	Low	Liquid
LAH	Very high	Low	Very high	Solid
Limonene	NA	NA	None	Liquid
MEA	Low	High	Low/Medium	High melting point**
Methane	High	NA	Low	Gaseous
Methanol	Medium	NA	Low	Liquid
Monosilanes	High	NA	Low	Gaseous
Morpholine	NA	High	NA	High melting point**

Table C.3: Criteria evaluations from the preliminary fuel selection involving 86 fuels - Part 3
(GREEN=Selected for PICE , YELLOW=Rejected for PICE/Accepted for reference , RED=Rejected for PICE)
(*Final evaluation made after preliminary feasibility assessment, **Liquid storage state*)

Fuel	Performance evaluation	Combustion evaluation	Toxicity evaluation	Storage evaluation
n-buthylamine	High	NA	High	Liquid
n-decane	NA	Medium	Low	Liquid
Nitromethane	High	Medium/High	None/Low	Liquid
Pentaborane	NA	Low/Medium	Very high	Liquid
Pentane	Low/Medium	NA	Low	Low boiling point**
Phenyl hydrazine	NA	NA	High	Solid
Propadiene	Medium	NA	Medium/High	Gaseous
Propane	Low/Medium	NA	Low	Gaseous
Propargyl amine	NA	Low/Medium	High	NA
Propyl amine	Medium/High	NA	Low	Liquid
Propyl ether	NA	NA	Low	Liquid
Propylamine	High	NA	High	Liquid
Propylene	High	NA	Low	Gaseous
Propyne	High	NA	Medium/High	Gaseous
Pyaz*	Medium	NA	Low	Liquid
Pyridine*	Medium/High	NA	Medium	Liquid
Pyrrole	NA	High	High	Liquid Poor storage
RP-1	High	High	None/Low	Liquid
RP-2	NA	NA	NA	NA
Stock-0	NA	High	Low	Unknown transition temperatures**
Stock-1	NA	NA	Low	Unknown transition temperatures** Poor storage
Stock-2	High	Medium/High	Low	Unknown transition temperatures** Poor storage
Stock-3*	High	Medium	Medium	Unknown transition temperatures**
TEAL	NA	NA	NA	Liquid
TEAL + Hexane	NA	High	NA	NA
Tetraglyme*	Medium	High	Low	Liquid

Table C.4: Criteria evaluations from the preliminary fuel selection involving 86 fuels - Part 4
(GREEN=Selected for PICE , YELLOW=Rejected for PICE/Accepted for reference , RED=Rejected for PICE)
(*Final evaluation made after preliminary feasibility assessment, **Liquid storage state*)

Fuel	Performance evaluation	Combustion evaluation	Toxicity evaluation	Storage evaluation
THF	Low/Medium	NA	Low	Liquid
TMEDA*	High	NA	Low/medium	Liquid
TMPDA	High	High	None/Low	Liquid
Toluene	Medium/High	NA	Low	Liquid
Toluidine	Low/Medium	NA	NA	NA
Triethylamine	High	NA	Medium/High	Liquid
Triglyme*	Medium	High	Low	Liquid
Turpentine	Medium/High	NA	Low	Liquid

Table C.5: Final evaluations from the preliminary fuel selection involving 86 fuels - Part 1
(GREEN=Selected for PICE , YELLOW=Rejected for PICE/Accepted for reference , RED=Rejected for PICE)
(*Final evaluation made after preliminary feasibility assessment, **Liquid storage state*)

Fuel	Final evaluation	Reason for disposal
1,2,4-Triazole	No	Lack of sources Storage state fail
1,2-diaminocyclohexane	No	Lack of sources Toxicity fail
1,3-diaminopropane	No	Lack of sources Toxicity fail
1,5-hexadiyne	No	Hiigh melting point Lack of sources
Acetaldehyd	No	Lack of sources Low boiling point Performance fail
Acythelene	No	Poor storage characterstics
Alpha-terpineol	No	Lack of sources Wrong state: solid
Ammonia	No	Performance fail Wrong state:gaseous
Benzaldehyde	No	Performance fail
Block O*	No	Poor storage characteristics Unknown transiton temperatures
BMIM SCN*	No	Lack of availability Unknown boiling point
Butane	No	Wrong state: gaseous
Cyclopropane	No	Toxicity fail Wrong state gaseous
Decaborane	No	Lack of sources Wrong state: solid
DETA*	No	Toxicity fail
Dibutyl ether	No	Toxicity fail Performance fail
Diglyme	No	Toxicity fail Wrong state: gaseous
Dimethylether	No	Wrong state: gaseous High procurrment cost
d-limonene	No	Lack of sources Performance fail
DMA	No	Lack of sources Wrong state: gaseous
DMAZ	Partial	Lack of availability
DMEA/DMAE*	No	Better alternative
DMF	No	Lack of sources
DMSO	No	Lack of sources

Table C.6: Final evaluations from the preliminary fuel selection involving 86 fuels - Part 2
(GREEN=Selected for PICE , YELLOW=Rejected for PICE/Accepted for reference , RED=Rejected for PICE)
(*Final evaluation made after preliminary feasibility assessment, **Liquid storage state*)

Fuel	Final evaluation	Reason for disposal
EDA	No	High melting point Lack of sources Performance fail
EMIM SCN*	No	Lack of availability Unknown boiling point
Ethane	No	Toxicity fail Wrong state: gaseous
Ethanol	Yes	-
Ethyl methyl ether	No	Toxicity fail Wrong state: gaseous
Ethylene	No	Wrong state: gaseous
Ethylene glycol	No	Lack of sources
Ethylenediamine	No	Lack of sources Toxicity fail
Furaldehyde	No	Lack of sources
Furfuryl alcohol	No	Performance fail
Furfuryl amine	No	Lack of sources
Heptane	No	Lack of sources Toxicity fail
Hydrogen	No	Wrong state: gaseous
Isoamyl alcohol*	No	Lack of availability Lack of sources
Isooctane	Yes	-
Isopropyl alcohol	Yes	-
Jet-A	Partial	Better alternative
JP-10	Partial	Better alternative
JP-4*	No	Better alternative
JP-5*	No	Better alternative
JP-8*	No	Better alternative
LAH	No	Combustion stability fail Toxicity fail Wrong state: solid
Limonene	No	Lack of sources
MEA	No	High melting point Performance fail
Methane	No	Wrong state: gaseous
Methanol	Yes	-
Monosilanes	No	Wrong state: Gaseous
Morpholine	No	High melting point Lack of sources
n-buthylamine	No	Toxicity fail
n-decane	No	Lack of sources
Nitromethane	Partial	-

Table C.7: Final evaluations from the preliminary fuel selection involving 86 fuels - Part 3
(GREEN=Selected for PICE , YELLOW=Rejected for PICE/Accepted for reference , RED=Rejected for PICE)
(*Final evaluation made after preliminary feasibility assessment, **Liquid storage state*)

Fuel	Final evaluation	Reason for disposal
Pentaborane	No	Lack of sources
		Toxicity fail
Pentane	No	Lack of sources
		Low boiling point
		Performance fail
Phenyl hydrazine	No	Lack of sources
		Toxicity fail
Propadiene	No	Wrong state: solid
		Toxicity fail
Propane	No	Wrong state: gaseous
		Performance fail
		Wrong state:gaseous
Propargyl amine	No	Combustion stability fail
		Lack of sources
		Toxicity fail
Propyl amine	No	Lack of sources
Propyl ether	No	Lack of sources
Propylamine	No	Toxicity fail
Propylene	No	Wrong state: gaseous
Propyne	No	Lack of sources
		Toxicity fail
		Wrong state: gaseous
Pyaz*	No	Lack of availability
Pyridine*	No	Lack of availability
		Toxicity fail
Pyrrole	No	Poor storage characteristics
		Toxicity fail
RP-1	Yes	-
RP-2	No	Lack of sources
Stock-0	No	Better alternative
		Unknown transition temperatures
Stock-1	No	Better alternative
		Unknown transition temperatures
Stock-2	No	Better alternative
		Poor storage characteristics
		Unknown transition temperatures
Stock-3*	No	Combustion stability fail
		Toxicity fail
		Better alternative
TEAL	No	Poor storage characteristics
		Unknown transition temperatures
TEAL + Hexane	No	Lack of sources

Table C.8: Final evaluations from the preliminary fuel selection involving 86 fuels - Part 4
(GREEN=Selected for PICE , YELLOW=Rejected for PICE/Accepted for reference , RED=Rejected for PICE)
(*Final evaluation made after preliminary feasibility assessment, **Liquid storage state*)

Fuel	Final evaluation	Reason for disposal
Tetraglyme*	No	Better alternative Lack of development Toxicity fail
THF	No	Performance fail
TMEDA*	No	Toxicity fail
TMPDA	Yes	-
Toluene	Yes	-
Toluidine	No	Lack of sources Performance fail Unfavourable storage state
Triethylamine	No	Lack of sources Toxicity fail
Triglyme*	No	Lack of development Toxicity fail
Turpentine	Yes	-

D.Fuel characteristics

Table D.1: Relevant characteristics for the candidate fuel ethanol

Fuel : Ethanol			
Toxicity			
Relevant GHS	H225, H319	NFPA Health	2
SVP [kPa]	5.8	TWA [ppm]	1000
Ease of use			
Metal compatibility	Mostly excellent	Plastics compatibility	Mostly excellent
NFPA Flammability	3	NFPA Reactivity	0
Freezing temperature [K]	203	Boiling temperature [K]	407
Development level			
Estimated TRL		6	
Coolant qualities			
Thermal conductivity [W/(m.K)]	0.166	Specific heat [J/(kg.K)]	2440
Dynamic viscosity [Mpa.s]	1.04		
Other relevant characteristics			
Density [kg/m^3]	789	Other names(s)	Ethyl alcohol

Table D.2: Relevant characteristics for the candidate fuel Isooctane

Fuel : Isooctane

Toxicity

Relevant GHS	H225, H315, H304, H336, H400, H411	NFPA Health	1
SVP [kPa]	5.2	TWA [ppm]	300

Ease of use

Metal compatibility	Excellent	Plastics compatibility	Mostly excellent
NFPA Flammability	3	NFPA Reactivity	0
Freezing temperature [K]	166	Boiling temperature [K]	372

Development level

Estimated TRL	

Coolant qualities

Thermal conductivity [W/(m.K)]	0.0978	Specific heat [J/(kg.K)]	2123
Dynamic viscosity [Mpa.s]	0.473		

Other relevant characteristics

Density [kg/m^3]	690	Other names(s)	2,2,4-trimethylpentane

Table D.3: Relevant characteristics for the candidate fuel Isopropanol

Fuel : Isopropanol

Toxicity

Relevant GHS	H225, H319, H336	NFPA Health	1
SVP [kPa]	4.4	TWA [ppm]	400

Ease of use

Metal compatibility	Mostly excellent	Plastics compatibility	Excellent
NFPA Flammability	3	NFPA Reactivity	0
Freezing temperature [K]	184	Boiling temperature [K]	355

Development level

Estimated TRL	

Coolant qualities

Thermal conductivity [W/(m.K)]	0.1407	Specific heat [J/(kg.K)]	2680
Dynamic viscosity [Mpa.s]	1.96		

Other relevant characteristics

Density [kg/m^3]	786	Other names(s)	Isopropyl alcohol, propan-2-o

Table D.4: Relevant characteristics for the candidate fuel Jet-A

Fuel : Jet-A			
Toxicity			
Relevant GHS	H226, H304, H315, H336, H351, H411	NFPA Health	2
SVP [kPa]	2	TWA [ppm]	29
Ease of use			
Metal compatibility	Excellent	Plastics compatibility	Mostly excellent
NFPA Flammability	2	NFPA Reactivity	0
Freezing temperature [K]	226	Boiling temperature [K]	448
Development level			
Estimated TRL			
Coolant qualities			
Thermal conductivity [W/(m.K)]	0.11	Specific heat [J/(kg.K)]	2120
Dynamic viscosity [Mpa.s]	1.1		
Other relevant characteristics			
Density [kg/m^3]	840	Other names(s)	Jet fuel, aviation kerosene

Table D.5: Relevant characteristics for the candidate fuel methanol

Fuel : Methanol			
Toxicity			
Relevant GHS	H225, H301, H311, H331, H370	NFPA Health	1
SVP [kPa]	12.9	TWA [ppm]	200
Ease of use			
Metal compatibility	Mostly excellent	Plastics compatibility	Good
NFPA Flammability	3	NFPA Reactivity	0
Freezing temperature [K]	175	Boiling temperature [K]	338
Development level			
Estimated TRL		4	
Coolant qualities			
Thermal conductivity [W/(m.K)]	0.196	Specific heat [J/(kg.K)]	2530
Dynamic viscosity [Mpa.s]	0.533		
Other relevant characteristics			
Density [kg/m^3]	792	Other names(s)	Methyl alcohol

Table D.6: Relevant characteristics for the candidate fuel RP-1

Fuel : RP-1			
Toxicity			
Relevant GHS	H225, H304, H315, H319, H336, H350, H411	NFPA Health	2
SVP [kPa]	1	TWA [ppm]	29
Ease of use			
Metal compatibility	Excellent	Plastics compatibility	Mostly good
NFPA Flammability	2	NFPA Reactivity	0
Freezing temperature [K]	213	Boiling temperature [K]	363
Development level			
Estimated TRL		8	
Coolant qualities			
Thermal conductivity [W/(m.K)]	0.11	Specific heat [J/(kg.K)]	2050
Dynamic viscosity [Mpa.s]	1.5		
Other relevant characteristics			
Density [kg/m^3]	773	Other names(s)	Rocket propellant 1, refined petrole

Table D.7: Relevant characteristics for the candidate fuel TMPDA

Fuel : TMPDA			
Toxicity			
Relevant GHS	H226, H302, H312, H314, H318, H335, H411	NFPA Health	3
SVP [kPa]	0.65	TWA [ppm]	N/
Ease of use			
Metal compatibility	Excellent	Plastics compatibility	Ba
NFPA Flammability	3	NFPA Reactivity	0
Freezing temperature [K]	203	Boiling temperature [K]	41
Development level			
Estimated TRL		4	
Coolant qualities			
Thermal conductivity [W/(m.K)]	0.145	Specific heat [J/(kg.K)]	216
Dynamic viscosity [Mpa.s]	1.2		
Other relevant characteristics			
Density [kg/m^3]	779	Other names(s)	N,N,N',N'–tetramethylp

Table D.8: Relevant characteristics for the candidate fuel toluene

Fuel : Toluene

Toxicity

Relevant GHS	H225, H304, H315, H336, H361, H373	NFPA Health	2
SVP [kPa]	3.01	TWA [ppm]	20

Ease of use

Metal compatibility	Excellent	Plastics compatibility	Bad
NFPA Flammability	3	NFPA Reactivity	0
Freezing temperature [K]	178	Boiling temperature [K]	384

Development level

Estimated TRL	1

Coolant qualities

Thermal conductivity [W/(m.K)]	0.131	Specific heat [J/(kg.K)]	1700
Dynamic viscosity [Mpa.s]	0.56		

Other relevant characteristics

Density [kg/m^3]	867	Other names(s)	Toluol, methylbenzene

Table D.9: Relevant characteristics for the candidate fuel turpentine

Fuel : Turpentine

Toxicity

Relevant GHS	H225, H302, H304, H315, H317, H319, H332, H410	NFPA Health	1
SVP [kPa]	4	TWA [ppm]	20

Ease of use

Metal compatibility	Mostly excellent	Plastics compatibility	Good
NFPA Flammability	3	NFPA Reactivity	0
Freezing temperature [K]	218	Boiling temperature [K]	427

Development level

Estimated TRL	4

Coolant qualities

Thermal conductivity [W/(m.K)]	0.128	Specific heat [J/(kg.K)]	1720
Dynamic viscosity [Mpa.s]	1.375		

Other relevant characteristics

Density [kg/m^3]	790	Other names(s)	

E. Rocket engines input data

Table E.1: Relevant input data for the engines considered in setting up the propulsion model performing and subsequent validation efforts

Name	Type	Stage	Pc [Mpa]	eta [-]	OF [-]	Fuel	Ox	At [m^2]	De [m]
RS-68A	Cryogenic	Core stage	10.9	21.5	5.97	LH	LOX	0.217486	2.44
RS-25	Cryogenic	Core stage	20.6	69	6.03	LH	LOX	0.065564	2.4
HM7B	Cryogenic	Upper stage	3.7	83.1	5	LH	LOX	0.009263	0.99
J-2	Cryogenic	Upper stage	5.26	27.5	5.5	LH	LOX	0.125949	2.1
RL10B-2	Cryogenic	Upper stage	4.412	280	5.88	LH	LOX	0.0137	2.21
Vinci	Cryogenic	Upper stage	6.08	240	5.8	LH	LOX	0.015127	2.15
Vulcain 2.1	Cryogenic	Core stage	11.8	61.5	6.03	LH	LOX	0.056319	2.1
Vulcain 2	Cryogenic	Core stage	10	45	5.3	LH	LOX	0.054063	1.76
LE-5B	Cryogenic	Upper stage	3.6	110	5	LH	LOX	0.020878	1.71
LE-7A	Cryogenic	Core stage	12.3	52	5.9	LH	LOX	0.05003	1.82
Viking 5C	Storable	Core stage	5.5	10	1.71	UDMH	NTO	0.076977	0.99
Vikas 4B	Storable	Second stage	5.85	30.8	1.71	UH-25	NTO	0.073695	1.7
RD-275M	Storable	Core stage	16.5	26.4	2.67	UDMH	NTO	0.062549	1.45